



CISM COURSES AND LECTURES NO. 241  
INTERNATIONAL CENTRE FOR MECHANICAL SCIENCES

---

# PLASTICITY IN STRUCTURAL ENGINEERING FUNDAMENTALS AND APPLICATIONS

CH. MASSONNET / W. OLSZAK / A. PHILLIPS

---

SPRINGER-VERLAG WIEN GMBH  
@Seismicisolation



INTERNATIONAL CENTRE FOR MECHANICAL SCIENCES

COURSES AND LECTURES - No. 241



PLASTICITY  
IN STRUCTURAL ENGINEERING  
FUNDAMENTALS  
AND APPLICATIONS

CH. MASSONNET  
UNIVERSITY OF LIEGE

W. OLSZAK  
POLISH ACADEMY OF SCIENCES  
INTERNATIONAL CENTRE FOR MECHANICAL SCIENCES  
UDINE

A. PHILLIPS  
YALE UNIVERSITY



This work is subject to copyright.  
All rights are reserved,  
whether the whole or part of the material is concerned  
specifically those of translation, reprinting, re-use of illustrations,  
broadcasting, reproduction by photocopying machine  
or similar means, and storage in data banks.

© 1979 by Springer-Verlag Wien

Originally published by Springer-Verlag Wien New York in 1979

ISBN 978-3-211-81350-8

ISBN 978-3-7091-2902-9 (eBook)

DOI 10.1007/978-3-7091-2902-9

## PREFACE

The rapid development of the Theory of Plasticity and of its methods is due to both the challenging new cognitive results and the demand for more realistic ways of assessing the inelastic response of engineering structures and machine parts when subjected to severe loading programmes. So, for instance, in order to determine the safety factor of structures or to explore their dynamic behaviour beyond the elastic range, we have to know the whole spectrum of their response up to failure.

The notable progress of the Theory of Plasticity concerns both its foundations and its engineering applications. These facts are clearly reflected in the lectures of the CISM course on “Engineering Plasticity. Part I : Civil Engineering” organized during its Saint-Venant Scientific Session. In this frame the following five course series have been delivered:

1. H. Lippmann (Munich): On the incremental extremum theorems for elastic-plastic media;
2. Ch. Massonnet (Liège): Fundamentals and some civil engineering applications of the Theory of Plasticity;
3. W. Olszak (Warsaw-Udine): Generalized yield criteria for advanced models of material response;
4. A. Phillips (New Haven, Con.): The foundations of plasticity. Experiments, theory and selected applications;
5. A. Sawczuk (Warsaw): Plastic plates.

The present volume contains the contributions 2, 3, and 4.

The course delivered by Ch. Massonnet presents, in Part One, in a condensed and clear manner, the fundamental laws governing the plastic response of materials and the ensuing subsequent theory whereupon, in Part Two, the methods of limit analysis and limit design of engineering structures are treated.

Under these headings, the topics treated are: The general theory of plasticity; the

*theorems of limit analysis in their both aspects, i.e. for proportional (one-parameter) loadings and for loading programmes depending on several parameters. Afterwards the concept of generalized variables and of the corresponding yield surfaces are introduced, whereupon problems of limit analysis and design as well as shake-down phenomena occurring in engineering structures are treated and discussed. Numerous examples and technical applications, with emphasis on problems pertaining to civil engineering, are presented and dealt with, so, e.g., frames, pile groups, grids, minimum-weight design, etc. Finally, the last Chapter is devoted to various approaches to the limit analysis of plates, disks, and shells.*

A. Phillips presents in his contribution new experimental evidence on the foundations of plasticity and re-evaluates on this basis the classical experimental work. The constitutive equations of plasticity are developed on the basis of the new experimental results and special emphasis is given to temperature changes. The initial and subsequent yield surfaces and the loading surface are discussed. The theory is extended to viscoplasticity and creep. Corners and norriality are examined. Applications are given to selected problems of low cycle fatigue, viscoplasticity, creep, and plastic stability.

Because the Author's lectures have been prepared well in advance of the course, some time has since elapsed during which considerable progress both in experimental and theoretical research has been achieved by the Author and his associates. To cover some of this progress which enhances the results presented in the lectures, an appropriate Appendix has been added. It is divided in two parts. The first one discusses new experimental findings, whereas the second treats new theoretical results. The related bibliography is also referred to.

The well known classical approach to formulating the yield criteria is based on the notion of mechanically isotropic and homogeneous media. The paper by W. Olszak shows how this approach has successively been generalized by taking into consideration new physical phenomena which originally were disregarded. First, the mechanical anisotropy and (macro)nonhomogeneity were taken into account. Afterwards rheological material response is considered in both its forms: (a) that which only sets in after the plastic limit has been exceeded; and (b) also that one –

considerably more difficult to be accounted for – which accompanies the deformation process from its very beginning. The next steps consist in investigating the consequences of a time-variable plasticity criterion, which may occur when, e.g., artificial irradiation effects or a time-variable humidity content of elastic-visco-plastic soils are being analyzed.

All these considerations assume that the (original) investigated deformation and stress fields are uniform (*homogeneous*). This assumption, as a rule, does not correspond to physical reality. So the consequent step consists in introducing (space and time dependent) nonhomogeneities of these fields. The influence of the stress tensor gradient on the yield criterion is found to be of importance [in an analogous manner as in the case of a (time) stress rate]. The ensuing consequences may, among others, result, under certain conditions, in a considerable increase of the plastic limit. This fact has already been known from experimental evidence for many years.

We hope the present volume will constitute a useful source of information on the problems presented by the lecturers.

W. Olszak

## CONTENTS

	page
Preface	I
<b>FUNDAMENTALS AND SOME CIVIL ENGINEERING APPLICATIONS OF THE THEORY OF PLASTICITY</b>	
by Ch. Massonet	
Introduction .....	3
<b>PART ONE : General Theory</b>	
1. General Theory of Plasticity .....	4
1.1. Structural Metals in Tension and Compression .....	4
1.2. Yield Condition Under Multiaxial States of Stress .....	9
1.3. Fundamental Laws of Plasticity – Perfectly Plastic Solids ...	16
1.4. Hardening Laws .....	23
1.5. Prandtl-Reuss Equations .....	29
1.6. Variation of the Global Coefficient of Lateral Contraction in the Course of a Tension Test .....	33
1.7. Stress Measurements, at the Surface of a Plastically Deformed Body, with the Help of Stress Rosettes .....	34
2. General Theorems of Limit Analysis - Proportional Loading .....	37
2.1. Introduction .....	37
2.2. Preliminary Concepts and Results .....	39
2.3. The Three Basic Theorems .....	43
2.4. Additional Remarks .....	46
2.5. Elastic-Plastic and Rigid-Plastic Bodies .....	50
2.6. Influence of Changes of Geometry .....	51
2.7. Uniqueness of the Solution .....	55
3. General Theorems of Limit Analysis - General Loading .....	56
3.1. Structure with non Negligible Dead Load .....	56
3.2. Loading Depending on Several Parameters .....	56

	page
<b>PART TWO : Limit Analysis and Design of Engineering Structures</b>	
<b>4. Generalized Variables .....</b>	<b>66</b>
4.1. The Concept of Generalized Variables .....	66
4.2. Choice and General Properties of the Generalized Variables ..	72
4.3. Elimination of the Reactions .....	73
4.4. Yield Conditions in Generalized Stress .....	76
4.5. Piecewise Linear Yield Surfaces .....	84
4.6. Discontinuities .....	87
<b>5. Frames – First Order Theory .....</b>	<b>89</b>
5.1. Specialized Versions of the Fundamental Theorems .....	89
5.2. Validity of the Fundamental Theorems for Carbon Steels ...	92
5.3. Proportional Loading – Practical Methods of Solution .....	94
5.4. Variable Repeated Loading - Shake Down Theorems .....	111
5.5. Minimum Weight Design .....	120
5.6. Practical Solution of all Problems of Plastic Analysis, Incremental Collapse and Minimum Weight Design by Reduction to Linear Programming .....	122
<b>6. Other Structures Made of Bars .....</b>	<b>133</b>
6.1. Pile Groups .....	133
6.2. Torsionless Grids Loaded Perpendicularly to their Plane .....	134
6.3. Torsionally Stiff Grids - Rigid Space Frames - Arches .....	134
6.4. Masonry Structures .....	135
<b>7. Various Approaches to the Limit Analysis of Plates, Shells and Disks .....</b>	<b>135</b>
7.1. Introduction .....	135
7.2. Limit Strength of a Wide-Flange I Beam with Circular Axis ..	136
7.3. Incremental Plasticity – Computer Solution of Plane Structure for Perfectly Plastic or Strain Hardening Metals .....	144
7.4. Illustrative Examples .....	152
7.5. Quasi-Direct Limit Analysis of Plane Structures Via the Finite Element Method .....	158
7.6. Illustrative Examples .....	172
<b>References .....</b>	<b>181</b>

	page
<b>THE FOUNDATIONS OF PLASTICITY</b>	
Experiments. Theory and Selected Applications by A. Phillips	
Preface . . . . .	189
1. Experimental Verification of a Theory. The Empirical Method . . . . .	191
2. Experimental Verification of a Theory. The Axiomatic Method . . . . .	192
3. Plastic Flow Under Uniaxial Stress . . . . .	193
4. The Initial Yield Surface . . . . .	207
5. The Subsequent Yield Surfaces . . . . .	215
6. The Loading Surface . . . . .	230
7. The Plastic Strain Increment Vector and the Creep Strain Vector . . . . .	233
8. Corners and Normality. Plastic Stability . . . . .	237
9. Analytical Expressions of the Motion of the Yield - and Loading Surfaces ..	241
9.1. Hardening Rules . . . . .	241
9.2. A New Hardening Rule . . . . .	244
9.3 Application . . . . .	246
9.4. Comparison of Rules . . . . .	248
10. The Theory of Plasticity . . . . .	251
11. Thermodynamic Considerations . . . . .	253
12. Creep and Viscoplasticity . . . . .	258
References . . . . .	262
Appendix . . . . .	265
References . . . . .	268
 <b>GENERALIZED YIELD CRITERIA FOR ADVANCED MODELS OF MATERIAL RESPONSE</b>	
by W. Olszak	
I. Introductory Remarks . . . . .	277
II. The Classical Approach . . . . .	279
III. Anisotropy. Nonhomogeneity . . . . .	281
IV. Rheological Effects . . . . .	284
V. Nonstationary Yield Criteria . . . . .	289

	page
VI. Space and Time Variable Stress and Strain Fields .....	293
VII. Final Methodical Remark .....	299
References .....	300

## **LIST OF CONTRIBUTORS**

Ch. Massonnet : Professor at University of Liège, Belgium.

W. Olszak : Professor, Polish Academy of Sciences; International Centre for Mechanical Sciences (C.I.S.M.), Udine, Italy.

A. Phillips : Professor of Engineering and Applied Science, Yale University, New Haven, Conn., U.S.A.

**THEORY OF PLASTICITY**  
(Civil Engineering I)

by

**Ch. MASSONNET**  
Prof. at University of Liège

## INTRODUCTION

The purpose of this course is to present, in condensed form, the methods of the theory of plasticity and especially of Limit Analysis and Design, with emphasis on problems pertaining to civil engineering.

The reader is assumed to know elementary calculus, as well as Mechanics of Materials and the elements of Mechanics of Continua.

Cartesian indicial notation will be used throughout. If repeated (dummy) indices are used, summation must be applied on these indices (EINSTEIN's Summation convention).  $\delta_{ij}$  represents the Kronecker delta. Partial derivatives of a function F with respect to the coordinates  $x_j$ , i.e.,  $\partial F / \partial x_j$ , will be represented by the notation  $\partial_j F$ .

## PART ONE: GENERAL THEORY

### 1. GENERAL THEORY OF PLASTICITY

#### 1.1. Structural Metals in Tension and Compression.

The basic information about metal behaviour is obtained by tension and compression tests.

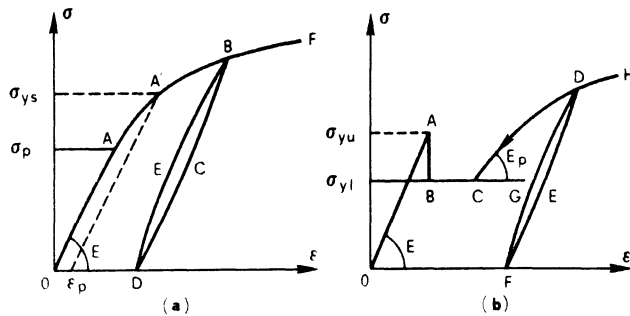


Fig. 1.1.

Most of the structural metals (brass, bronze, aluminium alloys, alloyed steels, etc.) exhibit the behavior depicted by Fig. 1.1.a, where the straight line  $OA$  corresponds to elastic (reversible) behavior, terminated in  $A$  at the limit of proportionality  $\sigma_p$  (in  $N/mm^2$ ). The slope of  $OA$  is YOUNG's modulus. No sharp yield point is discernible, and a yield strength must be defined arbitrarily. Ordinarily, one defines a offset yield point  $\sigma_{ys}$ , represented by point  $A'$  of the diagram, and corresponding to a certain amount of permanent strain  $\epsilon_p$  after unloading. The most used offset yield points are  $\sigma_{0.1}$ , corresponding to  $\epsilon_p = 0.001 \equiv 0.1\%$ , and  $\sigma_{0.2}$ , corresponding to  $\epsilon_p = 0.002 \equiv 0.2\%$ .

Above the proportional limit  $\sigma_p$ , the response of the metal is both elastic and plastic. Experiment shows that unloading at any stage (point B) reduces the strain along an almost completely elastic unloading line BCD. Subsequent reloading first retraces the unloading line with very small deviation (line DEB) and then continues approximately the behavior BF of the virgin material.

Usually, hot-rolled carbon steels exhibit the behavior represented by curve OBCDH at fig. 1.1.b. The yield point  $\sigma_{yl}$  (point b) is followed by an extended

horizontal yield plateau BC during which the material extends under constant stress. At C begins the strain hardening zone CDH with properties similar to zone ABF of fig. 1.1.a). A quantity important in practical limit analysis is the strain hardening modulus  $E_p$ , which is the tangent modulus of deformation  $d\sigma/d\epsilon$  at the beginning of the strain hardening zone. YOUNG's modulus for all structural steels is nearly constant and equal to  $210 \text{ kN/mm}^2$ . The strain hardening modulus varies with the carbon content between 5 and  $8 \text{ kN/mm}^2$ .

It is important to note that the plateau BC of the carbon steel curve, does not represent a continuous behavior of the material. The specimen exhibits plastic regions in form of thin strips, called yield lines, or LÜDERS–HARTMANN lines (easily visible on polished specimens), where the material is at point C, separated by completely elastic regions, represented by point B. The amount of plastified (C) material increases linearly along BC and, in the middle, of the plateau, half of the volume of the metal is plastified.

For above reasons, it is not possible to define a tangent modulus in the BC region.

Some carbon steels, especially those in the annealed condition, exhibit a peculiar behavior characterized, on Fig. 1.1.b), by the curve OABCDH. The position of point A is characterized by the upper yield stress  $\sigma_{yu}$  and that of point B by the lower yield stress  $\sigma_{yl}$ . The upper yield stress is highly sensitive to the axiality of the tension force in the specimen, the shape of this specimen and its surface condition. Any stress concentration due to the shape or to surface defects triggers yield lines which tend to round off the peak oAB.

Under very careful conditions, LEBLOIS and the writer could obtain for annealed mild steel, upper yield stresses exceeding the lower yield stress by up to 60 %. [L1].

The diagram of Fig. 1.2. shows how  $\sigma_{yu}$  and  $\sigma_{yl}$  depend on the strain rate  $\dot{\epsilon} \equiv d\epsilon/dt$  between  $10^{-7}$  and  $1. \text{ sec}^{-1}$ .

When the strains are small, it makes no difference to compute the stress from the original cross sectional area  $A_0$  or the actual area A. When the strains are

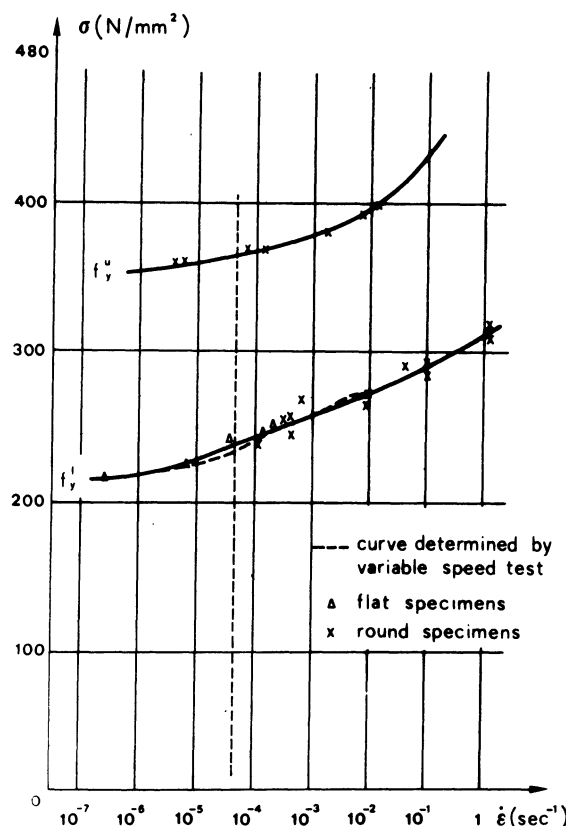


Fig. 1.2.

large, on the contrary, the difference is appreciable. We shall then distinguish between the nominal stress  $\sigma = P/A_0$  and the true stress  $P/A$ .

Similarly, for what regards the strains, we shall distinguish between the nominal strain

$$\epsilon = \frac{1 - l_0}{l_0} \quad \text{and the true strain } \epsilon = \int_{l_0}^1 \frac{1}{l} dl = \ln \frac{1}{l_0} .$$

At the end of the tensile test, necking of the test specimen occurs, but we shall not need the study of this phenomenon. The maximum value of the nominal stress,  $\sigma_B$ , is usually called the breaking strength of the metal.

The behavior of the virgin ductile metals in compression is the same as in tension, and corresponding limits  $\sigma_{0 \cdot 1}'$ ,  $\sigma_{0 \cdot 2}'$ ,  $\sigma_y'$ , may be defined, which have the same values as in tension.

However, after prestraining in tension, the stress-strain curve in compression (curve CDE - Fig. 1.3.) differs from the curve which could be obtained on reloading in tension (curve CBF) or on loading a virgin specimen in compression (curve oA'B').

Actually, the proportional limit in compression  $\sigma_p$  after a straining in tension is lower than the value of this limit,  $\sigma_p$ , for the virgin material. This phenomenon is called BAUSCHINGER effect and should be taken into account in the mathematical description of strain hardening.

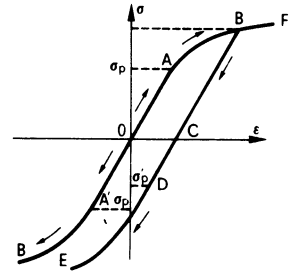


Fig. 1.3.

The stress-strain diagram of metals without yield plateau may be very accurately represented by the RAMBERG–OSGOOD formula

$$\epsilon = \epsilon_e + \epsilon_p = \frac{\sigma}{E} + \left(\frac{\sigma}{B}\right)^n \quad (1.1.)$$

where E is YOUNG's modulus, and B and n are material constants.

The tangent modulus is given by formula

$$E_t = \left( \frac{d\sigma}{d\epsilon} \right) = \frac{E}{1 + n \frac{E}{B} \left( \frac{\sigma}{B} \right)^{n-1}} \quad (1.2.)$$

From the definition given above of the 0.1 % and 0.2 % offset yield stresses, one deduces immediately the relations

$$0.001 = \left( \frac{\sigma_{0 \cdot 1}}{B} \right)^n \quad 0.002 = \left( \frac{\sigma_{0 \cdot 2}}{B} \right)^n \quad (1.3.)$$

from which

$$\frac{\sigma_{0 \cdot 2}}{\sigma_{0 \cdot 1}} = \sqrt{2} . \quad (1.4.)$$

This shows that the parameter  $n$  measures the steepness of the strain hardening part ABF of the  $\sigma$ ,  $\epsilon$  diagram ; it is therefore appropriate to call  $n$  strain hardening index.

The stress-strain curves discussed above have been tacitly assumed independent of the rate of straining. This is reasonably true for structural metals at room temperature, tested at the ordinary slow speeds of standard testing machines. The strain rate effect is usually very small. Most materials without yield plateau obey LUDWIK's logarithmic strain rate law

$$(1.5.) \quad \sigma = \sigma_1 + \sigma_0 \ln \frac{\dot{\epsilon}}{\dot{\epsilon}_0} \quad (\dot{\epsilon} > \dot{\epsilon}_0)$$

where  $\dot{\epsilon} \equiv d\epsilon/dt$  is the strain rate of the test considered and  
 $\dot{\epsilon}_0$  is a reference strain rate, usually taken as 1% per hour.

As the strain rate increases from zero to  $100 \text{ sec}^{-1}$ , the stress strain curve is raised by about 15 % in the plastic range.

However, here also, carbon steels exhibit a very distinctive behavior and, for the above increase in strain rate, their yield stress increases by about 100 % whereas the breaking strength  $\sigma_B$  is only slightly increased.

Under elevated temperatures, the material constants  $E$ ,  $\sigma_y$ ,  $\sigma_B$  diminish and tend to zero when the temperature nears to the melting point. Moreover, the strain in the tension specimen increases under constant stress (creep test) whereas the stress drops off under constant strain (relaxation test). We shall not analyze here these viscoelastic phenomena.

In summary, let us emphasise that the yield stress  $\sigma_s$  or  $\sigma_y$  depends always on the environment (temperature, strain rate, etc.) and, in theoretical applications, the yield stress value must always be chosen for the environmental conditions of the problem under discussion.

Physically, the plastic deformations are explained by the movement of dislocations. To get dislocations to move and to be generated takes time and this explains that, the less the time, the higher the stress needed. Yielding is therefore not instantaneous, but takes a certain time, called time delay, which is a decreasing

function of the stress level [L1]. Strain rate effects and delay time for yielding are two aspects of the same physical phenomenon.

## 1.2. Yield Condition Under Multiaxial States of Stress.

### 1.2.1. Basic physical facts.

The first basic ingredient of theory of plasticity is the yield criterion, that is the mathematical law specifying the condition for which the material yields in a triaxial state of stress  $\sigma_1, \sigma_2, \sigma_3$ . Two experimental facts will help to simplify the discovery of this criterion. The first, shown by BRIDGMAN and others, is that the influence of hydrostatic pressure on yielding and subsequent deformation is negligible. The stress-strain curve is not affected in the small strain range, whereas the ductility of the material is greatly enhanced. The second fact, related to the first, is that, in large plastic deformations, the density of the material changes very little, so that POISSON's ratio is equal to 0.5, and the plastic part of the cubical dilatation is constantly zero

$$\dot{\Delta}_p = \dot{\epsilon}_{1,p} + \dot{\epsilon}_{2,p} + \dot{\epsilon}_{3,p} = 0. \quad (2.1.)$$

This is true for the metals up to the end of the tension or compression test and, for plain concrete in compression, up to about seventy percent of the breaking strength ( $0.7 \cdot \sigma_B$ ). For higher stresses, internal cracks are formed in concrete and the volume increases in the compression test, giving an apparent POISSON's ratio larger than 0.5.

It is generally assumed that the yield criterion may be expressed in terms of stresses only, and that the stress gradients  $d\sigma_1/dl, \dots, d\sigma_3/dl$  do not play any role. Experiment shows this to be true, except when the stress gradient becomes very large, so that the stress varies appreciably within a single grain of the metal. In that case, the macroscopic peak stress in a grain will exceed appreciably the value of the average stress in the grain, and a size effect will be observed. This question may be of importance, e.g., for the behavior of specimens with acute notches, in which large stress gradients exist at the root of the notch.

### 1.2.2. Yield criteria for perfectly plastic metals.

We shall first discuss the case of metals presenting an extended yield plateau characterized by its yield stress  $\sigma_y$ . The most convenient way of expression the yield criterion is to write it

$$(2.2.) \quad \bar{\sigma} (\sigma_1, \sigma_2, \sigma_3) = \sigma_y$$

where the equivalent stress  $\bar{\sigma}$  is a suitable combination of the principal stresses, which reduces to the yield stress in simple tension.

It is assumed, in what follows, that the material is isotropic. As plastic flow must then depend only on the value of the three principal stresses, but not on their directions, any yield criterion must be of the form :

$$(2.3.) \quad f(I_1, I_2, I_3) = 0$$

where  $I_1, I_2, I_3$ , are the invariants of the stress tensor  $\sigma_{ij}$ , defined by the formulae

$$(2.4.) \quad I_1 = \sigma_1 + \sigma_2 + \sigma_3 = \sigma_{11} ; \quad I_2 = \sigma_1\sigma_2 + \sigma_2\sigma_3 + \sigma_3\sigma_1 ; \quad I_3 = \sigma_1\sigma_2\sigma_3 .$$

However, from the first experimental fact analyzed above, it results that plastic yielding does not depend on the hydrostatic part of the stress tensor

$$\sigma_m = \frac{\sigma_1 + \sigma_2 + \sigma_3}{3} = \frac{I_1}{3}$$

and only depends on the invariants of the stress deviator

$$s_{ij} = \begin{bmatrix} s_{11} & s_{12} & s_{13} \\ s_{12} & s_{22} & s_{23} \\ s_{13} & s_{23} & s_{33} \end{bmatrix} = \begin{bmatrix} \sigma_{11} - \sigma_m & \sigma_{12} & \sigma_{13} \\ \sigma_{12} & \sigma_{22} - \sigma_m & \sigma_{23} \\ \sigma_{13} & \sigma_{23} & \sigma_{33} - \sigma_m \end{bmatrix}$$

The first invariant  $I_1 = s_1 + s_2 + s_3$  of  $s_{ij}$  is evidently zero, because its value is  $I_1 - 3\sigma_m$ , and the yield criterion reduces to the form

$$(2.5.) \quad f(I'_2, I'_3) = 0$$

where

$$(2.6.) \quad I'_2 = (s_1 s_2 + s_2 s_3 + s_3 s_1) = \frac{1}{2} (s_1^2 + s_2^2 + s_3^2) = \frac{1}{2} s_{ij} s_{ij}$$

$$(2.7.) \quad I'_3 = s_1 s_2 s_3 = \frac{1}{3} (s_1^3 + s_2^3 + s_3^3) .$$

It is useful to introduce here a geometrical representation of the stress state. This state is completely determined by the values of the three principal stresses, so that every stress may be represented by a vector in a three-dimensional state where the

principal stresses are taken as cartesian coordinates. At figure 2.1.,  $\vec{OS}$  is the vector  $(\sigma_1, \sigma_2, \sigma_3)$ , whereas  $\vec{OP}$  is the vector representing the deviator  $(\sigma'_1, \sigma'_2, \sigma'_3)$ .  $\vec{OP}$  always lies in the plane whose equation is

$$\sigma_1 + \sigma_2 + \sigma_3 = 0, \quad (2.8.)$$

whereas  $\vec{PS}$ , representing the hydrostatic component  $(\sigma_m, \sigma_m, \sigma_m)$  of the stress tensor, has the direction cosines  $(1/\sqrt{3}, 1/\sqrt{3}, 1/\sqrt{3})$  and is perpendicular to  $\pi$ .

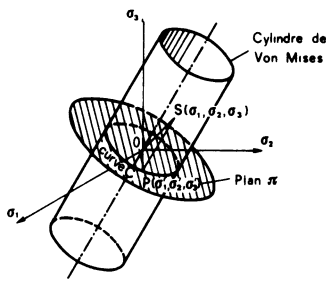


Fig. 2.1.

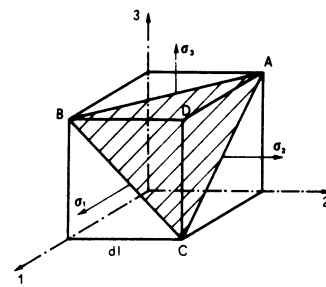


Fig. 2.2.

At present, the yield criterion (2.5) may be regarded as a surface in the space  $(\sigma_1, \sigma_2, \sigma_3)$ . As yielding is independent of the hydrostatic component of the stress tensor, it is evident that this surface is a right cylinder whose axis is the trisectrix of the axes, whose generatrices are perpendicular to  $\pi$  and which cuts  $\pi$  along a certain curve  $C$ . It suffices therefore to discuss the various possible shapes of this curve and to consider only stress states whose hydrostatic component is zero.

At figure 2.3.,  $\pi$  is the plane of the paper. The yield locus  $C$  and the orthogonal projections of the axes are represented. The locus may be convex or concave with respect to the origin, but visibly cannot be such that a ray cuts it twice. At present, if  $(\sigma_1, \sigma_2, \sigma_3)$  is a plastic state,  $(\sigma_1, \sigma_3, \sigma_2)$  is one also, because the metal is isotropic. The locus  $C$  is therefore symmetrical with respect to LL', and similarly to MM' and NN'. This is equivalent to say that the yield locus is a function of the invariants of the tensor.

We shall study, in the present section, the perfectly plastic metals, for

which the yield locus is fixed in the space of principal stresses, whatever be the intensity of the plastic strains sustained by this metal.

We shall examine then, in section 1.4., the strain hardening metals, namely those which harden by plastic deformation, and we shall study how the yield surface changes its shape as a function of the amplitude of the previous plastic deformation.

### 1.2.3. Criterion of the maximum shear stress (TRESCA)

On the basis of rather rough experiments, TRESCA postulated that, in all possible states, the plastic deformation occurs when the maximum shear stress reaches a determined value, characteristic of the metal considered. As the maximum shear stress is given by the formula  $\tau_{\max} = (\sigma_1 - \sigma_3)/2$ , where  $\sigma_1$  and  $\sigma_3$  are the algebraically maximum and minimum principal stresses, TRESCA's criterion may be written  $(\sigma_{\max} - \sigma_{\min})/2 = C$ , where  $C$  is a universal constant for the metal considered. Applying the criterion in pure tension, where  $\sigma_{\max} = \sigma_y$ ,  $\sigma_{\min} = 0$ , one obtains  $(\sigma_{\max} - \sigma_{\min})/2 = \sigma_y/2$ . It is equivalent to write :

$$(2.9.) \quad \bar{\sigma} \equiv \sigma_{\max} - \sigma_{\min} = \sigma_y$$

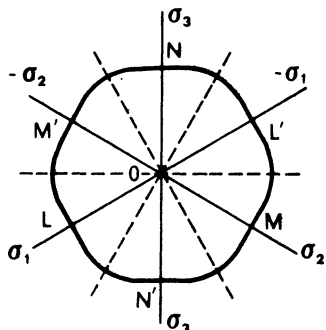


Fig. 2.3.

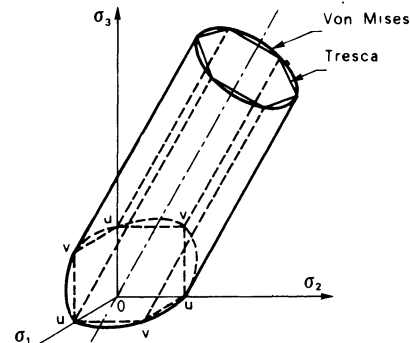


Fig. 2.4.

In the system of axes  $\sigma_1$ ,  $\sigma_2$ ,  $\sigma_3$  (fig. 2.4.), this criterion corresponds to the regular hexagonal prism of equations

$$(2.10.) \quad \sigma_1 - \sigma_2 = \pm \sigma_y; \quad \sigma_2 - \sigma_3 = \pm \sigma_y; \quad \sigma_3 - \sigma_1 = \pm \sigma_y.$$

The corresponding yield locus in the  $\pi$  plane is a regular hexagone (fig. 2.5.).

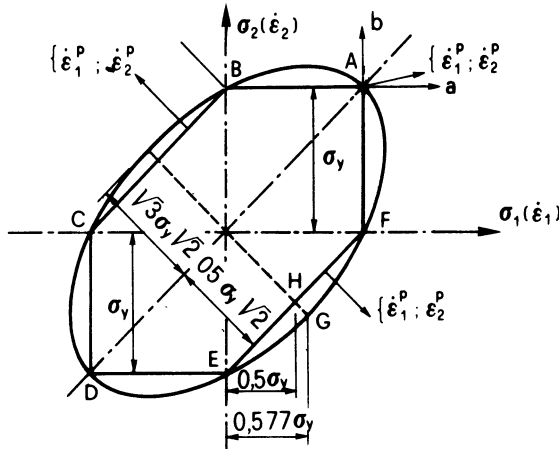


Fig. 2.5.

#### 1.2.4. Criterion of the maximum octaedral shear stress of of the maximum distortion energy. (MAXWELL – HUBER – HENCHY – VON MISES).

The hexagonal prism representing TRESCA's criterion fig. 2.4.) is a discontinuous surface possessing six distinct analytical expressions. This discontinuity yields evident mathematical difficulties in the application of the criterion.

To avoid them, VON MISES proposed in 1913 [M1] to modify slightly this prism and to replace it by the circum-scribed right cylinder (fig. 2.4.) of equation

$$(\sigma_1 - \sigma_2)^2 + (\sigma_2 - \sigma_3)^2 + (\sigma_3 - \sigma_1)^2 = 2 \sigma_y^2 \quad (2.11.)$$

The equivalent stress is obtained by writing (2.11.)

$$\bar{\sigma} = \frac{1}{\sqrt{2}} \sqrt{(\sigma_1 - \sigma_2)^2 + (\sigma_2 - \sigma_3)^2 + (\sigma_3 - \sigma_1)^2} = \sigma_y \quad (2.12.)$$

The yield locus in the  $\pi$  plane is the circumference circumscribed to TRESCA's hexagone (fig. 2.5.). It will be easily verified that the equation of this cylinder may also be written, taking (2.6.) into account

$$I'_2 \equiv \frac{1}{2} s_{ij} s_{ij} = \frac{\sigma_y^2}{3} , \quad (2.13.)$$

or

$$(2.14.) \quad \bar{\sigma} = \sqrt{\frac{3}{2}} (s_{ij} s_{ij})^{1/2},$$

which proves that is the simplest of the forms

$$(2.5.) \quad f(I'_2, I'_3) = 0.$$

With the aid of formulae (2.3.), one verifies directly that

$$(2.15.) \quad \bar{\sigma} = \sqrt{I_1^2 - 3I_2}$$

If the stress tensor is given in non principal orthogonal axes  $x, y, z$ ,  $\bar{\sigma}$  may be obtained by replacing in (2.15) the invariants  $I_1$  and  $I_2$  by their values in these axes, which gives

$$(2.16.) \quad \begin{aligned} \bar{\sigma} &= \left( \frac{3}{2} \sigma_{ij} \sigma_{ij} - \frac{1}{2} \sigma_{ij} \sigma_{ij} \right)^{1/2} \\ &= \sqrt{(\sigma_x + \sigma_y + \sigma_z)^2 - 3(\sigma_x \sigma_y + \sigma_y \sigma_z + \sigma_z \sigma_x - \tau_{xz}^2 - \tau_{yz}^2 - \tau_{xy}^2)} \end{aligned}$$

In 1924, H. HENCKY showed that the yield condition (2.11.) had a determined physical significance : it means that yielding occurs when the elastic distortion strain energy stored in the unit volume of the body reaches the characteristic value  $(1 + \nu)\sigma_y^2/3 E$ .

In 1926, ROŚ and EICHINGER remarked that the equivalent stress was proportional to the shear stress acting on a face of the octahedron inscribed in the cube built on the three principal directions. In fact, detailed calculation shows that

$$(2.17.) \quad \tau_{0C} = \frac{1}{3} \sqrt{(\sigma_1 - \sigma_2)^2 + (\sigma_2 - \sigma_3)^2 + (\sigma_3 - \sigma_1)^2} = \frac{\sqrt{2}}{3} \bar{\sigma}.$$

This shows that VON MISES criterion may also read as follows :

The first permanent deformations occur when the octahedral shear stress reaches

the definite value  $\frac{\sqrt{2}}{3} \sigma_y$ .

In most engineering structures, the stress state may be considered as plane, that is, one of the principal stresses (say  $\sigma_3$ ), is zero, and the stress vectors on any plane

element at the point considered of the material, are parallel to the  $(\sigma_1, \sigma_2)$  plane.

In that particular case, the plastic behavior is represented by the section of the three dimensional yield loci of fig. 2.4. by the plane  $\sigma_3 = 0$ . The result is figure 2.5. The hexagon ABCDEF represents TRESCA's yield condition, which can be expressed by the equation

$$\max [|\sigma_1|, |\sigma_2|, |\sigma_1 - \sigma_2|] = \sigma_y \quad (2.18.)$$

and the circumscribed ellipse, of equation

$$\sigma_1^2 + \sigma_2^2 - \sigma_1 \sigma_2 = \sigma_y^2 , \quad (2.19.)$$

the VON MISES criterion(\*) .

The two criteria coincide for the stress states represented by points A, B, C, D, E, F, that is for uniaxial tension or compression or for equal biaxial tension or compression. The maximum discrepancy occurs for pure shear ( $\sigma_1 = -\sigma_2$ ) (points G and H of the figure), where VON MISES criterion predicts

$$\tau = \frac{\sigma_y}{\sqrt{3}} = 0.577 \sigma_y , \quad (2.21.)$$

while TRESCA's criterion predicts

$$\tau = \frac{\sigma_y}{2} = 0.5 \sigma_y .$$

The maximum percentage difference is 15.4 % and can be reduced to the half (7.7 %) by adjusting the value of the yield stress. Often, it is much less than that values, which shows that the choice between the two criteria is mostly a matter of convenience.

As we shall see in section 4.5., the advantage of TRESCA's criterion is to

(\*) In orthogonal non principal coordinates, the equation of this ellipse [obtained by putting  $\sigma_z = \tau_{xy} = \tau_{yz} = 0$  in (2.16.)] is

$$\sigma_x^2 + \sigma_y^2 - \sigma_x \sigma_y + 3 \tau_{xy}^2 = \sigma_y^2 \quad (2.20.)$$

be linear. But it is discontinuous at the vertices. On the other hand, VON MISES criterion is continuous, but it is non linear, which complicates enormously the mathematical developments.

The meaning of the normality law may be seen on fig. 2.5., if  $\dot{\epsilon}_1$  and  $\dot{\epsilon}_2$  axes are superposed to the  $\sigma_1$  and  $\sigma_2$  axes. The vector plastic strain rate  $\dot{\epsilon}_j^p$ , with components  $\dot{\epsilon}_1^p$ ,  $\dot{\epsilon}_2^p$ , is normal to the hexagon, or the ellipse. At a vertex like A or B, it is contained within the “cone” of normals hatched.

### 1.3. Fundamental Laws of Plasticity – Perfectly Plastic Solids.

#### 1.3.1. Perfectly plastic solid.

A solid will be called perfectly plastic if it can undergo unlimited plastic deformations under constant stress when it is subjected to a homogeneous state of stress with  $\bar{\sigma} = \sigma_y$ .

The value  $\sigma_y$  is well defined for each material in a given environment (see section 1.1.), and is the limiting value that  $\bar{\sigma}$  cannot exceed. States of stress with  $\bar{\sigma} > \sigma_y$  are called impossible.

In the following, we shall frequently be interested in purely plastic strains  $\epsilon_{ij}$  and strain rates and we shall disregard the corresponding elastic elements (except when the contrary is explicitly stated). This mathematical model is called the rigid-plastic model.

When dealing with incipient plastic flow, we assume that the strains remain very small. Hence, strains  $\epsilon_{ij}$  and displacements  $u_i$  are related through the classical equations of Mechanics of Continua

$$(3.1.) \quad \epsilon_{ij} = \frac{1}{2} (\partial_i u_j + \partial_j u_i),$$

whereas the strain rates are given by the expression

$$(3.2.) \quad \dot{\epsilon}_{ij} \equiv \frac{\partial \epsilon_{ij}}{\partial t} = \frac{\partial}{\partial t} \left[ \frac{1}{2} (\partial_i u_j + \partial_j u_i) \right] = \frac{1}{2} (\partial_i v_j + \partial_j v_i)$$

where  $v_i = \frac{\partial u_i}{\partial t}$ .

### 1.3.2 Power of dissipation.

During incipient plastic flow at a given particle, where the state of stress is described by  $\sigma_{ij}$  and the state of strain rate by  $\dot{\epsilon}_{ij}$ , the power of the stresses per unit volume of material is

$$d = \sigma_{ij} \dot{\epsilon}_{ij} . \quad (3.3.)$$

For purely plastic strains, this power is dissipated into heat during plastic flow. Therefore, it is called “power of dissipation”. It is essentially positive.

### 1.3.3. Geometrical representation.

In a six-dimensional euclidean space, consider a rectangular cartesian coordinate system with the origin 0. The six-dimensional vectors  $\underline{\sigma}$  and  $\underline{\dot{\epsilon}}$  that have the components  $\sigma_{11}, \sigma_{22}, \sigma_{33}, \sigma_{12}, \sigma_{13}, \sigma_{23}$  and  $\dot{\epsilon}_{11}, \dot{\epsilon}_{22}, \dot{\epsilon}_{33}, 2\dot{\epsilon}_{12}, 2\dot{\epsilon}_{23}$  respectively, with respect to this coordinate system, will be called the stress vector and the strain rate vector, and the point P with the radius vector  $OP = \underline{\sigma}$  will be called the stress point. Equation (3.3.) indicates an important property of this geometrical representation : the specific power of the stress on the strain rate is given by the scalar product of the vectors  $\underline{\sigma}$  and  $\underline{\dot{\epsilon}}$

$$d = \underline{\sigma} \cdot \underline{\dot{\epsilon}} . \quad (3.4.)$$

If elastic strain rates are neglected, so that  $\underline{\dot{\epsilon}}$  represents the plastic strain rate, this scalar product is the specific rate of dissipation, which will be denoted by D.

The surface with the equation

$$\bar{\sigma}(\sigma_{ij}) - \sigma_y = 0 \quad (3.5.)$$

is called the yield surface, because states of stress at the yield limit are represented by stress points P on this surface. For the perfectly plastic materials considered here, the reference stress depends only on the state of stress but not on the state of strain, because these materials do not exhibit strain hardening. The yield surface is therefore a fixed surface in our six-dimensional space. The yield surface divides this space into two regions : the region  $\bar{\sigma} < \sigma_y$ , which consists of stress points representing attainable states of stress, and the region  $\bar{\sigma} > \sigma_y$ , which corresponds to stress states that cannot be attained in the considered perfectly plastic material. For convenient reference, interior points of the attainable region will be described as lying inside the yield surface, while stress points representing unattainable stress states will be described as being outside the yield surface. The origin of coordinates,

which represents the stress-free state, must lie inside the yield surface, because the material will not yield in the absence of stress.

### 1.3.4. Fundamental assumptions on the power of dissipation

As far as plastic deformations are concerned, we consider that a given material is characterized by its constitutive equations relating the stress tensor  $\sigma_{ij}$  to the tensor  $\dot{\epsilon}_{ij}$  of the plastic strain rates. Substitution of these expressions into relation (3.4.) makes the specific power of dissipation  $D$  a function of the strain rate components only.

We further assume that :

1. This specific power of dissipation is a single-valued function of the strain rate components ;
2. This dissipation function  $D(\dot{\epsilon}_{ij})$  is homogeneous of the order one.

According to this last assumption, multiplying every strain rate component by a positive scalar  $\lambda$  means multiplying the power of dissipation by  $\lambda$  :

$$D(\lambda \dot{\epsilon}_{ij}) = \lambda D(\dot{\epsilon}_{ij}), \quad \lambda > 0.$$

Using the geometrical representation introduced in Section 1.3.3., we rewrite the preceding relation in the form

$$(3.6.) \quad D(\lambda \underline{\dot{\epsilon}}) = \lambda D(\underline{\dot{\epsilon}}), \quad \lambda > 0.$$

This second assumption expresses the inviscid nature of the considered perfectly plastic material.

If the strain rates at a particle are specified to within a common positive factor, they are said to determine a local flow mechanism at this particle.

The strain rate vectors  $\underline{\dot{\epsilon}}$  and  $\lambda \underline{\dot{\epsilon}}$  in equation (3.6.), when  $\lambda$  is positive, thus determine the same local flow mechanism, and this mechanism is completely defined by the unit vector  $\underline{\dot{\epsilon}}$  along  $\underline{\dot{\epsilon}}$ ,

Let now a local flow mechanism  $\underline{\dot{\epsilon}}$  be given. According to assumption 1

above, this flow mechanism determines a unique specific rate of dissipation  $D(\dot{\epsilon})$ . It follows from equation (3.4.) that a state of stress  $\underline{\sigma}$  for which

$$\underline{\sigma} \cdot \dot{\epsilon} < D(\dot{\epsilon}) \quad (3.7.)$$

cannot produce the mechanism  $\dot{\epsilon}$ .

Now, the stress points with radius vectors  $\underline{\sigma}$  satisfying the relation (3.7.) are interior points of the half-space that contains the origin 0 and is bounded by a plane normal to  $\dot{\epsilon}$  at the distance  $D(\dot{\epsilon})$  from 0. As we let the vector  $\dot{\epsilon}$  of the flow mechanism rotate about the origin, the interior points that all corresponding half spaces have in common are the points inside the yield surface and the bounding planes of the half-spaces envelop the yield surface (Fig. 3.1.).

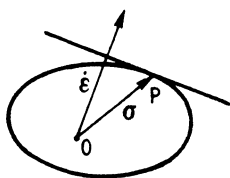


Fig. 3.1.

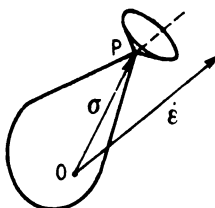


Fig. 3.2.

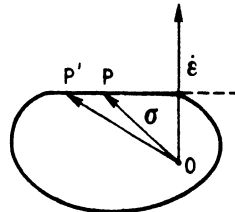


Fig. 3.3.

As the boundary of the domain common to all half-spaces, the yield surface is convex. It may :

1. be strictly convex, that is, it may have a continuously turning normal (as does the VON MISES surface); in this case, there is one-to-one-correspondence between the stress point and the flow mechanism (fig. 3.1.);
2. exhibit vertices as in fig. 3.2.; at a vertex P, all outward pointing vectors that lie on or within the cone of normals define possible flow mechanisms; the vector  $\dot{\epsilon}$  of a flow mechanism still determines the stress point P, but the converse is no longer true;
3. exhibit flat parts as in fig. 3.3. (as does the TRESCA yield surface); the stress point then determines the flow mechanism, but the converse is not true when  $\dot{\epsilon}$  is normal to a flat of the yield surface.

Despite the possible lack of one-to-one correspondence between the stress vector  $\underline{\sigma}$  and the vector  $\dot{\underline{\epsilon}}$  of the flow mechanism, it is readily verified that, for all kinds of yield surfaces, the specific dissipation  $D = \underline{\sigma} \cdot \dot{\underline{\epsilon}}$  is single valued function of the strain rate vector  $\dot{\underline{\epsilon}}$ .

The main result from preceding discussion is that the vector  $\dot{\underline{\epsilon}}$  is normal to the plane drawn tangentially to the yield surface at the stress point P. In other words, it is parallel to the normal to the yield surface at P. It is known from analytical geometry that the normality of a vector  $\dot{\underline{\epsilon}}$  to a surface with equation  $\bar{\sigma}(\sigma_{ij}) = \sigma_y$  is expressed by the relations

$$(3.8.) \quad \dot{\epsilon}_{ij}^P = \mu \frac{\partial \bar{\sigma}}{\partial \sigma_{ij}} \quad (\mu \geq 0)$$

where  $\mu$  is a positive scalar factor.

Therefore, the function  $\bar{\sigma}(\sigma_{ij})$  plays for the strain rates  $\dot{\epsilon}_{ij}$  the role of a potential, and the **normality law** first cited, with its generalizations to vertices and flats, is also called the **law of plastic potential**. It is widely accepted, though introduced in various manners in the literature.

In the following, we call **flow mechanism of a body** (or structure) a field of plastic strain rate vectors  $\dot{\underline{\epsilon}}$  whose magnitudes are defined to within a common positive scalar factor, whereas a vector  $\dot{\underline{\epsilon}}$  (or  $\underline{\epsilon}$ ) is called a **local flow mechanism**. Note that a given stress field may be related by the normality law to several fields of strain rate vectors  $\dot{\underline{\epsilon}}$ . These fields have in common the field of unit vectors  $\dot{\underline{\epsilon}}$ .

When the solid is isotropic, at least as far as its yield condition is concerned, the normality law, expressed in the  $\underline{\sigma}$  and  $\dot{\underline{\epsilon}}$  spaces, ensures that principal directions of the stress tensor and of the strain rate tensor coincide. Hence, when principal directions of these two tensors are known, or otherwise determinable, spaces of principal stresses and strain rates may as well be used. As a rule, all spaces in which the dissipation is unambiguously determined may be used. All properties obtained above remain valid.

### 1.3.5. Illustrating examples.

Let us first express the power of dissipation for the VON MISES yield condition. We use the principal stresses and strain rates as components of the vectors  $\underline{\sigma}$  and  $\dot{\underline{\epsilon}}$  (fig. 3.4.). The yield surface is the circular cylinder with the equation (2.11.). Let P be a generic stress point on the surface and C the foot of the perpendicular from P on the axis of the cylinder. The line CP is normal to the cylinder at P. According to relation (3.4.), the power of dissipation corresponding to the stress vector  $\underline{\sigma} = \underline{OP}$  will be given by the modulus  $|\dot{\underline{\epsilon}}|$  of the strain rate vector  $\dot{\underline{\epsilon}} = \underline{OQ}$  (parallel to line CP), multiplied by the projection of  $\underline{OP}$  on the direction of line OQ. This projection has the length of CP, that is the magnitude  $\sqrt{2/3} \sigma_y$  of the radius of the cylinder. Hence,

$$D = \sqrt{2/3} \sigma_y |\dot{\underline{\epsilon}}| = \sqrt{2/3} \sigma_y \sqrt{\dot{\epsilon}_1^2 + \dot{\epsilon}_2^2 + \dot{\epsilon}_3^2} \quad (3.9.)$$

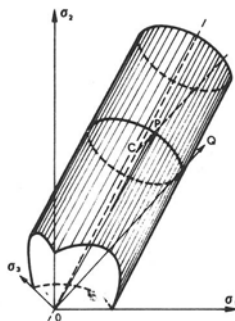


Fig. 3.4.

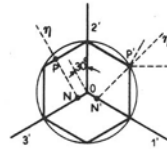


Fig. 3.5.

Consider next TRESCA's yield condition. When the three principal stresses are taken as rectangular cartesian coordinates in stress space, this yield condition is represented by a hexagonal prism (fig. 2.4.). Fig. 3.5. shows the normal cross section through a point P of this prism that does not lie on an edge. The normal to the prismatic surface at P is the perpendicular in the cross-sectional plane to the corresponding side of the regular hexagon. The projection of  $\underline{\sigma} = \underline{OP}$  on  $\eta$  is the segment NP. Its magnitude is that of the distance from 0 to any side of the hexagon, namely  $\sigma_y/\sqrt{2}$ . Consequently, we have

$$D = \underline{\sigma} \cdot \dot{\underline{\epsilon}} = \frac{\sigma_y}{\sqrt{2}} |\dot{\underline{\epsilon}}| \quad (3.10.)$$

When the stress point lies on an edge of the yield prism (e.g. P' in fig. 3.5.) and when the direction of the strain rate vector is intermediate between those of the normals to the adjacent planes (as  $\eta'$  on fig. 3.5.), relation (3.10) is no longer valid. A strain rate vector with direction  $\eta'$  can be considered as resulting from the linear combination of strain rate vectors corresponding to adjacent planes. Hence, we have the general expression

$$(3.11.) \quad \dot{\epsilon} = \alpha \dot{e}_a + \beta \dot{e}_b ,$$

where  $\dot{e}_a$  and  $\dot{e}_b$  are the unit strain rate vectors for the two adjacent planes, and  $\alpha$  and  $\beta$  are arbitrary nonnegative scalar factors. From equations (3.4.), (3.10.) and (3.11.), we obtain

$$(3.12.) \quad D = \frac{\sigma_y}{\sqrt{2}} (\alpha + \beta) .$$

Clearly, from relation (3.12.) it is seen that the dissipation depends on the orientation of  $\dot{\epsilon}$ , except for vanishing  $\alpha$  or  $\beta$  (when relation (3.10.) is valid).

The preceding results can be more directly obtained when remembering that, as shown in section 1.3.4., the dissipation for a unit vector  $\dot{\epsilon}$  is measured by the distance from the origin to the tangent plane to the yield surface at the stress point P. This distance is  $\sigma_y \sqrt{2/3}$  for VON MISES condition. It is  $\sigma_y / \sqrt{2}$  for TRESCA's, except at points on the edges where it varies with the inclination of the tangent plane.

We shall finally show that the basic assumptions made in section 1.3.4. on the power of dissipation imply, for the yield conditions of both VON MISES and TRESCA, that plastic flow occurs with no volume change, a law verified experimentally. To this purpose we have to prove formula

$$(3.13.) \quad \dot{\epsilon}_1 + \dot{\epsilon}_2 + \dot{\epsilon}_3 = 0 .$$

As we have seen, the yield condition of VON MISES is represented by a cylinder in the space of principal stresses, whereas TRESCA's yield condition is represented by an hexagonal prism. But, in both cases, the generatrices are normal to the plane with equation

$$(3.14.) \quad \sigma_1 + \sigma_2 + \sigma_3 = 0 .$$

Hence, any strain rate vector must be parallel to this plane and by analytical geometry, its components must satisfy eq. (3.13.).

## 1.4. Hardening Laws.

### 1.4.1. Introduction

We call hardening rule a law which describes explicitly the shape of the successive yield surfaces  $\bar{\sigma} = \bar{\sigma}(\sigma_1, \sigma_2, \sigma_3)$  when plastic deformations increase.

The two practically usable laws are :

- a) The law of isotropic hardening (HILL 1950 [H1]), which postulates essentially that the current yield surface is obtained by a uniform expansion of the initial yield surface in all directions. This law is in direct contradiction with the BAUSCHINGER effect (see section 1.1.) and conserves isotropy (which justifies its name);
- b) The law of linear kinematical hardening (PRAGER 1954 [P1]), which supposes essentially that the yield surface keeps the same shape as the initial yield surface, but that it moves by translation in the stress space. This law introduces partially the BAUSCHINGER effect, as well as the anisotropy produced by the plastic deformations. In spite of the critics that might be directed to it, we shall adopt here the first law (of isotropic hardening), because the BAUSCHINGER effect plays especially a role in load cycles and no load cycles occur in the main problems that we wish to solve, namely the search of "limit loads".

### 1.4.2. Summary of the isotropic hardening postulates

The assumptions of isotropic hardening are as follows :

- a) isotropic is preserved ;
- b) whatever be the path followed in the strain space to reach a stress state, the final yield surface is the same.

As a consequence of these assumptions, the current yield locus has the same shape as the initial yield locus and only the value of the yield stress  $\sigma_y$

contained in the equation ((2.10.) or (2.11.)) of the yield locus becomes function  $\bar{\sigma}$  of a certain measure of the hardening (parameter  $k$ ). The experimental determination of this function is independent of the stress state, that is it may be obtained by a pure tension test, for instance.

For the experimental proofs of these assumptions, see [M9].

These assumptions lead, geometrically, to an expansion of the initial yield surface and are represented mathematically, by the following formulation

$$(4.1.) \quad F(\sigma_{ij}, k) = f(\sigma_{ij}) - \sigma_y(k) = 0,$$

where  $f(\sigma_{ij}) \equiv \bar{\sigma}(\sigma_{ij})$  is the equivalent stress,  $\sigma_y(k)$  is the current yield stress in simple tension. The fundamental effect of the plastic strain rate  $\dot{\epsilon}_{ij}^p$  on the loading function  $F$ , which seems to have disappeared, is in fact maintained through the effect of  $k$ , which depends on the history of the plastic deformations.

To measure the hardening and obtain the explicit form of  $\bar{\sigma}(k)$ , three assumptions have been made in the literature.

**a) Assumption of the work hardening.**

The parameter  $k$  is identified with the plastic work dissipated :

$$(4.2.) \quad dK \equiv dW^P = \sigma_{ij}^P d\epsilon_{ij}^P \quad \text{with} \quad W^P = \int_0^P \epsilon_{ij}^P \sigma_{ij}^P d\epsilon_{ij}^P \quad (\geq 0)$$

and one sets

$$(4.3.) \quad \bar{\sigma}(k) \equiv f_1(W_P).$$

**b) Assumption of the stress hardening.**

It is postulated that, in the general flow rule

$$(4.4.) \quad d\epsilon_{ij}^P = d\mu \frac{\partial \bar{\sigma}}{\partial \sigma_{ij}}$$

equivalent to the normality law (3.8.), the scalar differential  $d\mu > 0$  is linearly related to the increments of stress by some functions of  $\bar{\sigma}$ , i.e. :

$$(4.5.) \quad d\mu = f_2(\bar{\sigma}) d\bar{\sigma}$$

## c) Assumption of the strain hardening.

The parameter  $k$  is identified with the sum of effective plastic strain increments sustained by the material particle under consideration :

$$dk = d\bar{\epsilon}^P \quad \text{with} \quad \bar{\epsilon}^P = \int_0^P \epsilon_{ij}^P d\bar{\epsilon} \quad (4.6.)$$

and one sets

$$\bar{\sigma}(k) = f_3(\bar{\epsilon}^P). \quad (4.7.)$$

The differential  $d\bar{\epsilon}^P$  (following the particle, and to be discussed below), is a nonnegative invariant in terms of the plastic strain increments.

The functions  $f_1$ ,  $f_2$  and  $f_3$  entering into the three assumptions are to be determined in such a way that the assumed behavior specializes to some known reference state. Usually, this state is the uniaxial state of stress provided by the classical tension test, in which case

$$\sigma = h(\epsilon^P) \quad (4.8.)$$

or

$$\frac{d\sigma}{d\epsilon^P} = h'(\epsilon^P) = g(\sigma) \quad (4.9.)$$

where  $\epsilon^P = \int d\epsilon^P$  is the total plastic strain along the axis of the specimen,  
 $\sigma$  is the tensile stress and  
 $g$  the plastic tangent modulus.

## 1.4.3. Definitions of equivalent stress and strain.

The current yield surface of the isotropically hardening solid has for equation

$$\bar{\sigma}(\sigma_{ij}) = \sigma_y \quad (4.10.)$$

where  $\bar{\sigma}$  is the equivalent stress and  $\sigma_y$  the current value of the tensile yield stress.

By definition, the equivalent stress  $\bar{\sigma}$  is a normalized invariant of the stress tensor  $\sigma_{ij}$  such that

$$\bar{\sigma} = \sigma \text{ if } \sigma_{11} = \sigma \quad \text{and} \quad \text{if } \sigma_{ij} = 0 \text{ for } i + j > 2 \quad (4.11.)$$

This implies that  $\bar{\sigma}$  is an homogeneous function of the order 1 in  $\sigma_{ij}$

To arrive at a physical interpretation of the scalar  $d\mu$  in formula (4.4.), one may substitute (4.4.) in the expression (4.2.) for the increment of plastic work, to obtain

$$(4.12.) \quad dW^P = \sigma_{ij} \frac{\partial \bar{\sigma}}{\partial \sigma_{ij}} d\lambda = \bar{\sigma} d\mu = \sigma_y d\mu,$$

because

$$\sigma_{ij} \frac{\partial \bar{\sigma}}{\partial \sigma_{ij}} = \bar{\sigma}$$

by EULER's theorem about homogeneous functions.

Formula (4.12.) shows that  $d\mu$  plays the role of a generalized plastic strain increment  $d\bar{\epsilon}^P$  associated to the generalized stress  $\bar{\sigma}$ . It seems natural that, by definition,  $d\mu$  should be identified as the increment of effective strain. Thus, we set

$$(4.13.) \quad d\mu = d\bar{\epsilon}^P, \quad dW^P = \bar{\sigma} d\bar{\epsilon}^P$$

so that equation (4.4.) transforms into

$$(4.14.) \quad d\epsilon_{ij}^P = d\bar{\epsilon}^P \frac{\partial \bar{\sigma}}{\partial \sigma_{ij}}.$$

A general expression for  $d\bar{\epsilon}^P$  follows from (4.14.), as the invariant

$$(4.15.) \quad d\bar{\epsilon}^P = [d\epsilon_{ij}^P d\epsilon_{ij}^P / (\frac{\partial \bar{\sigma}}{\partial \sigma_{K1}} \frac{\partial \bar{\sigma}}{\partial \sigma_{K1}})]^{1/2}.$$

This general definition includes the two following special cases for the TRESCA and VON MISES materials :

### TRESCA Material.

Using the principal direction (1, 2, 3) of stress as the (arbitrary) basis for calculating  $d\bar{\epsilon}$ , one has by (2.4.)

$$(4.16) \quad \bar{\sigma} = \sigma_1 - \sigma_3, \text{ assuming } \sigma_1 \geq \sigma_2 \geq \sigma_3$$

and thus,

$$\frac{\partial \bar{\sigma}}{\partial \sigma_{K1}} \quad \frac{\partial \bar{\sigma}}{\partial \sigma_{K1}} = 2 ,$$

whereby

$$d\bar{\epsilon}^P = \left( \frac{1}{2} d\epsilon_{ij}^P d\epsilon_{ij}^P \right)^{1/2} . \quad (4.17.)$$

If principal strain increments are introduced, with  $d\epsilon_3^P = -d\epsilon_1^P$  and  $d\epsilon_2^P = 0$ , (4.17.) provides simply

$$d\bar{\epsilon}^P = d\epsilon_1^P \quad (4.18.)$$

### VON MISES Material.

Introducing the expression (2.16.) of the equivalent stress

$$\bar{\sigma} = \left( \frac{3}{2} \sigma_{ij} \sigma_{ij} - \frac{1}{2} \sigma_{ii} \sigma_{jj} \right)^{1/2}$$

in (4.15.), one finds

$$\frac{\partial \bar{\sigma}}{\partial \sigma_{K1}} \quad \frac{\partial \bar{\sigma}}{\partial \sigma_{K1}} = 3/2 ,$$

whereby

$$d\bar{\epsilon}^P = \left( \frac{2}{3} d\epsilon_{ij}^P d\epsilon_{ij}^P \right)^{1/2} . \quad (4.19.)$$

#### 1.4.4. Equivalence of the three isotropic hardening assumptions.

The flow rule is derived below principally from the assumption (2) of “stress hardening”. In the process, the equivalence of the three approaches will be demonstrated.

With the representation (4.14.), one includes the assumption (4.5.) in the flow rule by stating

$$d\bar{\epsilon} = f_2(\bar{\sigma}) d\bar{\sigma} . \quad (4.20.)$$

This immediately shows that there exists a unique relation between  $\bar{\sigma}$  and  $\bar{\epsilon}$ , and thus proves the equivalence of assumptions b) and c). (4.20.) combined with (4.2.) and (4.13.) further leads to

$$(4.21.) \quad dW^P = \sigma_{ij} d\epsilon_{ij}^P = \bar{\sigma} f_2(\bar{\sigma}) d\bar{\sigma} ,$$

which shows that assumption b) [ or c)] implies “work-hardening”, in the sense that  $\bar{\sigma}$  is uniquely related to  $\int dW_P$ . Conversely, assumption a) with the use of (4.13.), i.e.

$$(4.22.) \quad \bar{\sigma} = f_1 (\int \bar{\sigma} d\bar{\epsilon}^P)$$

implies (4.20.), that is “stress (or strain) hardening”. This concludes the proof of general equivalence [ H3] .

Proceeding from (4.14.) and (4.20), one finds in uniaxial tension, in view of the property (4.11. bis)

$$(4.23.) \quad d\bar{\epsilon}^P = f_2(\sigma) d\sigma ,$$

which may be compared with (4.9.) to give

$$(4.24.) \quad f_2 = \frac{1}{g} .$$

Through (4.14.), (4.20.) and (4.24.), the flow rule (valid for  $d\bar{\sigma} > 0$ ,  $\bar{\sigma}$  not exceeded by any past value), is complete. Thus

$$(4.25.) \quad d\epsilon_{ij}^P = \boxed{\frac{d\bar{\sigma}}{g(\bar{\sigma})} \frac{\partial \bar{\sigma}}{\partial \sigma_{ij}}} .$$

In an actual tension test (fig. 4.1.) elastic and plastic deformations occur simultaneously.  $d\bar{\epsilon}^P$  reduces to  $d\epsilon_{11}^P$ . The figure shows that one has

$$d\bar{\sigma} = E_t d\bar{\epsilon} ,$$

where  $E_t$  is the tangent modulus of deformation. But

$$d\bar{\epsilon} = d\bar{\epsilon}^e + d\bar{\epsilon}^p ,$$

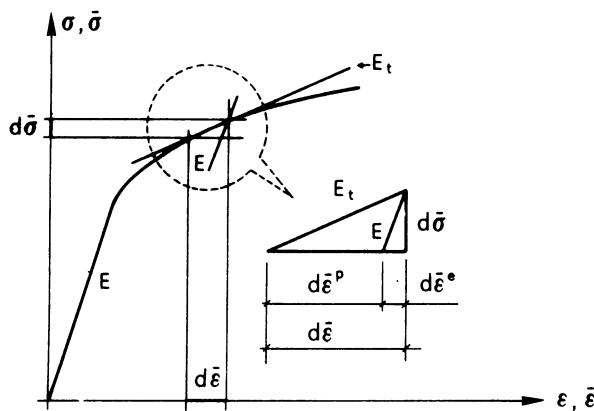


Fig. 4.1.

so that

$$d\bar{\sigma} = E_t (d\bar{\epsilon}^e + d\bar{\epsilon}^p) = E_t \left( \frac{d\bar{\sigma}}{E} + d\bar{\epsilon}^p \right)$$

whence

$$\frac{d\bar{\sigma}}{d\bar{\epsilon}^p} = \frac{1}{E_t} - \frac{1}{E} = \frac{1}{E'} = \frac{1}{g(\bar{\sigma})} \quad (4.26.)$$

where  $E' \equiv g$  is the plastic tangent modulus.

With VON MISES criterion (2.14.), one has the relation

$$\frac{\partial \bar{\sigma}}{\partial \sigma_{ij}} = \frac{3}{2} \frac{s_{ij}}{\bar{\sigma}} \quad (4.27.)$$

which, introduced in (4.27.), gives

$$d\epsilon_{ij}^p = \frac{3}{2} \frac{d\bar{\sigma}}{\bar{\sigma} E}, s_{ij} . \quad (4.28.)$$

### 1.5. Prandtl - Reuss Equations.

If the elastic strains are not negligible in comparison to the plastic strains, the total strain increment at a point of the body is given by the relation

$$d\epsilon_{ij} = d\epsilon_{ij}^e + d\epsilon_{ij}^p . \quad (5.1.)$$

The elastic part of the increment is governed by HOOKE's law, which, for an isotropic material, reads

$$(5.2.) \quad \epsilon_{ij}^e = \frac{1}{2G} [\sigma_{ij} - \frac{\nu}{1+\nu} \delta_{ij} \sigma_{kk}]$$

or, in inverted form,

$$(5.3.) \quad \sigma_{ij} = 2G [\epsilon_{ij}^e + \frac{\nu}{1-2\nu} \epsilon_{kk}^e \delta_{ij}] .$$

To condense further developments, we shall write these two relations as follows

$$(5.4.) \quad \epsilon_{ij}^e = A_{ijkl} \sigma_{kl} ,$$

$$(5.5) \quad \sigma_{ij} = D_{ijkl} \epsilon_{kl}^e ,$$

where the fourth order tensors A and D have well known symmetry properties, e.g. :

$$(5.6.) \quad D_{klmn} = D_{mnlk} \dots \text{etc.}$$

Differentiating (5.2.), we have

$$(5.7.) \quad d\epsilon_{ij}^e = \frac{1}{2G} [d\sigma_{ij} - \frac{\nu}{1+\nu} \delta_{ij} d\sigma_{kk}] .$$

Adding these elastic increments to the plastic increments given by (4.28.), we obtain the PRANDTL-REUSS equations in their general form :

$$(5.8.) \quad d\epsilon_{ij} = \frac{1}{2G} (d\sigma_{ij} - \frac{\nu}{1+\nu} \delta_{ij} d\sigma_{KK}) + \frac{3}{2} \frac{d\bar{\sigma}}{\bar{\sigma}E'} s_{ij} .$$

For the future computer solutions of plasticity problems (Section 7.3.) we need an inverted expression of PRANDTL-REUSS formulae. This will be obtained as follows. From expression (2.14.) of  $\bar{\sigma}$ , we have first :

$$(a) \quad s_{kl} ds_{kl} = \frac{1}{2} d(s_{kl} s_{kl}) = \frac{1}{2} d(\frac{2}{3} \bar{\sigma}^2) = \frac{2}{3} \bar{\sigma} d\bar{\sigma} .$$

Therefore (4.27.) may be written

$$(b) \quad d\epsilon_{ij}^P = \frac{3}{2} \frac{1}{\bar{\sigma}E'} s_{ij} s_{kl} ds_{kl} \frac{3}{2\bar{\sigma}} = \frac{9}{4\bar{\sigma}^2 E'} s_{ij} s_{kl} ds_{kl} .$$

Now, by (5.3.bis) and (5.1.) :

$$s_{kl} ds_{kl} = s_{kl} d\sigma_{kl} = s_{kl} D_{klmn} d\epsilon_{mn}^e = s_{kl} \cdot D_{klmn} (d\epsilon_{mn} - d\epsilon_{mn}^p).$$

From (5.6.) and the definition (5.3.) of  $D_{ijkl}$ , we have

$$s_{kl} D_{klmn} = s_{kl} D_{mnkl} = 2G s_{mn} \quad (c)$$

whence, by (b) and (2.14.),

$$\begin{aligned} s_{kl} ds_{kl} &= 2Gs_{mn} d\epsilon_{mn} - 2Gs_{mn} d\epsilon_{mn}^p \\ &= 2Gs_{mn} d\epsilon_{mn} - 2Gs_{mn} \left( \frac{9}{4\bar{\sigma}^2 E} s_{mn} \cdot s_{kl} ds_{kl} \right) \quad (d) \\ &= 2Gs_{mn} d\epsilon_{mn} - \frac{3G}{E'} s_{kl} ds_{kl}. \end{aligned}$$

Solving (c) for  $ds_{kl}$  gives

$$s_{kl} ds_{kl} \left( 1 + \frac{3G}{E'} \right) = 2Gs_{mn} d\epsilon_{mn}$$

and

$$s_{kl} ds_{kl} = \frac{2G E'}{3G + E'} s_{mn} d\epsilon_{mn} \quad (e)$$

Introducing (e) in (b) gives

$$d\epsilon_{ij}^p = \frac{9}{4\bar{\sigma}^2 E'} \frac{2G E'}{3G + E'} s_{ij} s_{mn} d\epsilon_{mn} = \frac{9G}{2\bar{\sigma}^2 (E' + 3G)} s_{ij} s_{mn} d\epsilon_{mn}. \quad (f)$$

Now, by (5.1.) and (5.5. bis), we have

$$d\sigma_{ij} = D_{ijkl} (d\epsilon_{kl} - d\epsilon_{kl}^p)$$

then, by (f)

$$d\sigma_{ij} = D_{ijkl} d\epsilon_{kl} - D_{ijkl} \frac{9G}{2\bar{\sigma}^2 (E' + 3G)} s_{kl} s_{mn} d\epsilon_{mn}$$

By (c)

$$d\sigma_{ij} = D_{ijkl} d\epsilon_{kl} - \frac{9G}{2\bar{\sigma}^2(E' + 3G)} 2Gs_{ij} d\epsilon_{kl}$$

and finally

$$(5.9.) \quad d\sigma_{ij} = [D_{ijkl} - \frac{9G^2}{\bar{\sigma}^2(E' + 3G)} s_{ij} s_{kl}] d\epsilon_{kl}$$

In engineering notation, PRANDTL–REUSS formulae for the VON MISES case, (5.9.) may be written

$$(5.10.) \quad \begin{aligned} d\epsilon_x &= \frac{1}{E} [d\sigma_x - \nu(d\sigma_y + d\sigma_z)] + \frac{d\bar{\sigma}}{\bar{\sigma}E'} [\sigma_x - \frac{1}{2}(\sigma_y + \sigma_z)] \dots (x, y, z) \\ d\gamma_{xy} &= \frac{d\tau_{xy}}{G} + 3 \frac{d\bar{\sigma}}{\bar{\sigma}E'} \tau_{xy} \dots (x, y, z). \end{aligned}$$

Changes in stress which move the stress point on or inside the current yield surface call for the elastic terms alone.

In general, it is not allowed to use integrated forms of the equations (5.7.), (5.9.) or (5.10.), because the plastic increments depend on the whole strain history.

However, the use of these integrated forms is licit when the loading of the body is radial, that is when, in all points of the body, the principal trihedron keeps a fixed position and the principal stresses increase proportionnally to each other. In that case, one obtains from (5.8.) with

$$(5.11.) \quad \frac{d\bar{\sigma}}{\bar{\sigma}E'} = \phi$$

$$(5.12.) \quad \epsilon_{ij} = \frac{1+\nu}{E} \sigma_{ij} - \frac{\nu}{E} \delta_{ij} \sigma_{kk} + \frac{3}{2} \phi s_{ij} .$$

In engineering notation, this formula becomes :

$$(5.13.) \quad \epsilon_x = \frac{1}{E} [\sigma_x - \nu(\sigma_y + \sigma_z)] + \phi [\sigma_x - \frac{1}{2}(\sigma_y + \sigma_z)] \dots (x, y, z)$$

$$\gamma_{xy} = \frac{\tau_{xy}}{G} + 3\phi\tau_{xy} \dots (x, y, z) \quad (5.13.)$$

These equations belong to the simplified version of the theory of plasticity, called **deformation theory**, which was founded by HENCKY and NADAJ [N1] and has been especially developed in USSR by ILYUSHIN [I1], SOKOLOWSKY [S1] and others.

The deformation theory being much simpler than the complete differential theory, it enables to solve many practical problems. BUDIANSKY has shown that the solutions so obtained are a satisfactory approximation provided that the loading is not too far from radial at all points of the body where the material yields.

### 1.6. Variation of the Global Coefficient of Lateral Contraction in the Course of a Tension Test.

Consider a specimen made of an hardening material subject to a tension test beyond the limit of proportionality.

The stress tensor in all point of the specimen is uniaxial and the principal trihedron has an invariable orientation (fig. 6.1.). We have therefore radial loading and we can use the PRANDTL-REUSS equations in their integrated form (5.13.). In the present case,  $\sigma_1 = \sigma$ ,  $\sigma_2 = \sigma_3 = 0$  and the equations (5.13.) reduce to

$$\epsilon_1 = \left( \frac{1}{E} + \phi \right) \sigma_1 ; \epsilon_2 = \epsilon_3 = - \left( \frac{\nu}{E} + \frac{\phi}{2} \right) \sigma_1 \quad (6.1.)$$

but fig. 6.2. shows that  $\sigma_1/\epsilon_1$  is the secant modulus  $E_{S_1}$  that is, the shape of the straight line joining the origin 0 to point A ( $\sigma, \epsilon$ ). One has then

$$\frac{\sigma_1}{\epsilon_1} = \frac{E}{1 + \phi E} = E_S \quad (6.2.)$$

On the other hand, the ratio  $(-\epsilon_2/\epsilon_1)$  represents a global elastoplastic POISSON's ratio, variable with the degree of yielding, and that we shall represent by the symbol  $\eta$ . (6.1.) gives, with account taken of (6.2.) :

$$\eta = -\frac{\epsilon_2}{\epsilon_1} = \frac{\nu + \frac{E\phi}{2}}{1 + E\phi} = \frac{\frac{1}{2} + \frac{E\phi}{2}}{1 + E\phi} - \frac{\frac{1}{2} - \nu}{1 + E\phi} = \frac{1}{2} - \frac{E_S}{2E} (1 - 2\nu) \quad (6.3.)$$

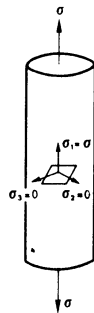


Fig. 6.1.

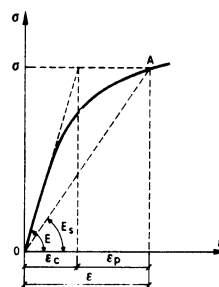


Fig. 6.2.

Using (6.1.) and (6.2.), we can write the integrated PRANDTL–REUSS equations (5.9.) in the form :

$$(6.4.) \quad \epsilon_1 = \frac{1}{E_S} |\sigma_1 - \eta(\sigma_2 + \sigma_3)|, \dots (1, 2, 3)$$

Formula (6.3.) shows that the global POISSON's ratio varies progressively, along a tension test, from the value  $\nu$  of the elastic domain to the purely plastic value  $1/2$ ; this formula is in good agreement with the highly accurate measurements executed by the National Bureau of Standards [S4] and represents in this way a verification a posteriori of the laws of plasticity of hardening materials.

### 1.7. Stress Measurements, at the Surface of a Plastically Deformed Body, with the Help of Strain Rosettes.

Suppose that we glue, on the free surface of a body, an electric resistance strain gage rosette with at least three independent circuits. It is easy, by using the formulae of plane strain or the MOHR circle of plane strain with coordinates  $\epsilon, \gamma/2$ , to obtain the principal strains  $\epsilon_1, \epsilon_2$ , and the angle  $\alpha$  made by the first principal direction with the horizontal. Now, the problem is to deduce, from these values  $\epsilon_1, \epsilon_2$ , the values of the principal stresses  $\sigma_1, \sigma_2$ , when the body has undergone elastoplastic deformations at the considered point of the surface.

The classical equations

$$(7.1.) \quad \sigma_1 = \frac{E}{1-\nu^2} (\epsilon_1 + \nu \epsilon_2) \quad \sigma_2 = \frac{E}{1-\nu^2} (\epsilon_2 + \nu \epsilon_1) ,$$

given by Theory of Elasticity, are no longer valid and the problem is to establish the equations which replace them.

If one admits that the loading at the considered point is radial, one may utilize the formulae (6.4.) of the Deformation Theory of elasto-plastic body. Putting  $\sigma_3 = 0$ , we find

$$\epsilon_1 = \frac{1}{E_S} (\sigma_1 - \eta\sigma_2), \quad \epsilon_2 = \frac{1}{E_S} (\sigma_2 - \eta\sigma_1) \quad (7.2.)$$

whence

$$\sigma_1 = \frac{E_S}{1-\eta^2} (\epsilon_1 + \eta\epsilon_2); \quad \sigma_2 = \frac{E_S}{1-\eta^2} (\epsilon_2 + \eta\epsilon_1)$$

with  $\eta = \frac{1}{2} - \frac{E_S}{2E} / (1 - 2\nu)$  (7.3.)

The value of  $E_S$  is the slope, measured on the stress-strain diagram of the material (fig. 7.1.) obtained in pure tension, of the straight line 0A joining the origin to the point whose ordinate is the equivalent stress

$$\bar{\sigma} = \sqrt{\sigma_1^2 + \sigma_2^2 - \sigma_1\sigma_2} \quad (7.4.)$$

If this diagram can be represented with sufficient accuracy by the law (1.1.) of RAMBERG–OSGOOD, the secant modulus may be computed by the formula

$$E_S = \frac{\bar{\sigma}}{\epsilon_c} = \frac{E}{1 + \frac{E}{B} \left(\frac{\bar{\sigma}}{B}\right)^{n-1}} \quad (7.5.)$$

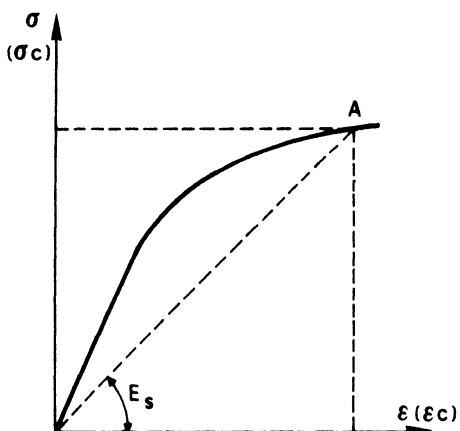


Fig. 7.1.

The equations (7.3.), (7.4.) must be solved simultaneously by iteration to determine the values of  $\sigma_1$  and  $\sigma_2$ . If many computations of this type must be effected, it is recommended to write a small computer program.

The stresses deduced from strain rosettes by the method developed here have been compared [A1], in the case of a tubular thin-walled specimen in aluminium alloy

subjected to axial tension and internal pressure, with the stresses calculated directly by the formulae

$$\sigma_1 = \frac{P}{A} \quad \sigma_2 = p \frac{r}{t} .$$

The agreement was found excellent.

It must be feared, however, to obtain a less good agreement in the case of steels with yield plateau, where yielding proceeds in a discontinuous way, as explained in section 1.1.

## 2. GENERAL THEOREMS OF LIMIT ANALYSIS – PROPORTIONAL LOADING

### 2.1. Introduction

Let a body or structure be subjected to a system of loads that are increased quasi-statically and in proportion, starting from zero. The term quasi-statically means that the loading process is sufficiently slow for all dynamic effects to be disregarded. The term “in proportion” signifies that the ratio of the intensities of any two loads remains constant during the loading process. Such a loading is also called “proportional loading” or “radial loading” in the literature. The points of application and the lines of action of the loads and the constant ratios of their intensities will be said to determine the type of loading.

In the general theory developed in present section, we shall use the models of Mechanics of Continua. In a certain reference state (which usually represents in practice the service conditions), the volume forces are  $F_i$  and the surface forces,  $T_i$ . A proportional loading is obtained when these forces become  $\lambda F_i$  and  $\lambda T_i$ , respectively, and when the multiplier  $\lambda$  increases slowly.

Suppose that we consider an engineering structure (for instance a mild steel beam or a rigid-jointed frame) and that we increase the load multiplier  $\lambda$  from the value 1 it has under service conditions.

At first, the behavior of the structure is purely elastic.

From a certain value  $\lambda_a > 1$ , yielding occurs, in certain parts of the structure. This behavior is called contained plastic flow, because the deformations of the structure are still controlled by the parts of it which remain elastic.

For a certain value  $\lambda_1$  of the multiplier, called the plastic collapse or limit value or limit load, the load  $\lambda$  hardly changes while the deflections increase to magnitudes several times larger than the maximum deflections in the elastic range. This behavior is caused by the development of plastic flow in the structure, to such an extent that the remaining elastic material does not contribute effectively to sustaining the load. It has been called uncontained plastic flow, to distinguish it from the contained flow

defined above.

The occurrence of the limit load may be accompanied by a real collapse of the structure ; this will be the case for most rigid frame or shell structures. In other cases, notably that of plates subjected to bending, the structure remains stable under the limit load, but its deformations become so large that it is no longer usable. In both cases, the knowledge of the limit load is very important for the civil engineer, because he must design his structure so as to present a definite factor of safety against the limit load.

The aim of Theory of Plasticity is the detailed study of the stress and strain fields in structures in a state of contained plastic flow.

In the present course, we are especially interested to develop methods for obtaining the value of the plastic collapse load of structures.

This part of Theory of Plasticity is called Limit Analysis.

As in all physical theories, the theory of Limit Analysis will be based, for mathematical purposes, on a series of simplifying assumptions. Specifically, it will be assumed :

- 1) that the body or structure is made of an elastic-perfectly plastic material with indefinite yield plateau ;
- 2) that the body or structure obeys the equilibrium equations written for its undeformed configuration. In other words, Limit Analysis will be a first-order theory ;
- 3) that no troublesome phenomenon occurs such as brittle or fatigue fracture, instability phenomena, etc. . . .

Collapse will be defined as the condition in which deflections can increase without limit while the load (i.e. the multiplier  $\lambda$ ) is held constant.

In practice, the behavior is influenced by strain hardening, changes of geometry, residual stresses, etc. . . . Nevertheless, the value  $\lambda_l$  determined by the methods of Limit Analysis is, most of the time, an important information for the designer.

The subject of Limit Analysis will be divided into two parts. The first one is the

general three-dimensional theory, which is developed in present chapter and uses the language of Mechanics of Continua: stresses  $\sigma_{ij}$ , strain rates  $\epsilon_{ij}$ , power of dissipation  $D$ , volume forces  $F_i$  and surface  $T_i$  etc. . . The second part is the application of this general theory to engineering structures, (chapter 5) which are always composed of thin elements. If these elements are undimensional (bars), we speak of trusses, beams, rigid-jointed frames, arches and grillages. If they are bidimensional, we speak of plates and shells and structures composed of these elements.

In all cases, it is possible to simplify the study of the behavior of these engineering structures by using simplifying assumptions : BERNOULLI assumption that plane sections remain plane, in the case of beams ; KIRCHHOFF – LOVE assumption in the case of plates or shells. As we shall see in Chapter 4, it will then be possible, instead of using stresses and strain rates, to deal with internal stress resultants – such as the normal and shear forces, bending and torsional moments and with the corresponding deformations (center-line displacements, curvature and torsion rates, etc. . .)

The use of these generalized stresses and strain rates, that will be called  $Q_i$  and  $\dot{q}_i$  as in LAGRANGE's Analytic Mechanics, will entail a substantial economy of mathematics.

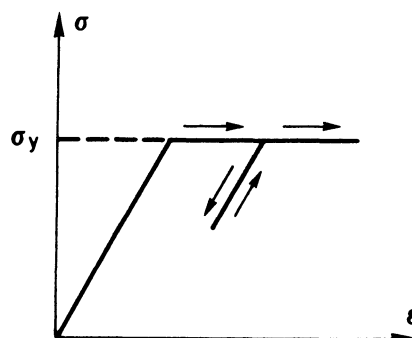


Fig. 1.1.

## 2.2. Preliminary Concepts and Results

### 2.2.1. Concepts of statically admissible stress field and kinematically admissible flow mechanism.

Because the elastic deformations are small compared to the plastic deformations at the limit load and because the limit theory of Analysis and Design

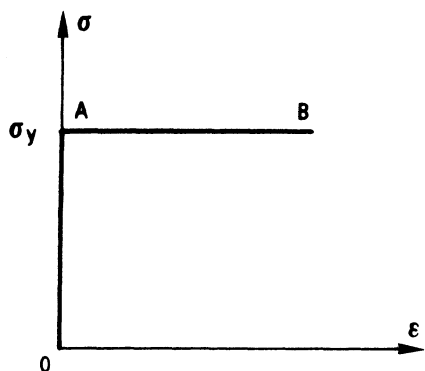


Fig. 2.1.

that we wish to develop is a first order theory, we can, in this theory, disregard completely the elastic deformations. This is equivalent to assuming that the stress-strain diagram of the material has the shape OAB of fig. 2.1., which is called the rigid-plastic model.

Let us analyze now the properties of the stress and strain rate fields in a rigid plastic body in his limit state of incipient uncontained plastic flow.

- 1) The stresses  $\sigma_{ij}$  are in equilibrium with the applied loads (volume loads  $\lambda_1 F_i$ , surface loads  $\lambda_1 T_i$ ), so that the  $\sigma_{ij}$  satisfy the equations of internal equilibrium

$$(2.1.) \quad \partial_j \sigma_{ij} + \lambda_1 F_i = 0,$$

the conditions of equilibrium at the surface of the body

$$(2.2.) \quad \sigma_{ij} v_j = \lambda_1 T_i$$

where  $v_j$  represents the unit vector along the external normal to the surface of the body.

- 2) The stresses respect everywhere the yield condition

$$(2.3.) \quad \bar{\sigma} \leq \sigma_y.$$

Any stress field respecting conditions (2.1.) and (2.2.) should be called statically admissible and a stress field respecting condition (2.3.) should be called plastically admissible. In practice, the research men who have developed the Theory of Limit Analysis have coined the term statically admissible for a stress field satisfying simultaneously relations (2.1.), (2.2.) and (2.3.); correctly speaking, such a field should have been called "statically and plastically admissible" but we shall follow the general practice.

- 3) The actual flow mechanism composed of the velocities  $v_i$  and strain rates  $\epsilon_{ij}$  in the body at collapse satisfies the kinematical boundary conditions of the body. In addition, the first principle of Thermodynamics requires that the power of the applied loads  $\lambda_1 F_i$ ,  $\lambda_1 T_i$  be equal to the (positive) power dissipated in the plastic flow.

Any mechanism  $(v_i, \dot{\epsilon}_{ij})$  satisfying the kinematical boundary conditions of the body is called kinematically admissible.

The demonstration of the two fundamental theorems is based on two preliminary results.

### 2.2.2. The principle of virtual powers.

One of the main tools in the Mechanics of Deformable Bodies is the Principle of virtual displacements : the necessary and sufficient condition for a body to be in equilibrium is that, for any stress field  $\sigma_{ij}$  in equilibrium with the volume and surface forces and for any infinitely small kinematically admissible virtual displacement field  $\delta u_i$ , the external work be equal to the deformation work.

This is expressed mathematically by the equality

$$\int_v F_i \delta u_i dV + \int_s T_i \delta s_i dS = \int_v \sigma_{ij} \delta \epsilon_{ij} dV, \quad (2.4.)$$

where  $\delta \epsilon_{ij}$  represent the virtual strains corresponding to the virtual displacements  $\delta u_i$ .

By differentiating (2.4.) with respect to the time, and introducing the virtual velocities  $\delta v_i = d\delta u_i/dt$  and strain rates  $\delta \dot{\epsilon}_{ij} = \delta(d\epsilon_{ij}/dt)$ , we obtain the principle of virtual powers

$$\int_v F_i \delta v_i dV + \int_s T_i \delta v_i dS = \int_v \sigma_{ij} \delta \dot{\epsilon}_{ij} dV. \quad (2.5.)$$

This theorem reads as follows :

If a body is in equilibrium, the power produced by the external forces is equal to the power dissipated in the plastic deformations for any virtual kinematically admissible field of velocities  $\delta v_i$  and strain rates  $\delta \dot{\epsilon}_{ij} P_j$ .

This theorem gives a simple means for computing the value of the limit multiplier  $\lambda_l$ , corresponding to the collapse of the structure. Indeed, applying the theorem to the actual collapse forces  $\lambda_l F_i, \lambda_l T_i$  and to the actual field of velocities  $v_i$  and strain rates  $\dot{\epsilon}_{ij}$  at collapse, we find

$$\lambda_l [\int_v F_i v_i dV + \int_s T_i v_i dS] = \int_v \sigma_{ij} \dot{\epsilon}_{ij} dV. \quad (2.6.)$$

### 2.2.3. The power equation.

Consider a structure subjected to service forces  $F_i$  and  $T_i$ . If we give ourselves a kinematically admissible flow mechanism  $(v_i +, \dot{\epsilon}_{ij} +)$  the power of dissipation  $D$  is, by section (1.3.4.), as well defined single valued function of the  $\dot{\epsilon}_{ij} +$  through the yield condition and the normality law.

The stress field (or fields)  $\sigma_{ij} +$  corresponding to above flow mechanism through the normality law (1.3.8.) is not, in general, a stress field in equilibrium and, therefore the principle of virtual powers (2.5.) is not valid.

We can ever decide, however, to apply equation (2.5.) formally. This gives the equation

$$(2.7.) \quad \lambda_+ [\int_V F_i v_i + dV + \int_S T_i v_i + dS] = \int_V \sigma_{ij} + \dot{\epsilon}_{ij} + dV.$$

This equation is called the **power equation**. By means of the power equation, it is always possible to associate to each kinematically admissible flow mechanism a definite value  $\lambda_+$  of the multiplier. This multiplier is said to correspond to the flow mechanism considered.

### 2.2.4. The principle of maximum energy dissipation.

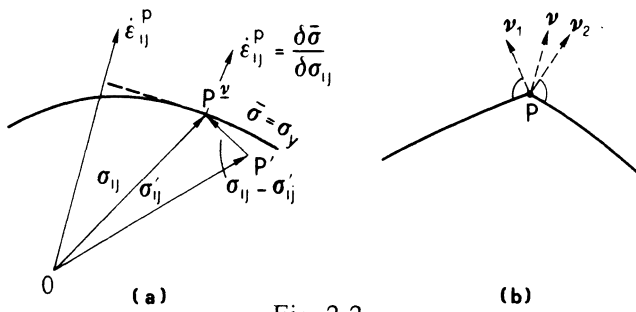


Fig. 2.2.

Suppose that the stress state at a definite point of the body,  $\sigma_{ij}$ , be a point on the yield surface (fig. 2.2.a.). Let us call  $\sigma'_{ij}$  any other point on or within the yield surface. The corresponding stress vectors  $\underline{OP}$  and  $\underline{OP'}$  are shown on the figure, as well as the vector  $P'P = \sigma_{ij} - \sigma'_{ij}$ . Due to the convexity of the yield surface, the angle  $P'P\nu$  is always larger than  $\pi/2$ , which shows that the scalar product of the vector  $P'\hat{P} = \sigma_{ij} - \sigma'_{ij}$  by the vector  $\nu = \partial\bar{\sigma}_e/\partial\sigma_{ij}$  cannot be negative. Hence, the convexity property together with the normality rule

$$\dot{\epsilon}_{uj}^P = \mu \frac{\partial \bar{\sigma}}{\partial \sigma_{ij}} \quad (\mu > 0) \quad (2.8.)$$

requires

$$(\sigma_{ij} - \sigma'_{ij}) \dot{\epsilon}_{ij}^P \geq 0 \quad (2.9.)$$

If the stress state  $\sigma_{ij}$  is inside the yield surface,  $\bar{\sigma}(\sigma'_{ij}) < \sigma_y$  and the inequality sign holds in equation (2.9.).

If the stress point P falls on a corner of the yield surface (fig. 2.2.b.), the normal  $\nu$  is not defined, but is only strained to lie between  $\nu_1$  and  $\nu_2$ . However, it is easily seen that for any realizable stress state  $\sigma'_{ij}$ , the inequality (2.9.) is still valid.

As inequality (2.8.) is valid for any particle, it may be integrated over the entire volume of the body, which gives

$$\int_V \sigma_{ij} \dot{\epsilon}_{ij}^P dV \geq \int_V \sigma'_{ij} \dot{\epsilon}_{ij}^P dV. \quad (2.10.)$$

Note that the left-hand member represents the power of dissipation  $D(\dot{\epsilon}_{ij}^P)$  of the whole body. We have therefore the Theorem of maximum dissipation : is not less than the fictitious power dissipated in this mechanism by any attainable state of stress.

## 2.3. The Three Basic Theorems

### 2.3.1. Statical or lower bound theorem.

Theorem.

*If a stress field  $\bar{\sigma}_{ij}$  can be found which satisfies the equations of equilibrium (2.1.), (2.2.) and which nowhere violates the yield conditions (2.3.), then the corresponding multiplier  $\lambda_-$  cannot exceed the limit multiplier  $\lambda_l$*

**Proof :** The limit load  $\lambda_l$  is composed of surface tractions  $\lambda_l T_i$  and volume forces  $\lambda_l F_i$ . Let  $\sigma_{ij}$ ,  $v_i$ ,  $\dot{\epsilon}_{ij}^P$  represent actual stresses, velocities and strain rates at collapse.

We express the fact that both the stress field  $\bar{\sigma}_{ij}$  and the actual stress field at

collapse,  $\sigma_{ij}$ , are in equilibrium by applying twice the principle of virtual powers. In the two applications of this principle, we can take as fields of virtual velocities and strain rates, the actual field  $v_i, \dot{\epsilon}_{ij}^P$  of the collapsing structure, because it is kinematically admissible.

The use of the principle for the  $\sigma_{ij}$  field gives

$$(2.11.) \quad \lambda_- [\int_V F_i \delta v_i dV + \int_S T_i \delta v_i dS] = \int_V \bar{\sigma}_{ij} \delta \dot{\epsilon}_{ij}^P dV.$$

The use of the principle for the actual collapse stress field  $\sigma_{ij}$  gives

$$(2.12.) \quad \lambda_1 [\int_V F_i \delta v_i dV + \int_S T_i \delta v_i dS] = \int_S \sigma_{ij} \delta \dot{\epsilon}_{ij}^P dV.$$

Subtracting (2.11.) from (2.12.), we find :

$$(2.13.) \quad \int_V \sigma_{ij} \delta \dot{\epsilon}_{ij} dV - \int_V \bar{\sigma}_{ij} \delta \dot{\epsilon}_{ij} dV = (\lambda_1 - \lambda_-) [\int_V F_i \delta v_i dV + \int_S T_i \delta v_i dS]$$

But the  $\bar{\sigma}_{ij}$  are a field of attainable stresses. Therefore, by the theorem of maximum dissipation (formula (2.9.)), the left hand member of (2.13.) is non negative. The bracket in the right hand member being an essentially positive work, it follows that

$$(2.14.)$$

$$\boxed{\lambda_- < \lambda_1}$$

Q.E.D.

By using the concept of statically admissible stress field defined in section 2.2.1., we can give of the statical theorem the following condensed version :

#### Statical theorem :

*A multiplier  $\lambda_-$  corresponding to a statically admissible stress field cannot exceed the actual collapse multiplier.*

This theorem is, in the opinion of the author, one of the most important of the entire Theory of Structures. It expresses the physical fact that :

If an equilibrium path can be found for the stresses, which leads the external forces to the abutments of the structure, this equilibrium will be effectively realized by suitable yielding of the material, provided this material has a sufficient (theoretically an infinite) ductility. In other words, the theorem proves that, in an elastic-perfectly

plastic structure subjected to dead loads, only the equilibrium equations are really vital. The compatibility equations can be violated.

### 2.3.2. Kinematical or upper-bound theorem.

**Theorem:**

*Any multiplier  $\lambda_+$  corresponding to a kinematically admissible flow mechanism by the power equation is not less than the limit multiplier  $\lambda_l$ .*

**Proof :** Let  $v_{i+}$  and  $\dot{\epsilon}_{ij+}$  be the velocities and strain rates of the kinematically admissible flow mechanism. The corresponding multiplier  $\lambda_+$  is given, by definition, by equation (2.7.).

Let  $\sigma_{ij}$  be the actual stress field at the limit state of the structure, in equilibrium with the external forces  $\lambda_l P_i$  and  $\lambda_l T_i$ . The principle of virtual powers, applied this stress field and adopting as virtual kinematically admissible field of velocities and strain rates the flow mechanism ( $v_{i+}$ ,  $\dot{\epsilon}_{ij+}$ ), gives the equation

$$\lambda_l \left[ \int_V P_i v_{i+} dV + \int_S T_i v_{i+} dS \right] = \int_V \sigma_{ij} \dot{\epsilon}_{ij+} dV. \quad (2.15.)$$

Because  $\sigma_{ij}$  is an attainable stress field, that normally does not correspond to the field  $\dot{\epsilon}_{ij+}$  by the normality law, the principle of maximum energy dissipation (2.9.) gives

$$\int_V \sigma_{ij+} \dot{\epsilon}_{ij+} dV \geq \int_V \sigma_{ij} \dot{\epsilon}_{uj+} dV. \quad (2.16.)$$

Substracting (2.15.) from (2.7.), and taking account of (2.16.), we find

$$|\lambda_+ - \lambda_l| \left[ \int_V P_i v_{i+} dV + \int_S T_i v_{i+} dS \right] = \int_V \sigma_{ij+} \dot{\epsilon}_{ij+} dV - \int_V \sigma_{ij} \dot{\epsilon}_{ij+} dV \geq 0. \quad (2.17.)$$

The bracket in the left-hand member represents an essentially positive power. Therefore,

$\lambda_+ > \lambda_l$
-------------------------

Q.E.D. (2.18.)

In more physical terms, the kinematical theorem states that, if any kinematically admissible mechanism of collapse can be found, for which the rate of work of the

given external loads exceeds the rate of plastic energy dissipation in the body, then this body cannot support these external loads.

### 2.3.3. Complete solutions – The combined theorem.

Assume that we have found a statically admissible stress field and a kinematically admissible mechanism that correspond to the same multiplier  $\lambda$ . According to the two fundamental theorems, this multiplier belongs simultaneously to the set of the statically admissible multipliers  $\lambda_- \leq \lambda_l$  and to the set of the kinematically admissible multipliers  $\lambda_+ \geq \lambda_l$ . Therefore, it is the unique common bound of these sets. This proves that the limit multiplier  $\lambda_l$  has always a unique value.

The situation above occurs when it is possible to associate a statically admissible stress field and a kinematically admissible mechanism by the law of the plastic potential (1.3.8.). In that case, the power equation (2.7.) defining  $\lambda_+$  can be regarded as a virtual power equation expressing the equilibrium of the associated stress field. Consequently,  $\lambda_+ = \lambda_-$  and, denoting by  $\lambda$  this common value, we have  $\lambda = \lambda_l$ . This leads to :

**Combined theorem :**

*When it is possible to associate by the plastic potential flow law a statically admissible stress field and a kinematically admissible mechanism, the multiplier  $\lambda$  corresponding simultaneously to both fields is the exact limit multiplier  $\lambda_l$ .*

The two fields above form what is called a **complete solution** of the Limit Analysis of the structure. In practical problems, one starts either from a mechanism, or from a statically admissible stress field, and tries to obtain the other field. Numerous examples of this technique will be given in chapters 5, 6 and 7 of this course.

## 2.4. Additional Remarks

### 2.4.1. Constancy of the stresses during plastic flow.

**Theorem**

*If all changes of geometry are disregarded, all stresses remain constant while plastic deformations take place at the limit load ; only plastic, but not elastic increments of strain occur.*

**Proof :** Disregarding changes of geometry is justified because we are concerned exclusively with the incipient uncontained plastic flow, which is of infinitesimal magnitude. This flow occurs under constant load  $\lambda_l$ . Assume for a moment that some changes  $\dot{\sigma}_{ij}$  occur in the stress field during the flow. They are in equilibrium with vanishing load changes,  $\lambda = 0$ . We can therefore write the equation of virtual power as follows

$$\dot{\lambda} \left[ \int_V F_i v_i dV + \int_S T_i v_i dS \right] = \int_V \dot{\sigma}_{ij} \dot{\epsilon}_{ij}^e dV. \quad (4.1.)$$

$\dot{\lambda}$  being zero, the right-hand member must also be zero. Now,  $\dot{\epsilon}_{ij} = \dot{\epsilon}_{ij}^e + \dot{\epsilon}_{ij}^P$ . Therefore, we have

$$\int_V \dot{\sigma}_{ij} (\dot{\epsilon}_{ij}^e + \dot{\epsilon}_{ij}^P) dV = 0.$$

But it follows from the normality law that  $\dot{\sigma}_{ij} \dot{\epsilon}_{ij}^P = 0$ , since the stress variation vector  $\dot{\sigma}_{ij}$  is tangential to the yield surface and therefore normal to  $\dot{\epsilon}_{ij}^P$ . Therefore,

$$\int_V \dot{\sigma}_{ij} \dot{\epsilon}_{ij}^e dV = 0. \quad (4.2.)$$

But the last integral represents the double of the strain energy of the elastic body subjected to the stresses  $\dot{\sigma}_{ij}$ . It is well known from Theory of Elasticity that the strain energy is an essentially positive quantity, which cannot be zero, unless

$$\sigma_{ij} = 0 \text{ everywhere (Q.E.D.)} \quad (4.3.)$$

#### 2.4.2. Addition and subtraction of material – FEINBERG's theorem.

*If some material is added to a perfectly plastic structure and if the dead weight of the additional material is neglected, the limit load  $\lambda_l$  of the structure cannot decrease.*

**Proof :** Let  $\sigma_{ij}$  be the stress field at collapse in the original structure.

Consider now the stress field consisting of the field  $\sigma_{ij}$  in the original structure and zero stresses in the additional material. This stress field is discontinuous at the boundary between the original and the additional material, but it will be shown later

(section 4.6.) that these discontinuities are acceptable. Anyway, this stress field corresponding to  $\lambda_1$  original struct. is statically admissible for the modified structure. According to the statical theorem, we have then

$$\lambda_1^{\text{original struct.}} < \lambda_1^{\text{reinforced struct.}} \quad (\text{Q.E.D.})$$

FEINBERG's theorem is in opposition to theory of elasticity. Indeed, it is easy to show that, by welding on an elastic bar of rectangular section two thin appendices

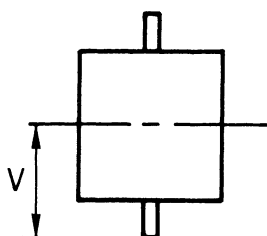


Fig. 4.1.

(fig. 4.1.), we can decrease the section modulus  $S = I/v$ , because the effect of these appendices is to increase  $v$  more than the moment of inertia  $I$ . Similarly, in the elastic theory of groups of piles, due to NÖKKENTVED, it can occur that the addition of a new pile to the group results in a decrease of the elastic strength (section 6.1.).

By FEINBERG's theorem, similar paradoxes can never occur in Limit Analysis.

#### 2.4.3. Effect of residual stresses.

In the demonstrations of the various theorems of sections 2.3. and 2.4.1., no assumption has been made concerning an initial stress-free state. Therefore, the possible presence of residual stresses does not invalidate the proofs of the theorems, nor the existence of small initial deformations of the structure, provided the deformations do not significantly change the geometry of the structure, so that the equilibrium conditions can be set up without taking account of these deformations. Hence, we can state that unknown initial stresses (including thermal stresses), and deformations have no effect on the limit load, provided they do not significantly affect the geometry of the structure.

Foregoing result is extremely important in the case of steel structures, whose members are usually full of residual stresses due to unequal cooling rate after rolling, cold straightening, flame cutting, welding and cold forming. Numerous experiments support this property, which was implicitly used by practicing engineers when they designed their steel structures by elastic theory, but ignoring the effect of residual stresses. The most striking one is that imagined by MAIER–LEIBNITZ [M2].

A symmetrical two-span continuous I beam is loaded by two equal loads  $\lambda P$ .

In a first test, the three supports are exactly aligned. The beam fails by the mechanism shown dotted, involving three plastic hinges and the limit load is  $\lambda_1$ . In a second test (fig. 4.2.b.), the central support is displaced downward 5 mm until the stress in the lowermost fiber of the

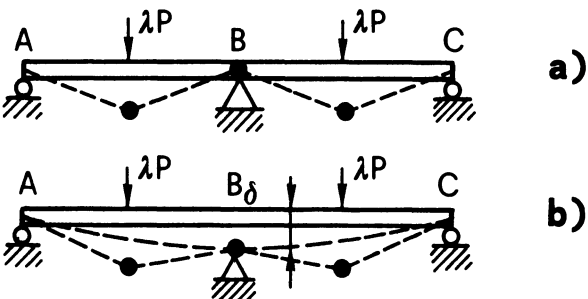


Fig. 4.2.

central section reaches the allowable tensile stress. From the point of view of the classical safety concept, the beam then could not support any further load. Nevertheless, the experimental limit load reaches the same value  $\lambda_1$  as before, and the same is true when the central support is displaced upward to produce the allowable tensile stress in the uppermost fiber of the central cross section.

However, if the residual stresses have no effect on the limit load, they change completely the elastoplastic behavior of the steel members.

The limit of proportionality in bending is lowered, and becomes sometimes less than  $\sigma_y/2$  and the moment-curvature diagram is completely changed.

Therefore, the residual stresses have a pronounced effect on all instability phenomena, which must be analyzed by second order theory and which are therefore influenced by any change in the elastoplastic behavior.

#### 2.4.4. Generality of the theorems.

The proofs of the basic theorems of Limit Analysis are based on the assumption that all external loads applied to the structure increase in proportion, or, in other terms, that any two of these loads keep a constant ratio throughout the loading. However, the actual loading program needs not to adhere to this scheme.

What is of paramount importance is that the prescribed load ratios must be respected at the limit load. Any program of loading can in fact be followed that brings the component loads up to their final proportions at the limit load, provided only that the limit load of the structure corresponding to some other proportions is not exceeded on the way.

Anyway, the type of loading considered represents a severe limitation because, in civil engineering, the dead load does not practically vary, while the live loading can

increase up to collapse. A more general type of loading reflecting this fact is considered in Section 3.1.

The most general type of loading which has been studied thus far considers loads  $P$  which can vary independently between fixed limits known in advance,  $P_1$  and  $P_u$ . This problem is studied in detail in section 3.2.

## 2.5. Elastic-Plastic and Rigid-Plastic Bodies

The three fundamental theorems were established by GVOZDEV [G1], HILL [H2] and PRAGER [P2] [P3] in the case of the rigid perfectly plastic body, and by DRUCKER, PRAGER AND GREENBERG [D1] for the elastic-perfectly plastic material. The fundamental theorems are absolutely identical for both idealizations. They are based exclusively on the concepts of statically admissible stress fields and kinematically admissible plastic strain rate fields, with no reference to the elastic or rigid nature of the material not at yield.

The question we now wish to discuss is whether one idealization is better than the other.

If the elastic-plastic idealization is used, the limit state corresponds to incipient uncontained plastic flow. For any point of the structure, the graph of the displacement  $\delta$  versus the multiplier  $\lambda$  is initially a straight line OA (fig. 5.1.a.)

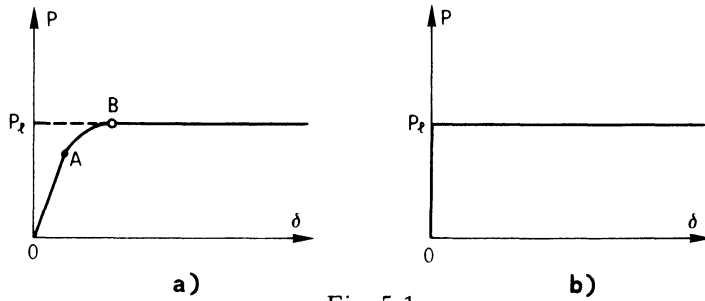


Fig. 5.1.

(elastic range), then a curve AB (elastic plastic range : contained plastic flow) and finally, when plastification has spread sufficiently through the body, the horizontal BC representing the uncontained plastic flow.

If, on the contrary, we use the rigid-plastic idealization, the rigid parts of the body

prevent all deformations up to the onset of the unrestrained plastic flow at the limit multiplier  $\lambda_l$ , so that this load is also called sometimes yield point load (fig. 5.1.b.).

Clearly, both idealizations are only acceptable if the elastoplastic deformations  $\delta_l$  at impending collapse (fig. 5.1.a.) are small enough, so as not to change too much the initial geometry of the body. If these deformations change appreciably the initial behavior of the body – as it is the case for example in a thin plate subjected to bending by transverse loads, where membrane stresses change completely the behavior as soon as the transverse displacements become of the order of the thickness – both approaches above are equally poor and the structural behavior can only be studied by a step by step non linear procedure, involving intricate computations and therefore the use of an electronic computer.

## 2.6. Influence of Changes of Geometry

The real purpose of Limit Analysis is to predict the ultimate behavior of civil engineering structures made from elastoplastic materials. As seen in section 2.5., the limit load is a concept valid only for an idealized structure, which has preserved its initial geometry at the moment of collapse.

Experimental and theoretical behavior differ for two main reasons :

- 1) due to the elastoplastic deformations, the actual structure presents at impending collapse some deviation from above ideal shape (one could add to these deviations the inevitable imperfections of shape due to the fabrication process) ;
- 2) When large plastic deformations occur, the real material exhibits some work hardening that was neglected in the theory.

In the study of elastic structures, a first order theory is generally sufficient. Only in structures based on funicular action (suspension bridges and large arch bridges) become the second order effects sufficiently large to must be included in the analysis.

In plastic analysis of structures, the relative importance of the second order effects is much larger, because these effects are roughly proportional to the square of the relative deflections  $\delta/l$ . If we consider that the deflections at impending collapse are between 2 and 3 times the service deflections, the second order effects at impending collapse are from 4 to 9 times larger than in service conditions.

The main problem in practice is to ascertain whether the theoretical limit load will effectively be reached, and, if yes, to appreciate the behavior of the structure after the limit load has been exceeded. To answer this question, one has to examine whether the displacements present at impending collapse will tend to increase or to lower the theoretical limit load.

To show how this principle may be applied, we shall study in succession a plane frame, a plate and a shell.

Consider first the very simple problem of a rectangular portal frame hinged at its feet, formed of infinitely rigid bars connected at points B and C by ductile joints yielding perfectly plastically under the limit moment  $M_p$ .

The first order theory gives, for both cases represented at figures 6.1. a and b,

$$(6.1.) \quad P_l \dot{\theta} = 2 M \dot{\theta}, \text{ whence } P_l = 2 M_p / l.$$

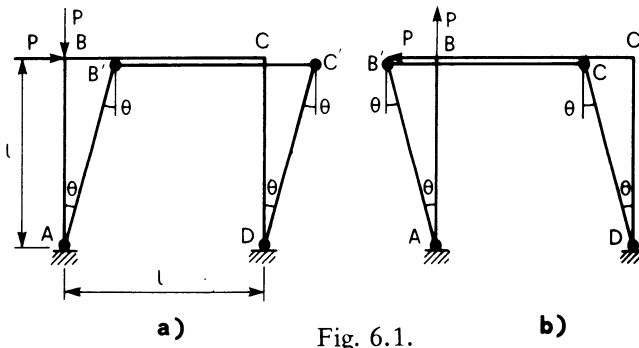


Fig. 6.1.

so that the law  $(P, \delta)$  is an horizontal (fig. 6.2.).

On the contrary, if  $\theta$  is considered as a finite angle, it is seen that the horizontal and vertical velocities of point B are respectively

$$v_h = l \sin \dot{\theta} \quad \text{and} \quad v_v = l(1 - \cos \dot{\theta})$$

From the theorem of virtual powers, the limit load for the deformed frame is obtained by giving to this frame a virtual infinitely small deformation  $d\dot{\theta}$ , in the course of which  $v_h$  and  $v_v$  take variations

$$dv_h = l \cos \dot{\theta} d\dot{\theta} \quad \text{and} \quad dv_v = l \sin \dot{\theta} d\dot{\theta}$$

The equality of the internal and external powers gives then, for the problem of fig.

6.1.a.,

$$Pdv_h + Pdv_v = 2M_p d\theta$$

that is

$$P_1 = \frac{2M_p}{l(\cos \theta + \sin \theta)} \quad (6.2.)$$

This shows that the limit load decreases with  $\theta$  along the full line marked (1) in fig. 6.2. For not too large deformations, the sine and cosine may be expanded into Mac-LAURIN series truncated after the terms in  $\theta^2$ ; one obtains in this way the approximation

$$P_1^{app} = \frac{2M_p}{l(1 + \theta - \theta^2/2)} \quad (6.3.)$$

This formula is represented on fig. 6.2. by the dashed curve marked (1'). For the problem of fig. 6.1.b., the vertical displacement of point B occurs against the vertical force  $P$ ; the sign of the corresponding power must be changed, so that formulae (6.2.) and (6.3.) become respectively

$$P_1 = \frac{2M_p}{l(\cos \theta - \sin \theta)} \quad \text{and} \quad P_1^{app} = \frac{2M_p}{l(1 - \theta - \theta^2/2)}. \quad (6.4.), (6.5.)$$

In figure 6.2., these formulae are represented by the curves (2) and (2') respectively. It is seen that the second order effects have a stabilizing or destabilizing influence according to the sign of the axial force  $P$  on column AB.

Let us now consider a circular simply supported plate, loaded by a transverse concentrated force in its middle. The deflections will tend to transform this plate in a membrane and the membrane forces exert evidently a stabilizing effect. Indeed, the experimental load-deflection diagram obtained (fig. 6.3.) shows that there exists a large post-limit domain.

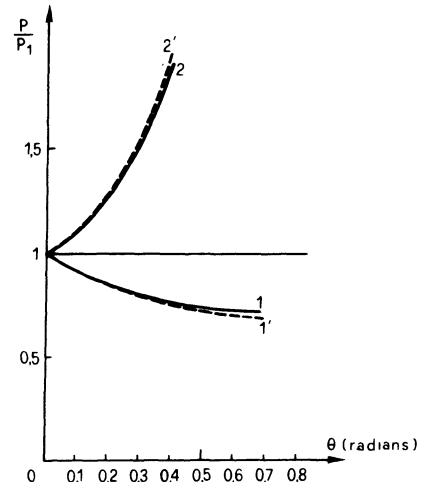


Fig. 6.2.

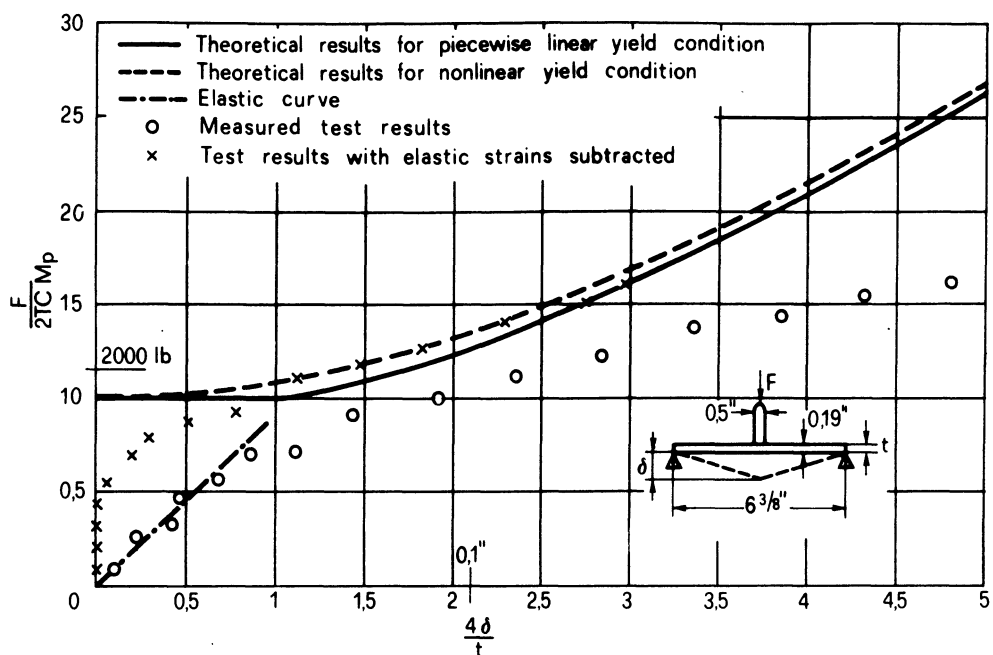


Fig. 6.3.

Fig. 6.4. gives similar load deflection curves for four different truncated shallow

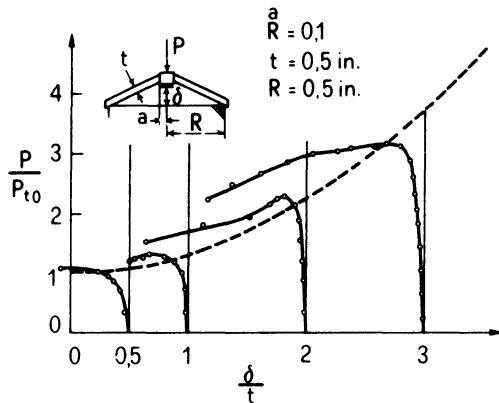


Fig. 6.4.

conical shells subjected to a uniform load at the upper edge. The dashed curve showing the theoretical load versus the deflection is obtained by taking account of the changes of geometry.

In the case of the plate, the changes of geometry have a favorable effect on the strength of the structure whereas, in the case of the shell, the limit state is unstable and results in plastic collapse of the structure.

## 2.7. Uniqueness of the Solution

As already noted in section 2.3.3., the value of the limit multiplier  $\lambda_l$  for proportional loading is unique. Are the fields  $\sigma_{ij}$  and  $\dot{\epsilon}_{ij}$  also unique ?

Suppose first that we consider a definite stress field  $\sigma_{ij}$ . As emphasized at the end of section 1.3.4. to this field may correspond, by the normality law, several mechanisms, all of them furnishing the same multiplier  $\lambda_l$  by their power equation (2.7.). Hence the flow mechanism clearly need not be unique.

Now, is the stress field necessarily unique ? This problem was investigated by PRAGER [P3]. He proved that, when two complete solutions  $(\sigma_{ij})_1$ ,  $(\epsilon_{ij})_1$  and  $(\sigma_{ij})_2$ ,  $(\epsilon_{ij})_2$  are known, the stress fields of the two solutions were identical except possibly :

1. in the common rigid regions ;
2. where both states of stress are represented by stress points on the same flat part of the yield surface.

Practical examples of this possibility may be found when studying the limit behavior of reinforced concrete plates (see the lectures by Prof. SAWCZUK).

### 3. GENERAL THEOREMS OF LIMIT ANALYSIS – GENERAL LOADING.

#### 3.1. Structure with non Negligible Dead Load.

We have already mentioned in Section 2.4.4. that proportional loading represented a too restricted loading case for civil engineering structures, where the dead load represents always an appreciable part of the total loading and does not vary very much in practice. Assuming the dead load to be completely determined and given and the live loads to consist of a one parameter loading controlled with the multiplier  $\lambda$  whose magnitude at collapse is  $\lambda_v$ , one defines statically and kinematically multipliers  $\lambda_{v-}$  and  $\lambda_{v+}$  as follows :

1.  $\lambda_{v-}$  is the intensity of the live load which, together with the fixed dead load, corresponds to a statically admissible stress field ;
2.  $\lambda_{v+}$  is the intensity of the live load which, together with the fixed dead load, corresponds by the power equation to a kinematically admissible mechanism.

The actual limit multiplier is defined as the intensity of the live load that produces uncontained plastic flow when associated to the dead load.

It is easy, by generalizing slightly the demonstrations, to show that

$$(1.1.) \quad \lambda_{v-} < \lambda_v < \lambda_{v+} .$$

Historically, the limit theorems first obtained by GVOZDEV [G1] have precisely been established under present conditions.

An implicit condition for the validity of (1.1.) is obviously that the dead load alone cannot cause the collapse of the structure.

#### 3.2. Loading Depending on Several Parameters.

##### 3.2.1. Introduction.

The various loads acting on a structure vary often independently of each other and can be reapplied many times. It is of primary importance to the designer to determine the permissible ranges of variation of these loads to avoid some kind of plastic collapse.

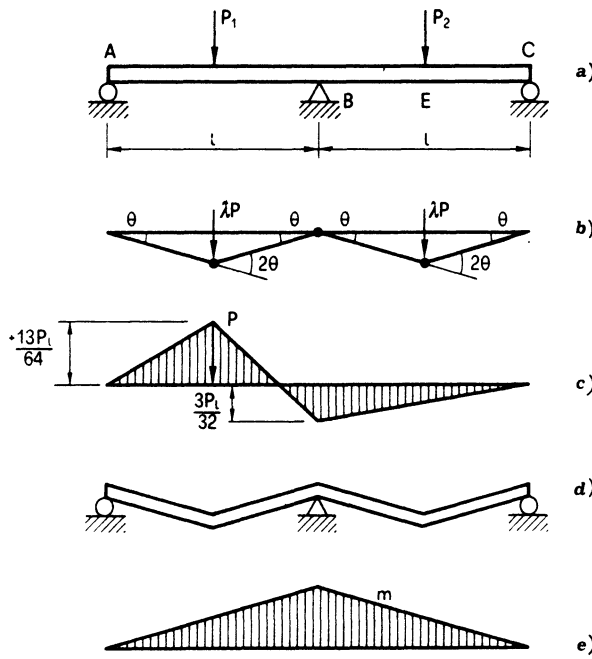


Fig. 2.1.

power equation ; indeed, the external power is

$$P_e = 2 \lambda P \frac{1}{2} \dot{\theta}$$

whereas the internal power dissipated in the three plastic hinges is

$$P_i = M_p (2 \dot{\theta} + 2 \dot{\theta} + 2 \dot{\theta}).$$

Equating these powers, we obtain

$$\lambda_1 = \frac{6M_p}{P_1}. \quad (a)$$

However, it is easily found that, if the loads vary independently, the maximum magnitude of the multiplier must be less than (a). Indeed, it is easily found by elastic analysis that, if the left force  $\lambda P$  is applied alone, the bending moment diagram has the shape depicted by fig. 2.1.c). The maximum moment occurs under the load and its value is  $M_D = + \frac{13 \lambda P l}{64}$ . If the value (a) of  $\lambda_1$  is substituted in the expression, one finds

In order to understand more fully the nature of the problem, consider (fig. 2.1.) a symmetrical two-span continuous I beam in steel, which supports two concentrated loads,  $P_1$  and  $P_2$ , applied in the middle of each span.

To have a concrete case, suppose that the dead weight of the beam is negligible and that the loads  $P_1$  and  $P_2$  can in service vary independently between 0 and  $P$ .

If both loads are equal, their limit value producing the collapse of the beam by the collapse mechanism of fig. 2.1.b is easily found by the

$$M_D = \frac{78}{64} M_P ,$$

which proves that a plastic hinge will occur in D as soon as  $\lambda$  exceeds the value

$$\lambda' = \frac{64}{78} \lambda_l . \quad (b) .$$

on the other hand, if two equal forces  $\lambda P$  are applied in D and E, it is easily seen that the bending moment in B is  $-\frac{12\lambda P l}{64}$  and that a negative plastic hinge will occur in B for any value of  $\lambda$  exceeding

$$\lambda'' = \frac{64}{72} \lambda_l \quad (c) .$$

If, now, load cycles are applied to the beam according to (fig. 2.2.), it can easily be

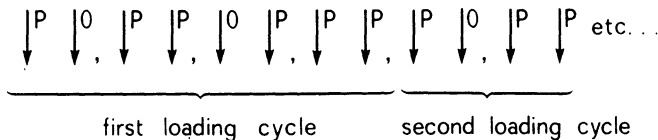


Fig. 2.2.

conceived that plastic deformations of increasing magnitude will accumulate in D, B and E and that permanent deformations will ultimately occur that render the beam unserviceable (fig. 2.1.d) by failure by progressive plastic deformation, also called incremental collapse.

It could also happen that, because the bending moments in section D and E become positive, then negative, in the course of the same loading cycle (fig. 2.2.) the metal would fail by a fatigue type of failure called low-cycle fatigue. In the following, the term failure by alternating plastic deformation will be used instead to accentuate the contrast between the two types of failures.

However, due to its permanent deformations, this once statically indeterminate structure becomes non-concordant with its supports, so that a field of self-stresses must necessarily develop if the supports at A, B, C are bilateral. This field of selfstresses is a diagram of residual moments  $m$ , which has necessarily the shape of fig. 2.1.e.). It is well known that residual stresses due to plastic deformations are

helpful in supporting the loads, as long as the external loads do not change their signs. We may therefore very well imagine that, after a certain number of loading cycles (fig. 2.2.), the plastic deformations will ultimately cease because of the help given by the diagram of residual moments  $m$ . The amounts of plastic deformation that occur in consecutive cycles of loading may decrease as the terms of a convergent infinite series, or plastic deformation may stop altogether after the first cycle or the first few cycles of loading. In either case, the structure is said to shake down. If shakedown does not occur, the plastic deformations are said to be unstable. The fundamental theorems to be established in present chapter are concerned with the determination of the shakedown multiplier, that is the greatest value  $\lambda_s$  of the multiplier  $\lambda$  (affecting simultaneously the lower and upper limits of each load in service) for which the structure will shake down, that is the plastic deformations will tend to stable values.

The study of above problems – called in English the shakedown theory – constitutes a natural complement to the theory of Limit Analysis for the case of variable loads. This is the reason why the shakedown analysis has raised renewed interest in the last few years, though the basic theory had been initiated in the early thirties by BLEICH [B1] and MELAN [M3].

Two fundamental theorems regarding the shakedown are due to MELAN [M3] and KOITER [K1]; these theorems are essentially appropriate generalizations of the theorems of Limit Analysis (sections 2.3.1. and 2.3.2.).

In many cases of practical importance, a structure is acted upon not only by variable mechanical actions but also by a variable temperature field. The introduction of temperature brings three new problems :

- 1) thermal strains affect the stress field ;
- 2) the yield stress of the material changes with temperature ;
- 3) elastic moduli vary with temperature.

The first two effects have already been studied in theory of Limit Analysis and in the Shakedown Analysis by PRAGER [P2] as well as by other authors.

The demonstration given here follows the paper by J.A. KÖNIG [H2] and incorporates also the third effect above.

To be more specific about the magnitude of the two last effects cited above, let us say that :

- 1) in the case of mild steel, the yield stress remains almost constant up to  $300^\circ$  centigrades, but then decreases significantly within the temperature range  $300^\circ < T < 600^\circ\text{C}$ .
- 2) for a very wide range of temperatures, YOUNG's modulus  $E$  changes by 5 - 10 per cent per every  $100^\circ$  centigrades according to following linear relation

$$(2.1.) \quad E(T) = E(0) (1 - KT).$$

In present study, we shall neglect all viscoelastic effects, and restrict the analysis to an ideally elastic-plastic behavior.

### 3.2.2. Basic assumptions.

The strain tensor in an elastic-plastic body subjected to thermal actions is given by the expression

$$(2.2.) \quad \epsilon_{ij}^E = \epsilon_{ij}^E + \epsilon_{ij}^P + \epsilon_{ij}^T,$$

where  $\epsilon_{ij}^E = A_{ijkl} \sigma_{kl}$  and  $A_{ijkl}$  is the tensor of the elastic moduli,

$\epsilon_{ij}^P$  is the plastic strain tensor and

$\epsilon_{ij}^T$  is the thermal strain tensor.

By the elastic stress field  $\sigma_{ij}^E$ , we shall designate the solution of the actual boundary value problem obtained under condition  $\epsilon_{ij}^P = 0$ . The field  $\sigma_{ij}^E$  – which, in general, differs from  $\sigma_{ij}^E$  – concerns the solution for an elastic-perfectly plastic solid, where the constitutive relations are given by a yield condition (section 1.2.) and by a flow rule (section 1.3.4.). The difference

$$(2.3.) \quad \rho_{ij} = \sigma_{ij} - \sigma_{ij}^E$$

is a residual stress field satisfying the zero stress boundary conditions.

It is important to observe that, as soon as the tensor of elastic moduli  $A_{ijkl}$  varies with temperature, the plastic deformation field  $\epsilon_{ij}^P$  does not specify uniquely the field of residual stress  $\rho_{ij}$ . Indeed, the field  $\rho_{ij}$  depends now also on the actual

temperature and may vary with temperature even for an invariable field  $\epsilon_{ij}^P$ .

Let us assume now that the mechanical loads and temperature vary arbitrarily within the prescribed limits. We neglect the inertia forces and any thermoelastic and thermoplastic coupling and assume that the displacements remain sufficiently small so that the principle of virtual displacements is valid. Then, we have the following theorem :

### 3.2.3. First shake-down theorem or generalized MELAN's theorem.

If a real number  $s > 1$  and a time independent plastic strain field  $\epsilon_{ij}^P$  can be found such that the associated field of residual stresses  $\bar{\rho}_{ij}$  satisfy the inequality

$$\bar{\sigma} \{ s [\sigma_{ij}^E(x_i, t, T) + \bar{\rho}_{ij}(x_i, T)] \} < \sigma_y(x_i, T) \quad (2.4.)$$

for all loads and temperatures admitted by the loading program, then the structure will shake down. The relation  $\bar{\sigma}(\sigma_{ij}) = \sigma_y$  is the yield condition and  $s$  plays the role of a safety factor. Fig. 2.3. shows how the total stress may be plastically admissible even if  $\sigma_{ij}^E$  does not satisfy the yield criterion.

In the particular case where  $\partial A_{ijkl}/\partial T = 0$ , the above theorem reduces to MELAN's theorem and may be formulated solely in terms of elastic and residual stresses, because a steady plastic deformation is equivalent to a constant residual stress field in this case.

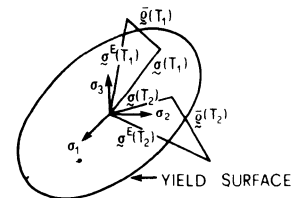


Fig. 2.3.

**Proof :** In order to prove the theorem, we generalize the proof of MELAN's theorem as given by KOITER [K1]. The asymptotic stability of plastic deformations will be demonstrated by using the appropriately generalized positive functional of residual stress and temperature :

$$Y = \frac{1}{2} \int_V A_{ijkl} (\rho_{ij} - \bar{\rho}_{ij})(\rho_{kl} - \bar{\rho}_{kl}) dV + \frac{1}{2} \int_0^t \int_V A_{ijkl} (\rho_{ij} - \bar{\rho}_{ij})(\rho_{kl} - \bar{\rho}_{kl}) dV dt + \frac{1}{2} \int_V \bar{A}_T R^2 T dV \quad (2.5.)$$

The first integral coincides with the original functional as introduced by KOITER [K1]. The second one is introduced because of the variation of the elastic moduli. The third is to keep the whole sum positive.

A dot denotes a differentiation with respect to time,  $\partial_T$  stand for  $\partial \dots / \partial T$ ,  $\rho_{ij}$  designates the field of actual residual stresses. In addition, the following notations are introduced :

$$\begin{aligned}
 |\underline{\alpha}| &= \sqrt{\alpha_{ij} \alpha_{ij}} ; R = \sup_{\{T\}} \sup_{\{\underline{\sigma}(\underline{\sigma}) = \sigma_y\}} |\underline{\sigma}| + \sup_{\{T\}} |\bar{\rho}| + \sup_{\{t\}} |\underline{\sigma}^E| \\
 (2.6.) \quad \bar{A}_T &= \sup_{\{T\}} \sup_{\{|\underline{\sigma}| = 1\}} |\partial_T A_{ijkl} \sigma_{ij} \sigma_{kl}| ; \bar{T} = \sup_{\{t\}} |T| \\
 \bar{A} &= \sup_{\{T\}} \sup_{\{|\underline{\sigma}| = 1\}} A_{ijkl} \sigma_{ij} \sigma_{kl} ; r = \sup_{\{T\}} |\bar{\rho}|
 \end{aligned}$$

The symbol  $\sup [\dots]$  denotes the upper bound of the quantity within brackets when  $T$  varies arbitrarily within the limits prescribed by the loading program. Similarly, the symbols  $\sup_{\{\underline{\sigma}(\underline{\sigma}) = \sigma_y\}} [\dots]$  and  $\sup_{\{|\underline{\sigma}| = 1\}} [\dots]$

$$\{\underline{\sigma}(\underline{\sigma}) = \sigma_y\} \quad \{|\underline{\sigma}| = 1\}$$

denote the respective upper bounds for cases whrn the stress tensor may become any tensor satisfying the condition  $\underline{\sigma}(\underline{\sigma}) = \sigma_y$  or  $|\underline{\sigma}| = 1$ , respectively.

The symbol  $\sup_{\{t\}} [\dots]$  denotes the upper bound of the expression in brackets over all positive times.

It may be shown that the third integral in (2.5.) is always greater than the second one. Indeed, we have

$$\begin{aligned}
 \int_0^t \int_V A_{ijkl} (\rho_{ij} - \bar{\rho}_{ij})(\rho_{kl} - \bar{\rho}_{kl}) dV dt &= \int_0^t \int_V \partial_T A_{ijkl} (\rho_{ij} - \bar{\rho}_{ij})(\rho_{kl} - \bar{\rho}_{kl}) \dot{T} dV dt \\
 &< \int_0^t \int_V \bar{A}_T |\rho - \bar{\rho}|^2 \dot{T} dV dt < \int_0^t \int_V A_T R^2 \dot{T} dV dt < \int_V A_T R^2 \bar{T} dV
 \end{aligned}$$

Hence

$$(2.7.) \quad Y > 0.$$

Differentiating Y with respect to time, we obtain

$$\dot{Y} = \int_V A_{ijkl}(\rho_{ij} - \bar{\rho}_{ij})(\dot{\rho}_{kl} - \dot{\bar{\rho}}_{kl}) dV + \int_V \dot{A}_{ijkl}(\rho_{ij} - \bar{\rho}_{ij})(\rho_{kl} - \bar{\rho}_{kl}) dV \quad (2.8.)$$

From the principle of virtual displacements, it follows that

$$\int_V (\rho_{ij} - \bar{\rho}_{ij}) |\dot{A}_{ijkl}(\rho_{kl} - \bar{\rho}_{kl}) + A_{ijkl}(\dot{\rho}_{kl} - \dot{\bar{\rho}}_{kl}) + \dot{\epsilon}_{ij}^P - \dot{\bar{\epsilon}}_{ij}^P| dV = 0 \quad (2.9.)$$

Hence, from (2.8.) and since, moreover,  $\dot{\bar{\epsilon}}_{ij}^P = 0$ , we have

$$\dot{Y} = - \int_V (\rho_{ij} - \bar{\rho}_{ij}) \dot{\epsilon}_{ij}^P dV = - \int_V [(\sigma_{ij}^E + \rho_{ij}) - (\sigma_{ij}^E + \bar{\rho}_{ij})] \dot{\epsilon}_{ij}^P dV \leq 0. \quad (2.10.)$$

The last inequality follows from the principle of maximum energy dissipation (2.2.8.), since  $(\sigma_{ij}^E + \rho_{ij})$  is the exact stress state corresponding to the plastic strain rates  $\dot{\epsilon}_{ij}^P$  by normality law (1.3.8.), whereas  $(\sigma_{ij}^E + \bar{\rho}_{ij})$  is only an attainable stress state.

This inequality yields, for  $t > 0$

$$Y(t) \leq Y(0) \quad \text{and} \quad Y \rightarrow 0, \quad Y \rightarrow \text{constant for } t \rightarrow \infty \quad (2.11.)$$

From the definitions of  $\rho_{ij} = \sigma_{ij} - \sigma_{ij}^E$ , where  $\sigma_{ij}$  is the actual stress, and the stress field

$$\sigma_{ij}^S = \sigma_{ij}^E + \bar{\rho}_{ij}$$

postulated in the statement of present theorem, we have

$$\rho_{ij} - \bar{\rho}_{ij} = \sigma_{ij} - \sigma_{ij}^S, \quad (2.12.)$$

so that the expression (2.10.) of Y may be written

$$\dot{Y} = - \int_V (\sigma_{ij} - \sigma_{ij}^S) \dot{\epsilon}_{ij}^P dV. \quad (2.13.)$$

Now, if the total amount of plastic work performed in the loading program is acceptable as criterion for assessing the overall deformation, boundedness of the overall deformation may be proved. Indeed, condition (2.4.) proves that

$$s(\bar{\rho}_{ij} + \sigma_{ij}^E) = s \sigma_{ij}^S \quad (2.14.)$$

is a plastically admissible stress field for all loads within the prescribed limits. Hence, by the principle of maximum energy dissipation (2.2.8.)

$$(2.15.) \quad (\sigma_{ij} - s \sigma_{ij}^P) \dot{\epsilon}_{ij}^P \geq 0,$$

and the integrand of (2.10.) satisfies the inequality

$$(2.16.) \quad (\sigma_{ij} - \sigma_{ij}^P) \dot{\epsilon}_{ij}^P \geq \frac{s-1}{s} \sigma_{ij} \dot{\epsilon}_{ij}^P$$

Combination of (2.13.) and (2.16) yields an inequality for the rate at which plastic work  $W_P$  is performed in the loading program :

$$(2.17.) \quad W_P = \int_V \sigma_{ij} \dot{\epsilon}_{ij}^P dV = \frac{s}{s-1} \int_V (\rho_{ij} - \bar{\rho}_{ij}) \dot{\epsilon}_{ij}^P dV \leq \frac{s}{s-1} (-\dot{Y})$$

By integrating with respect to time, we obtain finally an estimate of the total plastic work dissipated during an arbitrary process :

$$(2.18) \quad W_P = \int_0^\infty dt \int_V \sigma_{ij} \dot{\epsilon}_{ij}^P dV = \frac{s}{s-1} \int_V (\bar{A}r^2 + A_T R^2 T) dV .$$

As the plastic work is bounded, the theorem is proved and therefore the shakedown is assured.

### 3.2.4. Bounds of the plastic displacements.

The basic shakedown theorem established in preceding section permits the evaluation of the shakedown multiplier  $\lambda_s$ . If the loads and temperatures applied to the body exceed their shakedown values, it is certain that the structure will become unserviceable. On the other hand, if all loads and temperatures remain within their respective shakedown limits, the only true statement is that the plastic deformations will ultimately cease, but it may very well occur that these displacements are excessive and render the structure unserviceable. It is therefore of a high practical interest to dispose of calculable upper bounds of the magnitude of the plastic displacements produced before shakedown has taken place. Such bounds have been obtained recently by PONTER [P4] and KÖNIG [K3]. We shall not develop these bounds here, but we shall investigate this problem again when we shall discuss, in chapter 5, the application of the general theory to rigidly jointed plane frames. In this application, we shall consider that external loads can fluctuate between their limits  $\lambda P_1 \leq P \leq \lambda P_u$ , but we shall disregard any thermal effect.

In that particular case, the plastic work  $W_p$  given by (2.13.) reduces to

$$W_p = \frac{s}{s-1} \int_v \frac{1}{2} A_{ijkl} \bar{\rho}_{ij} \bar{\rho}_{kl} dV \quad (2.19.)$$

The volume integral represents the strain energy of the residual stresses.

In closing their section, let us mention the Russian book by HOCHFELD, where the elastoplastic behavior of machine elements subjected to temperature variations is discussed in detail [H5].

**PART TWO :**  
**LIMIT ANALYSIS AND DESIGN OF ENGINEERING STRUCTURES**

## 4. GENERALIZED VARIABLES

### 4.1. The Concept of Generalized Variables.

#### 4.1.1. Introduction.

As already mentioned in section (2.1.), we designate by engineering structures those for whose analysis it is permissible and convenient, for practical purposes, to use certain stress resultants and corresponding generalized strains, rather than the general stress and strain tensors. These structures comprise beams, plane walls loaded in their plane, plates and shells. Their study in the case of elastic behavior is the subject of Advanced Mechanics of Materials whereas the general study of elastic bodies belong to the realm of Theory of Elasticity. These structures have in common that, for them, simplifying assumptions regarding the deformations are accepted as direct consequences of the fact that they are “thin” in certain directions. (Normal to the axis of a beam or to the median surface of a wall, a plate or a shell).

For beams, the hypothesis of BERNOULLI (which, in the particular case of pure bending, becomes a rigorous law easily proved by symmetry considerations [M7]) states that plane cross sections remain plane and orthogonal to the deformed material axis. For plates and shells, the natural generalization of BERNOULLI's hypothesis is KIRCHHOFF – LOVE hypothesis, according to which straight segments normal to the median surface remain straight and normal to the deformed median surface.

The reason why these hypotheses procure a great simplification in Limit Analysis is just the same as in the elastic Mechanics of Materials. In this last case, it is well known that the behavior of a beam is known as soon as we know at each point the curvature of its axis. Similarly, the knowledge of the extensions and of the two curvatures and twist of the median surface of an elastic plate or shell is sufficient to furnish the bending and torsional moments as well as the stresses in this plate or shell. Quite similarly, we shall see in the present chapter that the knowledge of the plastic curvature (and eventually twist) rates of the axis or the median surface of a

plastically deformed beam, plate or shell suffices for the complete knowledge of its limit behavior.

#### 4.1.2. Beams without axial force.

Consider a beam whose generic cross section is subjected to a bending moment  $M$  and a shear force  $V$ .

From BERNOULLI hypothesis,, shear strains are found to be zero. The transverse strains due to lateral contraction are uninteresting; so that the only strains to consider are the longitudinal strains  $\epsilon_x$  , given by

$$(1.1.) \quad \epsilon_x = yK$$

where  $y$  is the distance from the neutral axis taken positively downward and  $K$  the curvature of the beam axis.  $K = 1/\rho$  , where  $\rho$  is the radius of curvature.

The strain rate is therefore given by

$$(1.2.) \quad \dot{\epsilon}_x = y \frac{\partial K}{\partial t} = y \dot{K} .$$

The influence of the shear stresses is neglected in the yield condition, which reads simply

$$(1.3.) \quad \sigma_x = \sigma_y$$

Because the state of stress is assumed uniaxial, the power dissipated per unit length of the beam in a plastic region is

$$(1.4.) \quad D = \int_{-h/2}^{+h/2} \sigma_y |\dot{\epsilon}_x| b(y) dy$$

where  $h$  is the depth of the section and  $b(y)$  the width at the level  $y$  (Fig. 1.1.)

With the use of equation (1.3.), equation (1.4.) can be written

$$(1.5.) \quad D = \int_{-h/2}^{+h/2} \sigma_y |y \dot{K}| b(y) dy = |\dot{K}| \int_{-h/2}^{+h/2} \sigma_y |y| b(y) dy = |\dot{K}| M_p$$

where

$$(1.6.) \quad M_p \equiv \int_{-h/2}^{h/2} \sigma_y |y| b(y) dy$$

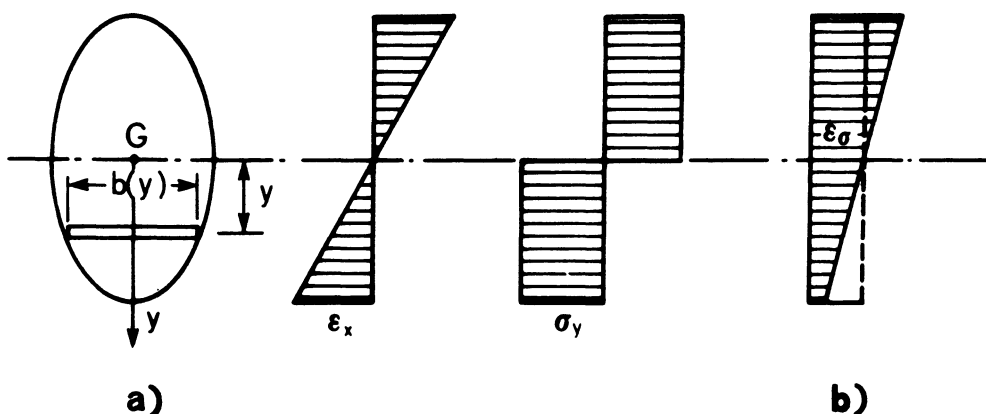


Fig. 1.1.

is called the full plastic moment capacity or, simpler, the plastic moment. For all layers of the lower half of the section,  $\dot{\epsilon}_x$  is positive with  $y$  and  $\sigma_x = +\sigma_y$ , whereas for all layers of the half of the section  $\dot{\epsilon}_x$  is negative with  $y$  and  $\sigma_x = -\sigma_y$ . The diagram of the longitudinal stresses  $\sigma_x$  over the cross section is thus birectangular.

Formula (1.6.) may be written

$$(1.7.) \quad M_p = \sigma_v Z$$

with

$$(1.8.) \quad Z = \int_{-h/2}^{+h/2} |y| b dy$$

The quantity  $Z$ , called the **plastic modulus**, has the dimension  $L^3$  and is equal to twice the statical moment  $S_{nx}$  of one half of the section with respect to the neutral axis.

For a rectangular section with depth  $h$  and width  $b$ , we have  $Z = bh^2/4$  and  $M_p = \sigma_y \frac{bh^2}{4}$ . It is useful to compare  $M_p$  with the yield moment

$$(1.9.) \quad M_y = \sigma_y S,$$

which is the maximum moment the beam can sustain purely elastically. As  $S = \frac{bh^2}{6}$ , we see that, for a rectangular section

$$\frac{M_p}{M_v} = 1.5 \text{ .}$$

The ratio

$$f = M_p / M_y , \quad (1.10.)$$

called the **shape factor**, provides a convenient means to estimate the strength benefit derived from the passage from the purely elastic bitriangular stress distribution (moment  $M_y$ ) to the fully plastic birectangular one (moment  $M_p$ ).

It is easy to evaluate  $f$  from the formula

$$f = \frac{Z}{S} = \frac{2S_x}{S} \quad (1.11.)$$

derived from (1.10.), taking account of (1.9.) and (1.7.). For the rolled I and H sections,  $f$  varies from about 1.10 to 1.25, and it is customary, in practical applications, to use the value  $f = 1.12$ .

For a solid circular section,  $f = 16/3 \pi$ ; for a very thin-walled hollow circular tube,  $f = 4/\pi = 1.27$ .

The rate of dissipation for the whole structure is, from (1.5.)

$$D_t = \int_{\text{Struct}} |K| M_p dS \quad (1.12.)$$

From elementary Mechanics of Materials, it is known that, for a I rolled profile, the actual moment-curvature diagram has the shape of figure 1.2.a, where

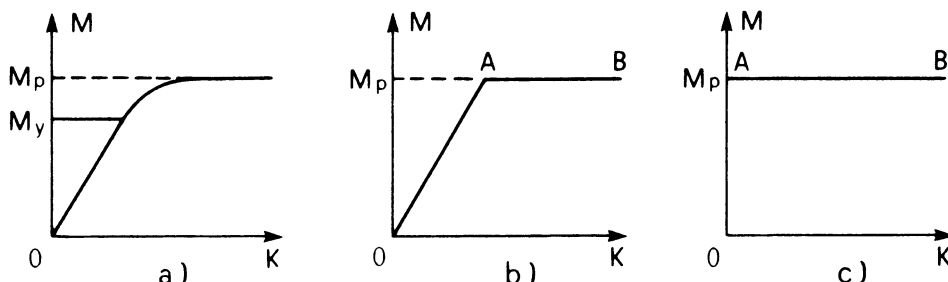


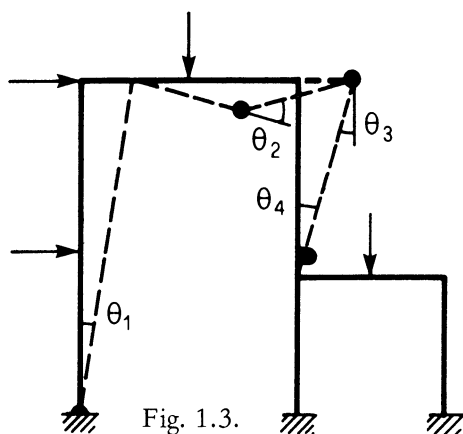
Fig. 1.2.

$M_p / M_y \approx 1.12$ . The shape of this diagram shows that the curvature increases very fast as soon as the yield moment is exceeded and tends to infinity for  $M$  tending to  $M_p$ . This means that, in a plane rigid-jointed structure composed of beams and columns and loaded in its plane, the plastic deformations are concentrated in narrow zones around the various sections where  $M$  is a local maximum equal to the plastic

moment of the bar.

If the small part of the web in the resistance to bending is disregarded, the I profile may be replaced by a sandwich beam composed only of two thin flanges. With this simplification,  $f = M_p / M_y = 1$  and the  $(M, K)$  diagram becomes the contour OAB of fig. 1.2.b), identical in shape to the stress-strain diagram. If, finally, the elastic deformations are neglected, the  $(M, K)$  diagram becomes contour OAB of figure 1.2.c).

In this rigid plastic approximation, the plastic deformation of the framed structures are concentrated in the sections where  $M = M_p$ , so that a discontinuity of slope occurs at these “critical” sections. One says that “plastic hinges” have formed in these sections. In this simplified model, the deformed rigid-jointed frame at collapse is replaced by a system of rigid bars linked by friction pins, such that motion of the system takes place through rotation of the pins (fig. 1.3.).



Let us call  $\theta_i$  ( $i = 1, 2, 3, 4$ ) the angle of rotation at the plastic hinges. The curvature rate  $K$  is everywhere zero except at the locations of the plastic hinges, where  $K$  is infinite. The function  $K$  is therefore a sum of DIRAC functions and formula (1.12.) transforms into

$$(1.13.) \quad D_t = \sum M_{pi} |\dot{\theta}_i|$$

Summarizing, we see that, here :

1. The yield condition reduces to  $|M| = M_p$  and the flow rule to  $\text{sign } \theta_i = \text{sign } M_i$ , or  $M_i \theta_i \geq 0$  ;
2. The stress field reduces to the  $M$  diagram ;
3. The strain rate field reduces to the (discontinuous) distribution of the rate of curvature.

#### 4.1.3. Arches

In shallow arches, the axial force  $N$  is considerable, and the corresponding part of the power or dissipation cannot be neglected. Calling  $\epsilon_0$  the strain at the axis, we see that the longitudinal strain at the level  $y$  is given by the relation

$$\epsilon(y) = y K + \epsilon_0 \quad (1.14.)$$

The total rate dissipation is

$$D_t = \int_{\text{arch}} (M \dot{K} + N \dot{\epsilon}_0) dS, \quad (1.15.)$$

Where  $M$  and  $N$  combine to produce complete plastification of the section. Interaction curves  $M$  versus  $N$  of various sections may be found in textbooks of Mechanics of Materials or Limit Analysis [M7].

Assuming that the shear force does not influence yielding, the functions  $M$ ,  $N$ ,  $\dot{K}$  and  $\dot{\epsilon}_0$  of the abscissa  $s$  are sufficient to solve the problem.

#### 4.1.4. Simple plate and shell examples.

In both plates and shells, the thickness  $t$  must be small compared to the other dimensions. A plate has a plane median surface and is subjected only to forces normal to this median plane (when the applied forces are parallel to this plane, the structure is called a disk). A shell has a median surface with at least one finite radius of curvature. A membrane is a shell with no bending rigidity.

In the particular case of circular plates loaded axisymmetrically (fig. 1.4.) the torsional moments  $M_{r\theta}$  vanish by symmetry on the radial and circumferential sections, so that  $M_r$  and  $M_\theta$  are principal moments, which depend only of the coordinate  $r$ . By KIRCHHOFF's assumption :

$$\dot{\epsilon}_r = z \dot{K}_r, \quad \dot{\epsilon}_\theta = z \dot{K}_\theta \quad (1.16.)$$

where  $K_r$  and  $K_\theta$  are the radial and circumferential (principal) rates of curvatures. The dissipation per unit area of the median plane is, by analogy to the beams,

$$D = M_r \dot{K}_r + M_\theta \dot{K}_\theta \quad (1.17.)$$

In relation (1.17.),  $M_r$  and  $M_\theta$  must combine to completely plastify the volume element  $tr dr d\theta$  represented at fig. 1.4.

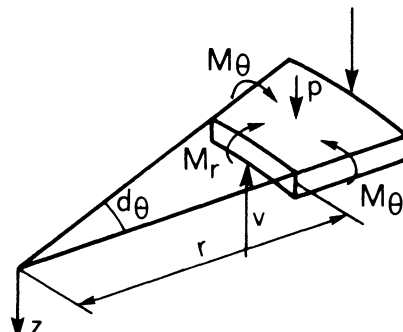


Fig. 1.4.

Since the yield condition can be expressed in terms of  $M_r$  and  $M_\theta$  only, the functions  $M_r, M_\theta, \dot{K}_r, \dot{K}_\theta$  of  $r$  are sufficient for the limit analysis of the plate.

Usually, in a plate referred to cartesian coordinates, the state of bending is defined by the moment tensor, which is composed of two bending moments,  $M_x$  and  $M_y$ , and two torsional moments,  $M_{xy}$  and  $M_{yx}$ , equal by the reciprocity of shear stresses. By KIRCHHOFF's assumption, the strains are proportional to the curvatures  $K_x$ ,  $K_y$ , the twist  $K_{xy}$  and to the distance  $Z$  to the median plane

$$(1.18.) \quad \epsilon_x = z K_x, \quad \epsilon_y = z K_y, \quad \gamma_{xy} = z K_{xy}.$$

The dissipation per unit area of the median plane is

$$(1.19.) \quad D = M_x \dot{K}_x + M_y \dot{K}_y + 2 M_{xy} \dot{K}_{xy}.$$

#### 4.2. Choice and General Properties of the Generalized Variables.

As indicated in the introduction of present chapter (section 4.1.1.), our aim is to solve problems of Limit Analysis of "thin" structures by using as kinematical variables the rates of extension and curvature of the axis of the beam or of the median surface of the disk, plate or shell, which describe the collapse mechanisms of these structures. We shall denote these kinematical variables by symbols  $q_1, q_2, \dots, q_n$  and call them the **generalized strain rates**.

Now, we wish to keep the advantage obtained by LAGRANGE in his Analytical Mechanics by introducing his generalized forces  $Q_i$  and displacements  $q_i$ , namely to preserve the fundamental notion of **energy**. We are thus compelled here to take, as generalized stresses  $Q_i$  associated to the  $\dot{q}_i$ , the stress-type variables which preserve the fundamental notion of **power**, that is which are such that the specific rate of dissipation is still given by

$$(2.1.) \quad D = Q_1 \dot{q}_1 + Q_2 \dot{q}_2 + \dots + Q_n \dot{q}_n = Q_i \dot{q}_i$$

and representable, in the  $Q_i$  space with superimposed  $\dot{q}_i$  space, by the scalar product of vector  $Q_i$  by vector  $\dot{q}_i$ .

We now call "reactions" the generalized stresses that do not a priori vanish for reasons of symmetry or equilibrium and that nevertheless do not appear in equation (2.1.) because they correspond to generalized strain rates that, in the considered

problem, have been assumed to vanish throughout the structure. For example, in beams, plates and shells, transversal shear forces are always reactions because normals are assumed to remain normal to the deformed median surface.

Not only is it always possible to solve problems of limit analysis using only the generalized variables (with no reference to the reactions), but it is also the most efficient way for solving problems. To that purpose, the reactions must be eliminated from the yield condition, which becomes

$$F(Q_1, Q_2, \dots, Q_n) = K^2, \quad (2.2.)$$

where  $K$  is an appropriate constant for a given point of the axis of the beam or the median surface of the shell. This elimination process is discussed in the following section.

The fundamental advantage of the generalized variables  $Q_i$  and  $\dot{q}_i$  will now become apparent. As the notion of power is preserved, the demonstrations of the three basic theorems of Section 2.3., of the theorems about shakedown (section 3.3.) and of the other properties established in Sections 1.3.4., 2.2.4. and 2.4. (convexity of the yield surface, law of normality, constancy of the stresses during plastic flow, FEINBERG's theorem, etc. . . .) are also preserved. It suffices to replace everywhere in these demonstrations  $\sigma_{ij}$  by  $Q_i$  and  $\dot{\epsilon}_{ij}$  by  $\dot{q}_i$  to obtain the demonstrations of the same theorems expressed in terms of generalized stresses and strain rates.

Practically, that means that all the fundamental theorems, stated before for bodies of general shape in the language of Mechanics of continua, furnish the corresponding theorems written in the language of the Mechanics of Materials (approximate theory of beams, disks, plates and shells) when the appropriate stress resultants are inserted in place of the general stress components and the corresponding generalized strain rates in place of the strain rate components. Thus, for example, a lower bound will be obtained by showing that a field of stress resultants  $Q_1, Q_2, \dots, Q_n$  nowhere violates the appropriate yield condition.

#### 4.3. Elimination of the Reactions..

##### 4.3.1. Introduction.

Consider a structural element like a beam, plate and shell and denote by  $Q_1, \dots, Q_n$ , is the  $n$  stress – type variables acting on it. Suppose first that none is a

reaction ; the yield condition of this element can then be written in the form (2.2.). As demonstrated in section 4.2. the normality law applies to the surface with equation (2.2.) represented in the generalized stress space  $(Q_1, \dots, Q_i, \dots, Q_n)$  with superimposed generalized strain rate space  $(\dot{q}_1, \dots, \dot{q}_i, \dots, \dot{q}_n)$  and we have

$$(3.1.) \quad \dot{q}_i = \frac{\partial F}{\partial Q_i} \quad (\mu \geq 0) \quad (i = 1, \dots, n)$$

Suppose now that, on the contrary,  $(n-K)$  the generalized strain rates  $(\dot{q}_{K+1} = \dot{q}_{K+2} = \dots = \dot{q}_n)$  are zero.

According to the normality law (3.1.), equations

$$(3.2.) \quad \dot{q}_{K+1} = \dot{q}_{K+2} = \dots = \dot{q}_n = 0$$

will select a set of points on the yield surface (2.2.) where the projections of a normal vector on the axes  $(k+1), (k+2), \dots, n$ , vanish. This set of points forms part of the original yield surface (2.2.). By projecting this part on the  $(Q_1, \dots, Q_K)$  space, one obtains the simplified yield condition

$$(3.3.) \quad \Phi(Q_1, \dots, Q_K) = K^2$$

that contains only the active generalized stresses, and none of the reactions  $Q_{K+1}, \dots, Q_n$ .

#### 4.3.2. Direct elimination of the reactions through the use of the dissipation function.

We have seen in section 1.3.4. how we could generate the yield surface as the envelope of the hyperplanes normal to  $e$  and distant  $D(\dot{e})$  from the origin. For a given problem where the "active" generalized strain rates are  $\dot{q}_1, \dots, \dot{q}_K$ , the same technique may obviously be applied in the stress space of the  $Q_1, \dots, Q_K$ , if we know the dissipation function  $D(\dot{q}_1, \dots, \dot{q}_K)$ . It may be shown [S3] that the surface obtained in this way is identical with the surface (3.3.) obtained by projection, and that, consequently, the normality law applies to the latter surface.

#### 4.3.3. Values taken by the reactions.

The reactions correspond to generalized strain rates equal to zero.

These can vanish, either :

- a) because of the very definition of the structure, or
- b) because of special symmetry conditions.

The most important cases of the first kind is a beam obeying BERNOULLI assumption or a plate, or shall, obeying KIRCHHOFF–LOVE assumption. In all these cases, there cannot exist a transversal rate of shear. Because of the normality law, the yield surface is a cylinder with its axis parallel to the shear force axis (fig. 3.1.).

In that case, the shear forces may take any value. They cannot be determined from mechanism and normality law, but may possibly be obtained from equilibrium conditions. (See section 7.2. for an example discussed in detail).

If, on the contrary, the generalized stress variable is a reaction because of special symmetry conditions, it is assigned a definite value deduced from the normality law. For example, in plane stress,  $\dot{\epsilon}_2 = 0$  imposes  $\sigma_2 = \sigma_1/2 = 1.154 \sigma_y/2$  for the MISES yield condition (fig. 3.2. (a)) or  $0 < \sigma_2 < \sigma_y$  (fig. 3.2.(b)) for the TRESCA condition. But, at the same time, the equilibrium equations do not contain these reactions because of the special symmetry conditions above.

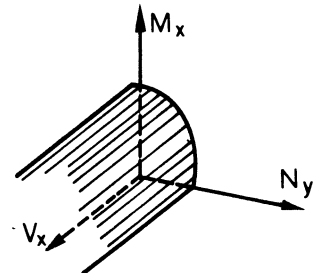


Fig. 3.1.

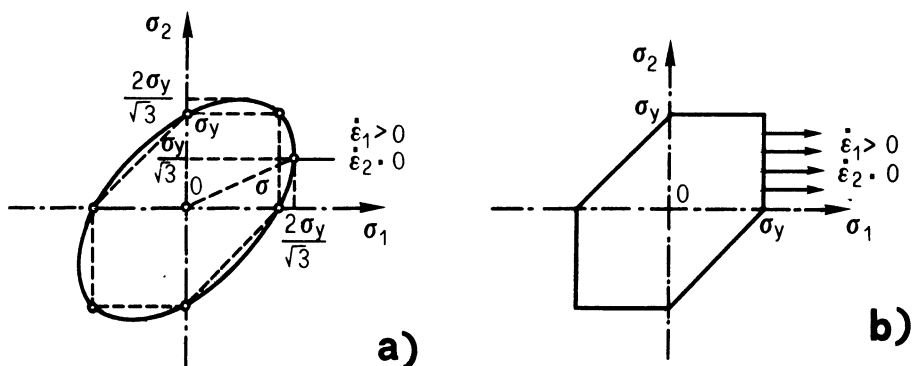


Fig. 3.2.

Hence, when equilibrium and yield conditions are satisfied in terms of generalized stresses only, they can also always be satisfied when reactions are considered. Moreover, it is known that the equilibrium equations can be obtained from the principle of virtual work by a variational procedure. No reaction will enter the

virtual work equation. This remark proves that it is always possible to eliminate the reactions from the equations of equilibrium.

#### 4.4. Yield Conditions in Generalized Stresses.

##### 4.4.1. Introduction.

It is possible to establish the most general yield condition (2.2.) for a shell in metal or reinforced concrete and then to obtain the simplified yield surfaces valid for particular problems by section or projection [S2]. However, we shall prefer, in what follows, to obtain the simplified yield condition directly. To this purpose, there are several methods available. We shall consider two of them. The first one is an integration method which bases directly on the definition of generalized stresses as resultants of the actual stresses through the thickness. The second is the method of lower and upper bounds, which brackets the yield surface between lower and upper bounds furnished by the fundamental theorems.

##### 4.4.2. Method by integration.

The method by integration may be summarized as follows:

By KIRCHHOFF–LOVE assumption that normals to the mean surface remain normals after deformation, the generalized strain rates of the median surface are directly related to the components of the strain rate tensor at any level through the thickness. Then, the strain rate tensor is related to the stress tensor by the normality law. Integration over the thickness furnishes the yield condition in generalized stresses.

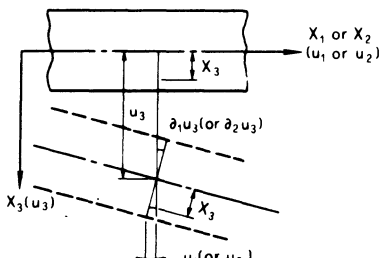


Fig. 4.1.

We shall illustrate this method by considering a metalplate transversely loaded whose material obeys the VON MISES or TRESCA yield condition.

We assume with KIRCHHOFF that material normals remain normal to the deformed median plane and that the transversal displacements  $u_3$  are small with respect to the constant thickness  $t$ .

The field of displacements in the deflected plate is given by (fig. 4.1.)

$$u_1 = -x_3 \frac{\partial u_3}{\partial x_1}$$

$$u_2 = -x_3 \frac{\partial u_3}{\partial x_2} \quad (4.1.)$$

$$u_3 = u_3(x_1, x_2)$$

Using the classical expression of the strain tensor

$$\epsilon_{ij} = \frac{1}{2} (\partial_i u_j + \partial_j u_i),$$

we obtain

$$\begin{aligned} \epsilon_1 &= -x_3 \frac{\partial^2 u_3}{\partial x_1^2}, & \epsilon_2 &= -x_3 \frac{\partial^2 u_3}{\partial x_2^2}, & \epsilon_3 &= 0 \\ \epsilon_{12} &= -x_3 \frac{\partial^2 u_3}{\partial x_1 \partial x_2}, & \epsilon_{13} &= \epsilon_{23} &= 0 \end{aligned} \quad (4.2.)$$

or, in more compact form,

$$\epsilon_{ij} = -x_3 \partial_{ij} u_3 \quad (i, j = 1, 2). \quad (4.3.)$$

Hence the various horizontal lamellae of thickness  $dx_3$  composing the plate are in a state of plane stress and subjected to stresses  $\sigma_{11}$ ,  $\sigma_{22}$ ,  $\sigma_{12}$ , whose direct resultants through the thickness are zero, and whose moment resultants are given by the general formula

$$M_{ij} = \int_{-t/2}^{+t/2} \sigma_{ij} x_3 dx_3 \quad (i, j = 1, 2). \quad (4.4.)$$

It is clear that the three non-zero components  $M_{11}$ ,  $M_{22}$ ,  $M_{12}$ , form as the  $\sigma_{ij}$ , a plane tensor representable by a unique MOHR circle.

The energy dissipated per unit area of the median plane is

$$\mathcal{E} = \int_{-t/2}^{+t/2} \sigma_{ij} \epsilon_{ij} dx_3. \quad (4.5.)$$

Introducing (4.3.) into (4.5.), we obtain :

$$\mathcal{E} = -\partial_{ij} u_3 \int_{-t/2}^{+t/2} \sigma_{ij} x_3 dx_3 \quad (4.6.)$$

Within the framework of small deflection theory, the quantities  $-\partial_{11}u_3, -\partial_{22}u_3$  and  $-\partial_{12}u_3$  are respectively the two curvatures and the geometric torsion of the deflected median plane, and form together a plane tensor

$$(4.7.) \quad K_{ij} = \partial_{ij} u_3 \quad (i, j = 1, 2)$$

called the curvature tensor. With the definitions (4.4.) of the moments, relation (4.6.) can therefore be written

$$(4.8.) \quad \mathcal{E} = M_{ij} K_{ij}$$

and the specific power of dissipation is

$$(4.9.) \quad D = M_{ij} \dot{K}_{ij}.$$

The three generalized stresses are the moments  $M_{ij}$  and the corresponding generalized strain rates are the three  $\dot{K}_{ij}$ .

Because we have shown above that each layer of thickness  $dx_3$ , is in plane stress, the yield condition is

$$(4.10.) \quad \bar{\sigma}(M_{ij}) = \sigma_y.$$

On the other hand, (4.3.) may be written, with help of (4.7.)

$$(4.11.) \quad \epsilon_{ij} = x_3 K_{ij}$$

whence

$$(4.12.) \quad \dot{\epsilon}_{ij} = x_3 \dot{K}_{ij}.$$

This shows that the strain rate vector in the six-dimensional space considered in section 1.3.3. has components proportional to  $x_3$ . Hence, the local flow mechanism, as defined in section 1.3.4., is the same for every point of the lower half of the plate ( $x_3 \geq 0$ ). If we now assume that the yield surface with equation (4.10.) is symmetric with respect to the origin, (as it is the case for the VON MISES and TRESCA condition, see figure 1.2.4.) the stress point P remains fixed (fig. 4.2.) for all the laminae of the lower half plate. For the laminae of the upper half plate,  $x_3$  changes sign, and the unit vector  $\underline{0q}$  representing the flow mechanism changes its sense. The corresponding stress point P' goes to a position symmetric with respect to the origin (fig. 4.2.) and the stress state, which was  $\sigma_{ij}$  becomes  $(-\sigma_{ij})$ .

Therefore, the components  $\sigma_{11}, \sigma_{22}, \sigma_{12}$  are constant in each half-plate, and the

components of the moment tensor (4.4.) are simply

$$M_{ij} = \sigma_{ij} \int_{-t/2}^{+t/2} |x_3| dx_3 = \sigma_{ij} \frac{t^2}{4} \quad (4.13.)$$

Because moments are seen to be proportional to the stress components, the yield surface in the plane space of moments will have the same form as in the plane space of stress components. (fig. 1.2.5.).

It often proves convenient to use non-dimensional, or reduced, variables. Stress components are rendered nondimensional by division by  $\sigma_y$ , and relation (4.10.) takes the "canonic" form

$$\Phi\left(\frac{\sigma_{ij}}{\sigma_y}\right) = 1. \quad (4.14.)$$

Similarly, we define reduced moments

$$m_{ij} = \frac{M_{ij}}{M_p} \quad (i, j = 1, 2) \quad (4.15.)$$

where

$$M_p = \sigma_y \frac{t^2}{4} \quad (4.16.)$$

is the plastic moment for uniaxial bending. From (4.13.), (4.15.) and (4.16.), we deduce

$$m_{ij} = \frac{\sigma_{ij}}{\sigma_y} \quad (i, j = 1, 2). \quad (4.17.)$$

With these relations, yield condition (4.14.) becomes

$$\Phi(m_{ij}) = 1 \quad (4.18.)$$

We see that the yield condition (4.18.) in reduced moments is identical to that in reduced stresses.

For example, VON MISES condition (1.2.19.) for plane stress, using reduced stresses, becomes

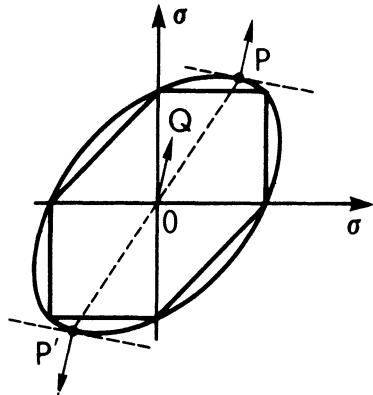


Fig. 4.2.

$$(4.19.) \quad \left(\frac{\sigma_{11}}{\sigma_y}\right)^2 + \left(\frac{\sigma_{22}}{\sigma_y}\right)^2 - \frac{\sigma_{11}}{\sigma_y} \frac{\sigma_{22}}{\sigma_y} + 3\left(\frac{\sigma_{12}}{\sigma_y}\right)^2 = 1 .$$

Hence, the corresponding yield condition for a plate is simply

$$(4.20.) \quad m_{11}^2 + m_{22}^2 - m_{11}m_{22} + 3m_{12}^2 = 1 .$$

Similarly, TRESCA's condition (1.2.17.) gives

$$(4.21.) \quad \max [|m_1|, |m_2|, |m_1 - m_2|] = 1 .$$

#### 4.4.3. Method of lower and upper bounds.

Let us consider an isolated element of a beam, plate or shell (fig. 4.3.).

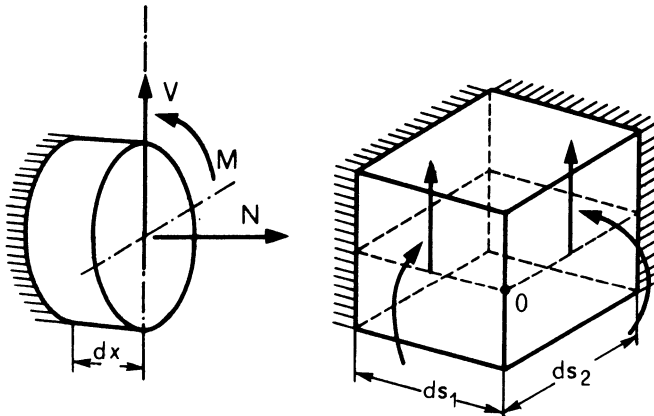


Fig. 4.3.

This element may be regarded as a free body subjected to the resultant forces and couples of the stresses transmitted by neighboring elements, and these actions may be "exteriorized", that is regarded as directly applied to the considered element. Any combination of stress resultants that causes the element to yield represents a point of the yield locus in generalized coordinates. Now, we can use the two fundamental theorems of Limit Analysis (sections 2.3.1. and 2.3.2.) to obtain informations about the shape of this yield locus. Indeed.

- 1) Any statically admissible stress distribution on the element will furnish generalized stresses that will be the coordinates of a point on or within the yield surface ;

- 2) Any kinematically admissible strain rate distribution through the element will be associated, through the normality law, with generalized stresses that will be the coordinates of a point on or outside the yield surface.

The yield surface can thus be bounded in this way from the interior and exterior. We illustrate this method by considering :

### The yield locus of a cylindrical shell without axial force.

Consider the cylindrical shell represented by fig. 4.4.. It is subjected to an internal pressure that may depend only on the coordinate  $x$ . Because of axisymmetry and the absence of axial load, the only non-vanishing stress resultants and moments are those shown in fig. 4.4. Shear force  $V_x$  is a reaction because of KIRCHHOFF-LOVE assumption and bending moment  $M$  also because the circumferential rate of curvature  $\dot{K}_\theta$  is zero by symmetry (to the first order).

Stresses  $\sigma_x$  and  $\sigma_\theta$  are principal and TRESCA's yield condition may be written

$$\max[|\sigma_x|, |\sigma_\theta|, |\sigma_x - \sigma_\theta|] = \sigma_y \quad (4.22.)$$

Let us introduce the dimensionless variables

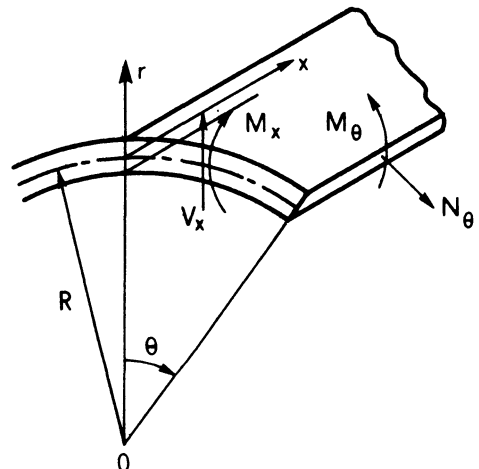


Fig. 4.4.

$$\begin{aligned} m_x &= \frac{M_x}{M_p} = \frac{M_x}{\sigma_y t^2/4} \quad \text{and} \\ n_\theta &= \frac{N_\theta}{N_p} = \frac{N_\theta}{\sigma_y t} . \end{aligned} \quad (4.23.)$$

As the stress  $\sigma_x$  are equilibrated by a moment  $M_x$  alone, the algebraic area of their diagram through the thickness must be zero. Therefore, the only two possibilities are those represented at fig. 4.5(a) and (b).

Consider the first possibility fig. 4.5.(a) . For the stress point to be on TRESCA's

hexagon shown in the insert of fig. 4.7. and  $N_\theta$  to be maximum, the distribution of the  $\sigma_\theta$  must be that on the right side of fig. 4.5.(a), showing the three different plastic "regimes" D, A, B, through the thickness. Regime A is supposed to extend on a layer of thickness  $\alpha t$  with  $0 \leq \alpha \leq 1/2$ . Visibly,  $m_x = 1$  while  $0 \leq n_\theta \leq 1/2$ . This relationship is represented by the horizontal segment 1B in the reduced variables  $m_x$ ,  $n_\theta$  of diagram fig. 4.7..

Consider now the second type of distribution of  $\sigma_x$  stresses Fig. 4.5.(b). Again, we choose the  $\sigma_\theta$  stresses corresponding to yield and try to maximize the value of  $N_\theta$ . For this reason, we assume that the upper layer of the shell is in regime D (with  $\sigma_\theta = 0$ ) and not in regime DE ( $\sigma_\theta < 0$ ), because this would diminish the value of  $N$ . We obtain from the figure

$$(4.22.) \quad m_x = 1 - 4 \alpha^2 \quad n_\theta = \frac{1}{2} + \alpha.$$

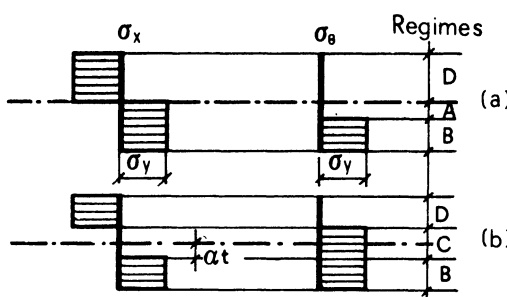


Fig. 4.5.

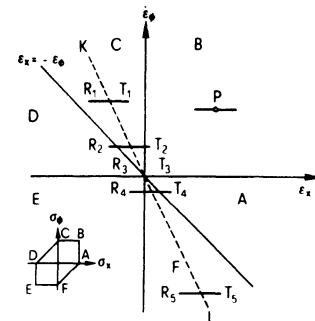


Fig. 4.6.

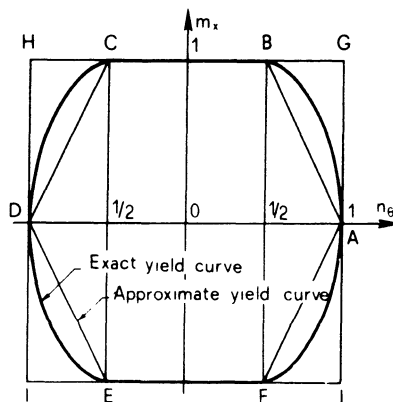


Fig. 4.7.

Elimination of the parameter  $\alpha$  between these equations gives the parabola with vertical axis

$$m_x = 1 - 4 \left( n_\theta - \frac{1}{2} \right)^2 , \quad (4.25.)$$

which passes through A and B (fig. 4.7.). The full yield locus in the first quadrant is therefore the curve 1BA. Since similar results holds in each quadrant, the complete yield curve is obtained by symmetry ; it is the solid curve ABCDEFA of fig. 4.7.

Note that, in the case of fig. 4.5.a., we have as reaction the reduced circumferential moment

$$m_\theta = \frac{1}{2} - 2 \alpha^2 \quad \text{with } 0 < \alpha < 1/2 .$$

This expression remains valid in the case of fig. 4.5.b.

As said in Section 4.3.3.,  $m_\theta$  does not play any role in the problem based on the consideration of generalized stresses and strain rates. This will be seen on a practical example in section 7.2.

The solid curve of fig. 4.7. was deduced from purely static considerations. It represents therefore – according to the statical theorem – only a lower bound of the true (reduced) yield locus. To prove that this curve is the exact yield locus, we must be able to associate, to the stress distributions of fig. 4.5., corresponding strain rate distributions. To do this, we consider the strain rates  $\dot{\epsilon}_x$ ,  $\dot{\epsilon}_\theta$  which are associated to  $\sigma_x$  and  $\sigma_\theta$  respectively and superpose these coordinates to  $\sigma_o$  and  $\sigma_\theta$  in the TRESCA diagram of fig. 4.6.

KIRCHHOFF–LOVE assumption gives in general

$$\dot{\epsilon}_x = \dot{\epsilon}_{x_0} + z \dot{K}_x, \quad \dot{\epsilon}_\theta = \dot{\epsilon}_{\theta_0} + z \dot{K}_\theta , \quad (4.26.)$$

where  $\dot{\epsilon}_{x_0}$  and  $\dot{\epsilon}_{\theta_0}$  are the rates of extension and  $\dot{K}_x$ ,  $\dot{K}_\theta$ , the rates of curvature of the middle surface of the shell. Now, we have seen in beginning that, in the problem under discussion,  $\dot{K}_\theta$  was zero because of axisymmetry.

Therefore, (4.26.) reduces to :

$$\dot{\epsilon}_x = \dot{\epsilon}_{x_0} + z \dot{K}_x, \quad \dot{\epsilon}_\theta = \dot{\epsilon}_{\theta_0} . \quad (4.27.)$$

This shows that, in the  $\dot{\epsilon}_x, \dot{\epsilon}_\theta$  plane of fig. 4.6., if the strain rates at the middle surface are represented by the point P, then the strain rates across the thickness will be represented by a line segment of length  $2tK_x$ , which is centered at P and parallel to the  $\dot{\epsilon}_x$  axis. But, because the axial force  $N_x$  must vanish, there must be as many layers in regime D as in regime B (see the insert fig. 4.6.). In other terms, the strain rate point P for the middle surface must lie on the dashed line KL.

We can now distinguish five possibilities, represented in fig. 4.6. by the line segments  $R_1T_1$  to  $R_5T_5$ .  $R_1T_1$  implies that  $\sigma_x = 0, \sigma_\theta = \sigma_y$  across the thickness, and leads to the reduced stress resultants  $m_x = 1, n_\theta = 1$ . The segment  $R_2T_2$  corresponds (for  $K_x > 0$ ) to the stress distribution

$$(4.28.) \quad \left\{ \begin{array}{lll} \sigma_x = -\sigma_y, & \sigma_\theta = 0, & -t \leq z \leq -\alpha t \\ \sigma_x = 0, & \sigma_\theta = \sigma_y, & -\alpha t \leq z \leq +\alpha t \\ \sigma_x = \sigma_y, & \sigma_\theta = \sigma_y, & \alpha t \leq z \leq t. \end{array} \right.$$

This is precisely the second stress distribution (fig. 4.5.b.) that we have discussed above in the static approach. Similarly, it can be shown that the line segment  $R_3T_3$  corresponds to the stress distribution of fig. 4.5.a.  $R_4T_4$  and  $R_5T_5$  corresponds to distributions symmetrical to those of fig. 4.5. Thus, we see that present kinematic approach leads again to the yield curve of fig. 4.7., which is therefore the exact yield curve in generalized coordinates.

## 4.5. Piecewise Linear Yield Surfaces.

### 4.5.1. Advantage of a piecewise yield surface.

A piecewise yield condition is very attractive from the mathematical point of view. Indeed, if the yield surface consists of plane faces, as long as the stress point remains on a given plane, the stress vector at yield retains the same direction normal to that plane (fig. 5.1.) and the flow mechanism does not change. All possible flow mechanisms can thus be classified into a finite number of plastic “regimes”, each of them corresponding to the contact of the stress point P with one plane, one edge or one vertex of the yield polyhedron (fig. 5.1.). As we shall see in detail in the example of section 7.2., the differential equations of the problem are linear and easy to integrate, while they would be non linear if the yield surface were curved. These reasons explain the preference given to TRESCA’s yield condition over the yield

condition of VON MISES when analytical solutions are sought(\*). Let us observe, however, that, when generalized stresses are used, the linearity of TRESCA's yield condition does not guarantee a piecewise linear yield surface in terms of generalized stresses. Indeed, we have found parabolic segments in the yield curve established in Section 4.4.3. In this case, the exact yield surface must then be replaced by a polyhedron, either inscribed (polygon ABCEDFA of fig. 4.7.), or circumscribed (polygon GHIJG of fig. 4.7.).

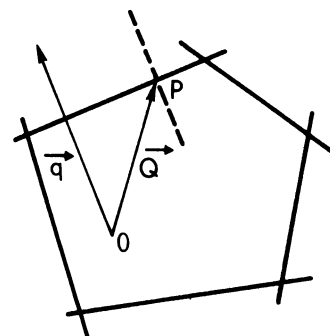


Fig. 5.1.

#### 4.5.2. Influence on the limit load of the linearization of the yield condition.

To have a graphical support, consider a yield condition that involves only two generalized stresses  $Q_1$  and  $Q_2$ . Let the exact yield curve be represented by the full line in fig. 5.2., and let  $\lambda_1$  be the corresponding exact limit multiplier for a given proportional loading. If, instead of the exact yield curve  $e$ , the inscribed polygon  $i$  (in dashed lines) is used, the state of the stress at collapse for polygon  $i$  is statically admissible for curve  $e$ . If the corresponding limit multiplier is  $\lambda_i^-$ , the static theorem yields the inequality

$$\lambda_i^- < \lambda_1. \quad (5.1.)$$

If  $\lambda_c^-$  is a statically admissible multiplier for  $i$ , we have

$$\lambda_c^- < \lambda_i^- . \quad (5.2.)$$

On the other hand, the use of the circumscribed polygon  $c$  would give

$$\lambda_1 < \lambda_c^+ . \quad (5.3.)$$

If  $\lambda_c^+$  is a kinematically admissible multiplier for  $c$ , the kinematic theorem proves that

$$\lambda_c^+ < \lambda_c^- . \quad (5.4.)$$

(\*) On the contrary, VON MISES yield condition could be preferred, because of its continuity, in the numerical solution of limit analysis problems on electronic computers.

Inequalities (5.1.) to (5.4.) may be combined in the continued inequality

$$(5.5.) \quad \lambda_i^- < \lambda_i < \lambda_l < \lambda_c < \lambda_c^+.$$

Note that no definite statements can be obtained about statically admissible multipliers for  $c(\lambda_c^-)$  or kinematically admissible multipliers for  $i(\lambda_i^+)$ . Note also that the scale of the yield locus and the limit multiplier of a structure are directly proportional to the yield stress  $\sigma_y$  of the material. If  $\sigma_y$  is multiplied by a factor  $k$  greater or smaller than unity, the yield surface is similarly expanded or contracted with respect to the origin. Hence, polygons  $i$  and  $c$  are homothetical with factor  $k$  and we have for the exact limit multipliers  $\lambda_c$  and  $\lambda_i$  which correspond to the curves  $c$  and  $i$

$$(5.6.) \quad \lambda_c = k \lambda_i.$$

If we want to obtain bounds on  $\lambda_l$ , it suffices therefore to calculate  $\lambda_i$ , and then to determine the lowest expansion factor  $k$  that makes polygon  $i$  circumscribed to  $e$ . Note also that, if, in the problem at hand, the stress point, for all plastic regions of the structure, remains on a certain part of curve  $e$ , as  $AB$  in fig. 5.3., the yield

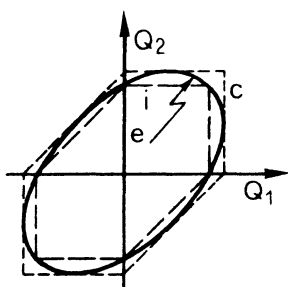


Fig. 5.2.

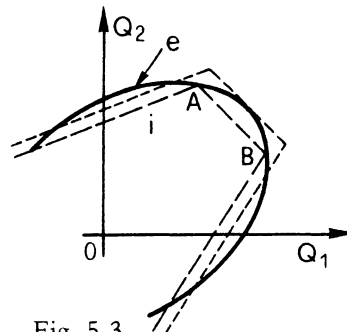


Fig. 5.3.

Polygon obtained by expansion of polygon  $i$  must be external to curve  $e$  in that part only. This remark enables us to use the smallest possible expansion factor  $k$ .

#### 4.5.3. Linearization processes.

The first obvious method for obtaining a piecewise linear yield surface is to find the exact yield surface and then inscribe (or circumscribe) more or less arbitrarily a polyhedron, in order to simplify the subsequent analysis. This will be done in Section 7.2., where we shall replace for convenience the exact yield locus of fig. 4.8. by the inscribed polygon (in dashed lines) ABCDEF.

A second method consists of using an approximation, not to the yield surface, but to the structure itself by replacing the actual solid beam, plate or shell by the corresponding “ideal sandwich” structure shown by fig. 5.4., composed of two sheets and a core. The stress state in each (thin) sheet is assumed constant through the thickness  $t^*/2$  (plane stress) and the core is assumed to carry exclusively shear stresses, to which it can resist indefinitely.

It is evident that such a structure is geometrically linear in the sense that no nonlinearity will arise by integration through the thickness, because all internal stress resultants are obtained by simply summing the contributions of the two sheets. Therefore, the use of a linear yield criterion (such as TRESCA's) will guarantee a piecewise linear yield condition in generalized stresses. For this reason, ideal sandwich structures are extremely popular in research papers, what does not justify really the mathematical trick introduced.

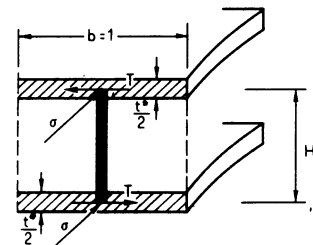


Fig. 5.4.

The reader will establish himself the expressions of the internal stress resultants  $N$ ,  $M$ ,  $M_t$  of a sandwich shell, and their limit values  $N_p$ ,  $M_p$ ,  $M_{tp}$ . (For the solutions, see [S3]).

#### 4.6. Discontinuities.

The proofs of the two fundamental theorems given in Sections 2.3.1. and 2.3.2. were based on the consideration of continuous stress and strain rate fields.

However, discontinuous fields are actually very useful in practical applications, be it in actual or in generalized stress and strain rates. The most familiar discontinuities are the stress discontinuity at the neutral axis of a beam bent plastically (fig. 4.1.) and the concept of plastic hinge (fig. 4.1.3.) which corresponds to a discontinuous distribution of the rates of curvature  $K$  along the axis of the bar.

In what follows, we shall discuss briefly which discontinuities are admissible, and then show how the demonstrations of the fundamental theorems can be extended to such discontinuous fields .

To begin with, surface of stress discontinuity are clearly possible, provided the equilibrium equations (2.2.1.) and (2.2.2.) are satisfied at all points of these surfaces. Surfaces of velocity discontinuity can also be admitted, provided the power of dissipation is properly computed. These last surfaces are in fact the limiting cases of continuous velocity fields, in which one or more velocity components change very rapidly a thin transition layer, which becomes at the limit a discontinuity surface for convenience.

Now, the demonstrations of the two fundamental theorems are easily generalized for such discontinuous fields. The introduction of discontinuous stress fields satisfying equilibrium equations does not affect the statical theorem (section 2.3.1.). On the other hand, when surfaces of velocity discontinuity are considered in the kinematical theorem, the only modification necessary is to replace the expression (2.2.5.) of the principle of virtual powers by the following one<sup>(\*)</sup> :

$$(6.1.) \quad \int_v F_i \delta v_i dV + \int_v T_i \delta v_i dS = \int_v \sigma_{ij} \delta \epsilon_{ij} dV + \int_{S_D} \tau \Delta v dS_D$$

where  $S_D$  represents the discontinuity surface across which the velocity component tangential to the surface jumps by  $\Delta v$ , while the shear stress  $\tau$  parallel to this surface is assumed continuous.

In the use of above principle for a yield mechanism, the tangential stress at the discontinuity surface is the yield stress in pure shear,  $k$ . The power of dissipation per unit area of discontinuity surface is therefore  $D = k\Delta v$ . The total power dissipated in this way is simply added to that computed from the continuous velocity distribution.

---

(\*) This extended version is easily derived from the equilibrium conditions by using the divergence theorem as usual. The last term in the right hand member of (6.1.) is the additional internal power dissipated by the forces  $\tau d S_D$ .

## 5. FRAMES – FIRST ORDER THEORY.

### 5.1. Specialized Versions of the Fundamental Theorems.

As demonstrated in section 4.2., the fundamental theorems of Limit Analysis may be written in terms of generalized stress  $Q_i$  and generalized strain rate  $\dot{q}_i$ . Now, in the case of rigid jointed plane frames loaded in their plane, the effect of the normal and shear forces on the value of the plastic moment capacity can be neglected, at least on first approximation (see [M7] for more details). The bending moment  $M$  is thus the only generalized stress and, as discussed in Section 4.1.2., the corresponding generalized strain rate  $\dot{q}$  is the rate of curvature  $K$  of the bar axis. The fundamental theorems in forms appropriate to beams and frames are therefore as follows :

*Static or lower bound theorem : If, for a multiplier  $\lambda_-$  of the external loads, a diagram of bending moments  $M_-$  can be found that obeys the equation of statical equilibrium and nowhere violates the yield criterion  $|M| < M_p$ , then*

$$\lambda_- < \lambda_l \quad (1.1.)$$

If such a moment diagram is called in short a *statically admissible bending moment diagram*, the statical theorem may be expressed more compactly as follows :

*Static theorem : Any multiplier corresponding to a statically admissible moment diagram is a lower bound of the true limit multiplier  $\lambda_l$ .*

*Kinematic or upper bound theorem : A system of axis velocities which satisfies the kinematical support conditions of the frame furnishes, by the power equation*

$$\lambda_+ \sum P \dot{\delta} = \sum M \dot{\theta} \quad (1.2.)$$

*a value  $\lambda_+$  of the multiplier such that*

$$\lambda_+ > \lambda_l \quad (1.3.)$$

If such a system of axis velocities is in short called a *kinematically admissible mechanism*, the theorem can be expressed more compactly as follows :

*Kinematic theorem : Any multiplier  $\lambda_+$  deduced by the power equation (1.2.) from a kinematically admissible mechanism is an upper bound of the limit multiplier  $\lambda_l$ .*

**Combined theorem :** Suppose that, for a given multiplier  $\lambda$  of the external loads, a statically admissible bending moment diagram can be found such that the magnitude of  $|M|$  equals  $M_p$  in a sufficiently large number of sections to produce a kinematically admissible mechanism with plastic hinges in these sections. Suppose further that, at each of these sections, the sign of the bending moment corresponds to the sense of the hinge rotation of this mechanism. Then, the considered multiplier  $\lambda$  is exactly equal to the limit multiplier  $\lambda_l$ .

In using this theorem, caution should be exercised concerning the correspondence between bending moment diagram and mechanism. For instance, if a M diagram has been found in which  $|M| = M_p$  at a sufficiently large number of sections to produce a total of a partial collapse mechanism, it does not necessarily follow that the corresponding mechanism is an actual collapse mechanism.

Consider, for instance, the built-in portal frame shown in fig. 1.1.(\*) . The plastic moment capacity of the columns is 500 kNm and that of the beam 1000 KNm. Service loads P and H are shown in the figure. Find the value of the multiplier that must be applied to these loads to obtain the limit loads.

An erroneous solution of this problem, which corresponds to the multiplier  $\lambda = 2$ , is given in fig. 1.1.b. It is obvious that the condition  $|M| < M_p$  is satisfied. Moreover,  $|M|$  reaches  $M_p$  in sections 2, 3 and 4. Thus, there are three plastic hinges, corresponding to the collapse mode of the beam that is indicated in fig. 1.1.c. For the frame, this is a partial collapse mechanism. Nevertheless, this mechanism cannot occur because it corresponds to a negative bending moment at cross section 2 (fig. 1.1.c), whereas the considered moment is positive. The combined theorem therefore fails to be applicable.

The exact solution of the problem is given by the bending moment diagram in fig. 1.1.d, which corresponds to the multiplier  $\lambda = 2.88$ . The plastic moment is reached

---

(\*) Throughout this course, the following sign convention will be used:

One specifies first of all an extreme fiber of reference in each bar, which is indicated by a broken line parallel to the axis of the bar (see fig. 1.1.a). Bending moments that produce tension in this fiber are considered positive. A curvature K is regarded as positive when producing extension in the reference fiber. A rotation in a plastic hinge is considered positive when corresponding to very large positive curvature restricted to a very narrow segment of the member.

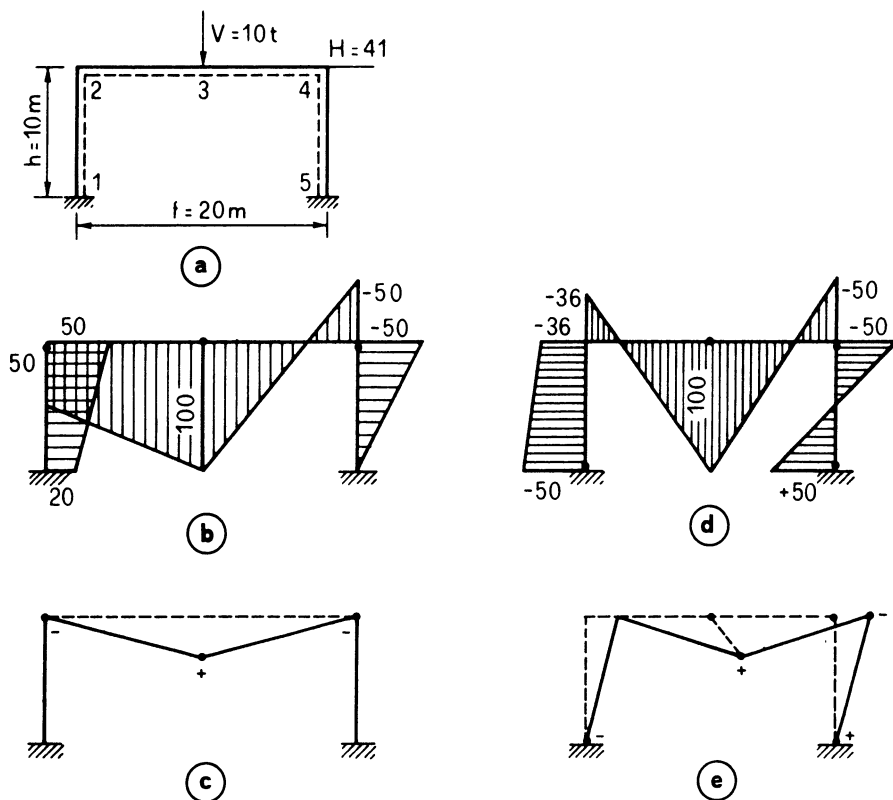


Fig. 1.1.

in four sections corresponding to a complete collapse of the frame, whose degree of redundancy is three. The collapse mechanism is shown in fig. 1.1.e, and it is seen that the moments in the four plastic hinges have signs agreeing with those of the bending moments.

This important theorem also allows us to check whether a given kinematically admissible mechanism is an actual collapse mechanism. In discussing this, let us first assume that the given mechanism corresponds to a complete collapse. For a frame with the degree of redundancy  $h$ , the given mechanism then involves  $(h + 1)$  plastic hinges, at each of which the bending moment must have the magnitude of the corresponding plastic moment and the sign of the hinge rotation. These  $(h + 1)$  bending moments being known, the bending moment distribution becomes statically

determined and is readily obtained by using the statical equations of equilibrium(\*). If it turns out that these bending moments satisfy everywhere the yield condition  $|M| < M_p$  and are thus statically admissible, the given mechanism is an actual collapse mechanism. A typical application may be found in section 5.3.6.6.

When the given mechanism corresponds to partial collapse, only the bending moments in the collapsing part are statically determinate. For the given mechanism to be an actual collapse mechanism, not only must the bending moments in the collapsing part be statically admissible, but they must also be extended in a statically admissible manner throughout the rest of the structure. Since this part of the structure is statically indeterminate, one of the classical methods of elastic structural analysis of statically indeterminate structures must be used to determine the corresponding part of the bending moment diagram.

## 5.2. Validity of the Fundamental Theorems for Carbon Steels.

The fundamental results of section 5.1. are based on the concept of the plastic hinge, introduced in section 4.1.2. Now, the concept of plastic hinge itself is deduced from the elastic-perfectly plastic behaviour of the tensioned and compressed parts of a beam subjected to bending, that is ultimately from the diagram of fig. 2.1.1.

As carbon steels show a discontinuous behavior along the yield plateau and may show a very marked upper yield point (fig. 1.1.2.), it may be questioned whether the theorems of section 5.1. are valid for carbon steels. This problem has been investigated by LEBLOIS and MASSONNET [L1], who have studied in detail the shape of the moment-curvature diagram for an annealed mild carbon steel showing a very pronounced upper yield point. They have shown that the consequence of  $\sigma_{yu} = 1.5 \sigma_{yl}$  in bending is to produce an elastic behavior up to the upper yield moment

$$M_{yu} = \sigma_{yu} S \quad (\text{where } S \text{ is the section modulus})$$

which surpasses the plastic moment calculated on the basis of the lower yield stress,

$$M_p = \sigma_{yl} Z ,$$

---

(\*) A simple and wholly general technique for producing all independent equations of statical equilibrium will be explained in section 5.3.6.

in all cases where

$$\frac{\sigma_{yu}}{\sigma_{y1}} > \frac{Z}{S} .$$

As a consequence of this, moment-curvature relationships of the type of fig. 2.1.a., where the beam section becomes suddenly fully plastic at point A ( $M_{yu} = M_p$ ) have been consistently obtained in bending of rectangular specimens.

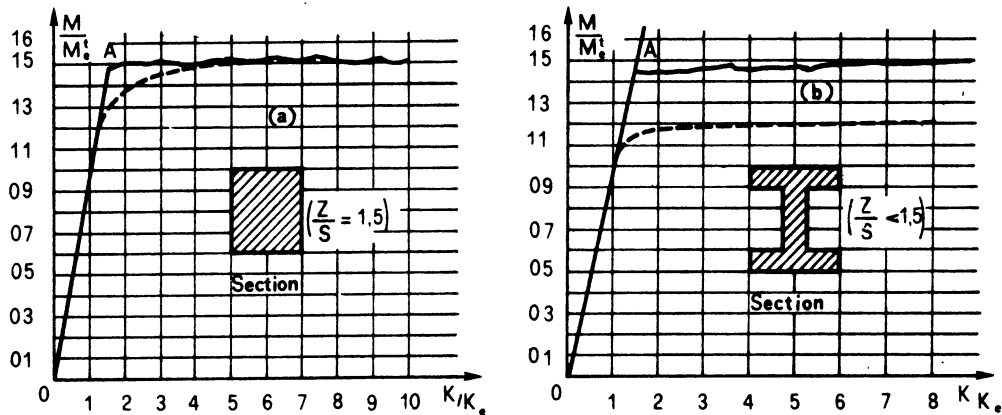


Fig. 2.1.

For carefully machined I profiles,  $Z/S$  was smaller than 1.5. and therefore  $M_{yu}$  was larger than  $M_p$  with the consequence that the  $(M, K)$  curve climbed elastically to  $M_{yu}$  at point A (fig. 2.1.b.) and did not fall afterwards to the curve of the classical theory.

Similar phenomena were observed in torsion of round and tubular specimens.

These phenomena could only be observed on carefully machined and annealed specimens, designed so as to avoid any stress raiser. In industrial practice, the steel rolled profiles contain always residual stresses and their rough rolled surface presents in addition innumerable stress raisers, which trigger the yield of the metal in the form of LUDERS bands, as soon as the lower yield stress is reached. For this reason, the classical moment-curvature diagram of fig. 4.2.a. may safely be used as a basis for the development of Limit Analysis and Design of industrial beams and frames made of carbon steel.

### 5.3. Proportional Loading – Practical Methods of Solution.

#### 5.3.1. Introduction.

In all this chapter, we shall restrict ourselves, at least in the illustrative examples, to structures formed on prismatic members. In a prismatic member, plastic hinges can form in cross sections other than the end sections only if the member is subjected to transverse loads. When these loads are concentrated, the eventual plastic hinges are necessarily located in sections where loads are applied.

In the present section, we shall first examine briefly two methods valid for simple statically indeterminate structures such as continuous beams and simple frames, the **kinematic** and the **static methods**. Then, we shall study more in detail a general method suitable for more complicated structures, the **Method on Combining Mechanisms**, which may lead to automatic computation on a digital computer, as we shall see in Section 5.6.

#### 5.3.2. Loadings to be considered.

Because the actual failure load of a statically indeterminate structure is its limit load, it is logical to define the service load of the structure as the quotient of the limit load by a plastic safety factor  $S_p$ . This new definition of the service load attributes to statically indeterminate structures the same actual safety that statically determinate structures have, whereas the actual safety of an elastically designed statically indeterminate structure may be unnecessarily high.

In the Specifications which accept plastic design, usually two loading cases must be considered :

**Loading case I** (comprising dead weight, live loads and snow, but not the wind)

**Loading case II** (comprising the loads of case I, less the snow, plus the wind)

For these two loadings cases, the safety factors of the elastic or allowable stress method of design are, say  $(S_{el})_I$  and  $(S_{el})_{II}$  respectively.

Under the loads  $S_{el}P$ , the maximum bending moments, in a statically determinate structure like a beam on simple supports, reach strictly the value  $M_y = \sigma_y S$  of the yield moment.

Effective collapse by formation of a mechanism only occurs when the maximum bending moments reach the value

$$M_p = f M_y , \quad (3.1.)$$

where, for the rolled profiles used in steel construction, the mean value of 1.12 may be adopted. So that the plastic safety factors of the statically determinate structure in question are

$$(S_p)_I = 1.12 (S_{el})_I \quad (S_p)_{II} = 1.12 (S_{el})_{II} . \quad (3.2.)$$

If the same actual safety against collapse for all beams and frames is desired, the preceding factors  $S_p$  must be adopted for all structures, either statically determinate or indeterminate.

The following table gives for the european mild steel AE24 the allowable stresses, elastic and plastic safety factors admitted in the belgian Specifications, and, for the american mild steel A36, the same quantities admitted in the AISC (American Institute of Steel Construction) 1969 Specifications.

Country	Belgium				United States		
	$\sigma_y = 240 \text{ N/mm}^2$			$\sigma_y = 36 \text{ ksi}$			
Loading case	allowable stress $\text{N/mm}^2$	$S_{el}$	$S_{pt} = f S_{el}$	allowable stress ksi	$S_{el}$	$S_{pl} = f S_{el}$	
I	160	1.5	$1.5 \times 1.12 = 1.68$		1.65	$1.65 \times 1.12 = 1.85$	
II	180	1.33	$1.33 \times 1.12 = 1.49$		1.25	$1.25 \times 1.12 = 1.40$	

### 5.3.3. Analysis – Restricted Design – Optimum Design.

Before going into the detail of the methods of solution, let us emphasize that we shall be concerned with two kinds of problems. Let  $M_p$  be the plastic moment and  $l$  the length of one of the bars, regarded as the reference bar in the framed structure. The plastic moments of the other bars may be written in the form  $\alpha_i M_p$ , where  $\alpha_i$  is a coefficient corresponding to the  $i$  th bar.

We assume these coefficients  $\alpha_i$  to be known.

The given service loading consists of several loads, one of which is taken as reference load and denoted by  $P$ . These forces are assumed to vary proportionally and thus, at collapse, their intensities will all be multiplied by the same multiplier  $\lambda$ .

The work equation furnished by the principle of virtual work then has the form

$$(3.3.) \quad \lambda P_l = k M_p ,$$

where  $k$  is a numerical coefficient. We may wish to determine either :

1. The value of the multiplier  $\lambda$  of the given loads that corresponds to collapse of a structure with a given plastic reference moment  $M_p$ ; this is a problem of analysis, or
2. The plastic moment  $M_p$  of the reference beam, for the reference limit load of the structure to be a given multiple  $\lambda$  of the known service load  $P$ ; this is a problem of restricted design, because only one  $M_p$  must be determined, the others having been chosen beforehand as certain multiples of this one.

Note that, because the  $\alpha_i$  are known, both problems are basically equivalent.

In closing, let us mention that we shall study later (section 5.5.) the most general design problem, which is called optimum design, and which is defined as follows : Find the plastic moments  $M_i$  of all the bars so as to obtain a structure which presents the safety factors required by the Building Code for the various loading cases (see section 5.3.2.) and which is optimum in a certain sense, for example, the structure of minimum weight.

#### 5.3.4. The kinematic method.

##### 5.5.3.4.1. Principle.

In its most elementary form, the kinematic method of determining the limit load consists in successively considering all possible collapse mechanisms.

From the power equation (1.2.), the load intensity corresponding to each of these mechanisms is obtained. According to the kinematic theorem, the actual intensity of the limit load is the smallest of all loads intensities obtained in this manner.

To make certain that no possible mechanism has been overlooked, the bending

moment diagram corresponding to the selected mechanism may be drawn. If this diagram turns out to be statically admissible, the combined theorem (section 5.1.) guarantees that the exact limit load has been found.

### 5.3.4.. Example : Doubly Built-In Beam subjected to a concentrated load at one third of the span (fig. 3.1.).

Because of the absence of horizontal loads, the degree of redundancy of the system is 2 ; its collapse will therefore involve three hinges, which can only be located at the end sections A and C at the loaded section B (Fig. 3.1.a). The only possible collapse mechanism with these hinges is represented in fig. 3.1.b. The power equation (section 5.1.) is

$$P \frac{\dot{\theta}_1}{3} = M_p (\dot{\theta} + \frac{\dot{\theta}}{2} + \frac{3\dot{\theta}}{2}) \quad (3.4.)$$

Thus

$$P_1 = 9 M_p / l \quad (3.5.)$$

In treating beam and frame problems, it is customary to drop the points representing the rates and to write, instead of the power equation (1.2.), the work equation

$$\lambda + \sum P\delta = \sum M\theta \quad (3.6.)$$

which, in the present problem simplifies to

$$P \frac{\theta_1}{3} = M_p (\theta + \frac{\theta}{2} + \frac{3\theta}{2}) . \quad (3.7.)$$

Both equations (3.4.) and (3.7.) (or generally, (1.2.) and (3.6.) would be identical if the deflections at B were neglected, i.e. if a small motion from the initial unloaded configuration is used, or also if the rigid-plastic model is used.

However, finite for instance, it is desired to study the effect to the increasing deflections on the value of the limit load. This possibility has already be illustrated in section 2.6.

The only possible bending moment diagram is shown in fig. 3.1.c. It can be verified

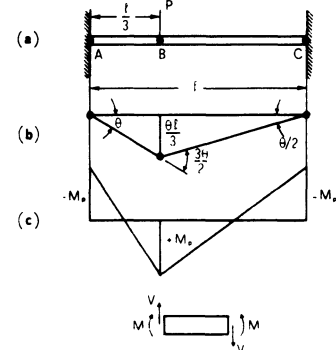


Fig. 3.1.

to be statically admissible (see section 5.3.6.3. hereafter) and hence we have obtained the complete solution of the problem and (3.4.) is the exact value of the limit load.

#### 5.3.4.3. Exercises.

Find the complete solution for the structure of fig. 3.2. and 3.3.  
beam of fig. 3.2., show that it can fail by two independent beam mechanisms of different amplitudes.

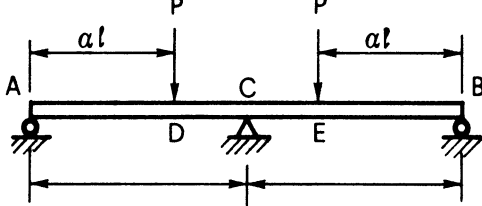


Fig. 3.2.

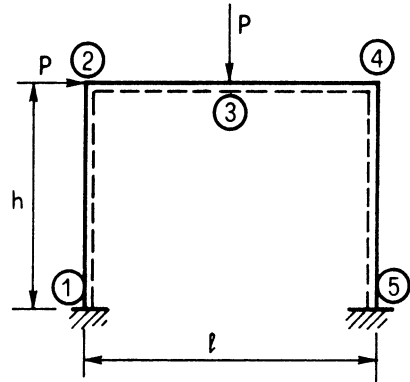


Fig. 3.3.

#### 5.3.5. The (semi-graphic) static method.

##### 5.3.5.1. Principle

The static method of determining the limit load essentially searches for a statically admissible bending moment distribution to which there is a corresponding kinematically admissible mechanism ; this method is particularly wellsuited for the treatment of rectangular or gabled pinned-base frames of one or several bays. (Fig. 3.4.) ; it is less useful for built-in beams or frames.

The detailed procedure is as follows :

1. Redundancies are chosen. These must form a complete set in the sense that the structure becomes statically determinate when all the redundancies are given the value zero. This statically determinate structure will be called the **primary structure** ;
2. The bending moment diagram for the primary structure is drawn.  
It will be called the **statically determinate bending moment diagram** ;

3. The bending moment diagrams corresponding to unit values of the various redundancies are sketched, and, by superposition, the M diagram corresponding to litteral unspecified values of the redundancies is obtained. This diagram is called the **statically indeterminate bending moment diagram** ;

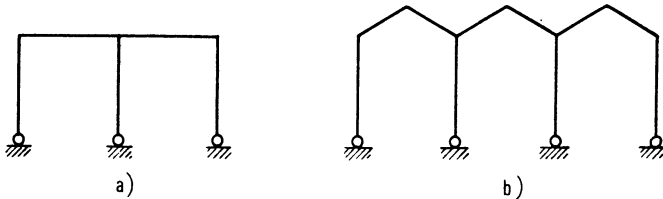


Fig. 3.4.

4. The actual bending moment diagram is constructed by superposition of the diagrams under 2 and 3 above, the values of the redundancies being determined to satisfy the following conditions : (a) the magnitude of the actual bending moment must nowhere exceed the plastic moment and  
 (b) the insertion of hinges at the sections at which the magnitude of the actual bending moment equals the plastic moment must transform the structure into a mechanism ;
5. A deformation of this mechanism for which the total work done by the loads is positive is now sketched to check whether the signs of the relative rotations in the plastic hinges agree with the signs of the actual bending moments at the hinge sections.

#### 5.3.5.2. Illustrative example : Clamped based gabled frame.

The frame is shown at fig. 3.5. All bars are prismatic and have the same cross section. The applied forces that the frame must carry are shown in fig. 3.5. and involve the dead weight of the roof, the loads applied by a crane girder, and the wind pressure. The faces acting on the roof are transferred to the portal frames by 10 purlins. The unknown is the common cross section of the bars.

1. The primary structure chosen is shown in Figure 3.6. The redundancies are the bending moments  $M_A$  and  $M_G$  at the feet of the columns and the thrust  $H_6$  ;
2. The statically determinate bending moment diagram produced in this primary structure by the loads shown in fig. 3.5. is determined. This diagram is drawn in broken lines in fig. 3.7. and its ordinates are given in Table 3.1.
3. The bending moment diagrams produced by the unit redundancies  $M_A = 1$ ,  $M_G = 1$  and  $H_G = 1$ , acting alone on he primary structure are also determined.

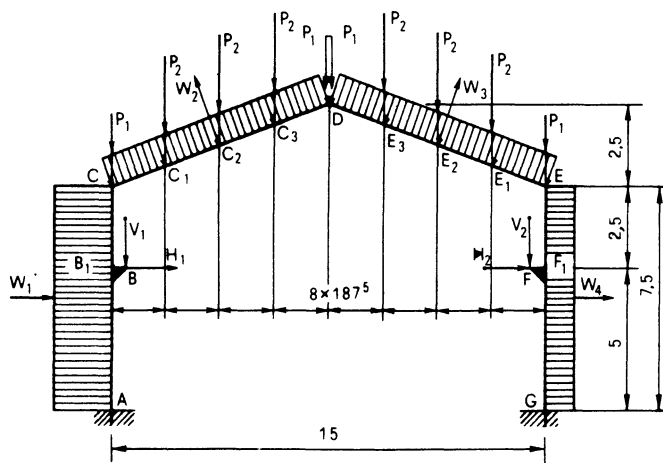


Fig. 3.5.

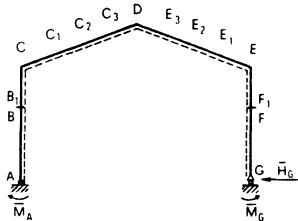


Fig. 3.6.

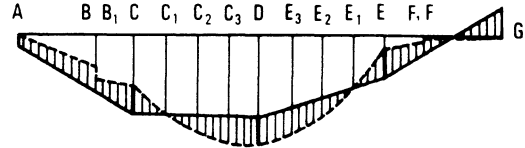


Fig. 3.7.

Their ordinates are given in Table 3.2.

- We assume that the absolute value of the moment reaches  $M_p$  at sections C, D, E and G. Moreover, we except the moments in D and G to be positive, and the moments in C and E to be negative. Hence,

$$M_C = -M_p, \quad M_D = +M_p, \quad M_E = -M_p, \quad M_G = +M_p.$$

Tables 3.1. and 3.2. enable us to write the equations :

$$M_C \equiv 32,465 + M_A - 7.5 H_G = -M_p$$

$$M_D \equiv 70,199 + 0.5 M_A + 0.5 M_G - 10 H_G = +M_p$$

$$M_E \equiv 7653 + M_G - 7.5 H_G = -M_p$$

$$M_G = + M_p .$$

The solution of this set of equations is

$$M_p = + 17850 \text{ DNm} ; \quad M_A = - 7142 \text{ DNm}$$

$$M_G = + 17850 \text{ DNm} ; \quad H_G = + 5780 \text{ DN.}$$

The actual bending moments in the frame at collapse are obtained from Tables 3.1. and 3.2. using the general formula

$$M^j = M_{st \text{ det}}^j + k_A^j M_A + k_G^j M_G + k_H^j H_G ,$$

where the  $k^j$  are the coefficients of column  $j$  in Table 3.2.

Table I. – Isostatic Moments

Sections	A	B	B <sub>1</sub>	C	C <sub>1</sub>	C <sub>2</sub>	C <sub>3</sub>	D	E <sub>3</sub>	E <sub>2</sub>	E <sub>1</sub>	E	F <sub>1</sub>	F	G
Moments (kgm)	0	20 505	27 955	32 645	50 926	63 036	69 487	70 199	63 181	50 417	31 886	7 653	4 023	668	0

Table II. – Hyperstatic Moments

M <sub>A</sub>	1	1	1	-1	~ 975	0,750	0,625	0,500	0,375	0,250	0,125	0	0	c	0
M <sub>L</sub>	0	0	0	0	0,125	0,250	0,375	0,500	0,625	0,750	0,875	1	1	i	1
H <sub>G</sub>	0	- 5	- 5	- 7,5	- 8,125	- 8,750	- 9,375	- 10	- 9,375	- 8,750	- 8,125	- 7,5	- 5	- 5	0

Table III. – Actual Moments

Sec-tions	A	B	B <sub>1</sub>	C	C <sub>1</sub>	-		D	E <sub>3</sub>	E <sub>2</sub>	E <sub>1</sub>	E	F <sub>1</sub>	F	G
	- 142	- 15 537	- 8 087	- 17 847	- 84	+ 11 606	+ 17 527	+ 17 753	+ 17 451	+ 11 432	- 356	- 17 847	- 7 027	- 10 382	+ 17 850

The values specifying the actual bending moment diagram are indicated in Table 3.3., the diagram itself being represented by the hatched ordinates in fig. 3.7. It is seen that no bending moment exceeds

$$M_p = 17.850 \text{ DNm}$$

in absolute value. The assumed collapse mechanism (fig. 3.8.) is therefore simultaneously kinematically and statically admissible and hence furnishes the exact solution of the problem.

Had we assumed the plastic moment to be attained in other sections, we should have obtained, using the same procedure, a bending moment diagram in which  $M$  would have exceeded  $M_p$  somewhere. For instance, if we had assumed (fig. 3.9.)

$$M_A = -M_p, M_{C_3} = +M_p, M_E = -M_p, M_G = +M_p,$$

we would have found bending moments larger than  $M_p$  in absolute value at B, C, D and E, the two largest ones occurring at C and D. If we replace condition  $M_A = -M_p$  and  $M_{C_3} = +M_p$  by  $M_C = -M_p$  and  $M_D = +M_p$ , we obtain once again the previously considered mechanism, which is the correct one.

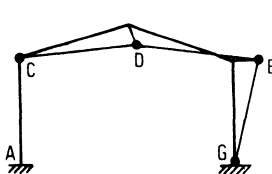


Fig. 3.8.

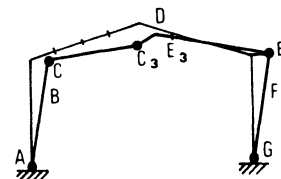


Fig. 3.9.

**Remark :** the semi-graphic method may run into difficulties if the structure fails by partial collapse, which is the rule in rectangular multiple frames. Indeed, whereas the  $M$  diagram is readily drawn for the part of the structure that is transformed into a mechanism, it is not at all easy to continue this  $M$  diagram throughout the rest of the structure.

We shall see in the next section that the method of combining mechanisms does not possess this drawback.

### 5.3.6. The method of combining mechanisms (NEAL and SYMONDS [N2])

#### 5.3.6.1. Principle of the method.

A structure subjected to given loads is considered, and it is intended to solve the restricted design problem presented in section 5.3.3., that is to determine the value of the plastic moment of the reference bar for collapse to occur under the given loads.

The principle of the method is to construct the collapse mechanism as the combination of a certain number of simple and independent mechanisms. To begin with, these simple mechanisms are identified and their work equations established.

According to the kinematic theorem, the actual mechanism is characterized, among all possible mechanisms, by the largest value of  $M_p$  (see section 5.3.3.). Consequently, the method will consist in selecting the simple mechanism with the largest  $M_p$  and combining it with one or more other simple mechanisms to obtain a complex mechanism with a still larger value of  $M_p$ .

The most likely combinations are examined in this manner until it is believed that the actual collapse mechanism has been found. To verify the correctness of this belief, the M diagram is determined from statics, taking account of the known bending moments in the plastic hinges of the considered mechanism. If this M moment is admissible, that is if the magnitude of  $|M|$  nowhere exceeds the local plastic moment, the combined theorem of Section 5.1. proves that the problem has been solved. When the bending moment diagram only violates the condition  $|M| < M_p$  at a few cross sections, it is often possible to adjust the locations of some hinges to render the diagram statically admissible and thus obtain the correct solution of the problem.

#### 5.3.6.2. Illustrative example : Rectangular frame with two bays.

Consider the rectangular frame with two bays shown in fig. 3.10. The structure has ten critical sections at which plastic hinges could form. They are marked in fig. 3.10. by small black circles labeled 1 to 10. The knowledge of the bending moments in these critical sections suffices to determine completely the bending moment diagram. The location of the possible plastic hinge in the uniformly

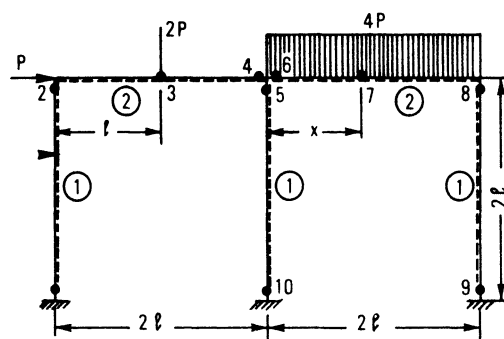


Fig. 3.10.

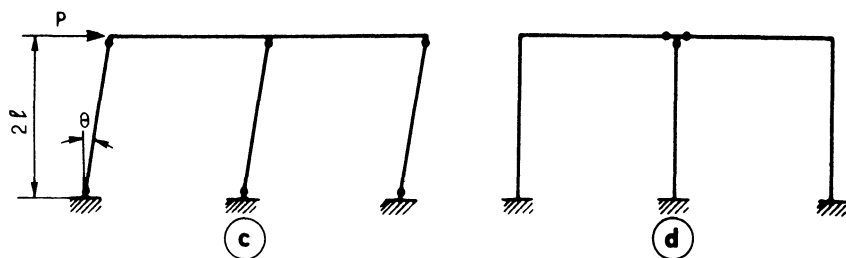
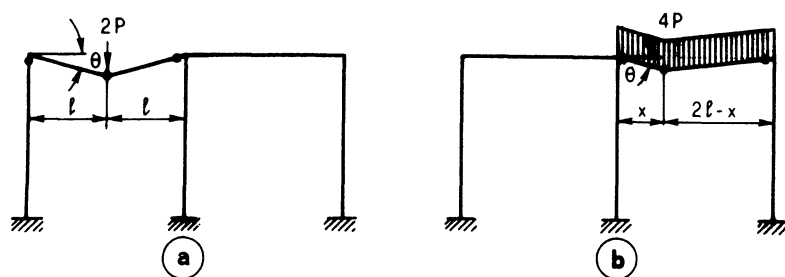


Fig. 3.11.

loaded beam is specified by its (unknown) abscissa  $x$ . The numbers in circles are the  $\alpha_i$  factors discussed in section 5.3.3. and defining the values of the plastic moments of the various bars.

In the study of multistory multibay rectangular frames, for which the present method is especially developed, it is convenient to choose the three types of independent mechanisms as shown in figures 3.11. a), b), c), d), called beam, panel and joint mechanisms, respectively.

#### 5.3.6.3. Number of independent mechanisms and equations-of equilibrium.

From the  $m$  values of the bending moment at the critical sections that we need for determining completely the  $M$  diagram in the frame,  $h$  are statically indeterminate. That means that the remaining  $(m - h)$  values are statically determinate, which means that the number of independent equations of equilibrium relating the unknown moments is

$$e = m - h$$

Now, we shall show that each of these equations of equilibrium could be deduced from the independent mechanisms by using the principle of virtual work and the following technique :

- a) Insert perfect hinges at all the critical sections ;
- b) Consider the frame as a set of rigid bars linked by these pins ;
- c) Establish the equilibrium with the given external forces  $P$  by applying a pair of positive couples of intensities  $M_1, M_2, \dots, M_{10}$  on the two sides of each of these hinges ;
- d) With these preliminaries, each of the independent equations of equilibrium can now be obtained by applying the principle of virtual work valid for rigid bodies to the various independent mechanisms (fig. 3.11. a) to d)) considered as systems of virtual displacements. Note that bending moments must here be considered as external forces.

Above operations are represented, for the four independent mechanisms of fig. 3.11., by the sketches of fig. 3.12. a) to d).

For instance, for the left beam mechanism of fig. 3.12.a, we obtain the equation

$$P\theta + M_2\theta - M_32\theta + M_4\theta = 0 ,$$

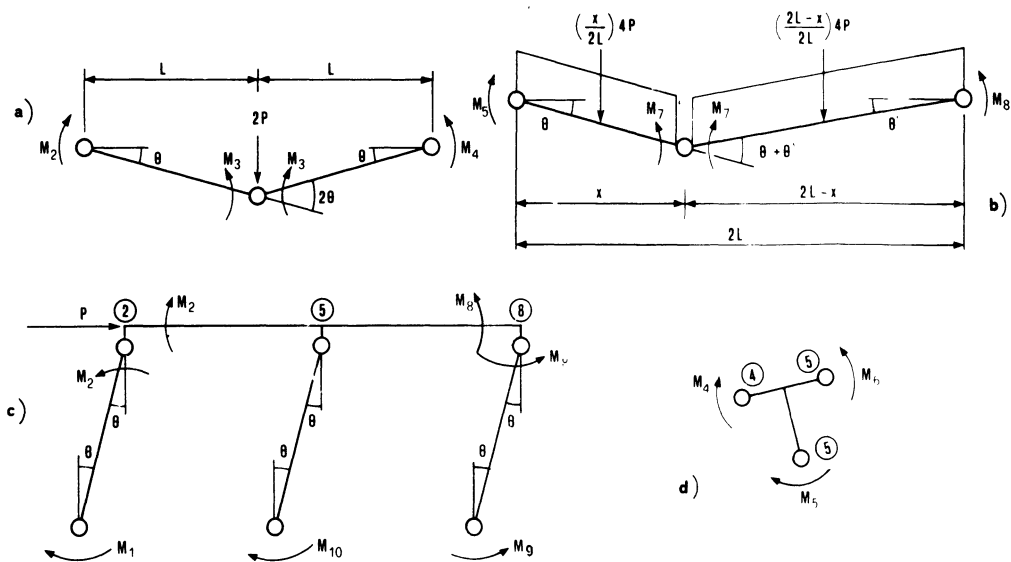


Fig. 3.12.

whence

$$2M_3 - M_2 - M_4 = 2Pl \quad (a)$$

Similarly, the mechanisms (b), (c), (d) of fig. 3.12. furnish the equations

$$2M_7 - M_6 - M_8 = 2Pl \quad (b)$$

$$M_2 - M_1 + M_5 - M_{10} + M_9 - M_8 = 2Pl \quad (c)$$

$$M_4 + M_5 - M_6 = 0 \quad (d)$$

From above discussion, we see that each mechanism furnishes an equation of statical equilibrium. The number  $x$  of independent mechanisms is thus exactly equal to the number of independent equations of statics and fundamental relation (3.8.) can be completed as follows :

(3.9.)

$$x = e = m - h$$

In the case of the frame of fig. 3.10, there are 10 critical sections ( $m = 10$ ) and the degree of redundancy  $h = 6$ . (3.9.) gives then  $x = e = 4$ . It is this result that forces us to consider, aside of the three beam and panel mechanisms of fig. 3.11.a), b), c), the "funny" joint mechanism of fig. 3.11.(d), which corresponds, by the above technique of "exteriorization" of bending moments, to the well known equation of

equilibrium of the joint 4, 5, 6.

#### 5.3.6.4. Plastic moments derived from the basic mechanisms.

Next, the plastic moments derived from the basic mechanisms of fig. 3.11. are computed. For the beam mechanism shown in fig. 3.11.a), the work equation is(\*) :

$$2P(l\theta) = M_p \theta + (2M_p)(2\theta) + (2M_p)\theta \quad (a')$$

from which

$$M_p = Pl/3.5 = 0.286 Pl \quad (a'')$$

This result could have been obtained by replacing the moments in (a) by their plastic values :

$$M_2 = -M_p, \quad M_3 = 2M_p, \quad M_4 = -2M_p$$

The signs used result from the sense of rotation of the hinges shown in figure 4.6.a.

For the second mechanism, we find

$$M_p = Pl \frac{2x(2l-x)}{1(8l-x)}. \quad (b')$$

In particular, if  $x = 1/2$ , we have

$$M_p = Pl/3.5 = 0.286 P. \quad (b'')$$

Finally, the panel mechanism of fig. 3.11.(c) gives

$$P(2l\theta) = 6M_p \quad (c')$$

and

$$M_p = Pl/3 = 0.333 Pl. \quad (c'')$$

The joint mechanism shown in fig. 3.11.(d) does not give us any value of  $M_p$  because its work equation reduces to the identity  $0 = 0$ . This kind of mechanism is

(\*) It must be remembered that the plastic moment of the beams is  $2M_p$ , and not  $M_p$  and that the moment at section 2 occurs in a column with plastic moment  $M_p$ .

sometimes called a **false mechanism**.

### 5.3.6.5. Obtaining the collapse mechanism by combining basic mechanisms.

The next step of the method is to combine the four basic mechanisms to obtain the greatest possible value of the reference plastic moment. The general work equation

$$(3.10.) \quad \sum P_i \delta_i = \sum M_{pj}(\theta_j)$$

established in section 5.3.4.2. shows that, for this goal to be reached, the work of the applied loads must be as large as possible, while the work dissipated in the hinges must be reduced as much as possible. The following rules can be deduced from this fact :

1. When combining two simple mechanisms, one must always eliminate at least one of the common hinges. Only in this case will the combined mechanism eventually give a plastic moment larger than the plastic moments of the component mechanisms.
2. If necessary, one can “rotate” a joint connecting two or more bars such as joint 4 - 5 - 6 of fig. 3.10., to diminish the internal work in this joint.  
This rotation corresponds to the mechanism shown in fig. 3.12.d.
3. When a mechanism with a hinge under a distributed load is used in a combination, it proves convenient to assume temporarily that this hinge is located at mid-span. If the actual collapse mechanism contains this hinge, its abscissa can be determined later on to maximize  $M_p$ .

Practically, the variation in the hinge position resulting from this hinge adjustment is usually small and may be neglected.

In discussing the present problem, we start with mechanism (c), because its plastic moment is the largest ( $M_p = P1/3$ ). To modify this mechanism, we must use a mechanism that makes it possible to suppress a hinge. We are thus led to considering the first beam mechanism (fig. 3.11.a). Choosing the same magnitude for angle  $\theta$  in both mechanisms, we obtain the mechanism shown in fig. 3.13. The corresponding work equation could be obtained directly, but it is simpler to proceed by addition of the rotations and the external works of the two component mechanisms (a') and (c'). One obtains

$$P(2l\theta) + 2P(l\theta) = M_p |\theta + (\theta - \theta) + \theta + \theta + \theta + \theta| + 2M_p(2\theta + \theta)$$

whence

$$M_p = 4 Pl/11 = 0.364 Pl \quad (e')$$

This mechanism gives the best of all results (a''), (b''), (c''), (e'') obtained so far. We must now try to still improve it, by combining it with the two simple mechanisms (b) and (d), which have not been used yet. These two mechanisms may jointly be combined with the mechanism (e) of figure 3.13. to eliminate the hinge in section 5, and at the same time avoiding introducing a hinge at 6. The new combination may be favorable or not, depending on the intensity of the distributed load.

It is represented in figure 3.14.

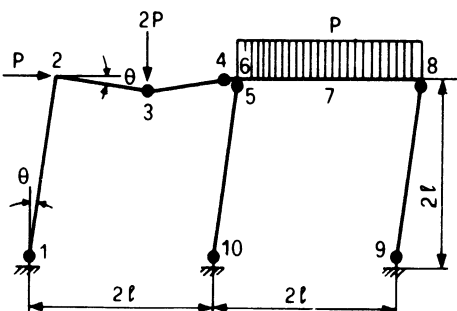


Fig. 3.13 .

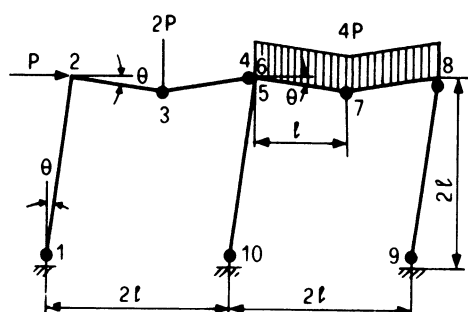


Fig. 3.14.

The work equation of this mechanism is

$$4 Pl\theta + 4 P(l\theta/2) = M_p(5\theta) + 2 M_p(6\theta), \quad (f')$$

from which

$$\dot{M}_p = \frac{6}{17} Pl = 0.353 Pl.$$

This result is approximate because, according to rule 3 above, the hinge under the distributed load has been arbitrarily located at mid-span. If  $x$  is the distance of this hinge from the left end section (fig. 3.15.), equation (f') becomes :

$$4Pl\theta + 4 P \left(\frac{x\theta}{2}\right) = 12M_p\theta + 2 M_p \frac{2l\theta}{2l-x} + M_p \frac{x\theta}{2l-x}$$

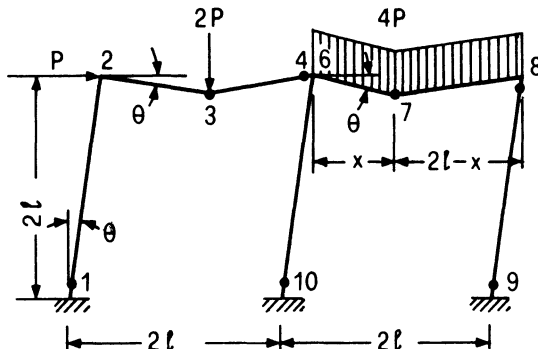


Fig. 3.15.

from which

$$M_p = p \frac{4l + 2x}{12 + (4l + x)/(2l - x)} .$$

The value of  $x$  which maximizes  $M_p$  is found to be  $x = 0.982 l$ , and the corresponding maximum value of  $M_p$  is again  $M = 0.353 P_l$  (the first three significant figures being unchanged). Practically, this determination of  $x$  is necessary only if the mechanism involving a hinge under a distributed load gives us the largest plastic moment, or one every close to it. (say, within 2 %).

#### 5.3.6.6. Verification of the collapse mechanism.

We must check whether the mechanism in fig. 3.13. effectively represents the correct solution of the problem. According to the combined theorem of section 5.1., a necessary and sufficient condition for this is that the corresponding bending moment diagram be statically admissible. To draw this diagram, it suffices to substitute the values

$$M_1 = -M_p, M_3 = +2M_p, M_4 = -2M_p, M_5 = +M_p, M_8 = -M_p, M_9 = +M_p, M_{10} = -M_p ,$$

into the equations of equilibrium (a) to (d) established in section 5.3.6.3. and solve for  $M_2$ ,  $M_6$  and  $M_7$ (\*). One obtains :

$$M_2 = M_p/2 ; M_6 = -M_p ; M_7 = 1.75 M_p .$$

(\*) The fourth unknown in this set of four equations is the value of  $M_p$ , which would be found identical to that furnished by the mechanism, because the work equation of the mechanism is also an equation of equilibrium which is not linearly independent of equations (a), (b), (c) and (d).

The resulting bending moment diagram is shown in fig. 3.16. It is readily verified that the plastic moment is nowhere exceeded; consequently, the collapse mechanism represented in fig. 3.13. is correct.

A fully automatic way of solving the analysis (or restricted design) problem, based on above method of combining mechanisms, will be described in section 5.6.

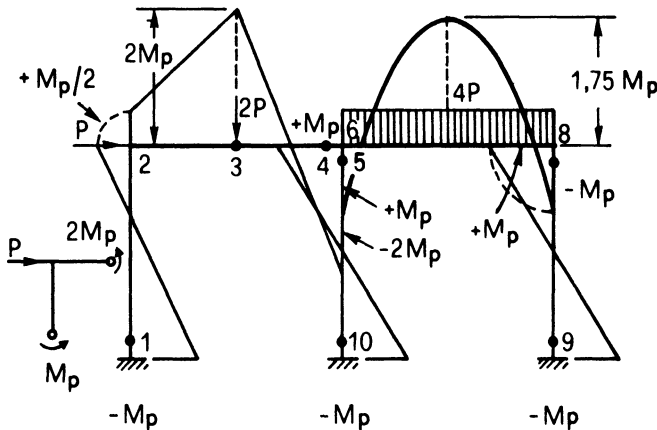


Fig. 3.16.

## 5.4. Variable Repeated Loading – Shake Down Theorems.

### 5.4.1. Introduction.

The problem of variable repeated loading has been discussed in most general terms in section 3.3. We have now, as in section 5.1., to specialize the results obtained for the particular case of structures whose behaviour only depends on a single parameter, the bending moment  $M$ . We shall use again the language of Theory of Structures and, instead of volume and surface forces  $F_i$  and  $T_i$ , consider concentrated or distributed forces  $P$  or  $q$ , applied to the axis of the bars composing the frame.

For each load acting on an elastic-perfectly plastic structure, let a range of variation

$$\lambda P_1 < P < \lambda P_u \quad (4.1.)$$

be prescribed for each load to within a multiplier  $\lambda$  that is common to all bounds. By choosing a sufficiently small value of  $\lambda$ , we may rule out failure by progressive or

alternating plastic deformations (section 3.2.1.), but this need not mean that no plastic deformations will occur when the loads vary within the ranges corresponding to the chosen value of this multiplier. The amounts of plastic deformations that occur in consecutive cycles of loading may decrease as the terms of a convergent infinite series, or plastic deformation may stop altogether after the first cycle or the first few cycles of loading.

In either case, the structure is said to shake down. The fundamental theorem to be established in this section is concerned with the determination of the shakedown multiplier  $\lambda_s$ , that is the greatest value of  $\lambda$  for which the structure will shake down.

Consider now a beam whose cross section has two axes of symmetry, like a I profile. By simple Mechanics of Materials, we can study how such a beam, made of an elastic perfectly plastic material, behaves when it is bent by positive moments, then unloaded and bent by negative moments. The computations (see e.g. [M/6]) show that, when the sense of the bending moment is reversed, the magnitude of the elastic range remains constant and equal to twice the maximum elastic moment of the virgin beam  $M_y$  (fig. 4.1.). This property is only valid if the cross section has two axes of symmetry, bending taking place about one of these axes.

#### 5.4.2. First theorem of incremental collapse.

This being settled, we shall endeavour to recast MELAN's theorem in the

language applicable to plane frames. We assume to simplify that no thermal effect do occur.

If the structure shakes down, there obviously exists a distribution of residual bending moments  $m^{(i)}$  satisfying the following conditions :

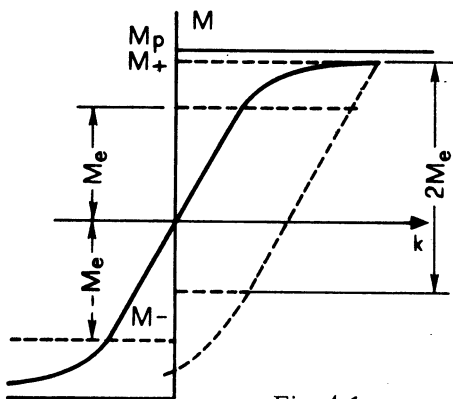


Fig. 4.1.

1. The moments  $m^{(i)}$  represent a state of self-stress of the structure, that is, they are in equilibrium in the absence of loads.

$M_e^{(i)}$  corresponding to any state of loading are superimposed on the residual moments  $m^{(i)}$ , the resulting bending moments nowhere exceed the plastic

moment  $M_p^{(i)}$  in absolute value.

3. As the loads vary within their prescribed ranges, the magnitude of the change  $(\Delta M)_e^{(i)}$  in the elastic bending moment nowhere exceeds the value  $2 M_e^{(i)}$ . Residual bending moments  $m^{(i)}$ , that satisfy these three conditions will be said to represent a virtual shakedown state of the structure for the given range of the loads. Mathematically, the three conditions are expressed by the inequalities :

$$\begin{aligned} m^{(i)} + M_e^{(i) \max} &\leq M_p^{(i)}, \\ m^{(i)} + M_e^{(i) \min} &\geq -M_p^{(i)}, \\ M_e^{(i) \max} - M_e^{(i) \min} &\leq 2M_e^{(i)}, \end{aligned} \quad (4.2.)$$

in which  $M_e^{(i) \max}$  and  $M_e^{(i) \min}$  are the extreme values of the elastic bending moments at the typical section  $i$  for all states of loading under consideration.

MELAN's general shakedown theorem (Section 3.2.3.) asserts that, if the necessary yield conditions (3.2.4.) for shake down are fulfilled with any safety factor  $S > 1$ , shakedown will occur. Now, in the present case, the corresponding necessary yield conditions are :

$$\begin{aligned} m^{(i)} + M_e^{(i) \max} &\leq \frac{1}{S} M_p^{(i)}, \\ m^{(i)} + M_e^{(i) \min} &\geq \frac{1}{S} M_p^{(i)}, \\ M_e^{(i) \max} - M_e^{(i) \min} &\leq \frac{2}{S} M_e^{(i)}. \end{aligned} \quad (4.3.)$$

MELAN's theorem specialized to frames reads therefore

**Static theorem of incremental collapse (MELAN's theorem).**

*If there exists a distribution of virtual bending moments  $m^{(i)}$  that satisfy yield conditions (4.3.), for  $s > 1$  and for the given ranges of the loads, the structure will shake down.*

It should be noted that the actual shakedown state, that is the distribution of residual moments found in the structure after it has shaken down, need not coincide with the virtual shakedown state from which we deduced that the structure will shakedown.

If thermal effects are present, all that is necessary is to extend the definitions of  $M_{e \max}^{(i)}$  and  $M_{e \min}^{(i)}$  to represent the maximum and minimum bending moments which can occur at any particular cross section  $i$  as the loads and temperatures vary between their prescribed limits, assuming wholly elastic behaviour of the structure.

#### 5.4.3. Kinematic theorem for incremental collapse.

The second theorem concerning incremental collapse yields from the kinematics of possible incremental collapse mechanisms. Suppose that the actual collapse mechanism is known, and let  $\theta_i$  represent the hinge rotation which occurs at section  $i$  during a small motion of this mechanism. If the loads on the structure are those corresponding to the incremental collapse multiplier  $\lambda_S$ , the structure will shakedown, and the residual moments  $m^{(i)}$  in it when it has shaken down will be such that the full plastic moment (positive or negative) will be just attained in each cross section  $(i)$  where a plastic hinge occurs in the incremental collapse mechanism. One has therefore

$$(4.4.) \quad \begin{aligned} m^{(i)} + M_{e \max}^{(i)} &= (M_p)^i && \text{if } \theta_i > 0 \\ m^{(i)} + M_{e \min}^{(i)} &= - (M_p)^{(i)} && \text{if } \theta_i < 0 . \end{aligned}$$

Since the  $m^{(i)}$  are in equilibrium with no external loads, and the  $\theta_i$  represent the hinge rotations of a mechanism, principle of virtual work gives the relation

$$(4.5.) \quad \sum m^{(i)} \theta_i = 0 .$$

Since the  $m^{(i)}$  are known from equations (4.4.) and the elastic moments  $M_{e \max}$ , and  $M_{e \min}$  are deductible from the multiplier  $\lambda$ , equation (4.5.) will determine the value  $\lambda_S$  of  $\lambda$  above which incremental collapse will occur.

A computation of this kind can be performed for any arbitrary choice of incremental collapse mechanism, and a corresponding value of  $\lambda$  can be determined. All these values  $\lambda_S^+$  of  $\lambda$  are governed by the

#### Kinematic theorem of incremental collapse :

*A kinematically admissible mechanism of incremental collapse yields, by equations (4.4.) and (4.5.), a multiplier  $\lambda_S^+$  which is never smaller than the actual multiplier of incremental collapse  $\lambda_S$  :*

$$\lambda_s^+ \geq \lambda_s . \quad (4.6.)$$

**Proof :** Consider a plane structure whose incremental collapse multiplier is  $\lambda_s$ .

Suppose that we strengthen the structure by increasing its plastic moment at several cross sections by increasing the yield stress, which leaves the elastic properties of the members unchanged. It results from the static theorem of section 5.4.2. that the incremental collapse multiplier for the reinforced frame cannot be less than  $\lambda_s$  because, if inequalities (4.2.) are satisfied for the original structure, they are a fortiori satisfied for the reinforced structure(\*). Now, we can reinforce the structure in such a way that no hinges will form in the reinforced structure, except precisely at the places where we have assumed hinges in our kinematically admissible mechanism.

Then, this assumed mechanism of incremental collapse will become the actual incremental collapse mechanism for the structure reinforced in this way, which can be written

$$\lambda_s^+ = (\lambda_s)_{\text{structure}}^{\text{reinforced}} \quad (4.8.)$$

Combining (4.7.) and (4.8.), we have

$$\lambda_s^+ \geq \lambda_s , \quad (4.9.)$$

which proves the theorem.

#### 5.4.4. Combined theorem of incremental collapse.

As in the case of collapse under proportional loading (Section 5.1.), we can combine the static and kinematic theorem for incremental collapse into a :

##### Combined theorem of incremental collapse :

Suppose that, for a given multiplier  $\lambda$  governing the bounds (4.1.) of the external loads, a statically admissible distribution of residual bending moments  $m^{(i)}$  can be found, such that, when the maximum and minimum elastic bending moments corresponding to this value of  $\lambda$  are added to the  $m^{(i)}$ , the fully plastic moment is

(\*) This result, incidentally, represents the generalization, for incremental collapse, of FEINBERG's theorem of section 2.4.2. It can be written

$$(\lambda_s)_{\text{struct}}^{\text{reinf}} \geq (\lambda_s)_{\text{struct}}^{\text{original}} \quad (4.7.)$$

nowhere exceeded, but is reached at enough cross sections to transform the structure into a mechanism if hinges are inserted at all these cross sections. Then, this value of  $\lambda$  is exactly equal to the incremental collapse multiplier  $\lambda_s$ .

Methods for calculating the incremental collapse multiplier can be deduced from above three theorems. In section 5.4.7., we develop only the most general method, which gives solutions in all cases.

#### 5.4.5. Upper bound for the maximum deflections in shake-down conditions.

The upper bound of the total energy  $W_p$  dissipated in the structure may be obtained by particularizing for a system of bars subjected to bending the general expression (3.2.14.) obtained in section 3.2.4. As the strain energy of the residual stresses given by the volume integral of (3.2.14.) reduces here to the strain energy

$\frac{1}{2} \int_{\text{structure}} \frac{m^2(x)dx}{EI}$  of the residual bending moments, we obtain

$$(4.10.) \quad W_p = \int_0^t \sum_i M_{pi} |\dot{\theta}_i^p| dt \leq \frac{S}{S-1} \frac{1}{2} \int \frac{m^2(x)dx}{EI}$$

In what follows, we consider plane frames acted upon by concentrated loads. All members are assumed to have an ideal sandwich cross section (section (4.5.) so that yield and plastic moments are equal :  $M_y = M_p = S\sigma_y$ . The loads are described by linear combinations of load parameters  $\mu_K(t)$ . The limits of variation of these parameters in service are known :

$$(4.11.) \quad \mu_K^{\min} < \mu_K(t) < \mu_K^{\max}.$$

The shakedown problem is assumed to have been solved, which means that we know the largest multiplier  $\lambda_s$  for which shake down still occurs ; the corresponding load parameters  $\mu_K$  obey the inequalities

$$\lambda_s \mu_K^{\min} < \mu_K(t) < \lambda_s \mu_K^{\max}.$$

We shall now show that the problem of finding an upper bound to the transverse displacements of this frame prior to shake down is a problem of linear programming. Indeed, the maximum deflection of the arbitrary cross section ( $x$ ) is

$$u(x) = u^E(x) + u^P(x), \quad (a)$$

where  $u^E(x)$  is the elastic part of the displacement and  $u^P(x)$  the plastic part.

Now, if we call  $u^{Ek}$  the elastic displacement due to unit concentrated load number  $k$ , and if the current value of the load  $P_K$  is defined by the parameter  $\mu_K$ , we have by the principle of superposition

$$u^E = \sum_k \mu_k u^{Ek} \quad (4.12.)$$

On the other hand, the rigid-plastic displacements are obtained by combining independent mechanisms (section 5.3.) and are of the general form

$$u^P(x) = \sum_j U_j(x) \theta_j^P \quad (4.13.)$$

where  $\theta_i^P$  are the plastic rotations and  $U_j(x)$  are known functions. Similarly, the diagram of residual moments  $m^{(i)}$  depends linearly on the plastic rotations  $\theta_i^P$  and we may write

$$m^{(i)} = \sum_{ij} K_{ij} \theta_{ii}^P \quad (4.14.)$$

Combining (a), (4.12.) and (4.13.), we have

$$u(x) = \sum_k \mu_k u^{Ek}(x) + \sum_j U_j(x) \theta_j^P. \quad (4.15.)$$

On the other hand, we may rewrite as follows the upper bound (4.10.) of the strain energy stored in the structure

$$\sum_i M_{pi} |\theta_i^P| < W_p < \frac{S}{S-1} \int \frac{m^2(x) dx}{2EI} = a \quad (4.16.)$$

This inequality is equivalent to the following one

$$\pm M_{p1} \theta_1^P \pm M_{p2} \theta_2^P + \dots < a \quad (4.17.)$$

Finally, by using (4.14.), the plasticity conditions (4.3.) may be written :

$$\begin{aligned} m^{(i)} &= \sum_j K_{ij} \theta_j^P < M_{pi} - M_{e \max}^{(i)} \\ &- M_{pi} - M_{e \min}^{(i)} < m^{(i)} = \sum_j K_{ij} \theta_i^P. \end{aligned} \quad (4.18.)$$

The mathematical problem to be solved is to find the maximum of the linear form (4.15.) under the constraints (4.11.), (4.17.) and (4.18.). This is a problem of linear programming (section 5.6.1.), which can be solved by known standard procedures.

For more details, the reader should consult the papers [ B2] and [ B3].

**Important remark.**

In the preceding estimation of the displacement bounds, it was assumed that the structure was initially stress free. If, now, we introduce at the beginning of the loading ( $t = 0$ ) and initial state  $m^o(x)$  of self-equilibrated bending moments, the upper bound of the total energy dissipated in the structure becomes

$$(4.19.) \quad W_p = \frac{S}{S-1} \int \frac{|m(x) - m^o(x)|^2}{2EI} dx .$$

This bound should now be used in the linear program, and thus a different programming problem results. In particular, if  $m^o(x) \equiv m(x)$ ,  $W_p$  becomes zero, which shows that the structure will shake down without any plastic deformations, or, in other words, behave plastically from the outset.

In practice, it is possible to subject the supports of hyperstatic structures to displacements such as to produce these initial moments and to eliminate any permanent deformation under shake-down loading.

#### 5.4.6. Illustrative example of the determination of the shake down multiplier and of the bounds to the plastic displacements.

Consider the portal frame of fig. 4.2. All bars have the same constant cross section, with moment of inertia  $I$  and plastic moment  $M_p$ . The frame is loaded by two independent forces  $V$  and  $H$ , which vary in service between the limits

$$0 < V < 3P$$

$$0 < H < 2P .$$

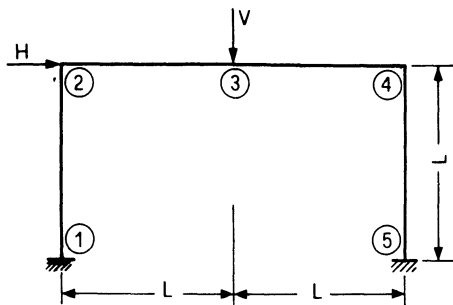


Fig. 4.2.

We consider now various limit problems related to the frame loaded by the increased loads  $\lambda V, \lambda H$ .

The value of  $\lambda$  ensuring a perfectly behavior of the frame is

$$\lambda_E = 1.026 M_p / PL . \quad (a)$$

The collapse load under proportional loading is

$$\lambda_l = 1.200 M_p / PL . \quad (b)$$

Shakedown takes place (see [N3] for the detailed solution) for

$$\lambda_s = 1.132 M_p / PL. \quad (c)$$

The field of the residual moments satisfying the inequalities (4.3.) for  $s = 1$  is unique and may be described by the following values of the redundants  $\mu, \nu, \tau$ , as defined in fig. 4.3.

$$\mu = 0.0188 M_p; \nu = 0.1508 M_p / L; \tau = 0.1225 M_p / L. \quad (d)$$

The upper bound of the total energy dissipated in the shakedown process, calculated by formula (4.10.), is :

$$a = \frac{s}{s-1} \frac{M_p^2 L}{EI} 2.6128 \cdot 10^{-2}. \quad (e)$$

For detailed solution of the linear programming leading to upper bounds of the plastic displacements at shakedown, see [B3].

The table below gives the minimum and maximum values of displacement  $u_4$  for various values of the safety factor(s) against shakedown

Table :  
Upper bounds of deflections  
(all values are to be multiplied by  $M_p L^2 / EI$ )

S	- min $u_4$	max $u_4$
1.0000	±	±
1.0127	0.8305	0.8259
1.0256	0.5446	0.4970
1.0526	0.3832	0.3284
1.1111	0.2935	0.2385

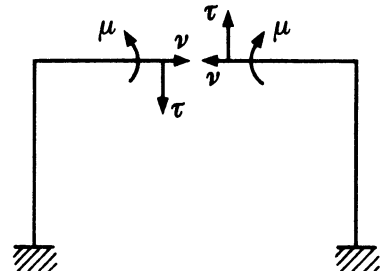


Fig. 4.3.

#### 5.4.7. Method of combining mechanisms [N3].

The method of combining mechanisms for the determination of  $\lambda_s$  is a direct generalization of the similar method for the calculation of the collapse multiplier  $\lambda_l$ , which has been explained in full detail in section 5.3.6.

The method is essentially based on the kinematic theorem of incremental collapse

which asserts that, for any assumed incremental collapse mechanism, a value of  $\lambda_s^+$  may be found by the process explained in section 5.4.3., and that the exact value of  $\lambda_s$  is the smallest of all the  $\lambda_s^+$ .

With this in mind, the method of combining mechanisms consists simply in :

- computing values of  $\lambda_s^+$  corresponding to the various independent mechanisms;
- combining these mechanisms with the aim of reducing  $\lambda_s^+$ , until it is believed that the lowest possible value has been found. One applies then, like in section 5.3.6., a statical check by determining the corresponding distribution of residual moments  $m^{(i)}$  and verifying the the maximum and minimum elastic bending moments can be added to the residual moment at every cross section without exceeding the plastic moment.

A fully automatic way of calculating  $\lambda_s$  on a computer based on above method, will be reviewed in section 5.6.1.

## 5.5. Minimum Weight Design.

### 5.5.1. Introduction.

The real purpose of all methods of analysis is to enable the designer to answer to the basic question : Given the loads and general dimensions of a structure, what strengths should the members have to produce an optimum solution ?

Now, as we shall see, it is possible to answer very simply to this question if elastic-perfectly plastic behaviour is assumed. In this respect, the plastic methods provide a major advance over the design efficiency possible with conventional elastic methods. This is so because the plastic method enables the design to be based on a definite factor of safety with respect of a real failure of the structure.

On the contrary, except for isostatic structures, the elastic designer has no knowledge of the real failure load and, thererore, of the corresponding factor of safety.

Now, to define an optimum design is a very difficult task, because a large number of considerations are involved : economic factors such as the relative costs of labor and steel, aesthetic considerations, etc. . . . The minimum weight solution, which is very important for aerospace structures, represents generally in Civil

Engineering an oversimplified version of the optimum solution (see [M10] for a detailed discussion of this point). However, in the particular case of plane frames made of rolled profiles, the cost of manufacturing the connections may be supposed to be roughly proportional to the cost of the bars themselves, and the total cost. For this reason, we shall study in what follows how to obtain the minimum weight solution.

### 5.5.2. Simplifying assumptions.

For each discrete series of available rolled profiles (in Europe, the narrow flange profiles IPE; the wide flange profiles HEA, HEB, HEM), a more or less definite relationship exists between plastic moment,  $M_p$ , and weight per unit length,  $w$ .

In some limited range, the actual (non linear) relationship may be replaced by a linear one, so that, for prismatic member  $i$ , of length  $l_i$ , the weight per unit length is

$$w_i = a + b M_{pi} \quad (5.1.)$$

where  $M_j$  is the (constant) plastic moment of the member and  $a$  and  $b$  are constants. The total weight of the structure is therefore

$$W = \sum_i w_i l_i = \sum_i l_i (a + b M_{pi}) = a \sum_i l_i + b \sum_i M_{pi} l_i. \quad (5.2.)$$

the summations being extended over all members of the structure.

The term  $a \sum_i w_i l_i$  is independent of the choice of particular cross sections within the range covered by the linear approximation (5.1.). Accordingly, the weight  $W$  is minimized by minimizing the quantity  $\sum M_{pi} l_i$ . For brevity, we call  $\sum M_{pi} l_i$  the weight function and denote it by  $G$ . HENCE, by definition

$$G = \sum M_{pi} l_i. \quad (5.3.)$$

The problem of plastic design for minimum weight can now be stated as follows : to design a structure, with given overall dimensions, that will support given limit loads (imposed by the Specifications) and simultaneously minimize its weight function.

### 5.5.3. Solution of the minimum weight design.

Minimum weight designs have very interesting properties, which have been discovered by FOULKES ([F1], [M6]). The present course does not permit, however, to study them. The main point is to find a convenient method for obtaining the minimum weight design. This will be done in the next section, where it

will be proved that the minimum weight design may be reduced to a linear program, for which convenient computer programs are available.

## 5.6. Practical Solution of all Problems of Plastic Analysis, Incremental Collapse and Minimum Weight Design by Reduction to Linear Programming.

### 5.6.1. Linear programming and limit analysis and design.

As they are books devoted to linear programming, it is clear that we cannot analyze thoroughly here this mathematical method. We shall content ourselves to say that a linear program may be appear under several forms, but that it is always possible to put it under the following standard form

find the minimum of  $\sum_{i=1}^n c_i x_i$

with the constraints

$$(6.1.) \quad \begin{aligned} \sum_{i=1}^n a_{ij} x_j &= b_i \quad (i = 1, 2, \dots, m) \\ x_i &\geq 0. \end{aligned}$$

In condensed matrix form, this becomes :

Find the minimum of  $C x$

with the constraints  $A x = b$ , (being a  $m \times n$ ) matrix and  $x \geq 0$ .

Above problem was solved in 1947 by G.B. DANTZIG, who devised the so-called “simplex” method. This method has been programmed for electronic computers, and it can be safely said that any serious computation center has presently at his disposal one or several programs for solving automatically at high speed linear programs, solving several hundred of variables.

The first paper recognizing that, for one-parameter structures like frames, the determination of the limit multiplier  $\lambda_1$  of rigid-plastic analysis under proportional loading was a problem of linear programming is that of CHARNES and GREENBERG [C1] (1951).

It has been shown, since, that all problems of plastic analysis and design were mathematical programming problems and could be solved by computer if the corresponding mathematical programs were available. These last years, the number

of papers devoted to such solutions has so increased that it is impossible, in the present short course, to make an exhaustive synthesis of them. We shall refer the reader, for this synthesis, to a very recent (unpublished) paper of professor D.E. GRIERSON [G2], which covers the following items :

**A. First-order analysis and design :**

1. Rigid-plastic analysis;
2. Incremental elastic plastic analysis;
3. Elastic-plastic analysis at collapse;
4. Optimal design.

**B. Second-order analysis and design :**

1. Incremental elastic-plastic analysis;
2. Elastic-plastic design;
3. Optimal elastic-plastic design.

In what follows, we shall cover only the items A 1), 2) and 4), for which the theory has been given in the preceding sections. To bring some order in the classification, let us remark that we distinguish, regarding :

the type of problem, between analysis and design;

the type of loading, between one proportional loading,

several proportional loadings prescribed by the Building Code,

Variable repeated loading (shake down).

the type of approach, between the static approach and the kinematic approach.

Combining these various types, we obtain the 10 different problems listed in the table below

Problem	Type	Loading	Approach
1	Analysis	proportional	static
2		kinematic	
3		static	
4		kinematic	
5	Optimal design	one proportional loading case	static
6		kinematic	
7		several proportional loading cases	static
8		kinematic	
9		shake down	static
10			kinematic

COHN, GHOSH and PARIMI [C2] have demonstrated that all these 10 problems could be identified as linear programs and have developed a computer program for solving them on computer.

As shake-down problems are not considered important in normal structures, because of probabilistic considerations developed by HORNE [H4], we shall drop problems 3, 4, 9 and 10. Moreover, the optimal design for several proportional loading cases is a rather straight forward extension of the same problem for one single loading case [C2]. We shall therefore investigate only, in what follows, problems 1, 2, 5 and 6.

A concrete problem will be given for illustration in each case and some general indications will be given for its solution. For the detailed treatment of these problems, we refer to the book of exercises by COHN [C3], from which these problems have been taken.

But, before reviewing problems 1, 2, 5 and 6, we have to explain how it is possible to obtain, on the computer, the :

#### 5.6.2. Automatic generation of a complete set of independent mechanisms.

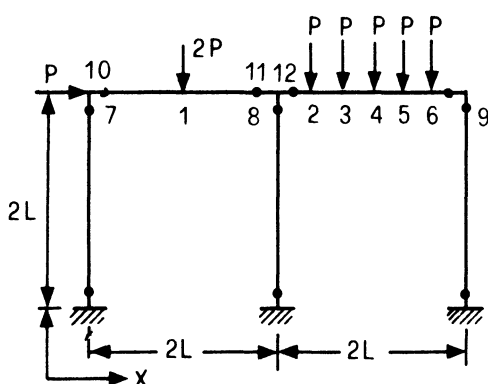


Fig. 6.1.

The method used has been explained in full detail in another paper of the author M8,. Lack of space forces us to give here only a condensed account. To be definite, let us consider the frame depicted by Fig. 6.1. It is referred to orthogonal axes  $x, y$ . We first number all the potentially critical sections, that is, all the sections where a plastic hinge may be formed. We call bars the rigid segments connecting two hinges.

The mechanisms of the frame are characterized by displacements of the hinges such that the elongations on the bars are zero and the support conditions are respected. Now, it is easy to calculate the elongations of the bars;  $\Delta l_j$ , as functions of the displacements  $u_{x,i}, u_{y,i}$  of the various hinges. In matrix notation, we can write

$$\underline{\Delta l} = \underline{A} \underline{U}$$

where  $\underline{\Delta l}$  is the vector of the bar elongations ;

$\underline{U}$  is the vector grouping the displacements of all hinges ;

$A$  is a rectangular  $m \times n$  matrix depending on the topology of the structure where  $m$  is the number of bars and  $n$  is twice the number of hinges.

The mechanisms of the frame will be obtained by searching the hinge displacements which produce no elongations in the bars. These displacements are solution of the homogeneous system

$$A \underline{U} = 0, \quad (6.2.)$$

where the trivial solution  $\underline{U} = 0$  must evidently be eliminated. It can be shown that the solution  $\underline{U} \neq 0$  of (6.2.) may be obtained systematically by applying the GAUSS – JORDAN elimination method. For the details, the reader is referred to [M8].

### 5.6.3. Limit analysis - Kinematic approach.

Consider a possible mechanism,  $i$ , associated with the kinematic multiplier  $\lambda_i^+$ , hinge rotations,  $\theta_{ij}$ , and external work of the applied service loads,  $e_i$ .  $\lambda_i^+$  is defined by the work equation (5.3.5.).

$$u_i = \sum_{j=1}^m M_{pj} \theta_{ij} = \lambda_i^+ e_i, \quad (6.3.)$$

where  $u_i$  is the total energy dissipated by plastic hinge  $J$  in mechanism  $i$  and  $s$  is the member of plastic hinges in this mechanism.

According to the kinematic theorem of Limit Analysis (section 5.1.), the exact limit multiplier  $\lambda_l$ , and the associated collapse mode, are given by the condition

$$\lambda_l = \min_i \lambda_i^+ = \min_i u_i / e_i = \min_i \left( \sum_{j=1}^s M_{pj} \theta_{ij} / e_i \right) (i = 1, 2, \dots, p) \quad (6.4.)$$

The method of combining mechanisms (section 5.3.6.) proves that all possible collapse mechanisms of a structure can be generated by linear combinations of  $m$  independent mechanisms. This number,  $m$ , the degree of statical indeterminacy,  $h$ , and the number of potential plastic hinges,  $s$ , are related by equation (5.3.7.), which, with present notations, becomes

$$m = s - h. \quad (6.5.)$$

The hinge rotations,  $\theta_{ij}$ , and external work,  $e_i$ , of the combined mechanism,  $i$ , are,

by definition, linear combinations of the corresponding hinge rotations,  $\theta_{Kj}$ , and external works,  $e_K$ , associated with the independent mechanism, i.e., :

$$(6.6.) \quad \theta_{ij} = \sum_{k=1}^m t_{ik} \theta_{jk} \quad \text{and} \quad e_i = \sum_{K=1}^m t_{iK} e_K,$$

where  $t_{ik}$  is a coefficient indicating the contribution of independent mechanism  $k$  to  $\theta_{ij}$  and  $e_i$  in the combined mechanism  $i$ .

Since an independent mechanism cannot result from a linear combination of any other mechanisms (because these form a complete set !),

$$(6.7.) \quad t_{ik} = \begin{cases} 1 & \text{for } i = k \\ 0 & \text{for } i \neq k \end{cases} \quad (i, k, = 1, 2, \dots, m).$$

A combined mechanism ( $i = m + 1, \dots, p$ ) is therefore characterized by at least two non-zero coefficients  $t_{ik}$ .

Assume now that the actual collapse mode ( $i = c$ ) has been identified.

( $i = c$ ,  $\lambda_c^+ = \lambda$ ), that the particular values of the variables for mechanism  $c$  are  $\theta_j$  ( $\equiv \theta_{cj}$ ) and  $t_K$  ( $= t_{cK}$ ), so that the subscript  $i (= c)$  can be dropped in equation (6.6.), for the collapse condition.

Now, it can be shown that the limit analysis problem can be formulated as a linear program (in its standard form (6.1.) as follows :

Find

$$\lambda, \theta_j, \text{ and } t_K (J = 1, 2, \dots, s; K = 1, 2, \dots, m)$$

such that

$$(6.8.) \quad (\lambda \pm) \sum_{J=1}^s M_{pj} \theta_J = \text{minimum}$$

with the constraints

$$(6.9.) \quad \theta_j - \sum_{K=1}^m t_K \theta_{kj} = 0, \quad (J = 1, 2, \dots, s)$$

$$(6.10) \quad \sum_{K=1}^m t_K e_K = 1.$$

However, the standard form soluble by the Simplex algorithm requires all the variables to be positive, while the rotations  $\theta_{ij}$  may be positive or negative.

To surmount this obstacle, we shall introduce in all problems to be discussed hereafter, the following trick. Let us call  $\theta_{ij}^+$  and  $\theta_{ij}^-$ , respectively the absolute values of the inelastic rotations in the positive and negative directions of bending, respectively, so that :

$$\begin{aligned}\theta_{ij}^+ &= \theta_{ij} \quad , \quad \theta_{ij}^- = 0 \quad \text{if} \quad \theta_{ij} > 0 \\ \theta_{ij}^+ &= 0 \quad , \quad \theta_{ij}^- = -\theta_{ij} \quad \text{if} \quad \theta_{ij} < 0.\end{aligned}\tag{6.11}$$

Let  $M_{pj}^+$  and  $M_{pj}^-$  be the (absolute) values of the plastic moment capacities of hinge J, corresponding to  $\theta_{ij}^+$  and  $\theta_{ij}^-$ , respectively. Then, we can recast the linear program above [equat. (6.8.) to (6.10.)] as follows :

Find

$$\lambda, \theta_J^+, \theta_J^- \text{ and } t_k \quad (J = 1, 2, \dots, s; k = 1, 2, \dots, m)$$

such that

$$(\lambda^+ =) \sum_{J=1}^s M_{pj}^+ \theta_J^+ + \sum_{J=1}^s M_{pj}^- \theta_J^- = \text{minimum} \tag{6.12.}$$

with the constraints :

$$\theta_J^+ - \theta_J^- - \sum_{K=1}^m t_K \theta_{kj} = 0 \quad (J = 1, 2, \dots, s) \tag{6.13.}$$

$$\sum_{K=1}^m t_K e_K = 1 \tag{6.14.}$$

and

$$\theta_J^+, \theta_J^- \geq 0$$

This program has  $(2s + m)$  variables and  $(s + 1)$  constraints.

#### 5.6.4. Limit Analysis - Static Approach.

The static approach is based on the consideration of a statically admissible bending moment diagram  $M_{ij}(J = 1, 2, \dots, s)$  under the external loads  $\lambda_i^- P$  ( $i = 1, 2, \dots, \infty$ ). By definition, these moments satisfy the  $m$  independent equilibrium equations and the plasticity conditions for all critical sections.

According to the static theorem of Limit Analysis (section 5.1.), the bending moment diagram at collapse corresponds to the largest value of  $\lambda_i$ , i.e.  $\lambda = \max \lambda_i^-$  ( $i = 1, 2, \dots, \infty$ ). Assume that the actual collapse mode ( $i = c$ ) has been identified (for  $i = c$ ,  $\lambda_c^- = \lambda_1^-$ ) and that the particular values of the moments for the collapse mode are  $\bar{M}_J$  ( $= \bar{M}_{cJ}$ ), so that the subscript  $i$  ( $= c$ ) can be dropped in subsequent equations.

The problem of Limit Analysis can then be reduced to the following Linear program:

Find

$$\lambda^-, \bar{M}_J \quad (J = 1, 2, \dots, s)$$

such that

$$(6.16.) \quad \lambda^- = \text{maximum}$$

with the constraints

$$(6.17.) \quad \sum_{J=1}^s \theta_{KJ} \bar{M}_J + \lambda^- e_K = 0 \quad (k = 1, 2, \dots, m)$$

and

$$(6.18.) \quad \bar{M}_J \leq M_{PJ}^+, \bar{M}_J \leq M_{PJ}^- \quad (J = 1, 2, \dots, s)$$

This program has  $(s + 1)$  variables and  $(2s + m)$  constraints.

As closer study of the linear programs (6.12.) to (6.15.) and (6.16) to (6.18) shows that these kinematic and static formulations of Limit Analysis are dual in the linear programming sense. They result therefore in the same collapse multiplier  $\lambda = \min_i \lambda_i^+ = \max_i \lambda_i^+$ , which demonstrates again the combined theorem of Limit Analysis (section 5.1.).

**Problems :** The hinged frame of fig. 6.2. is subjected to the service loads indicated.

Find his collapse multiplier  $\lambda_l$  successively by the kinematic and the static approaches.

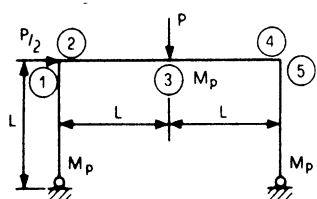


Fig. 6.2.

**hint :**  $h = 1$ . The  $s = 5$  critical sections to consider are numbered (1) to (5) on fig. 6.2. The  $s - h = 4$  independent mechanisms are shown on fig. 6.3. (a) to (d), with the values of the corresponding rotations

$\theta_{JK}$ .

The kinematic formulation possesses 6 constraints.

The static formulation possesses 4 constraints.

Answer : The collapse multiplier is :

$$\lambda_1 = \frac{2.667 M_p}{P L}$$

and corresponds to the mechanism of fig. 6.4. (a) and to the diagram of fig. 6.4. (b).

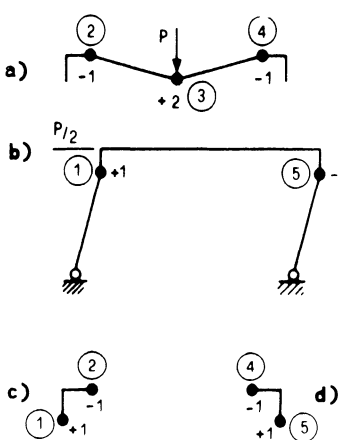


Fig. 6.3.

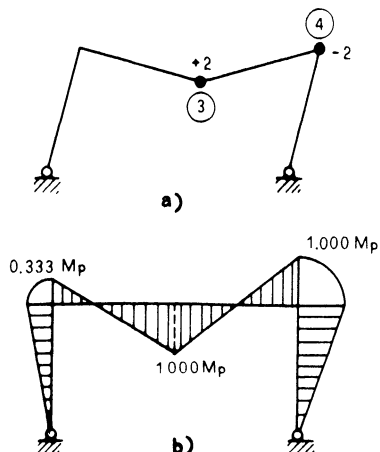


Fig. 6.4.

### 5.6.5. Optimum design - Introduction.

In this section and the next one the expression "optimum design" is used in short for a minimum weight design, that is a design that minimizes the weight function  $G$  given by expression (5.3.).

As defined in section 5.5., the optimum design consists of choosing for all bars of the frame plastic moment capacities such that the conditions of minimum weight (0), equilibrium (E), plasticity (P) and mechanism (M) are satisfied.

This problem can be solved by satisfying only three of the above conditions simultaneously.

If conditions (0), (E) and (P) are satisfied, we have the static approach.

If conditions (0), (E) and (M) are satisfied, we have the kinematic approach.

### 5.6.6. Optimum design - One proportional loading - Kinematic approach.

The kinematic formulation is

Find

$$M_{ph} \quad (h = 1, 2, \dots, n)$$

such that

$$(6.19.) \quad G = \sum_{h=1}^n M_{ph} l_h = \text{minimum}$$

with the constraints

$$(6.20.) \quad \sum_{h=1}^n a_{ih} M_{ph} \geq \lambda_l e_i \quad (i = 1, 2, \dots, p)$$

and

$$(6.21.) \quad M_{ph} \geq 0.$$

In these formulae,  $M_{ph}$  are the unknown plastic moments of the optimum design,  $l_h$  are the bar lengths over which  $M_{ph}$  are constants,  $G$  is the weight function of the frame,  $a_{ih}$  is the coefficient defining the contribution of  $M_{ph}$  in the  $i$  th equilibrium equation. Inequalities (6.20.) represent the equilibrium and mechanism conditions of the problem and state that the frame must not fail under loads below the ultimate loads specified in the Code by the multiplier  $\lambda_l$  in any of the  $p$  possible collapse modes (which can always be derived from any set of  $m < p$  independent mechanisms).

### 5.6.7. Optimum design - One proportional loading - Static approach.

The static formulation of the optimal design problem is :

Find

$$M_{ph}, \bar{M}_J \quad (h = 1, 2, \dots, n ; J = 1, 2, \dots, s)$$

such that

$$G = \sum_{h=1}^n p_{ph} l_h = \text{minimum}$$

with the constraints

$$\sum_{j=1}^s \theta_{kj} \bar{M}_j = \lambda_1 e_k \quad (k = 1, 2, \dots, m) \quad (6.22.)$$

$$M_{ph} - \bar{M}_j \geq 0 \quad (h = 1 \text{ for } j = 1, 2, \dots, s_1; \quad$$

$$M_{ph} + \bar{M}_j \geq 0 \quad \begin{array}{l} h = 2 \text{ for } j = s_1 + 1, \dots, s_2; \\ \vdots \\ h = n \text{ for } j = s_{n-1}, \dots, s_n \end{array} \quad (6.23.)$$

and

$$M_{ph} \geq 0.$$

Equations (6.22.) represent a set of independent equilibrium conditions and inequalities (6.23.), a set of 2s plasticity conditions.

### Problems :

Find the optimum design of the built-in frame of fig. 6.5., subjected to the ultimate loads indicated, by using successively the kinematic and the static approach.

**Hint :**the frame is 3 times statically indeterminate.

The critical sections are numbered (1) to (7) on fig. 6.5. The weight function to minimize is

$$G = L M_{p1} + \frac{3L}{2} M_{p2} + L M_{p3}.$$

In the kinematic approach, there are  $p = 10$  independent mechanisms, because the corner hinges may occur in (2) or (5), or in (4) or (7). The linear program contains therefore 10 inequalities (6.20.).

In the static approach, there are 4 independent equilibrium conditions (6.2.2.), corresponding to the 4 independent mechanisms 5-6-7; 1-2-3-4; 2-5 and 4-7.

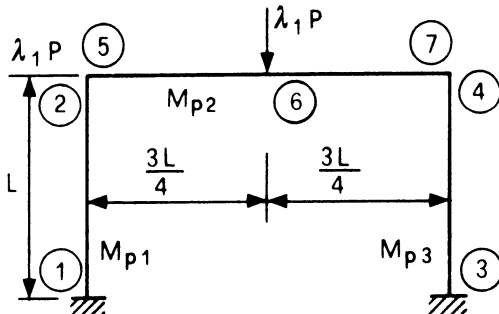


Fig. 6.5.

Answer :  $M_{p1} = 0.1875 \lambda_1 PL ; M_{p2} = M_{p3} = 0.3125 \lambda_1 PL.$

#### 5.6.8. "Realistic" optimum design.

The minimum weight design solution presented in Sections 5.5., 5.6.6. and 5.6.7. is an "academic" one, because a lot of practical considerations have been disregarded.

In actual practice, the following additional constraints must be considered :

1. The Building Code obliges to consider several independent (proportional) loading cases;
2. The plastic moment capacity,  $M_p$ , of a bar, may be reduced by the effect of normal force  $N$  and shear force  $V$  ;
3. The rolled profiles available form several discrete series, so that  $M_p$  is not a continuous variable ;
4. The design may be controlled by limits to the deflections in service, imposed by the Code ;
5. Stability of the various bars against local plate buckling, and individual or overall buckling (by bending or lateral torsional) must be controlled ;
6. Second order (also called  $P - \Delta$ ) effects must eventually be taken into account.

If this is done properly (that is by introducing suitable initial imperfections of the compressed bars), the consideration of  $P - \Delta$  effects guarantees against overall buckling. The danger of instability is thereby eliminated, provided local plate buckling is eliminated by rejecting the rolled profiles having insufficient thickness ratios.

The effect of the axial forces can rather easily be incorporated into the linear programs [C4]. For other contributions, we refer to the literature and especially to [G2]. To pinpoint the degree of development, we mention that :

- 1) In the department of the author, a program (due to R. ANSLIJN and the author) has been developed, which takes into account constraints 1, 2, 3 and 5 above. The program starts with an "academic" optimum design, then selects the sizes of the rolled profiles in the available series, by taking account iteratively of the effect of  $N$ . The constraints of individual buckling are applied afterwards and the bars reinforced accordingly.

- 2) Iterative programs, based on linear programming, written by HORNE and MORRIS [H5] and by EMKIN and LITTLE [E1], enable the optimum plastic design of multistory buildings. They take account, at least approximately, of all the additional constraints (1) to (6) listed above.

## 6. OTHER STRUCTURES MADE OF BARS

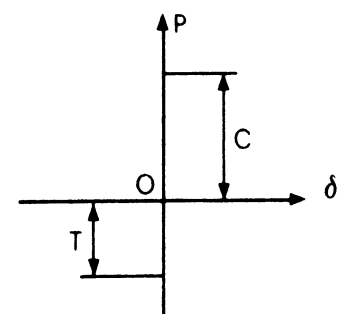
### 6.1. Pile Groups.

The control of the safety of foundations on pile groups is usually made by NÖKKENTVED's method, which is an elastic procedure based on the three following assumptions :

1. The piles are hinged at the foot and the head; transverse earth pressure is disregarded, so that they are axially loaded;
2. The axial component of the displacement of the pile's head is proportional to the load it sustains;
3. The foundation itself is rigid.

NÖKKENTVED's method does not enable to appreciate the effective safety of a pile foundation against collapse. Moreover, it leads to true paradoxes like the following : the adjunction of a supplementary pile to a group of piles may have as consequence to diminish the allowable force on the foundation. A similar paradox in the elastic theory of bending was already mentioned in Section 2.4.2.

In a paper written by H. MAUS and the author [M4], it is shown that the behavior of a pile may be idealized by the rigid-plastic model of fig. 6.1. The pile remains rigid for any axial effort  $P$  such that  $T \leq P \leq C$ . If  $P$  reaches the limit  $C$  in compression, the pile yields under constant force; the same occurs if  $P$  reaches the tension limit  $T$ .



In this way, a group of piles is reduced to a system of rigid-plastic hinged bars. The search for the collapse multiplier  $\lambda$  of a foundation subjected to a force  $Q$  in service can then visibly be

Fig. 6.1.

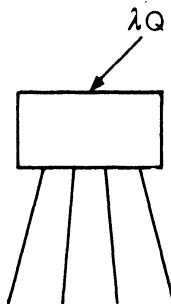


Fig. 6.2.

reduced to a linear program.

The method is developed and numerical examples given in the paper cited above. DEMONSABLON [D2] has generalized the study by considering the more realistic case of a heavy foundation whose dead weight remains constant, while (proportional) live loads may be added.

More details can be found in the book by M. SAVE and the author [M7].

## 6.2. Torsionless Grids Loaded Perpendicularly to their Plane.

In grids made of steel rolled profiles, the torsional rigidity is so small that torsional moments can be neglected. These grids are therefore one-parameter structures governed, like frames, by the bending moment. The solution of the problem of Limit Analysis or optimum design for these grids is similar to that obtained in Chapter 5 for plane frames loaded in their plane [M7]. These problems can, once again, be reduced to linear programs.

## 6.3. Torsionally Stiff Grids – Rigid Space Frames-Arches.

There exists an extensive literature on the limit analysis and design of space frames and similar structures. These are multiparameter structures, the behaviour of which is governed for each bar, by the yield condition  $f(N, M_x, M_y, M_z, T_x, T_y) = 0$  expressing the interaction at yield of the various stress resultants. These interaction laws have been extensively studied; they are always non linear. As an

example, the bending-torsion interaction in bars of I or rectangular cross section is represented by fig. 6.3. It can decently be approximated by the circumference of equation

$$\left(\frac{M_f}{M_{f_0}}\right)^2 + \left(\frac{M_t}{M_{t_0}}\right)^2 = 1.$$

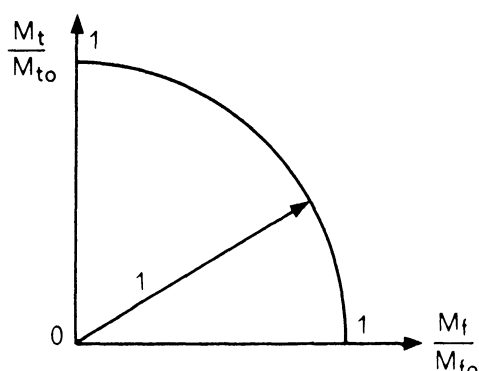


Fig. 6.3.

If these yield loci are approximated by piecewise linear curves or surfaces, it is possible to reduce all the problems of limit analysis and design mentioned in

the table of section 5.6.1. to a series of linear programs.

#### 6.4. Masonry Structures.

Limit Analysis has found an unexpected development in the field of masonry structures, due especially to the researches of HEYMAN [H4].

It provides, in the opinion of the author, the first satisfactory explanation of the stability and behaviour of the gothic cathedrals (see [M7] for a more detailed account).

### 7. VARIOUS APPROACHES TO THE LIMIT ANALYSIS OF PLATES, SHELLS AND DISKS.

#### 7.1. Introduction.

There exists an extensive literature on the limit analysis of plates, shells and disks in metal or reinforced concrete, which has been synthetized in the book [ S3 ] by professor SAVE and the author.

As the subject of plates is extensively covered by the lessons of Professor SAWCZUK at this course of Engineering Plasticity, I, Civil Engineering, it will not be treated here.

For development in this last chapter, three items have been selected among the research contributions of the author and his former or present collaborators :

- 1) The limit strength of a thin-walled beam with circular axis, because it provides an excellent illustration of the analytical theory of Limit Analysis, and especially of the various plastic "regimes" in the case of a piecewise linear yield criterion ;
- 2) The elastoplastic incremental analysis of structures by the method of finite elements and its application to problems of plane stress ;
- 3) The quasi-direct Limit Analysis via the finite element method.

In the first method, which is applicable to hardening as well as to perfectly plastic materials, the progressive extension of plastic zones in the structure under increasing load is followed step by step until, eventually, the limit load is reached.

The second method, on the contrary, computes directly the limit strength of elastic-perfectly plastic structures, without following the complete elastoplastic deformation history.

## 7.2. Limit Strength of a Wide-Flange I Beam with Circular Axis.

### 7.2.1. Introduction.

It is well known that the cross sections of thin walled beams with curved axis subjected to bending tend to be distorted due to the transverse forces  $q$  created by the axial stresses acting on neighboring cross sections forming the angle  $d\phi$  (Fig. 2.1.).

The first study of this kind, due to von KARMAN, was developed for the curved tube with thin-walled circular cross sections; it is showed the effect of the axis curvature on the distribution of stresses due to bending and on the flexural rigidity of the tube. This study, however, was restricted to elastic behaviour. It was later extended to other types of cross sections by TIMOSHENKO, STEINHARDT, ANDERSON and others. Our purpose, however, is entirely different; it is to show that such thin-walled beams possess a very large plastic strength reserve beyond the value of the bending moment  $M_y$ , for which the yield stress is reached in the most stressed point ([M11], [M12], [S3]).

In what follows, we consider a wide flange I beam with circular axis, subjected to a uniform bending moment diagram with magnitude  $M$  (Fig. 2.1.). Due to the constancy of  $M$  with  $\phi$ , the deformed axis will remain circular. We shall first study the limit behaviour of an isolated flange, then that of the web, and finally the behaviour of the complete I profile. The metal is supposed to follow TRESCA's yield criterion.

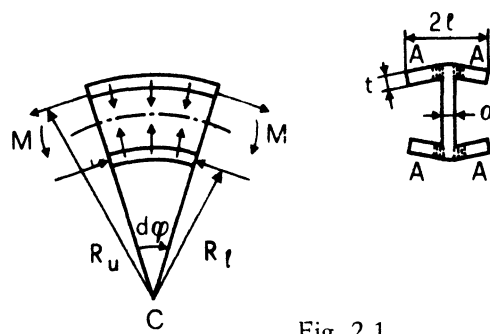
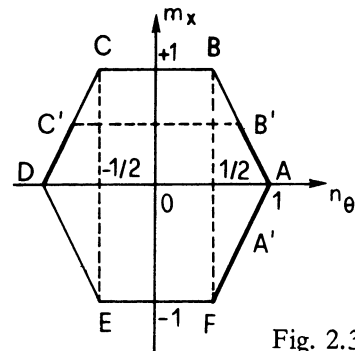
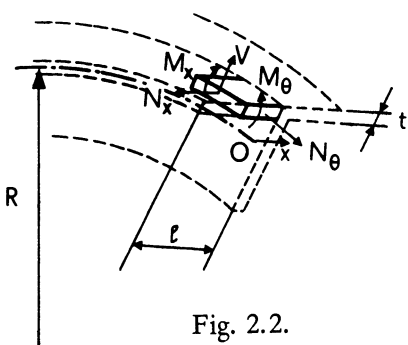


Fig. 2.1.



### 7.2.2. Limit behaviour of a flange.

Each flange behaves like a cylindrical, axisymmetrically loaded, shell, that is built-in at the web. An element of the upper flange is shown in fig. 2.2.  $N_x = 0$ , while  $V_x$  and  $M_\phi$  are reactions (see section 4.4.3.). The equilibrium equations of a shell element are

$$\frac{dV_x}{dx} + \frac{R_\theta}{R} = 0, \quad \frac{dM_x}{dx} = V_x \quad (2.1.)$$

Eliminating  $V_x$ , we find

$$\frac{d^2 M_x}{dx^2} + \frac{N_\theta}{N} = 0. \quad (2.2.)$$

To have linear differential equations to integrate, we use the piecewise linear hexagonal yield condition ABCDEFA, represented by dashed lines in Fig. 4.4.8., and shown again in fig. 2.3. As this is an inscribed approximation to the exact yield curve given in full line in fig. 4.4.8., the corresponding limit multiplier  $\lambda_i$ , by section 4.5.2., will satisfy the inequality  $\lambda_i < \lambda_l$ , where  $\lambda_l$  is the exact limit multiplier for the exact yield curve.

Introducing as in section 4.4.3. the reduced generalized stresses

$$m_x = \frac{M_x}{M_{pf}} \quad \text{and} \quad n_\theta = \frac{N_\theta}{N_{pf}}, \quad \text{with} \quad M_{pf} = \sigma_y \frac{t^2}{4}, \quad N_{pf} = \sigma_y t, \quad (2.3.)$$

we recast equation (2.2.) as

$$\frac{d^2 m_x}{dx^2} + \frac{4}{tR} n_\theta = 0. \quad (2.4.)$$

If the ratio of the span  $l$  of the half flange (fig. 2.2.) to its thickness is not too large, the bending moment at the web root will be smaller than the plastic moment. The stress regime of the half-flange will start from point A of the yield locus ( $m_x = 0$ ), and, since  $m_x$  is negative, extend along side AF, whose equation is

$$(2.5.) \quad m_x - 2 n_\theta = -2.$$

The boundary conditions at  $x = 0$  are

$$(2.6.) \quad m_x = 0, \quad \frac{dm_x}{dx} = 0.$$

Integration of equation (2.4.), taking account of (2.5.) and (2.6.), furnishes  $n_\theta = \cos(\sqrt{2x/tR})$ . If we introduce the parameter

$$(2.7.) \quad \alpha = 1 \sqrt{\frac{2}{tR}},$$

the expression of  $n_\theta$  becomes

$$(2.8.) \quad n_\theta = \cos \frac{\alpha x}{1},$$

valid for  $1 > n_\theta > 1/2$ , that is, for  $0 < x < \sqrt{0.548 tR}$ . As long as

$$(2.9.) \quad 1 < \sqrt{0.548 tR},$$

We can use equation (2.8.) to compute the plastic efficiency  $\rho_f$  of the flange, defined as

$$(2.10) \quad \rho_f = \frac{1}{l} \int_0^l n_\theta dx = \frac{1}{N_{pfl}} \int_0^l N_\theta dx.$$

When condition (2.9.) is not satisfied, the plastic regime must be changed. Since downward transversal bending deflections  $v$  produce compressive circumferential strains  $\epsilon_\theta = v/R$ , that is strains of sign opposite to the positive strains due to  $N_\theta$  in the circumferential fibers, the resulting strain  $\epsilon_\theta$  for large values of  $\alpha$  may become negative. Therefore, the transverse forces  $q$  also change sign in the vicinity of the tip of the flange (fig. 2.4.) and  $m_x$  becomes positive for small values of  $x$ . We are then led to choose the plastic regime DC'B'AF. The extremity of the flange, on a width  $d_1$ , is in regime DC', with  $\epsilon_\theta < 0$ , though the considered flange is, as an average, subjected to tension. The jump from C' to B' (discontinuity of  $n_\theta$  with  $x$ ) is admissible (see section 4.6.) because the continuity of  $m_x$  and  $dm_x/dx$  is preserved.

The situation is now as follows (Fig. 2.3. and 2.4.) :

- Regime DC' over  $0 \leq x \leq d_1$ . The yield condition is

$$m_x = 2 + 2 n_\theta \quad (2.11.)$$

with the boundary conditions (2.6.). The resulting stress distribution is

$$n_\theta = - \cos \frac{\alpha x}{l}, \quad m_x = 2 - 2 \cos \frac{\alpha x}{l} \quad (2.12.)$$

- Regime B'A over  $d_1 \leq x \leq d_1 + d_2$ . The yield condition is

$$m_x + 2 n_\theta = 2. \quad (2.13.)$$

Elimination of  $m_x$  between equations (2.4.) and (2.13.) and integration, gives :

$$n_\theta = A e^{\alpha x/l} + B e^{-\alpha x/l} \quad (2.14.)$$

- Regime AF over  $[l - (d_1 + d_2)]$ . The yield condition is

$$m_x = -2 + 2 n_\theta. \quad (2.15.)$$

Substitution of equation (2.15.) into (2.13.) and integration yields

$$n_\theta = C \sin \frac{\alpha x}{l} + D \cos \frac{\alpha x}{l}. \quad (2.16.)$$

The six unknowns A, B, C, D,  $d_1$  and  $d_2$  are obtained from the following six conditions; at:

$x = d_1$  discontinuity of  $n_\theta$  by mere sign change,

continuity of  $V_x$ , that is of  $\frac{dm_x}{dx}$

$x = d_1 + d_2$   $n_\theta = 1$

continuity of  $n_\theta$

continuity of  $V_x$ , that is, of  $\frac{dm_x}{dx}$ ,

$x = l$  :  $n_\theta = 1/2$ .

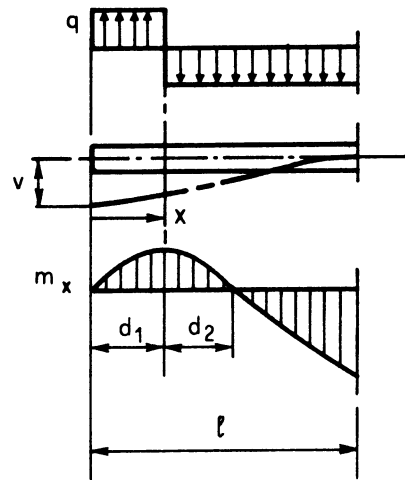


Fig. 2.4.

With the notations

$$(2.17.) \quad a_1 = d_1/l, \quad a_2 = d_2/l.$$

above conditions become :

$$\begin{aligned}
 \cos \alpha a_1 &= A e^{\alpha a_1} + B e^{-\alpha a_1} \\
 \sin \alpha a_1 &= -A e^{\alpha a_1} + B e^{-\alpha a_1} \\
 1 &= A e^{\alpha(a_1 + a_2)} + B e^{-\alpha(a_1 + a_2)} \\
 (2.18.) \quad 1 &= C \sin \alpha(a_1 + a_2) + D \cos \alpha(a_1 + a_2), \\
 C \cos \alpha(a_1 + a_2) - D \sin \alpha(a_1 + a_2) &= -A e^{\alpha(a_1 + a_2)} + B e^{-\alpha(a_1 + a_2)} \\
 C \sin \alpha + D \cos \alpha &= \frac{1}{2}.
 \end{aligned}$$

The system of equations (2.18.) was solved on the Bull computer of Liège University for  $\alpha$  varying from  $\alpha = 1.045$  (corresponding to  $\cos \alpha = 1/2$ ) to  $\alpha = 5.0$ .

With the curves of  $A$ ,  $B$ ,  $C$ ,  $D$ ,  $a_1$  and  $a_2$  versus  $\alpha$ , the efficiency of the flange can be calculated. It is found to be

$$\begin{aligned}
 \rho_f &= -\frac{\sin \alpha a_1}{a_1} + \frac{A}{\alpha} \left[ e^{\alpha(a_1 + a_2)} - e^{\alpha a_1} \right] \frac{B}{\alpha} \left[ e^{-\alpha(a_1 + a_2)} + B e^{-\alpha(a_1 + a_2)} \right] \\
 (2.19) \quad &- \frac{C}{\alpha} \left[ \cos \alpha - \cos \alpha(a_1 + a_2) \right] + \frac{D}{\alpha} \left[ \sin \alpha - \sin \alpha(a_1 + a_2) \right].
 \end{aligned}$$

The curve  $\rho_f$  versus  $\alpha$  is given in figure 2.5.

### 7.2.3. Limit behaviour of the web.

We now turn to the problem of the limit behaviour of the web, as influenced by the flanges. The total axial forces  $N_u$  and  $N_l$  in the upper and lower flanges, with radii  $R_u$  and  $R_l$ , respectively, can be determined from the analysis of preceding section. The radial stresses applied by the flanges to the web with thickness "a" are (see fig. 2.1. and 2.5.).

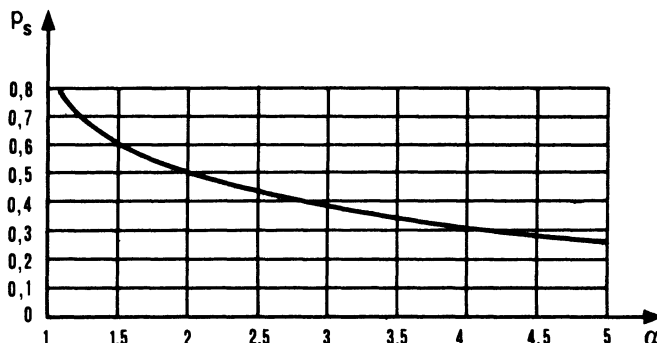


Fig. 2.5.

$$\sigma_{ou} = -\frac{N_u}{aR_u} < 0 , \quad \sigma_{ol} = \frac{N_l}{aR_l} < 0 . \quad (2.20.)$$

The web is also subjected to circumferential stresses  $\sigma_\theta$ . In region 1 (Fig. 2.5.), we have  $\sigma_\theta < 0$  and  $\sigma_r < 0$ . Hence, the yield criterion of TRESCA is simply

$$\sigma_\theta = -\sigma_Y \text{ with } -\sigma_Y < \sigma_r < \sigma_Y \quad (2.21.)$$

In region 2,  $\sigma_\theta > 0$  and  $\sigma_r < 0$ . The TRESCA yield condition is

$$\sigma_\theta - \sigma_r = \sigma_Y \quad (2.22.)$$

The only equilibrium equation, well known from the classical theory of thick elastic tubes is

$$\sigma_\theta - \sigma_r - r \frac{d\sigma_r}{dr} = 0 . \quad (2.23.)$$

With the considered yield conditions and the boundary conditions (fig. 2.6.)

$$\sigma_r = \sigma_{ou} \text{ for } r = r_u ; \quad (2.24.)$$

$$\sigma_r = \sigma_{ol} \text{ for } r = r_l ;$$

integration of equation (2.23.) yields following relations :

in region 1 :

$$\sigma_r = \frac{1}{r} | -\sigma_Y r + r_l(\sigma_{ol} + \sigma_Y) | , \quad \sigma_\theta = -\sigma_Y \quad (2.25.)$$

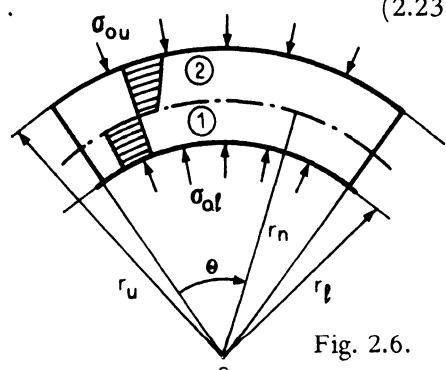


Fig. 2.6.

in region 2 :

$$(2.26.) \quad \sigma_r = \sigma_Y \ln \frac{r}{r_u} + \sigma_{ou}, \quad \sigma_\theta = \sigma_Y \left(1 + \ln \frac{r}{r_u}\right) + \sigma_{ou}$$

The radius  $r_n$  of the interface between regions 1 and 2 is obtained from the condition that the net resultant force over the cross section of the full I profile vanishes. We obtain in this manner

$$(2.27.) \quad r_n \ln \frac{r_u}{r_n} - (r_n - r_l) + \frac{2lt}{a} \left[ \rho_u \left(1 - \frac{r_u - r_n}{R_u}\right) - \rho_l \right] = 0,$$

where  $\rho_u$  and  $\rho_l$  are the efficiencies of the upper and lower flanges, respectively.

Finally, the plastic moment of the I beam is evaluated as the total moment of the internal forces with respect to the center of curvature :

$$(2.28.) \quad M_p = \sigma_Y \left[ 2tl(\rho_u R_u - \rho_l R_l) - \frac{a}{2} (r_u^2 - r_l^2) + \right. \\ \left. + \left( \frac{a}{4} - \frac{t\rho_u}{R_u} \right) (r_u^2 - r_n^2) + \frac{a}{2} r_n^2 \ln \frac{r_u}{r_n} \right].$$

The plastic moment  $M_{ps}$  of the reference I beam with straight axis is

$$(2.29.) \quad M_{ps} = 2lth\sigma_Y + a \frac{h_a^2}{4} \sigma_Y$$

with  $h = R_u - R_l + t$  and  $h_a = r_u - r_l$ .

The overall efficiency of the cross section is thus obtained as  $\rho = M_p / M_{ps}$  from equas. (2.28.) and (2.29.).

The theoretical results obtained above have been confronted with experiment on six small scale models of mild steel [S3]. The testing device is shown in fig. 2.6. Fig. 2.7. shows a typical moment versus curvature diagram, with the experimental value of  $M_p$ . In Fig. 2.8., plastically deformed cross section can be seen, while the diagram of fig. 2.9. enables a comparison of theoretical efficiencies with experimental values. Experimental values are larger than theoretical ones because the yield condition used. (fig. 2.3.) is wholly internal to the most realistic von MISES condition.

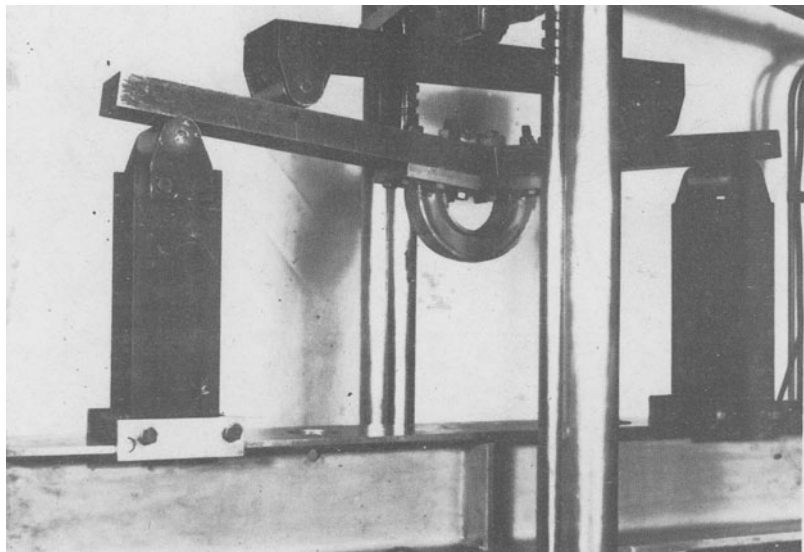


Fig. 2.7.

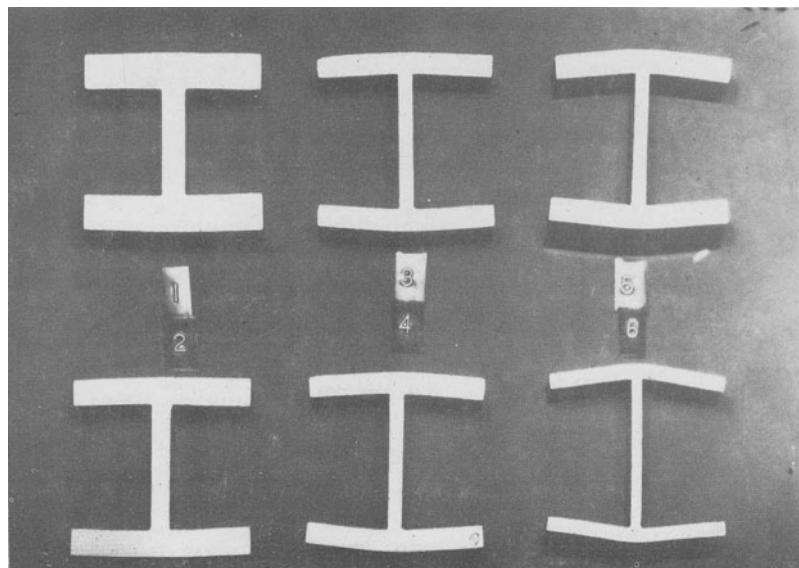


Fig. 2.8.

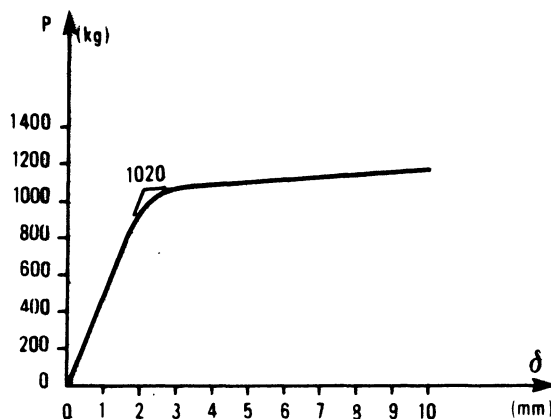


Fig. 2.9.

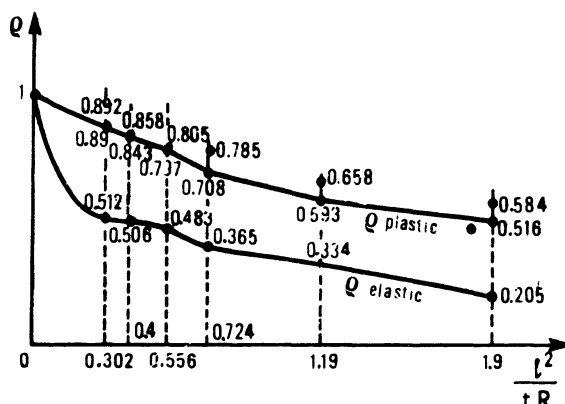


Fig. 2.10.

7.3. Incremental Plasticity - Computer Solution of Plane Structures for Perfectly Plastic or Strain Hardening Metals(\*) .

### 7.3.1. Specialization of Prandtl-Reuss equations for plane stress.

A state of plane stress in plane  $(x_1, x_2)$  is characterized by the relations

$$d\sigma_{i3} = 0 , \quad (i = 1, 2, 3)$$

$$d\epsilon_{j3} = 0 , \quad j = 1, 2)$$

(\*) This section and the next one represent a summarized version of a report written by F. FREY Assistant at the Chair of Mechanics of Materials and Theory Structures, University of Liège. The original internal report No. 33 (in french) is of July 1973.

Taking account of these relations and introducing matrix notations, the general PRANDTL-REUSS equations (1.5.7.) reduce to

$$\begin{Bmatrix} d\sigma_{11} \\ d\sigma_{22} \\ d\sigma_{12} \\ 0 \end{Bmatrix} = \underline{P} \begin{Bmatrix} d\epsilon_{11} \\ d\epsilon_{22} \\ d\gamma_{12} \\ d\epsilon_{33} \end{Bmatrix} \quad (3.1.)$$

where the coefficients of matrix  $\underline{P}$  are taken from (1.5.7.). The dependance of  $d\epsilon_{33}$  on the other components of the strain tensor increment is eliminated by applying GAUSS algorithm to the last equation of (3.1.) (Static condensation), which gives the constitutive law in plane stress

$$d\sigma = \underline{Q} \cdot d\epsilon \quad (3.2.)$$

where

$$\begin{aligned} d\sigma &= (d\sigma_{11} \ d\sigma_{22} \ d\sigma_{12})^T = (d\sigma_x \ d\sigma_y \ d\tau_{xy})^T \ (\text{T = transpose}) \\ d\epsilon &= (d\epsilon_{11} \ d\epsilon_{22} \ d\gamma_{12})^T = (d\epsilon_x \ d\epsilon_y \ d\gamma_{xy})^T \ (\text{with } d\gamma_{12} = 2 d\epsilon_{12}!) \end{aligned} \quad (3.3.)$$

$\underline{Q}$  is the elasto-plastic matrix, whose terms, derived from  $\underline{P}$ , are

$$Q_{ij} = P_{ij} - P_{i4} \cdot P_{j4} / P_{44} \quad (i, j = 1, 2, 3) \quad (3.4.)$$

It is not useful to derive the explicit analytical expressions of the coefficient  $Q_{ij}$ , which are complex.

The loading function  $F$ , based on von MISES criterion, is

$$F = \sqrt{\sigma_{11}^2 + \sigma_{22}^2 - \sigma_{11}\sigma_{22} + 3\sigma_{12}^2} \quad (3.5.)$$

The increment of equivalent plastic strain  $d\bar{\epsilon}^P$  is given by

$$d\bar{\epsilon}^P = \frac{1}{\sqrt{3}} \sqrt{[4(d\epsilon_{11}^P)^2 + 4(d\epsilon_{22}^P)^2 + 4d\epsilon_{11}^P d\epsilon_{22}^P + (d\gamma_{12}^P)^2]} \quad (3.6.)$$

and the total increment of equivalent strain is

$$d\bar{\epsilon} = \frac{E}{E - E_t} d\bar{\epsilon}^P \quad (3.7.)$$

Let  $\underline{S}$  be the matrix connecting the  $d\epsilon_{ij}^P$  with the  $d\epsilon_{ij}$  [ relation (f) of section 1.5.].

It is easy to show that  $\underline{S}$  may be computed from  $\underline{Q}$  by the formula

$$(3.8.) \quad \underline{S} = \underline{I} - \underline{H} \cdot \underline{Q}$$

where  $\underline{I}$  is the unit matrix and  $\underline{H}$  the elasticity matrix defined by (1.5.2.). This matrix  $\underline{S}$  furnishes the increments of plastic deformation

$$d\epsilon^P = \underline{S} d\epsilon$$

by (f.) of section 1.5., where  $d\epsilon^P = (d\epsilon_{11}^P \ d\epsilon_{22}^P \ d\gamma_{12}^P)^T$ .

### 7.3.2. Statement of the problem.

The numerical method used here for solving elastoplastic problems is that of finite elements coupled with the displacement method. The reader is supposed to know this technique (see e.g. [Z2]) which leads to the system of equations

$$(3.9.) \quad \underline{K} \cdot \underline{U} = \underline{R}$$

where  $\underline{K}$  is the stiffness matrix of the structure,  $\underline{U}$  the vector of the generalized nodal displacements,  $\underline{R}$  the vector of the (energetically equivalent) applied forces. This matrix equation express physically the equilibrium of the nodes.

The constitutive laws of the material play a role in the computation of matrix  $\underline{K}$ ; these laws depend, in an elastoplastic problem, on the history of the strains  $ij$ , that is, in general, on the displacements  $\underline{U}$ . Equation (3.9.) becomes thus

$$(3.10.) \quad \underline{K}(U) \cdot \underline{U} = \underline{R}$$

and represents therefore a system of non linear equations.

### 7.3.3. Solution of the non linear equations.

As the problem depends on the evolution of the strains and thus of the displacements, direct solution methods are not possible and recourse must be had to incremental methods, whose principle is to solve an incremental form of the equilibrium equations (3.10.), corresponding to increments of the loads, and with due account of the new boundary conditions at each iteration step.

The stiffness matrix being given by a relation of the form (see [Z2] and section

## 7.3.4. hereafter)

$$\underline{K}_t = \int_V \underline{a}^T \underline{P} \underline{a} dV$$

in which

$\underline{a}$  is an invariable matrix deduced from the linear strain-displacement relations

$$\epsilon_{ij} = \frac{1}{2} (\partial_j u_i + \partial_i u_j), \text{ and}$$

$\underline{P}$  is the incremental elastoplastic matrix (1.5.7.), depending on the state of the body, but connecting linearly the stress and strain increments.

The incremental equilibrium equations are necessarily linear. The major aim of the incremental method is precisely to linearize the equations (3.10.).

The simplest method of solution is EULER's step by step method. If  $n$  designates the number of the step, where everything is known, one determines the stiffness matrix  $\underline{K}_{tn}$  and one computes the displacement increments  $\Delta U_{n+1}$  of the following step, due to the corresponding loading increments  $\Delta R_{n+1}$ , by solving the linear system

$$\underline{K}_{tn} \cdot \Delta U_{n+1} = \Delta R_{n+1},$$

which furnishes the total displacements

$$U_{n+1} = U_n + \Delta U_{n+1}$$

of stadium ( $n+1$ ), from which the state of the body at this stadium may be found. And so on. The successive results of this procedure diverge increasingly from the exact solution, as seen on the unidimensional picture of fig. 3.1.

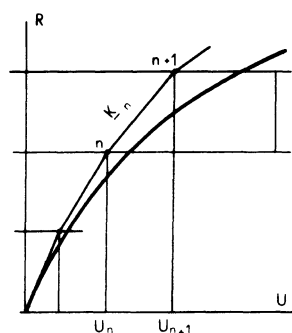


Fig. 3.1.

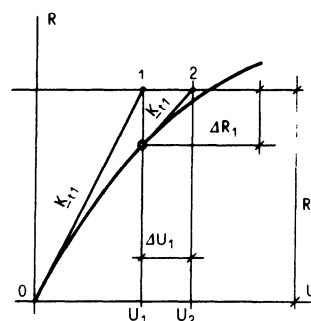


Fig. 3.2.

It is therefore necessary to introduce a corrective procedure, to let the approximate solution converge towards the exact solution. The most elegant method is that of NEWTON-RAPHSON, which is a simple extension of the classical NEWTON method for solving non linear equations with one unknown.

Let (fig. 3.2.) "1" be the state reached, whose characteristics enable to compute a new stiffness matrix  $\underline{K}_{ts}$ ; the correction to the displacements is given by the equation

$$(a) \quad \Delta R_1 = R - \int_V a^T \sigma_1(U_1) \cdot dV ,$$

where the second term of the right-hand member represents the internal forces developed at state 1 (see also section 7.3.4. hereafter). One obtains thus an improved value of the displacements

$$U_2 = U_1 + \Delta U_1 ,$$

and so on. The successive residues  $\Delta R_i$  constitute a measure of the accuracy obtained.

It is interesting to emphasize the close connection of this method with the so-called method of initial stresses, introduced in 1968 by ZIENKIEWICZ, VALLIAPPAN and KING [Z1], whose idea is the following : if the constitutive laws are expressed by the non-linear relationship

$$(b) \quad \sigma = f(\epsilon)$$

(which is the case in plasticity), they can be replaced by the classical linear laws

$$(c) \quad \sigma = D \epsilon + \sigma_o ,$$

where the initial stresses  $\sigma_o$  play the role of a correction necessary to satisfy (b), and thus represent the out of balance stresses, from which the corresponding forces

$$(d) \quad \Delta R = - \int_V \underline{a}^T \sigma_o \cdot dV$$

may be calculated.

Replacing (c) in (a), one finds (d), which demonstrates the analogy with NEWTON's method.

These last two methods may, however, be slightly modified. One calls tangential or incremental stiffness matrix the matrix  $\underline{K}_t$  calculated, before each new iteration, by taking account of the characteristics of the state reached by the preceding iteration. If, in the corrective procedure of a step, one keeps the matrix  $\underline{K}_t$ , characteristic of this step, constant, one obtains the so-called modified NEWTON-RAPHSON method (illustrated at fig. 3.3.), whose convergence is evidently slower.

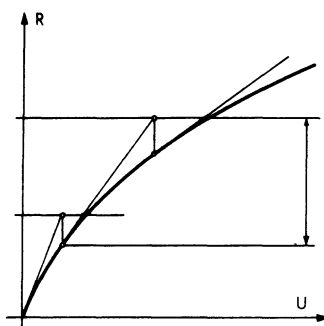


Fig. 3.3.

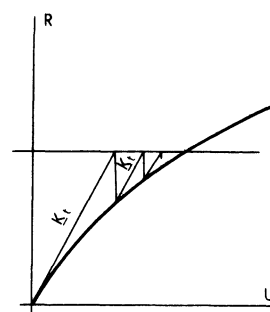


Fig. 3.4.

We show, finally a variant of the step by step method, called residual load step by step method, which is due to WILSON and MURRAY [M13].

It consists to add, to the loading increments of a step, the non equilibrated forces resulting from the preceding step (fig. 3.4.). By this procedure, the divergence of the step by step method from the exact solution is considerably reduced.

In conclusion, the non-linear problem is solved by the step by step method (with or without inclusion of residual loads), by applying regularly an eventually modified NEWTON-RAPHSON correction, in order to maintain the solution near to the exact solution.

#### 7.3.4. Finite element used.

To solve the problems of plane elastoplasticity, Mr. FREY has chosen, as finite element, the pure displacement quadrilateral isoparametric element of the second degree (fig. 3.6.).

The theory of the elements of this type is given in [Z2]; the stiffness matrix may be partitioned in submatrices  $\underline{k}_{ij}$ , with dimensions  $2 \times 2$ , whose expression is

$$\underline{k}_{ij} = t \int_{-1}^{+1} \int_{-1}^{+1} J \underline{a}_i^T Q \underline{a}_j d\xi d\eta = t \int_{-1}^{+1} \int_{-1}^{+1} G(\xi, \eta) d\xi d\eta ,$$

where  $J$  is the determinant of the jacobian of the coordinate transformation  $(x, y) \rightarrow (\xi, \eta)$ ,

a the matrix of strain displacement relations :

$$\epsilon = \begin{Bmatrix} \frac{\partial u}{\partial x} \\ \frac{\partial v}{\partial y} \\ \frac{\partial u}{\partial y} + \frac{\partial v}{\partial x} \end{Bmatrix} = \underline{a} \cdot \underline{p} ,$$

$Q$  the elasticity or elastoplasticity matrix,

$t$  the thickness of the element,

$i, j$ , the numbers of the element nodes.

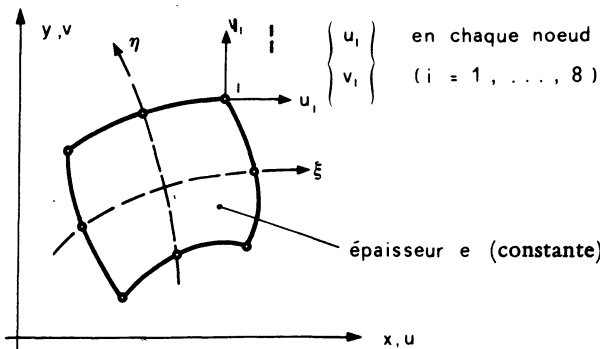


Fig. 3.5.

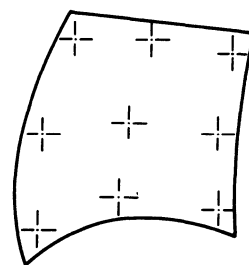


Fig. 3.6.

The numerical values of these submatrices are obtained by GAUSS numerical integration ; this process requires to define in the element a mesh of integration points in each of which the value of function  $G(\xi, \eta)$  must be computed (Fig. 3.6.); this is the reason why it is more rational to calculate at the same time the stresses in these same points, rather than at the nodes; in this way, the stress state in the element, defined by the stress state at the integration points, is variable, which enables to plasticify partially the element. This is an evident advantage of the elements of this type in comparison with the constant strain element used previously to solve the plastic problems ([Z1], etc.).

If  $\sigma_o$  designates a field of initial stresses in the element (residual stresses, non equilibrated stresses, etc..), the corresponding consistent nodal forces are

$$P_i = - t \int_{-1}^{+1} \int_{-1}^{+1} a_i^T \cdot \sigma_o \cdot J \cdot d\xi d\eta$$

and are also computed by numerical integration.

### 7.3.5. Computer program.

On the basis of preceding considerations, Mr. FREY has elaborated an entirely original computer program, based on the series of elementary FINEL programs devoted to the linear elastic computation of structures [F3]. This program is written in FORTRAN 4G language for the IBM 370-150 computer equipping presently the Computation Center of University of Liège. Recourse will be had to this publication for the programming details. The following stress-strain curves in tension are included in the program (fig. 3.7.).

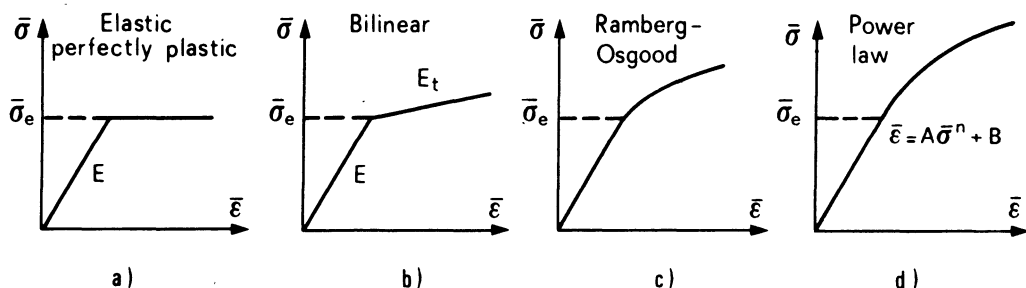


Fig. 3.7.

Regarding the performances, the time  $t$  necessary to execute an elastoplastic computation may be evaluated rather accurately by the following formula :

$$t = n \cdot N/10 \text{ seconds},$$

where  $n$  = number of iterations,

$N$  = number of unknowns.

It must be understood that, in a step followed by corrections, there are several iterations and that the initial linear elastic analysis counts for two iterations (computation plus scale factor).

## 7.4. Illustrative Examples.

### 7.4.1. Preliminary remark.

It is clear that only the non hardening materials lead to a limit load, characterized by :

- a) the formation of a yield mechanisms ;
- b) a continuous flow under constant load (the limit load).

In the examples which follow, it has been considered that the limit load was defined by the formation of the collapse mechanism ; beyond this stage, various behaviours are obtained which depend on the type of mechanism, type of loading, fineness of the discretization etc... These behaviours are essentially characterized by a sudden and considerable increase of the displacements and strains : the program stops if a certain strain is exceeded (1 to 5 % ).

For the hardening materials, the loading may, in principle, be increased indefinitely; practically, the numerical computations are stopped when a certain equivalent strain is obtained, or when the imposed level of loading is reached.

### 7.4.2. Cantilever beam : elastic perfectly plastic material.

The Cantilever defined at fig. 4.1. is subjected to pure bending. It contains a field of residual stresses with bitriangular distribution and maximum intensity 0.8  $\sigma_y$ . The beam is loaded up to a moment  $M = 108.8 \text{ tcm}$ , then completely unloaded (elastic unloading). Fig. 4.1. illustrates the load deflection diagram and compares it to the exact curve [F2]. This figure shows the flexibility of the program (various iterations, variation of the increments, loading-unloading etc...) Fig. 4.2. shows various distributions of  $\sigma_x$  in the cross section ; the obtained accuracy is perfect.

### 7.4.3. Vee notched specimen : elastic-perfectly plastic material.

The problem to be solved is presented at fig. 4.3. This is a classical problem treated by several authors, analytically as well as numerically. The results are compared by using the ratio  $\sigma_m/\sigma_y$  of the mean stress in the section at collapse, to the yield stress of the material (constraint factor). It is clear that  $\sigma_m/\sigma_y$  must be larger than or equal to unity, in virtue of the static theorem. The table in fig.4.3. illustrates several results. Fig. 4.4. shows one quarter of the specimen, with the progression of yield zones and the collapse mechanism. Fig. 4.5. illustrates the

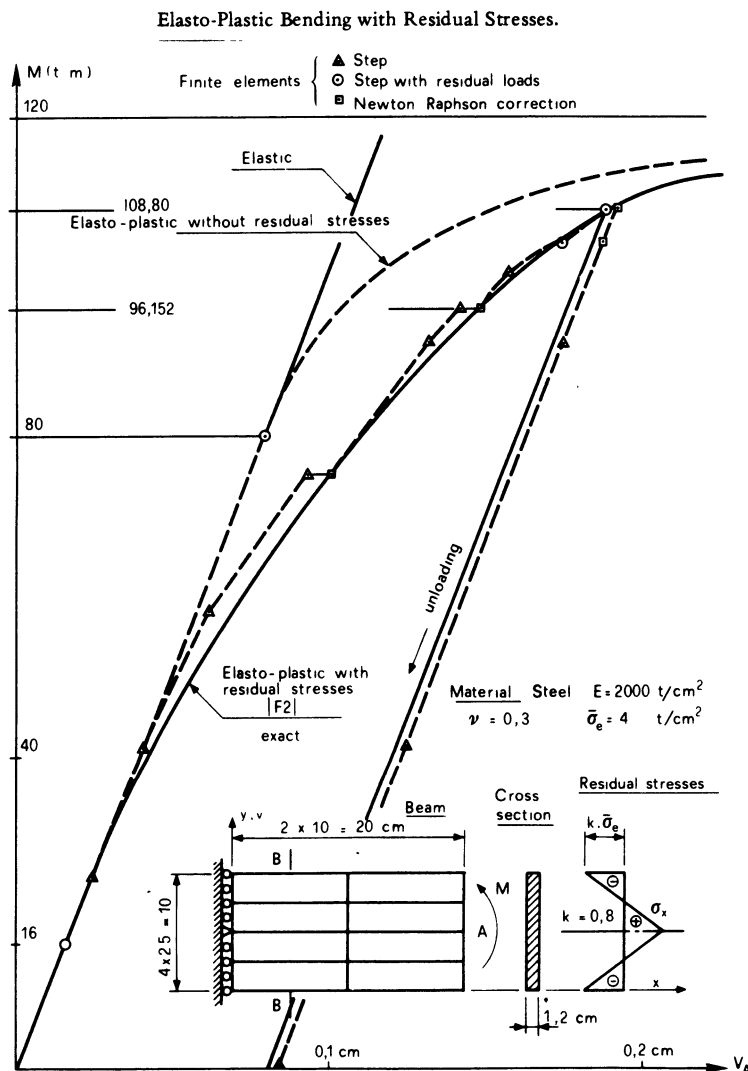


Fig. 4.1.

evolution of stress  $\sigma_y$  in the net section. Perfect agreement has been observed between these results and those obtained by NAYAK and ZINEKIEWICZ [N4].

#### 7.4.4. Strip with central circular hole-strain hardening material (aluminium).

This classical example is inspired from the tests by THEOCARIS and MARKETOS [T1]. The piece and the material are defined at fig. 4.6. The  $\bar{\sigma} - \bar{\epsilon}$

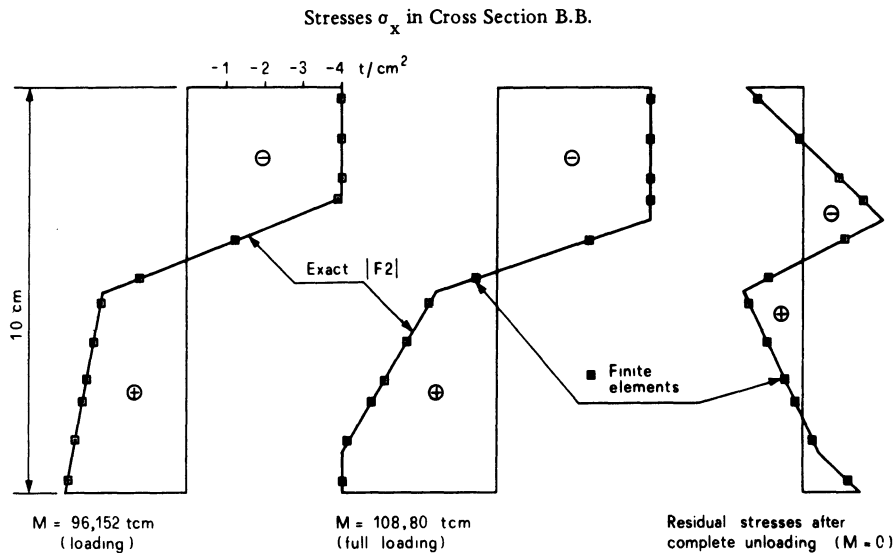


Fig. 4.2.

## V – Notched Specimen in Simple Tension.

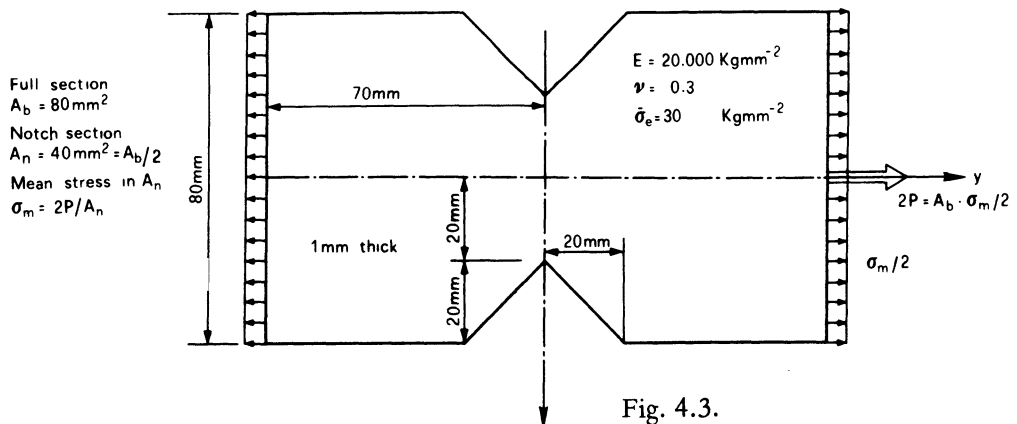


Fig. 4.3.

Comparison of Various Results With Ratio  $\sigma_m/\bar{\sigma}_e$   
Fig. 4.3. Cont

Source	$\sigma_m/\bar{\sigma}_e$	Number of unknowns	
HILL	$2\sqrt{3} = 1.155$	–	Exact (infinitely long strip)
YAMADA...	1.181	~ 290	
MARCAL...	0.967	~ 300	Poor result
NAYAK...	1.186	178	
NGUYEN D H	1.192	170	Rigid-plastic analysis
FREY	1.180	178	

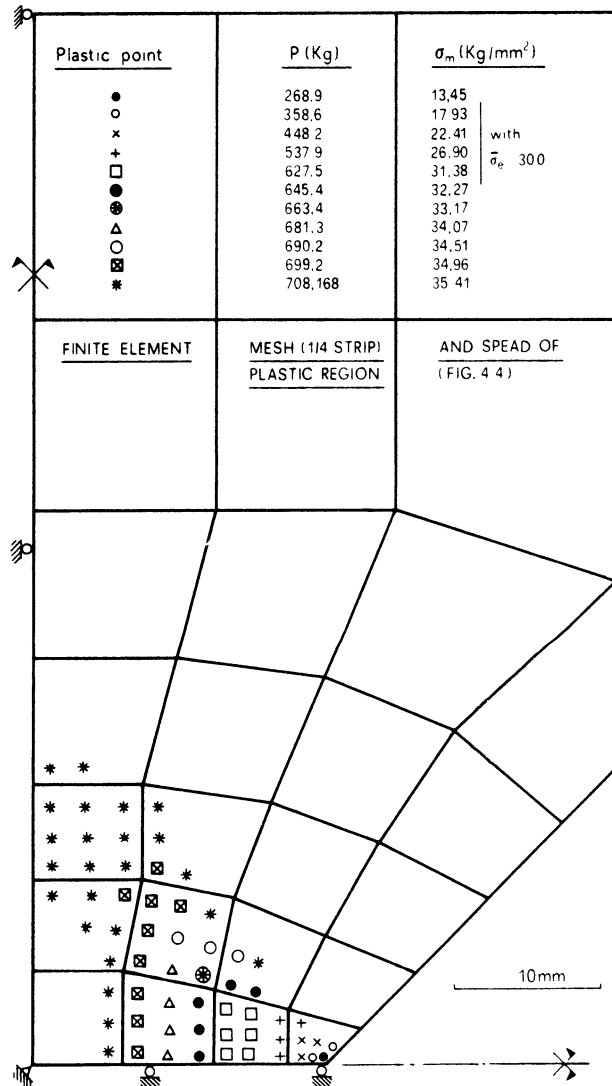


Fig. 4.4.

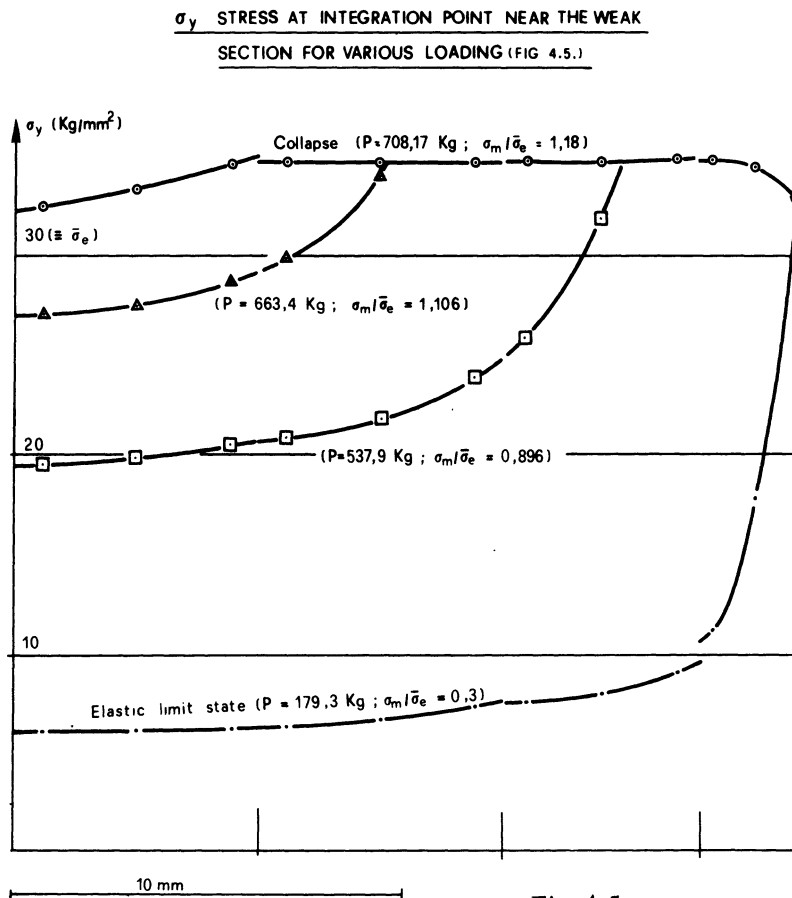


Fig. 4.5.

RAMBERG–OSGOOD law adopted for the material gives a curve practically identical to that defined graphically in [T1]. Fig. 4.7. gives the curve of the total equivalent strain  $\bar{\epsilon}_{et}$  at the most stressed point, as a function of the applied loads. This strain increases considerably from a mean stress  $\sigma_m$  in the net section of the order of 23 to 24 kg/mm<sup>2</sup>, which corresponds to the spreading of the plastic zone through the whole strip (see fig. 4.8.). This figure shows also the progression of the elasto-plastic interface corresponding to the value  $\bar{\epsilon}_{et} = 0.0035$  of the equivalent strain. The choice of this value enables a comparison with [T1].

Fig. 4.9. gives the evolution of the normal stresses in the net section. A comparison with [T1] shows that the general trend is the same, but that the agreement is not more than satisfactory, especially under large loads. The discrepancy should be attributed, partly to the errors in discretization, partly to the errors in the

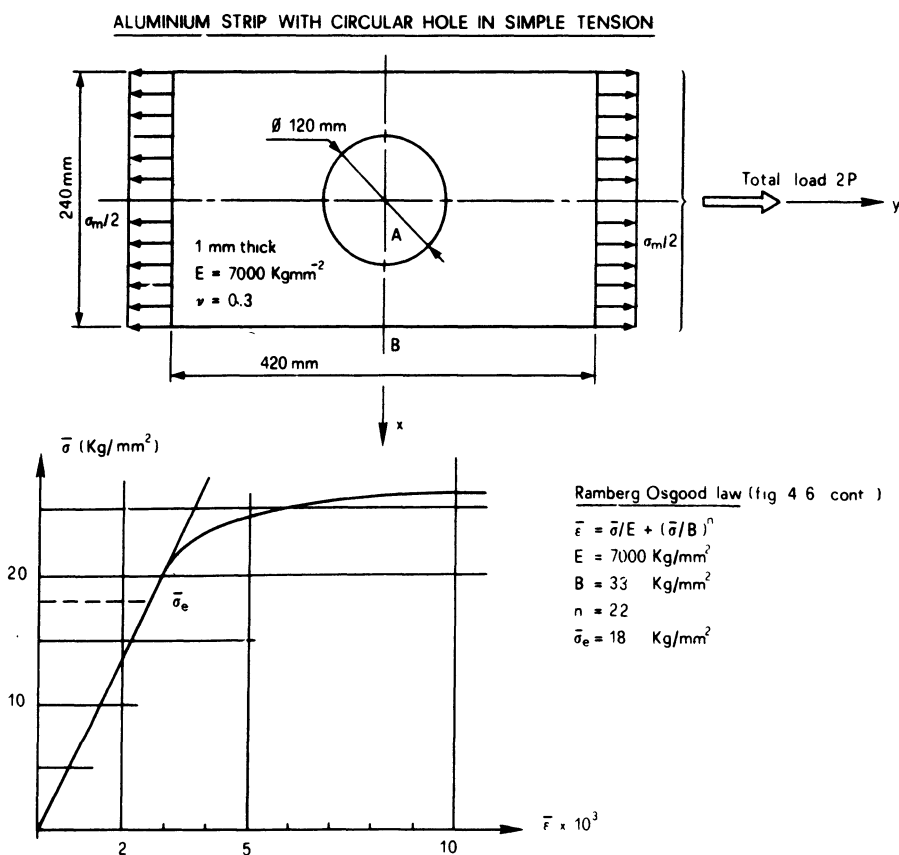


Fig. 4.6.

experimental measurements, but the best reason for it is that strains become large ( $> 1\%$ ) largely before the limit load is reached, so that errors due to second order effects may become significant.

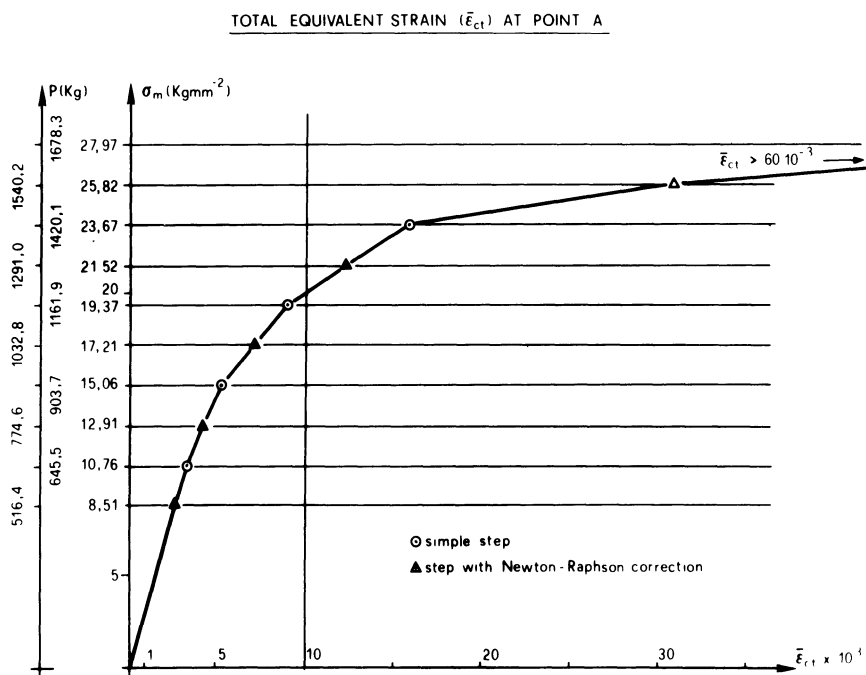


Fig. 4.7.

## 7.5. Quasi-Direct Limit Analysis of Plane Structures Via the Finite Element Method(\*)

### 7.5.1. Introduction.

Limit Analysis problems may be solved basically by two different approaches :

- the incremental study, which was illustrated by sections 7.3. and 7.4. ;
- the direct determination of the limit load, which is the subject of present section.

It has already been shown in section 5.6. that problems of Limit Analysis and Design

(\*) This section and the next one are a condensed version of the work of Mr. NGUYEN DANG HUNG, First Assistant at the Chair of Mechanics of Materials and Theory of Structures, which will be presented shortly to the Faculty of Applied Sciences of Liège University as a thesis of Doctorate in Applied Sciences.

FINITE ELEMENT MESH (1/4 STRIP) AND SPREAD  
OF PLASTIC REGION

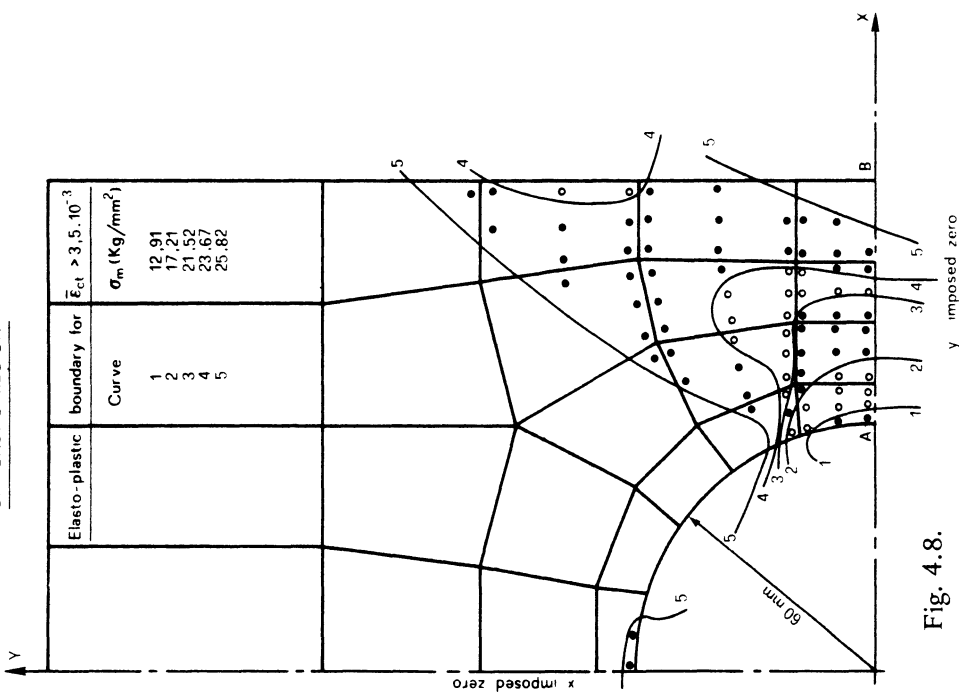


Fig. 4.8.

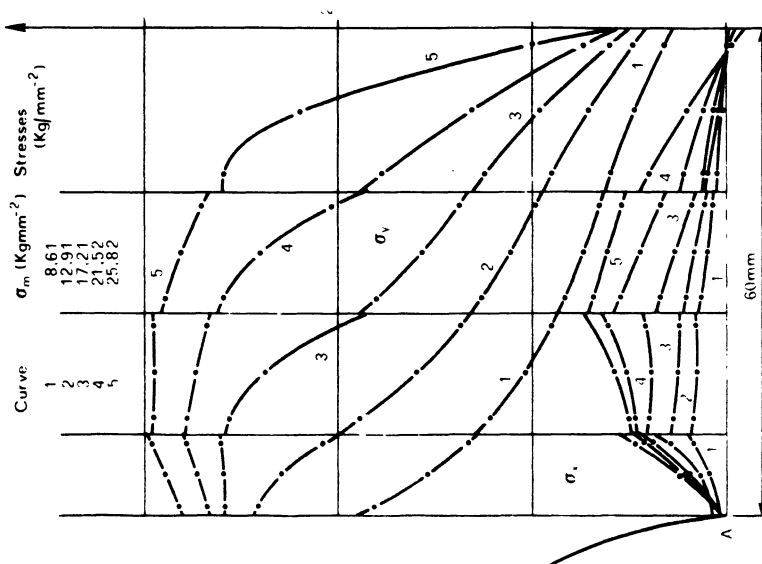
 $\sigma_v$  AND  $\sigma_u$  STRESSES IN WEAK SECTION AB

Fig. 4.9.

could be reduced to linear or non linear programs, depending on the degree of linearisation of the problem. The spatial discretization in finite elements is an indispensable tool in this study, as soon as the geometric shape of the body and its boundary conditions become complex. Researches along this line are presently very numerous. We may cite HODGE and BELYTSCHKO [H6], RANAWERA and LECKIE [R1] CASCiaro and di CARLO [C5], Faccioli and VITIELLO [F6], SAYEGH and RUBINSTEIN [S6], etc...

Present work considers only the case of proportional loading. Compared to the other researches, it seems to possess the following advantages :

- 1) Introduction of a criterion of yield “in the mean” leads to a considerable simplification, so that the solution is obtained by an iterative procedure direct and rapid, without any recourse to linear or non-linear programming ;
- 2) Emphasis on the similarity between rigid-plastic analysis and traditional elastic analysis leads to the following possibilities :
  - to use all existing (and already programmed) finite elements;
  - to obtain the code for rigid-plastic limit analysis by only slightly modifying the assembly and solution program of elastic analysis by finite elements ;
- 3) With the present program in use, called ADELEF (Approche Duale et directe des Etats Limites par la méthode des Elements Finis), it is possible to obtain both statically and kinematically admissible solutions, which provide lower and upper bounds of the collapse loads ;
- 4) By a generalization of classical variational principles, it appears that a rigid-plastic analysis of hybrid type, where PIAN’s hybrid element [P5] is used, is quite possible.

The method developed in present Section being based on the variational principles of plasticity theory, a summary of these principles will be given hereafter.  
For proofs and more detailed treatment, the reader is referred to the literature.

### 7.5.2. Survey of the variational principles in plasticity [W1].

With the definitions of a statically admissible stress field  $\sigma_{ij}$  and a kinematically admissible strain (or strain rate) field  $\epsilon_{ij}$  (or  $\dot{\epsilon}_{ij}$ ) given in section 2.2.1., the variational principles of plasticity read as follows(\*) .

### Deformation Theory – Hencky material

#### 1) KACHANOV's principle [K4]

Among the kinematically admissible and incompressible strain fields, the true one makes functional

$$\phi = k \sqrt{2} \int_V \sqrt{\epsilon_{ij} \epsilon_{ij}} dV - \int_S T_i v_i ds \quad (5.1.)$$

an absolute minimum.

### Flow Theory – von Mises material

#### 2) MARKOV's principle [M11]

Among the kinematically admissible and incompressible strain rate fields, the true one makes functional

$$\phi = k \sqrt{2} \int_V \sqrt{\dot{\epsilon}_{ij} \dot{\epsilon}_{ij}} dV - \int_S T_i v_i ds \quad (5.2.)$$

an absolute minimum.

#### 3) SADOWSKY's principle [S5]

Among the statically admissible stress fields, the true one makes functional

$$\Pi = - \int_{S_u} v_j \sigma_{ij} u_i dS \quad (5.3.)$$

an absolute minimum.

#### 4) HILL's principle [H1]

Among the statically admissible stress fields, the true one makes functional

$$\Pi = - \int_{S_u} v_j \sigma_{ij} v_i dS \quad (5.4.)$$

an absolute minimum.

---

(\*)  $k$  represents the yield stress in pure shear, which, for a von MISES materials, is equal to  $k = \frac{1}{\sqrt{3}} \sigma_y$ .

It must be remarked that KACHANOV's and SADOWSKY's principles – valid for the HENCKY material – on the one hand, and MARKOV's and HILL's principles – valid for the von MISES material – on the other hand, are perfectly similar. This is not surprising if it is recalled that these principles are the basis of fundamental theorems of Limit Analysis and that moreover the deformation and flow theories must coincide in the case of proportional loading.

### 7.5.3. Generalization of the variational principles for a von MISES material.Two-field principles.

Among the couples of stress field  $\sigma_{ij}$ , and strain rate field  $\dot{\epsilon}_{ij}$  such that  $\dot{\epsilon}_{ij}$  is compatible in V, that is satisfies

$$(5.5.) \quad \dot{\epsilon}_{ij} = \frac{1}{2}(\partial_j v_i + \partial_i v_j),$$

without satisfying the velocity boundary condition

$$(5.6.) \quad v_i = \bar{v}_i \text{ in } S_v,$$

$\sigma_{ij}$  satisfies the stress boundary condition

$$(5.7.) \quad \bar{\sigma}_{ij} v_j = T_i \text{ on } S_\sigma$$

without satisfying the equilibrium equations

$$(5.8.) \quad \partial_j \sigma_{ij} + F_i = 0,$$

the true couple ( $\sigma_{ij}$ ,  $\dot{\epsilon}_{ij}$ ) makes the functional

$$(5.9.) \quad \phi_G = k\sqrt{2} \int_V \sqrt{\dot{\epsilon}_{ij} \dot{\epsilon}_{ij}} dV - \int_{S_\sigma} v_j \bar{\sigma}_{ij} u_i dS + \int_{S_u} v_j \sigma_{ij} (\bar{u}_i - u_i) dS$$

stationary.

If, in the finite element approach, one considers that the border belongs entirely to  $S_u$ , then (5.9.) reduces to

$$(5.10.) \quad \phi_R = k\sqrt{2} \int_V \sqrt{\dot{\epsilon}_{ij} \dot{\epsilon}_{ij}} dV + \int_S v_j \sigma_{ij} (\bar{u}_i - u_i) dS,$$

which justifies the use of hybrid displacement elements of type 2 of PIAN [P5].

If, in the finite element approach, one considers that the border belongs totally to  $S_\sigma$ , then (5.9.) reduces to (5.3.), which will justify the use of the pure displacement model.

$$\begin{matrix} x \\ x \quad x \end{matrix}$$

Another possibility is the use of following functional

$$\Pi_G = - \int_{S_u} \nu_j \sigma_{ij} \bar{v}_i dS + \int_S \nu_j (\bar{\sigma}_{ij} - \sigma_{ij}) v_i dS , \quad (5.11.)$$

which is stationnary for the true couple  $(\sigma_{ij}, \dot{\epsilon}_{ij})$  among all couples satisfying following conditions :

$\sigma_{ij}$  statically admissible within the volume  $V$  (equations (5.8.))

$\sigma_{ij}$  plastically admissible, that is verifying

$$S_{ij} S_{ij} \leq 2 k^2 \quad (5.12.)$$

$\epsilon_{ij}$  compatible with the external constraints (5.6.) imposed on  $S_v$ .

In the finite element approach where the whole border is considered as belonging to  $S_\sigma$ , (5.11) reduces to

$$\Pi_R = \int_S \nu_j (\bar{\sigma}_{ij} - \sigma_{ij}) u_i dS , \quad (5.13.)$$

which will justify the use of the hybrid finite elements of equilibrium type of PIAN [P5].

On the contrary, if  $S_\sigma = 0$ , (5.11.) reduces to HILL's functional, and this justifies the use of the pure equilibrium elements of FRAEIJS de VEUBEKE [F5]. Von MISES yield criterion (1.2.13 or 16) may be written in matrix form as follows

$$I'_2 = \frac{1}{2} \sigma^T D \sigma = K^2 \quad (5.14.)$$

where

$I'_2$  is the second invariant of the stress deviator tensor,

$$\sigma^T = |\sigma_x \ \sigma_y \ \sigma_z \ \tau_{xy} \ \tau_{yz} \ \tau_{zx}| ,$$

$$(5.15.) \quad D = \begin{vmatrix} 2/3 & -1/3 & -1/3 & 0 \\ -1/3 & 2/3 & -1/3 & 0 \\ -1/3 & -1/3 & 2/3 & 0 \\ 0 & 0 & 0 & 2 \\ 0 & 0 & 0 & 2 \end{vmatrix}$$

#### 7.5.4. Criterion of the mean.

It was already stressed in Section 1.2. that the distortion energy density was  $W_d = I_2'/2G$ , so that von MISES criterion may be interpreted as follows : yielding occurs when the density of distortion energy reaches the limit value

$$(5.16.) \quad \bar{W}_d = \frac{k^2}{2G} .$$

Let  $V$  be a small, finite, domain of the structure. The mean value of the density of distortion energy is defined as

$$(5.17.) \quad \langle W \rangle = \frac{1}{V} \int_V W_d dV .$$

Basing on this interpretation, due to HENCKY [H5], we propose the following criterion of the mean : yielding occurs in a finite element when the mean density  $\langle W \rangle$  given by (5.17.) reaches the limit value (5.16.).

Combining (5.14.), (5.16.) and (5.17.), we obtain the criterion of the mean in matrix form

$$(5.18.) \quad \frac{1}{2V} \int_V \sigma^T D \sigma dV - k^2 = 0.$$

In the case of plane stress that interests us in the applications, the expression (5.15.) of the  $D$  matrix reduces to

$$(5.19.) \quad D = \begin{vmatrix} 2/3 & -1/3 & 0 \\ -1/3 & 2/3 & 0 \\ 0 & 0 & 2 \end{vmatrix}$$

### 7.5.5. Statically admissible approach.

#### 7.5.5.1. Introduction.

To find a lower bound of the load multiplier  $\lambda$ , one assumes that the stress field within the domain is a polynome depending on parameters  $\beta$  as follows

$$\sigma = \underline{S} \beta , \quad (5.20.)$$

where  $\beta$  is following column matrix :

$$\beta^T = |\beta_1 \ \beta_2 \ \dots \ \beta_n| .$$

From assumption (5.20.), one can define an appropriate system of generalized forces  $g$ , which can be expressed in terms of parameters  $\beta$  by

$$g = \underline{C} \beta . \quad (5.21.)$$

This system generates a parallel system of generalized displacements, determined by identifying both members of the principle of virtual powers.

$$g^T q = -\beta^T C^T q = - \int_{S_v} v_j \nu_i \sigma_{ij} dS , \quad (5.22.)$$

where  $v_j$  is the velocity vector,  $\bar{v}_j$  its imposed value on  $S_v$  and  $\nu_i$  the unit vector normal to the surface  $S_v$ .

Introducing expression (5.20.) of  $\sigma$  into the criterion of the mean (5.18), we can write this criterion

$$\frac{1}{2} \beta^T F \beta - k^2 = 0 \quad (5.23.)$$

with

$$F = \frac{1}{2} \int S^T D S dV . \quad (5.24.)$$

According to HILL's principle, the choice of the parameters  $\beta$  must be made so as to minimize the power dissipated, under the yielding condition (5.24.).

Introducing a LAGRANGE parameter  $\lambda$  to reduce the problem to an unconstrained minimum, we obtain the condition

$$-\beta^T C^T q + \lambda (\frac{1}{2} \beta^T F \beta - k^2) = \text{minimum} . \quad (5.25.)$$

Equating to zero the first variation of (5.25.) gives

$$\delta \beta^T (-C^T q + \lambda F \beta) = 0$$

and, because  $\delta\beta^T$  is arbitrary,

$$(5.26.) \quad \beta = \frac{1}{\lambda} F^{-1} C^T q .$$

Replacing  $\beta$  by this value in (5.20.) and (5.21.), we get

$$(5.27.) \quad \lambda g = K q$$

and

$$(5.28.) \quad \lambda \sigma = T q$$

where

$$(5.29.) \quad K = C F^{-1} C^T$$

$$(5.30.) \quad T = S F^{-1} C^T .$$

The value of parameter  $\lambda$  may be determined by relation (5.22.)

$$(5.31.) \quad \lambda = \frac{1}{k} \sqrt{\frac{1}{2} q^T K q} .$$

#### 7.5.5.2. Interpretation of $\lambda$ .

According to the law of plastic potential (1.3.4.), written in matrix form, the plastic strain rate is given by

$$\dot{\epsilon}_{ij}^P = \mu \operatorname{grad} \left( \frac{1}{2} \sigma^T D \sigma - k^2 \right) = \mu D \sigma ,$$

where  $\mu$  is a positive constant.

The distortion power reads

$$(5.32.) \quad \frac{1}{2} \int_V \sigma^T \dot{\epsilon}^P dV = \frac{1}{2} \mu \int_V \sigma^T D \sigma dV = \frac{1}{2} \mu \beta^T [\int_V S^T D S dV] \beta .$$

On the other hand, this power may be computed also by (5.25.)

$$(5.33.) \quad \frac{1}{2} \lambda \beta^T F \beta = \frac{1}{2} \lambda \beta^T \left[ \frac{1}{V} \int_V S^T D S dV \right] \beta .$$

Comparing (5.32.) and (5.33.), one finds

$$\lambda = V \mu . \quad (5.34.)$$

This shows that the parameter  $\lambda$  is proportional to the magnitude of the plastic strain rate. The proportionality constant is the measure of the finite domain considered.

#### 7.5.5.3. Direct solution in the case of a constant strain measure.

In the case where the strain measure  $\mu$  is constant throughout the structure, we have for each element  $i$  of the structure, according to (5.27.), (5.28.) and (5.34.),

$$\mu g_i = \frac{K_i}{S_i} q_i = K_i^* q_i \quad (5.35.)$$

$$\mu \sigma_i = \frac{T_i}{S_i} \cdot q_i = T_i^* q_i \quad (5.36.)$$

where  $g_i$  is the vector of the generalized forces corresponding to element  $i$ ,

$q_i$  is the vector of the corresponding generalized displacements,

$\sigma_i$  is the stress vector of the element,

$S_i$  is the area of element  $i$ .

Let  $g$  be the vector of the generalized forces of the whole structure,

$q$  the vector of the corresponding generalized displacements.

Any vector  $q_i$  may be considered as the projection of vector  $q$  on the space constituted by the element :

$$q_i = L_i q , \quad (5.37.)$$

where  $L_i$  is the so-called localisation matrix, which contains only terms 1 and 0.

The plastic power of dissipation of the structure is the sum of the plastic dissipation powers of each element

$$\dot{W}_p = q^T g = \sum q_i^T g_i . \quad (5.39.)$$

Introducing (5.35.), (5.36.) and (5.37.) into (5.39.), we get

$$\dot{W}_p = \frac{1}{2l} q^T \sum (L_i^T K_i^* L_i) q = \frac{1}{2l} q^T K^* q ,$$

where

$$(5.40.) \quad K^* = \sum L_i^T K_i^* L_i$$

Let  $\bar{g}$  be the vector of the generalized forces of the corresponding elastic problem whose structural stiffness matrix is  $K^*$ . The corresponding elastic energy is

$$W_e = \frac{1}{2} q^T K^* q .$$

The corresponding elastic solution is the solution of the linear problem is :

$$(5.41.) \quad \bar{g} = K^* q .$$

The plastic solution for the case of a constant strain measure is also linear :

$$(5.42.) \quad \mu q = K^* q .$$

Comparison (5.41.) with (5.42.) shows that the plastic problem differs from the corresponding elastic problem only by the scale factor  $\mu$ .

#### 7.5.5.4. Quasi-direct solution in the general case.

In the general case, the strain measure  $\mu_i$  varies from element to element. It is then necessary to make recourse to an iterative method to obtain the solution. We have

$$(5.43.) \quad \dot{W}_p = \frac{1}{2} \sum \frac{1}{\lambda_i} q_i^T K_i q_i = k^2 \sum \lambda_i$$

where

$$(5.44.) \quad \lambda_i = \frac{1}{k} \sqrt{\frac{1}{2} q_i^T K_i q_i}$$

It is assumed at the outset that  $\lambda_i$  is the same everywhere and equal to  $\lambda_0$ . In these conditions,

$$\dot{W}_p = \frac{1}{2\lambda_0} \sum q_i^{o T} K_i q_i^o = \frac{W_e^o}{\lambda_0} ,$$

where

$$W_e^o = \sum \frac{1}{2} q_i^{o T} K_i q_i^o .$$

The value of  $\lambda_o$  is defined by relation (5.43.)

$$\lambda_o = \frac{1}{k} \sqrt{\frac{W_e^o}{n}} ,$$

where n is the number of elements of the structure.

The plastic generalized forces will be known as soon as the equivalent elastic problem corresponding to  $W_e^o$  is solved. Let  $\bar{g}^o$  be the vector of the generalized forces of the elastic problem. We have

$$g^o = \frac{\bar{g}^o}{\lambda_o} , \quad \sigma_i^o = \frac{T_i^o}{\lambda_o} q_i^o .$$

Once the  $q_i^o$  are known, the following step is begun by computing the  $\lambda_i^1$  of each element

$$\lambda_i^1 = \frac{1}{k} \sqrt{\frac{1}{2} q_i^{oT} K_i q_i^o} .$$

Introducing the notation

$$\gamma_i^1 = \frac{\lambda_i^1}{\lambda_o} ,$$

we may compute an improved expression of the plastic power

$$\begin{aligned} \dot{W}_p^1 &= \sum \frac{1}{2\lambda_i^1} q_i^T K_i q_i = \frac{1}{\lambda_o} \sum \frac{1}{2} q_i^T \frac{K_i}{\gamma_i^1} q_i \\ &= \frac{1}{\lambda_o} \sum \frac{1}{2} q_i^T K_i^1 q_i = \frac{1}{\lambda_o} W_e^1 \end{aligned}$$

where

$$K_i^1 = \frac{K_i}{\gamma_i^1} .$$

Then, one solves the plastic problem corresponding to  $w_e^1 / \lambda_o$ , namely the system

$$\lambda_o g^1 = K^1 q^1$$

$$\lambda_o \sigma_i^1 = T_i^1 q_i^1$$

with

$$T_i^1 = \frac{T_i}{\gamma_i^1} .$$

One continues in this way until the total plastic power converges towards a definite value. At step  $n$ , the formulae are

$$\lambda_i^n = \frac{1}{k} \sqrt{\frac{1}{2} q_i^{n-1} K_i^{n-1} q_i^{n-1}} ; \quad \gamma_i^n = \frac{\lambda_i^n}{\lambda_o} , \dot{W}_p^n = \frac{1}{\lambda_o} W_e^n , \quad W_e^n = \sum \frac{1}{2} q_i^n K_i^n q_i^n$$

$$K_i^n = \frac{K_i^{n-1}}{\gamma_i^n} ; \quad T_i^n = \frac{T_i^{n-1}}{\gamma_i^n} ; \quad \lambda_o g^n = K^n q^n ; \quad \lambda_o \sigma_i^n = T_i^n q_i^n$$

Computations will stop as soon as

$$|\dot{W}_p^n - \dot{W}_p^{n-1}| < \epsilon_n ,$$

where  $\epsilon_n$  is the desired accuracy.

### 7.5.6. Kinematically admissible approach.

#### 7.5.6.1. Introduction.

To obtain an upper bound of the limit load, we use MARKOW's principle which is the correspondent, in rigid plastic theory, of the principle of total potential energy for elastic problems. This principle has been presented in Section 7.5.2. In the particular case of plane stress fields, which interests us, expression  $\dot{\epsilon}_{ij} \dot{\epsilon}_{ij}$  may be written in matrix form

$$(5.45.) \quad \dot{\epsilon}_{ij} \dot{\epsilon}_{ij} = \dot{\epsilon}^T C \dot{\epsilon}$$

with

$$\dot{\epsilon}^T = |\dot{\epsilon}_x \dot{\epsilon}_y \dot{\gamma}_{xy}|$$

and

$$(5.46.) \quad C = \begin{vmatrix} 2 & 1 & 0 \\ 1 & 2 & 0 \\ 0 & 0 & 1/2 \end{vmatrix}$$

The  $\dot{\epsilon}_z$  component has been eliminated by using the incompressibility condition

$$\dot{\epsilon}_{ii} = \dot{\epsilon}_x + \dot{\epsilon}_y + \dot{\epsilon}_z = 0.$$

Functional (5.2.) becomes

$$\phi = 2k \int_V \frac{\frac{1}{2} \dot{\epsilon}^T C \dot{\epsilon}}{\sqrt{\frac{1}{2} \dot{\epsilon}^T C \dot{\epsilon}}} - \int_{S_i} T_i v_i dS. \quad (5.47.)$$

The displacement formulation of finite element method is entirely classical :

$$V = N q, \quad (5.48.)$$

where the  $N$  are the shape functions, and

$$\dot{\epsilon} = B q. \quad (5.49.)$$

We introduce here an important assumption : there exists a mean value

$$\langle \frac{1}{\alpha} \dot{\epsilon}^T C \dot{\epsilon} \rangle = \frac{1}{V} \int_V \frac{1}{2} \dot{\epsilon}^T C \dot{\epsilon} dV = \frac{1}{2V^2} q^T K q, \quad (5.50.)$$

where

$$K = V \int_V B^T C B dV.$$

Matrix  $K$  is the rigid plastic correspondent of the stiffness matrix used in elastic theory. On the other hand, Hooke's matrix of elasticity being

$$C_e = \frac{Et}{1-\nu^2} \begin{bmatrix} 1 & \nu & 0 \\ \nu & 1 & 0 \\ 0 & 0 & \frac{1-\nu}{2} \end{bmatrix},$$

the  $C$  matrix defined by (5.46.) may be generated by taking  $E = 1.5$ ,  $\nu = 0.5$ ,  $t = 1$ . This shows that it is possible to use directly the existing finite elements in the rigid-plastic studies.

The power of external forces represented by the last integral of MARKOW's principle (5.47.) may be written in matrix form, taking account of (5.48.), as follows :

$$\int_{S_1} V^T T dS = q^T \int_{S_1} N^T T dS = -2q^T g, \quad (5.51.)$$

where the vector of the generalized forces is defined by the relation

$$(5.52.) \quad g = \frac{1}{2} \int_{S_1} N^T T dS .$$

In these conditions, functional (5.47.) may be written

$$(5.53.) \quad \phi = \frac{1}{\lambda} q^T K q - 2 q^T g ,$$

where  $\lambda$  is a parameter defined by equation (5.29.) in the formulation of the statically admissible approach.

Expressing the stationarity property of  $\phi$  by  $\delta\phi = 0$ , we obtain the simple relation

$$\lambda g = K q ,$$

which is identical to the relation (5.27.) obtained in the static approach.

This shows the very important fact that it is possible to develop the numerical computations of the kinematic approach by using the same algorithm as in the static approach.

### 7.5.7. Hybrid approach.

We indicate in passing that, to use the hybrid approach, one must use one of the two "two fields" approaches examined in Section 7.5.3. The numerical computations may be developed by using the same finite element code as in the static or kinematic approach.

## 7.6 Illustrative Examples.

### 7.6.1. Finite elements used.

To study the collapse state of structures in plane stress, the four following types of finite elements have been used :

a) Quadrilateral statically admissible element :

This is an equilibrium element with 8 degrees of freedom developed by FRAEIJ'S et VEUBEKE [F4] by superposing three fields of constant stress (Fig. 6.1.).

b) Triangular kinematically admissible element :

This is the classical displacement element with a quadratic displacement field and

degrees of freedom (Fig. 6.2.).

c) Isoparametric quadrilateral element :

This is the element used by F. FREY in section (7.4.) for his step by step approach. It is kinematically admissible with 16 degrees of freedom (Fig. 3.6.)

d) Hybrid triangular element :

This is a new element of the equilibrium type, due to PIAN, where the quadratic displacement field is defined at the border, while in the interior the stress field in equilibrium is given by polynomials of any degree (Fig. 6.3.).

### 7.6.2. Compression of a metal layer.

The first numerical example, rather academic, concerns the limit pressure of a metal layer between rigid and rough matrices. All the curves given correspond to the particular case where  $w/h = 2$ . (Fig. 6.4.).

Equilibrium quadrangle  
composed by 4 triangles

(QUADRI)

Stress field – Constant in each triangle

$$\sigma = \sigma(\beta_1, \beta_2, \beta_3, \beta_4, \beta_5)$$

Generalized displacement coordinates :

$$q^T = [u_1 \ v_1 \ u_2 \ v_2 \ u_3 \ v_3 \ u_4 \ v_4]$$

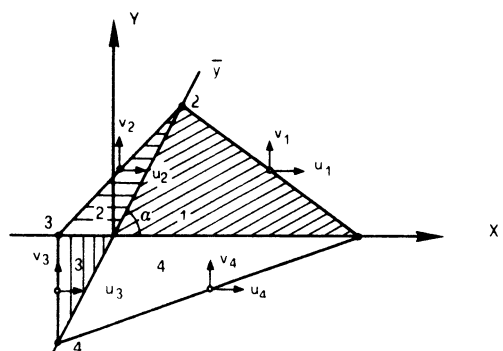


Fig. 6.1.

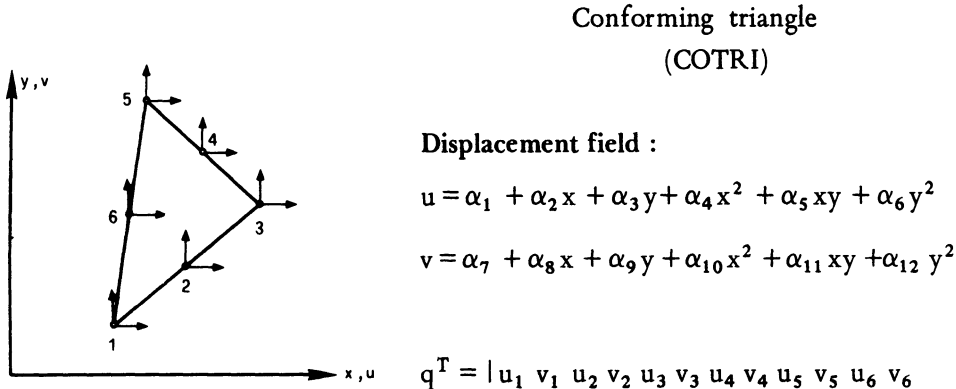


Fig. 6.2.

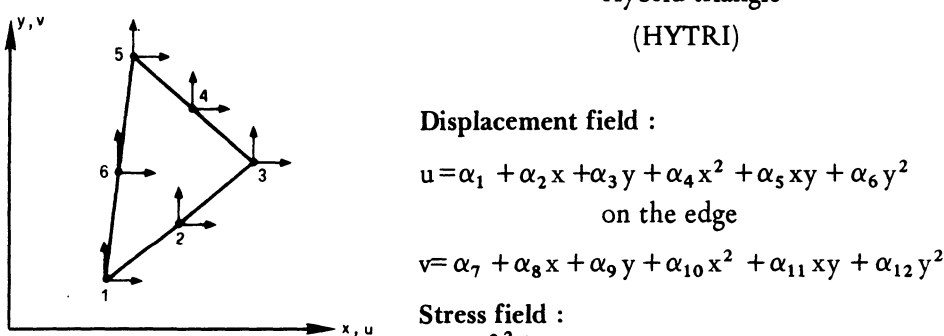
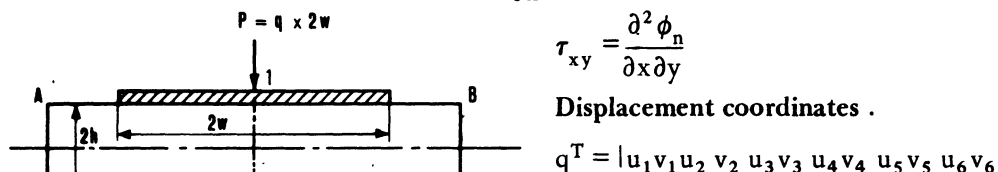


Fig. 6.3.



$$\tau_{xy} = \frac{\partial^2 \phi_n}{\partial x \partial y}$$

**Displacement coordinates .**

$$q^T = [u_1 \ v_1 \ u_2 \ v_2 \ u_3 \ v_3 \ u_4 \ v_4 \ u_5 \ v_5 \ u_6 \ v_6]$$

Compression of a metallic plate between rough rigid parallel platens

Fig. 6.4.

Table 1 compares the results obtained by the three types of approach studied above : static, kinematic and hybrid. Aside the value of the nondimensional limit pressure  $q/2k$ , the computation time is given for the IBM 370/158 computer of University of Liège. At the bottom of the table, we have mentioned the results obtained – and corresponding computation times – by the incremental approach (F. FREY) as well as by direct elastic – plastic analysis (NGUYEN DANG HUNG). The theoretical result obtained by PRANDTL, namely

$$q/2 k = 1.16 ,$$

corresponds to plane strain conditions. It can be roughly converted to plane stress conditions by multiplying it by  $\sqrt{3}/2$ , which gives

$$q/2 k = \frac{1.16\sqrt{3}}{2} = 1.0045 .$$

Table 1 : Comparison of the limit pressures obtained

Static approach			Hybrid approach			Kinematic approach		
Number of elements	time in seconds	$\frac{q}{2k}$	Number of elements	time in seconds	$\frac{q}{2k}$	Number of elements	time in seconds	$\frac{q}{2k}$
24	8	0.902	30	12	0.928	30	12	0.933
80	23	0.914	90	30	0.924	90	30	0.924
168	64	0.916	182	97	0.922	182	97	0.921

Elastoplastic step by step method (FREY) :  $q/2 = 0.89$  – Time Seconds

Direct elastic-plastic analysis (DANG) :  $q/2 = 0.887$  – Time Seconds

Fig. 6.5. illustrates the convergence of the value of the limit pressure towards the exact result for the three types of approach. The upper and lower bound character of the kinematic and static approaches is completely parallel to the result obtained in elastic theory [ N5 ].

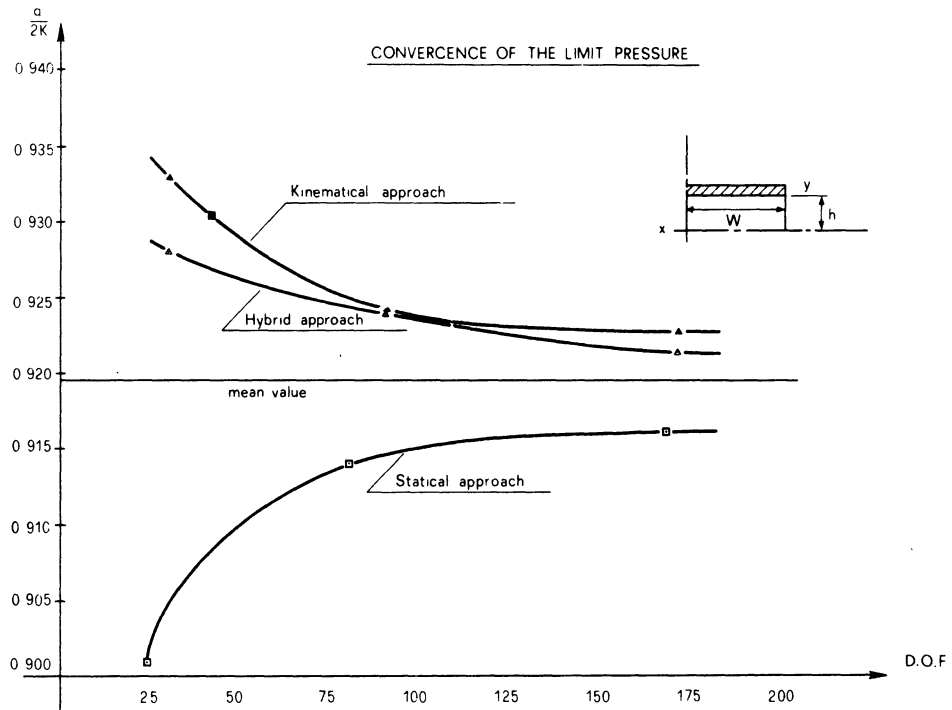


Fig. 6.5.

Fig. 6.6. represents the collapse mechanisms corresponding to the various discretizations and types of approach. The figure shows also the mechanism obtained by F. FREY by his step by step approach (sections 7.3. and 7.4.).

#### 7.6.3. Strip with vee notch subjected to tension.

Fig. 6.7. represents the collapse mechanism of a tensioned strip with a vee notch. The element used in the equilibrium quadrilateral element. The figure shows the results obtained by various authors,  $\sigma_m$  is the mean normal stress in the reduced cross section and  $\sigma_y$  is the yield stress.

#### 7.6.4. Strip with an eccentric circular hole.

Fig. 6.8. represents the notched strip subjected to tension. The results obtained by three authors are compared. In this example, the quadrilateral isoparametric element was used, which enables a good representation of the hole by arcs of parabola.

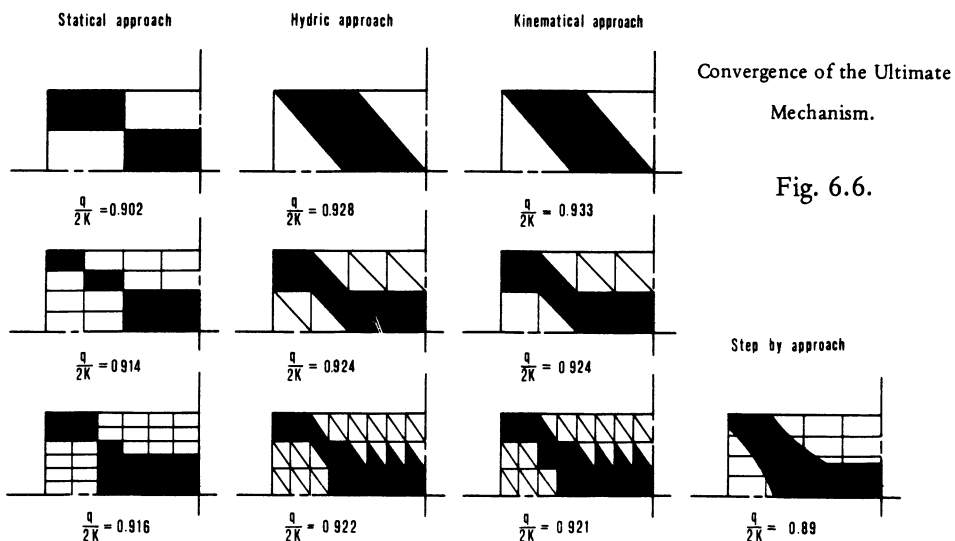


Fig. 6.6.

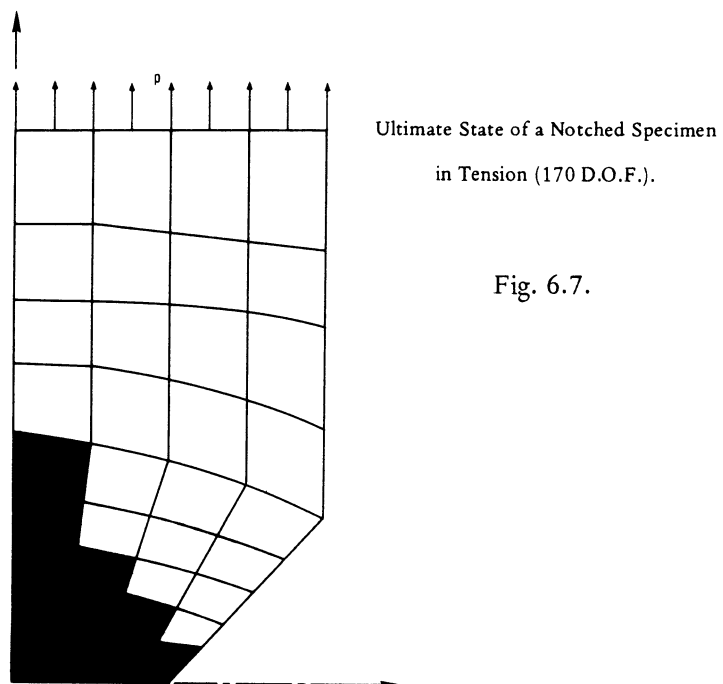


Fig. 6.7.

Authors	Comparison of the results					
	Hill [H 1]	Yamada [Y 1]	Nayak [N 4]	Marcal [M 15]	Frey	Nguyn Dang H
$\sigma/\sigma_y$	1.155	1.124	1.186	1.192	1.180	1.192
Details of the calculations	Exact	IBM(7090) 10'	ICT(1905E) 15'	IBM(7090) 15'	IBM(360) 5'	IBM(360) 2'30"

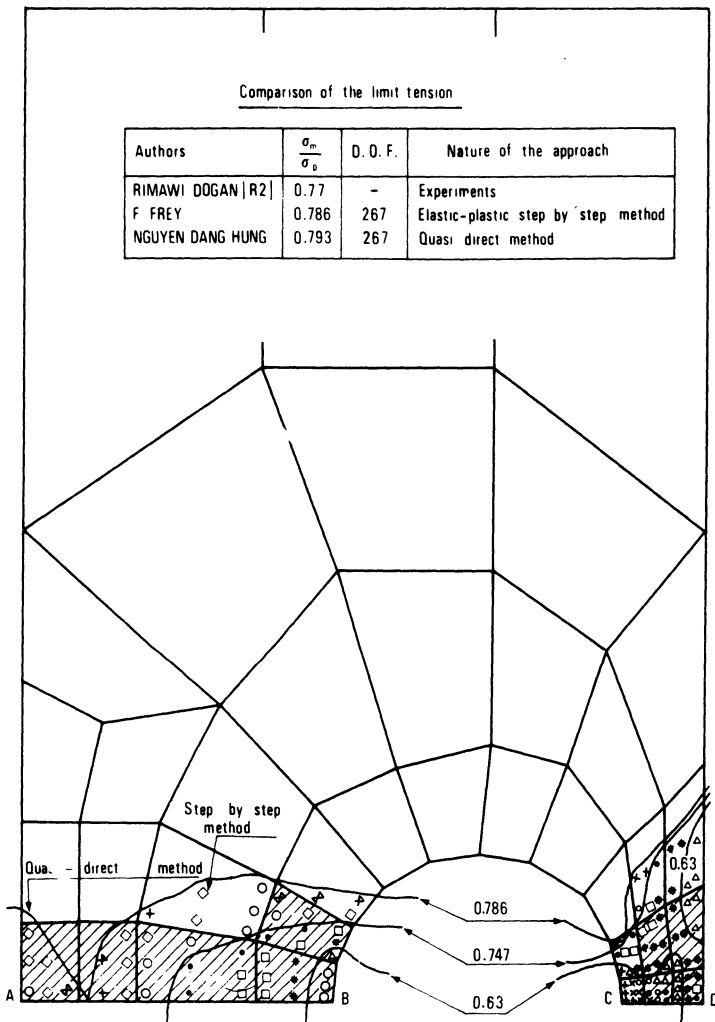


Fig. 6.8.  
Tension Specimen with Eccentric Hole.

### 7.6.5. Stability of a vertical cut.

This celebrated problem of soil mechanics was investigated by assuming that the soil is fully plastic material obeying von MISES criterion and the normality law.

Table 2 gives the values obtained by various methods – of the non dimensional height of the cut :

$$N_s = \frac{h\gamma}{k} ,$$

where  $\gamma$  is the specific weight of the material.

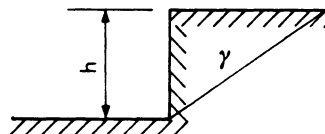


**Table 2. – Stability of a vertical cut.**

Author	$N_s = \frac{h\gamma}{k}$	Discretization (number of D.O.F)	Nature of the solution
COULOMB	4	–	upper bound
TAYLOR and CHEN	3.83	–	upper bound
DRUCKER and PRAGER	2	–	lower bounds
	2.83		
NGUYEN DANG HUNG	3.000	238	upper bound with COTRI
	2.906	164	Hybrid Analysis HYTRI
	2.826	164	lower bound with QUADRI

The results obtained by the dual analysis are excellent.

#### 7.6.6. Conclusions.

The first results of the direct and dual analysis are very encouraging.

The distinctive features of this new method are the possibility to use a whole series of finite elements of various types, the easiness with which the existing F.E. code of elastic analysis was modified and the speed of the computations.

Presently, the method is being applied to the Limit Analysis of plastes and shallow shells. Mr. NGUYEN DANG HUNG has also examined the possibility to take into account the elastic deformations, the strain hardening, as well as to extend the method to materials obeying yield criteria different of the von MISES criterion : MOHR – COULOMB – DRUCKER–PRAGER materials, etc. . . .

**REFERENCES**

- [ A1 ] ADES C.S. "Experimental Mechanics". 1962, p. 345-349.
- [ B1 ] BLEICH H. "Über die Bemessung statisch unbestimmter Stahltragwerke unter Berücksichtigung des elastisch – plastischen Verhaltens des Baustoffes". Bauingenieur, vol. 19-20, 1932, p. 261.
- [ B2 ] BRZEZINSKI R., KÖNIG J.A. "Evaluation of shakedown deflections of framed structures by linear programming". Proceedings of the Symposium on Plastic Analysis of Structures, vol. II, Jassy, 6-8 September 1972, p. 101-116.
- [ B3 ] BRZEZINSKI R., KÖNIG J.A. "Deflection Analysis of elastic-plastic frames at shakedown". Journal Struct. Mech., vol. II, 1973, p. 211-228.
- [ C1 ] CHARNES A., GREENBERG H.J. "Plastic collapse and linear programming". Amer. Math. Soc. Abs No. 506, 1951.
- [ C2 ] COHN M.Z., GHOSH S.K., PARIMI S.R. "A Unified approach to the theory of plastic structures". Proc. ASCE, Journ. E.M. Div., Oct. 1972.
- [ C3 ] COHN M.Z. "Analysis and Design of Inelastic Structures". Vol. 2 : Problems. University of Waterloo Press, 1972, 521 pp.
- [ C4 ] COHN M.Z., RAFAY T. "Collapse load analysis of frames considering axial forces". Proc. ASCE, Journ. Engng. Mech. Div., No. EM4, 1974, p. 773-794.
- [ C5 ] CASCIARO R. , DI CARLO A. "Formulazione dell'analisi limite delle piastre come problema di minimax mediante una rappresentazione agli elementi finiti del campo delle tensioni". Giorn. Genio Civile, 1970.
- [ D1 ] DRUCKER D.H., PRAGER W., GREENBERG H.J. "Extended limit design theorems for continuous media". Quart. Appl. Math., vol. IX, 1952, p. 381.
- [ D2 ] DEMONSABLON P. "Le calcul à la rupture des fondations sur groupes de pieux". Construction, vol. XX, 1965, p. 279-289.
- [ E1 ] EMKIN L.Z., LITTLE W.A. "Plastic design of multistory steel frames by computer". Proc. ASCE, Jour. Str. Div., Nov. 1970 and Jan. 1972.
- [ F1 ] FOULKES J. "The minimum weight design of structural frames". Proc. Royal Soc., London, Series A, vol. 223, 1954, p. 82.

- [ F2 ] FREY F. "Effet du dressage à froid des profilés laminés en double té sur leur force portante". Mémoires AIPC, vol. 29 II, 1969, p.
- [ F3 ] FREY F., RONDAL J., FOURNEAUX N. "Application de la méthode des éléments finis à la résolution des problèmes de structure de l'ingénieur civil". Mémoires CERES, Univ. de Liège, No. 48, Juillet 1974.
- [ F4 ] FRAEIJS DE VEUBEKE J.B. "Upper and lower bounds in Structural Analysis". Agardograph No. 72, July 1969. Pergamon Press, 1964.
- [ F5 ] FRAEIJS DE VEUBEKE J.B. "Displacement and equilibrium models in the finite element method". Chapter 9 in "Stress Analysis", editor O.C. Zienkiewicz, John Wiley ed., 1965.
- [ F6 ] FACCIOLO E., VITIELLO E. "Finite element, linear programming method for the limit analysis of thin plates". Int. Journ. for Numer. Method in Engng., vol. V, 1973, p. 311-325.
- [ G1 ] GVOZDEV A.A. "The determination of the value of the collapse load for statically indeterminate systems undergoing plastic deformation". Proc. of the Conf. on Plastic Deformations, Akademia Nauk U.S.S.R., Moscow, Dec. 1936.
- [ G2 ] GRIERSON D.E. "Computer based methods for the plastic analysis and design of building frames", Report to Technical Committee 15 of the IABSE-ASCE Committee on planning and design of tall buildings, August 1974. (Unpublished).
- [ H1 ] HILL R. "The Mathematical Theory of Plasticity". Clarendon Press, Oxford, 1950.
- [ H2 ] HILL R. "On the state of stress in a plastic-rigid body at the yield point". Phil. Mag., vol. 42, 1951, p. 868.
- [ H3 ] HELLAN K. "Journal of Engineering Materials and Technology". vol. 96, 1974, p. 78-80.
- [ H4 ] HEYMAN J. "The Stone Skeleton". Int. Journ. of Solids and Structures, vol. II, 1966, p. 249-279.
- [ H5 ] HENCKY H. "Zeitschrift für Angewandte Mathematik und Mech.", vol. IV, 1924, p. 323.
- [ H6 ] HODGE P.G. Jr., BELYTSCHKO T. "Numerical methods for the limit analysis of plates". Jour. Appl. Mech., vol. 35, 1968, p. 797-802.
- [ H7 ] HOCHFELD D.A. "Carrying capacity of Structures in conditions of temperature variations" (in russian). Maskinostr., Moscow 1970.

- [ H8 ] HORNE M.R. "The effect of variable repeated loads in building structures designed by the plastic theory". IABSE Publications, vol. 14, 1954, p. 53.
- [ H9 ] HORNE M.R., MORRIS L.J. "Optimum design of multistorey rigid frames". Chapter 14 of the book by Gallagher and Zienkiewicz : Optimum Structural Design, John Wiley ed., 1973.
- [ I1 ] ILYUSHIN A.A. "Plasticité". Eyrolles ed., Paris, 1956.
- [ K1 ] KOITER W.T. "General Theorems for Elastic-plastic Bodies . Chapter IV, p. 167-224 of Progress in Solid Mechanics", vol. I, edited by I.N. Sneddon and R. Hill-North-Holland Publishing Company, Amsterdam, 1960.
- [ K2 ] KÖNIG J.A. "On shakedown design of structures with temperature depending elastic modules". Proc. 1st International Conference on Structural Mechanics in Reactor Technology, vol. VI, part L, Berlin, Sept. 1972, p. 503-517.
- [ K3 ] KÖNIG J.A. "Deflection bounding at shakedown under thermal and mechanical loadings". Proc. 2nd International Conference on Structural Mechanics in Reactor Technology, vol. 5, part L, Berlin, Sept. 1973, p. 1-13.
- [ K4 ] KACHANOV L.M. "Foundations of the theory of plasticity". North-Holland Publ. Co., 1971.
- [ L1 ] LEBLOIS C. , MASSONNET C. "Influence of the upper yield stress on the behaviour of mild steel in bending and torsion". Inter. Journ. of Mech. Sciences, vol. 14, 1972, p. 95-115.
- [ M1 ] VON MISES R. "Göttinger Nachrichten". Math.-Phys. Klasse, 1913, p. 582.
- [ M2 ] MAIER-LEIBNITZ H. "Bautechnik", vol. 6, 1928, p. 11.
- [ M3 ] MELAN E. "Zur Plastizität des räumlichen Kontinuums". Ing. Archiv., vol. 9, 1938, p. 116.
- [ M4 ] MASSONNET C., MAUS H. "Force portante plastique des systèmes de pieux". Symposium on the Use of Computers in Civil Engineering, vol. I, No. 12, Lisbonne, 1962.
- [ M5 ] MASSONNET C., SAVE M. "Résistance limite d'une poutre courbe en double té à parois minces soumise à flexion pure". Publications AIBSE, vol. 23, 1964, p. 245.
- [ M6 ] MASSONNET C., SAVE M. "Plastic Analysis and Design". Vol. I : Beams and Frames. Blaisdell Publ. Co., New York, 1965.

- [ M7 ] MASSONNET C., SAVE M. "Calcul Plastique des Constructions". Vol. I : Structures dependant d'un paramètre. 2è édition, CBLIA éditeur, Bruxelles, 1967.
- [ M8 ] MASSONNET C. "Développement d'un programme automatique de dimensionnement plastique des structures planes en acier à l'aide de la programmation linéaire". Proc. pf the Symposium on Plastic Analysis of Structures, vol. 2, Jassy, 6-8 Sept. 1972, p. 238-259.
- [ M9 ] MASSONNET C. "Résistance des Maériaux". Tome II, 2è édition, G. Thone éditeur, 1973.
- [ M10 ] MASSONNET C., RONDAL J. "Structural Mechanics and Optimization". General Lecture at the 16 th Polish Solid Mechanics Conference, Krynica 26 August - 3 September 1974. (To be published).
- [ M11 ] MASSONNET C., SAVE M. "Résistance limite d'une poutre courbe en caisson soumis à flexion pure". Amici e Alumini, (The Campus Anniversary Volume), Liège, 1964.
- [ M12 ] MURRAY D.W., WILSON E.L. "Finite element large deflection analysis of plates". Proc. ASCE, J. Engng. Mech. Div., vol. 95, 1969, p. 143.
- [ M13 ] MARKOV A.A. "On variational Principles in Theory of Plasticity". Prikladnaia Matematika i Mekhanika, vol. II, 1947, p. 339-350.
- [ M14 ] MARCAL P.V. , KING I.P. "Elastic-plastic analysis of two-dimensional stress systems by the Finite Element method", Int. J. Mech. Sci. 9, 1967, 143.
- [ N1 ] NADAI A. "Plasticity". Mac GrawHill, New York, 1931.
- [ N2 ] NEAL B.G. , SYMONDS P.S. "The rapid calculation of the plastic collapse load of a framed structure". Proc. Inst. Civil Engineers, vol. 1, London, 1952, p. 58-71.
- [ N3 ] NEAL B.G. "The plastic methods of structural analysis". Second edition, Chapman and Hall, 1963.
- [ N4 ] NAYAK G.C., ZIENKIEWICZ O.C. "Elasto-plastic stress analysis; a generalization for various constitutive relations including strain softening". Int. Journ. for Num. Methods in Engrn., vol. 5, 1972, p. 113.
- [ N5 ] NGUYEN DANG HUNG "Displacement and equilibrium methods in matrix analysis of trapezoidal Structures". Collection des Publications de la Fac. des Sciences Appl. de l'Université de Liège, No. 21, 1970.
- [ N6 ] NUYEN DANG HUNG "Analyse limite rigide plastique par une méthode quasi-directe". Sciences et Techn. de l'Armement, 2è fasc., 1970.

- [ P1 ] PRAGER W. "A new method of analysing stress and strain in work-hardening solids". *Journ. Appl. Mech.*, vol. 23, 1956, p. 493.
- [ P2 ] PRAGER W. "Théorie générale des états limites d'équilibre". *Jour. Math. pures et appliquées*, vol. 34, 1955, p.4.
- [ P3 ] PRAGER W. "Problèmes de plasticité théorique". Dunod, Paris, 1958.
- [ P4 ] PRAGER W. "Shakedown in elastic-plastic media subjected to cycles of load and temperature". Symposium on "Plasticità nella Scienza delle Costruzioni", Bologna, 1957, p. 122 -125.
- [ P5 ] PONTER A.R.S. "Journal of Applied Mechanics", vol. 39, 1972, p. 953-958 and p. 959-963.
- [ P6 ] PIAN T.H.H. "Formulations of finite element methods for solid continua". US-Japan Seminar on Structural Analysis, Tokyo, 1969.
- [ R1 ] RANAWERA – LECKIE F.A. "Bound methods in limit analysis. "Proc. Seminar on F.E. Techniques in Structural Mechanics, H. Tottenham and C. Brebbia editors, University of Southampton, 1970.
- [ R2 ] RIMAWI W.H. – DOGANE "Experiments on yielding of tension specimens with notches and holes". *Experimental mechanics*, vol. 10, Oct. 1970.
- [ S1 ] SOKOLOWSKY V.V. "Theorie der Plastizität". V.E.B. Verlag Technik, Berlin, 1955.
- [ S2 ] SAWCZUK A., RYCHLLEWSKI J. "On Yield Surfaces for Plastic Shells". *Archiwum Mechaniki Stosowanej*, vol. I, 1960, p. 12.
- [ S3 ] SAVE M.A., MASSONNET C.E. "Plastic Analysis and Design of Plates, Shells and Disks". North-Holland Publishing Co., Amsterdam, 1972.
- [ S4 ] STANG A.H., GREENSPAN M., NEWMAN S.D. *Journ. Research Nat. Bur. Standards*, vol. 37, No. 4, Oct. 1946.
- [ S5 ] SADOWSKY N.A. "A principle of maximum plastic resistance". *Journ. Appl. Mech.*, vol. X, 1943, p. 65-68.
- [ S6 ] SAYEGH A.F., RUBINSTEIN M.F. "Elastic-plastic analysis by quadratic programming". *Proc. ASCE, Journ. Engng. Mech. Div.*, 1972, p. 1547-1572.
- [ T1 ] THEOCARIS P.S., MARKETOS E. "Elastic-plastic analysis of perforated thin strips of strain-hardening material". *Journ. of Mech. and Phys. of Solids*, vol. XII, 1964, p. 377.

- [ W1 ] WASHIZU K. "Variational methods in elasticity and plasticity". Pergamon Press, Oxford, 1968.
- [ Y1 ] YAMAHA Y., YOSHIMURA N., SAKURAI T. "Plastic stress-strain matrix and its application for the solution of elastic-plastic problems by the finite element method". Int. Journ. Mech. Sci., 10, 1968, p.343.
- [ Z1 ] ZIENKIEWICZ O.C., VALLIAPPAN S., KING I.P. "Elasto-plastic solutions of engineering problems : Initial stress, finite element approach". Int. Journ. for num. methods in engng., vol. I, 1969. p. 75.
- [ Z2 ] ZIENKIEWICZ O.C. "The finite element in engineering science." Mac Graw Hill, London, 1971.

**THE FOUNDATIONS OF PLASTICITY**

**Experiments. Theory and Selected Applications**

by A. Phillips  
Professor of Engineering and Applied Science  
Yale University, New Haven, Conn.

## *P R E F A C E*

*In the present monograph which is the text of my lectures given at CISM in October 1974, I have tried to present the foundations of plasticity from the experimentalist's point of view. The theory of plasticity is presented on the basis of several fundamental assumptions which can be verified experimentally independently of one another. The necessary experimental verification is provided whenever available and it is indicated where such a verification is not yet available.*

*The experimental verification of the basic assumptions of the theory of plasticity is provided from the author's experiments, of which a representative selection is given, but some additional experimental evidence of other authors is also given. It is hoped that the presentation which follows will stimulate the reader to some additional research.*

*For various reasons the printing of this text has been delayed for five years. During this time considerable progress was done by the author and his associates. Some of this progress has been indicated in the appendix.*

*My sincere thanks are due to Professor W. Olszak and to the late Professor L. Sobrero for kindly inviting me to present the lectures and in this way participate in the work of CISM.*

*Udine, April 1979.*

### 1. Experimental Verification of a Theory. The Empirical Method

The traditional method of experimental verification of an inelastic theory of metal deformation is the empirical one. In an empirical verification we compare the experimentally obtained stress-strain curve for a given stress path or strain path with the stress-strain curve predicted by the theory. Such an experimental verification requires a large number of experiments since each experiment verifies the validity of the theory for the particular path used. No conclusions can be drawn on whether the theory is correct for a different path, and consequently the empirical method is of limited validity. The limitations of the empirical method are even more apparent if the theory includes a number of arbitrary constants and/or functions which can be selected in such a manner that the theory agrees with the experiment for the given path. This is not a verification, it is only a method of selecting the values of the constants or functions in a way that an **apparent agreement** between theory and experiment will occur.

As an illustration of the empirical verification of a theory we shall consider the experiments by Morrison and Shepherd [1]. Figures 1 and 2 show the strains plotted in three dimensional diagrams. The solid curves represent the experimental results. The two broken curves represent the predictions of the total

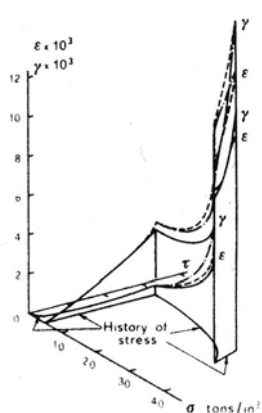


Fig. 1

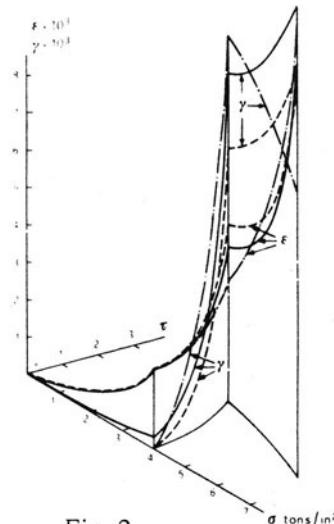


Fig. 2

strain theory of plasticity and of the incremental theory of plasticity, respectively. The two theories used are the simplest formulations of the respective groups of theories called total strain and incremental. It is seen that there is some disagreement between theory and experiment and that the disagreement seems to be more serious for the total strain theory than for the incremental theory. The above conclusion is valid for the stress paths which have been selected for the experiments shown.

These conclusions give no indication of whether the same type and amount of agreement or disagreement will be valid for other stress paths and in addition they give no guidance concerning the way the theories can be improved so that they will represent reality in a better way.

The above method of verification of a theory was standard at the time the experiments of Morrison and Shepherd were performed (twenty-five years ago). At the present time we have an alternative method for the verification of a theory. It will be discussed next.

## 2. Experimental Verification of a Theory. The axiomatic Method

Another method of experimental verification of a theory is the axiomatic method. The theory is presented on the basis of several fundamental assumptions or axioms which are selected in such a way that they can be verified experimentally independently of one another. Once each axiom of the theory is verified independently of the other axioms it follows that the entire theory is correct and depending on the range of validity of the axioms, the range of validity of the theory becomes known without ambiguity.

If one of the axioms of the theory is not verified it can always be modified so that the new version of the axiom will agree with the experiments. Thus, it is always possible to change the theory rationally so that its axioms will agree with the experiments. More generally a way is provided for theory and experiment to interact in a fruitfull way and generate new questions the answer of which provides for the advancement of understanding of the theory.

These lectures are based on the axiomatic method of verification of the theory of plasticity. Although we cannot say at present that we have a completely correct presentation of the theory of plasticity we believe that the axiomatic approach which already has yielded important results by fostering the interaction of theory and experiment, will help greatly in the development of the correct theory of plasticity.

We shall discuss first the uniaxial stress test from which conclusions will be drawn concerning the behavior of materials in the plastic range. Generalizations of these conclusions for the seven-dimensional stress-temperature space will be the basis of our considerations in the sections which will follow.

Next we shall consider the experimental evidence concerning a number of axioms or assumptions which are the basis of the theory of plasticity. This evidence will be first our own experiments but in addition some of the classical previous experiments will be re-evaluated in the light of our experimental findings. The experimental evidence will lead in some cases to modifications of the basic axioms. These modifications are excellent examples of the fruitfull interaction between theory and experiment which the axiomatic method enables us to achieve.

The theory of plasticity including some thermodynamic considerations will then be formulated. Here we must observe that the modified theory of plasticity is not yet complete and that additional experimental evidence is necessary.

In these lectures we shall also consider the implications of our experimental findings and of the modification of the theory of plasticity for some classical questions as for example, viscoplasticity, creep, repeated loading, and plastic stability.

The presentation of the material which follows is given from the point of view of the experimentalist. We shall try to base our considerations on available experimental evidence with the minimum amount of unproven assumptions. Such assumptions will be introduced only when the experimental evidence is lacking.

It is hoped that the material which will follow will stimulate the student to additional research in the spirit of the axiomatic method.

### 3. Plastic Flow Under Uniaxial Stress

The theory of plasticity is based on our experience with uniaxial stress experiments. To a given stress corresponds a strain which can be divided into an elastic portion and a plastic portion. The plastic portion is the only one which is of importance to plasticity. The division of the total strain  $e$  in to its elastic part  $e^e\ell$  and its plastic part  $e^p\ell$  can be achieved by means of the equation

$$e = e^e\ell + e^p\ell \quad (1)$$

provided that the strains are small. For finite strains we must use deformation

gradients and equation (1) is no longer valid. In what follows we shall restrict ourselves to small strains only so that equation (1) can be used. In eq. (1)  $e^{e\ell}$  is proportional to the stress and we can differentiate the plastic strain from the elastic one by means of observing the deviation from proportionality between stress and strain.

The proportional limit is the stress where we first observe a deviation from proportionality. The observation of the proportional limit is very difficult since it depends to some extent on the sensitivity of the measuring instruments and on the skill of the observer.

Our procedure for determining the proportional limit is by defining it on the stress-strain diagram as corresponding to the intersection of two straight lines, the elastic line and a strain-hardening line. The latter is the line passing through the first few consecutive points deviating to the same side of the linear elastic line.

It is necessary to follow the first small deviation from proportionality by a small unloading in order to decide whether the observed deviation from proportionality is a genuine permanent strain or not.

As an example of our procedure for determining the proportional limit we give Figure 3. It is seen that the loading occurred from O to A and that the

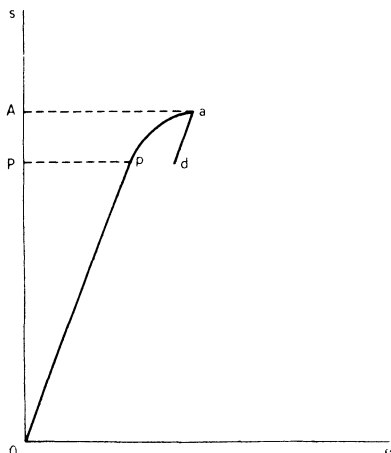


Fig. 3

proportional limit appeared at P, which corresponds to the intersection between a first straight line  $Op$  and a second straight line  $pa$ . At the level of A we decrease the load to verify the genuine appearance of the proportional limit. If  $ad$  is different than  $pa$  then  $p$  is a genuine proportional limit. The permanent strain at A need be only 2 to 3  $\mu\text{in/in}$  depending of course on the resolution of the instrumentation.

The argument can be made that since with increasing resolution in the instrumentation it may be possible to obtain nonlinearity at practically zero value of stress, there is no such quantity as a proportional limit. However, there

is a difference between what we consider as a proportional limit and the ideal proportional limit which may be zero. As Bauschinger noted nearly 100 years ago [2] the practical proportional limit, distinct from the ideal one, separates the region for which nonlinearity is reproducible upon repeated loading of the same specimen

from the region for which the permanent deformation differs from one experiment to the next.

In addition, above the proportional limit we observed measurable creep over a period of time when the load was allowed to remain unchanged, while below the proportional limit no measurable creep occurred. Figure 4 from [3] gives an illustration of the above mentioned observation. A bar of rectangular cross section

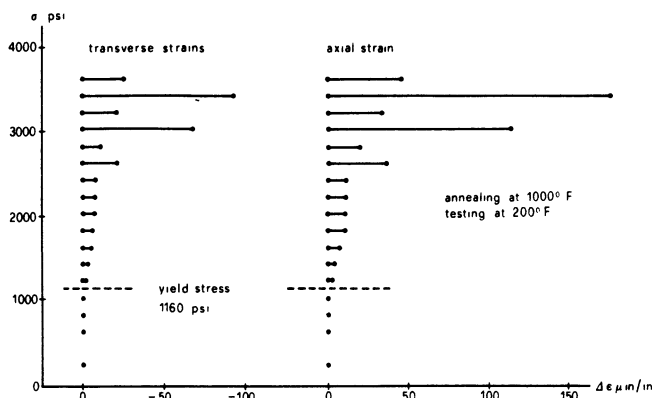


Fig. 4

was loaded in tension with the stress increasing stepwise every 3 minutes. The bar was of commercially pure aluminum annealed at  $1000^{\circ}\text{F}$  and tested at  $200^{\circ}\text{F}$ . Resistance strain gauges were applied on all four faces of the specimen measuring both axial and the transverse strains. It is seen that creep appears at the stress level indicated by our definition of the proportional limit. An analogous observation was made by Bauschinger 100 years ago.

Since the proportional limit is difficult to measure with certainty very often the proof strain method is used. The proof strain method is useful for intermediate strains or for large strains for which the plastic strain permitted diminishes in influence. For small strains, however, the influence of this plastic strain is quite significant.

It should be understood that in Fig. 3 the point P is the proportional limit and the point A is the proportional limit by the proof strain method when the proof strain is assumed to have the value say  $3\ \mu\text{in/in}$ . Obviously A is higher than P but in addition the point P is reproducible when the experiment is repeated if only a very few  $\mu\text{in/in}$  of plastic strain have been introduced. On the other hand the point A is not reproducible, since the slope of the second straight line is not the same every

time the experiment is repeated.

G.I. Taylor [4] used a backward linear extrapolation to the elastic line, first proposed by Lode [5]. The backward extrapolation technique relies on establishing an asymptotic strain hardening line.

The backward extrapolation technique is fundamentally different from our method since it requires a deep incursion into the plastic range while our method does not require it. The backward extrapolation method does not allow a unique determination of the proportional limit. Indeed, the backward extrapolation method assumes that there exists an asymptotic straight strain-hardening line when a deep incursion into the plastic range occurs. This is of course not true since the strain hardening line is anything but straight even for a deep incursion into the plastic range. It could also be said that by definition the backward extrapolation method does not pretend to define a proportional limit, but rather what is commonly called a yield limit.

Likewise, the proof strain method requires an incursion into the plastic range commensurate to the value of the proof strain. It assumes, in effect that plastic deformation occurs only after the proof strain has been reached. This assumption tends to give an increased value for the yield stress. As it will be seen in the next section both the backward extrapolation technique and the proof strain method make it impossible in effect to use the same specimen for the determination of more than one point of the yield surface.

Another reason why the observation of the proportional limit is difficult is because permanent deformation is truly time dependent deformation. For a given stress and temperature, although elastic strain occurs instantaneously, permanent deformation needs time to develop fully. An arbitrary division into plastic and creep strains does not represent physical reality although it might be convenient for solving boundary value problems.

The equilibrium tensile stress-strain curve at a given temperature is a sequence of equilibrium positions due to successively larger values of stress. Each increment of stress is assumed to be applied after the total permanent strain due to the previous stress increment had the time to appear fully. Therefore the equilibrium stress-strain curve is in reality an incremental stress-strain curve where the infinitesimal increments are in the stress. To each increment of stress  $\Delta\sigma$  at a given temperature corresponds an increment in elastic strain  $\Delta e^{el}$ , and an increment in the plastic strain  $\Delta e^{pl}$  which needs time to appear.

In fact each increment of stress is applied while the total plastic strain due

to the previous stress increments is still developing. Therefore, upon the application of an increment of stress not only that plastic strain appears which is due to that particular increment of stress but also plastic strain may continue to appear which is due to some of the previous stress increments. It is, of course, impossible to differentiate experimentally between the portions of appearing plastic strains due to different stress increments.

The time needed for the increment  $\Delta e^p \ell$  to appear may be infinite but for all practical purposes it can be assumed that it is finite when temperature and stress are smaller than certain limiting values which depend on the material.

If the material is forced to extend faster than it needs to express the entire permanent strain, as for example, when the deformation is with a constant stress rate, the stress-strain curve appears elevated, as curve OK instead of curve OL in Fig. 5, since the permanent portion of strain AB does not have the time to develop fully when the stress increases from the level  $s_A$  to a level  $s_A + ds$ . Thus, only the portion AC of the permanent strain appears. The equilibrium stress-strain curve OL is the lowest stress-strain curve possible at a given temperature. The curve OL could be obtained, in principle, if we could add small increments of stress in a deadweight machine but at each increment of stress would wait considerable time before the next increment of stress would be applied.

Suppose that in Fig. 6 curve OA represents the equilibrium stress-strain

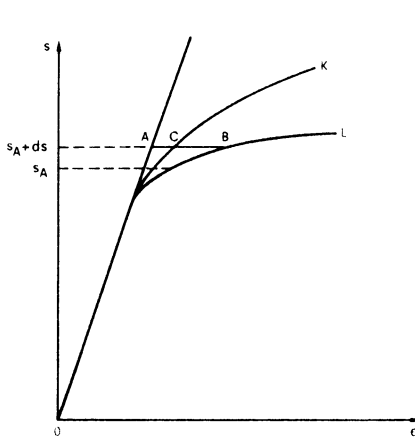


Fig. 5

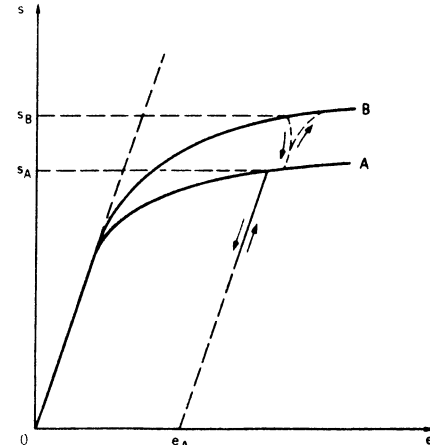


Fig. 6

curve. A moderate decrease of the stress below the value  $s_A$  at the permanent strain  $e_A$  will produce only elastic strain. Subsequent increase of the stress to  $s_A$  will produce only elastic strains. Only after  $s_A$  is exceeded plastic strain will again

appear. On the other hand if OB is a stress-strain curve obtained under nonequilibrium conditions, for example, under constant finite stress rate, then OB will always be higher than OA, and both a slow decrease in stress from  $s_B$  to  $s_A$  as well as a slow increase again of the stress from  $s_A$  to  $s_B$  will produce some plastic strains.

It is important when decreasing the stress below  $s_A$  not to go below the reverse proportional limit which may be situated above  $s = 0$ . Otherwise permanent strains of a negative value will be introduced and upon reloading  $s_A$  will again be affected since it will correspond to a different value of the total permanent strain. Cyclic plastic straining will then occur.

The equilibrium stress-strain curve can be obtained by first loading at a constant stress rate then unloading at selected strains followed by very slow reloading. In this way the equilibrium stress-strain curve will be the locus of all the points where the first deviation from proportionality during reloading occurs.

The experimental work which is the foundation of the research presented in these lectures was performed in dead-weight testing apparatus. The stress was the imposed variable and the strain was the response of the material. Dead-weight testing machines were used practically exclusively before the first world-war and then they were generally replaced in the laboratories with commercially made standardized hard testing machines which are designed to force upon the specimen a prescribed strain history. For a hard machine the strain is the imposed variable and the stress experienced by the loading element is the measured quantity.

These two different types of experimental apparatus give differences in the data which are significant and make comparison nearly impossible. In the dead-weight apparatus creep can develop freely. In the hard testing machines creep is impossible but relaxation appears. The relation between creep and relaxation is a very difficult not yet clearly understood problem, the solution of which is necessary before a comparison between sets of data obtained by means of the two types of machines can be made.

The recent introduction of testing machines with feedback controlled input – whether stress or strain – introduces the difficulty that their use makes it very difficult to differentiate between small amounts of loading and unloading which may be of importance in plasticity.

Let us now consider the idealized stress-strain diagram shown in Fig. 7. In this diagram we see illustrated the cases of loading OA and AC, unloading AB, and reloading BA. The point A presents the highest stress reached during loading before

unloading AB starts. This model used in the theory of plasticity specifies that during unloading and reloading the plastic strain and the point A remain unchanged. Obviously, then the point A corresponds to the proportional limit during reloading.

Experimental results [6] shown in Fig. 8 indicate that the model represented by Fig. 7 is not realistic. The model shown in Fig. 9 is a more realistic one. In this model it is assumed that the unloading produces only elastic strains but that the reloading will produce plastic strains if carried beyond the level represented by the point D. Thus, in this case we have two points instead of

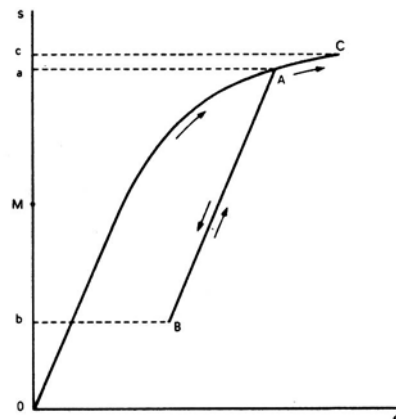


Fig. 7

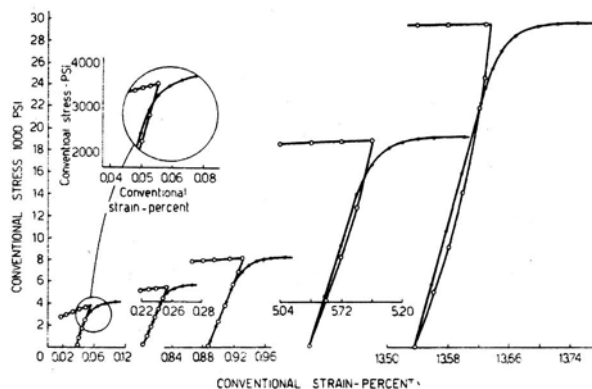


Fig. 8

one, the points A and D.

Let us reflect on the meaning of these two points and more generally on the model Fig. 9. Loading and reloading are assumed to occur with a certain stress rate and we shall also assume that the test is performed on a dead-weight testing machine. The unloading is assumed to occur very fast so that practically no time exists for plastic deformation to occur

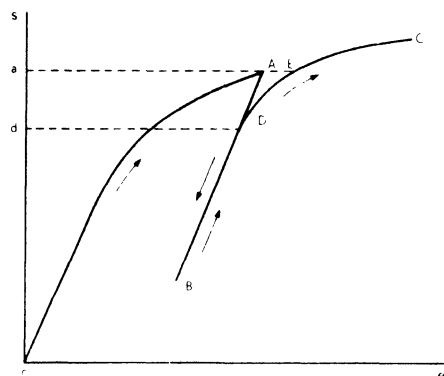


Fig. 9

while unloading. However, plastic deformation occurs during reloading as soon as the loading point moves above D. Hence D represents a point in the equilibrium stress-strain line.

Beyond D during reloading there is a small amount of plastic strain developing until the loading point reaches the point E which lies at the same stress level as A. Above A the development of the plastic strain increases with the stress at the same rate as it was increasing before the point A was reached.

Consider now the stress axis in Fig. 9. The points A and E are located at the stress level  $a$  which will be called the **loading stress**. The point D is located at the stress level  $d$  which will be called the **yield stress**. From the previous discussion it is obvious that  $d$  may be located at any point on the stress axis up to the level of the loading stress  $a$  depending on the length of time the stress remained at  $a$  before starting to decrease. However, this length of time will also determine the amount of plastic strain.

We should remark that the yield stress defined here is the proportional limit after the small amount of prestress to  $a$ . We next observe from Fig. 10 where

the equilibrium stress-strain line is given, that the point D of Fig. 9 lies on the equilibrium stress-strain line. A delay in the decrease of the stress from  $a$  means that additional plastic strain occurs while the stress remains at  $a$ . Thus, upon unloading the equilibrium stress-strain line will be reached at the point  $d'$  which will lie higher than  $d$ .

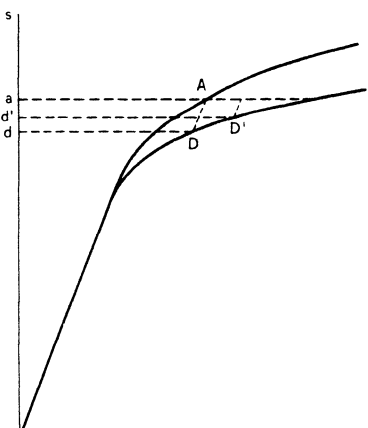


Fig. 10

The region below the yield stress is the elastic region. The region between the yield stress and the loading stress is the region of very small plastic strains and the region above the loading stress is the region with

fully developed plastic strain. Any decrease of the stress while the stress point is below  $a$  will produce no plastic strains if done sufficiently fast. It will produce small plastic strains if the decrease occurs slowly. Similarly, any increase of the stress while the stress point is below  $a$  but above  $d$  will produce no plastic strain if done sufficiently fast and it will produce small plastic strains if it occurs slowly.

In the next two sections we shall introduce the seven-dimensional generalizations of the points  $a$  and  $d$  in stress-temperature space. The generalization

of  $a$  is the **loading surface**, that of  $d$  is the **yield surface**. For the first loading, before any unloading occurs, the points  $a$  and  $d$  coincide and therefore the yield surface and the loading surface coincide. After the first unloading has occurred the two surfaces are distinct. We shall first consider the initial yield surface, next the subsequent yield surfaces, i.e., yield surfaces occurring after one or more unloadings occurred, and finally the loading surface.

In the simple tension test we have the stress acting in one direction but plastic strains occur in three directions. The plastic strains in the two directions perpendicular to the direction of application of the stress are of importance in order to obtain data regarding the value of Poisson's ratio for plastic strain and regarding the incompressibility of plastic deformation.

It has always been assumed in the literature of plasticity and creep that plastic and creep deformations produce no change in volume. For small strains and an isotropic material the above assumption is equivalent to the assumption that the Poisson's ratio has the value  $\nu = 0.5$ . The physical argument for this assumption of incompressibility is that plastic strain is due basically to simple slip. During slip the volume of the slipped and unslipped crystals remains the same so that the total volume will remain unchanged. In such a simple model the effect of the grain boundaries in the polycrystal and the dislocation generation within the grains are neglected. Therefore, direct experimental evidence of the incompressibility assumption of plastic and creep deformation is necessary in order for this axiom of incompressibility of such deformation to be accepted in the construction of the theory. A literature search has shown that very few appropriate experimental results, if any, are available concerning this problem for the region of plastic deformation and creep at the level of  $< 1\%$ . Consequently, we decided to perform our own experiments to obtain appropriate data.

M. Ricciuti and I performed tensile experiments with bars of square cross section made of commercially pure aluminum [3]. They were loaded in tension with the stress increasing stepwise every 3 minutes and the strains recorded in both the axial and lateral directions. The bars were annealed either at  $650^{\circ}\text{F}$  or at  $1000^{\circ}\text{F}$  and they were tested at  $70^{\circ}\text{F}$  or at  $200^{\circ}\text{F}$ .

Figures 11 to 16 show some of the results. The specimen in Figure 11 was loaded to 6040 psi axial stress with approximately  $8000 \mu\text{in/in}$  of total axial strain developed. Then the specimen remained at the 6040 psi stress for 1000 minutes while creep occurred. The specimen was annealed at  $650^{\circ}\text{F}$  and tested at  $70^{\circ}\text{F}$ . It yielded at 2050 psi axial stress. Figure 11 shows the development of the axial and

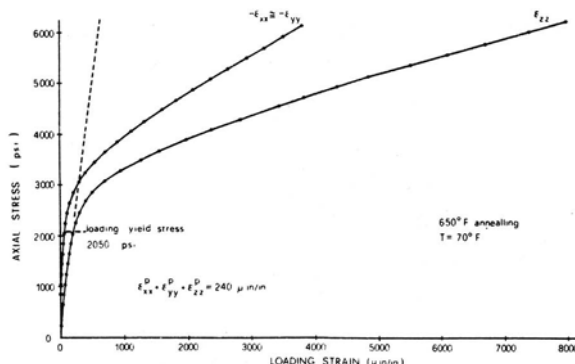


Fig. 11

the two transverse strains during loading to 6040 psi.

We first observe that the plastic strain develops isotropically. Indeed, we obtain for the lateral plastic strain  $\epsilon_x^{pl} = \epsilon_y^{pl}$  and in addition we observe that this lateral plastic strain is equal to 3400  $\mu\text{in/in}$  while the axial plastic strain is 7400  $\mu\text{in/in}$ . Consequently  $v^{pl} = 3400/7400 = .486$  which is very near to the ideal value of 0.50. The total change of volume measured by the sum  $\epsilon_x^{pl} + \epsilon_y^{pl} + \epsilon_z^{pl}$  is equal to 240  $\mu\text{in/in}$  which is a very small value compared to a total of 7400  $\mu\text{in/in}$  for the axial plastic strain.

Figure 12 shows, for the same specimen, the development of creep strains while the stress remains at 6040 psi. It will be observed that  $\epsilon_x \approx \epsilon_y$  but that  $v^{cr} = -\epsilon_x^{cr}/\epsilon_z^{cr} = .42$ . There is definitely a departure from the assumption of

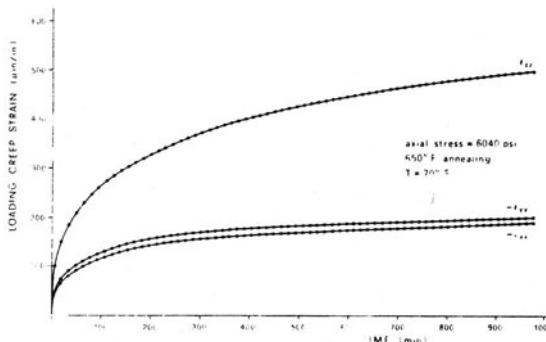


Fig. 12

incompressibility. An increase of approximately 100  $\mu\text{in/in}$  in the value of  $\Delta V/V$  takes place for a total of 500  $\mu\text{in/in}$  of axial creep strain. It is, of course to be expected that if the creep experiment would have been allowed to continue the

increase in the value of  $\Delta V/V$  would have stopped.

Figures 13 and 14 show the experimental results for a specimen annealed at 650°F and tested at 209°F. The specimen in Figure 13 was loaded incrementally

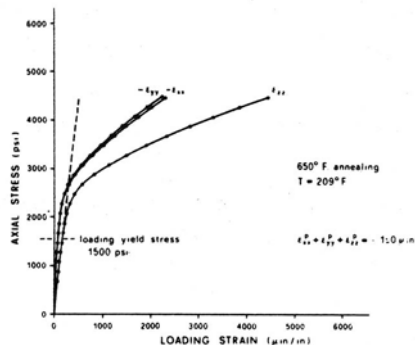


Fig. 13

to an axial stress of 4440 psi with approximately 4500  $\mu\text{in}/\text{in}$  of total axial strain developed. Then the specimen remained at the 4440 psi stress for 1200 minutes, while creep occurred.

Figure 13 shows the development of the axial and the two transverse strains during the axial loading. It will be observed that again the plastic strain develops isotropically. Indeed, we obtain  $\epsilon_x^{pl} \approx \epsilon_y^{pl}$  and the lateral plastic strain is nearly one-half of the axial plastic strain, i.e.  $\nu = 0.5$ . The total change of volume measured by the sum  $\epsilon_x^{pl} + \epsilon_y^{pl} + \epsilon_z^{pl}$  is equal to  $-180 \mu\text{in}/\text{in}$ , a very small value compared to the total of  $4000 \mu\text{in}/\text{in}$  for the axial plastic strain.

Figure 14 shows for the same specimen the development of creep strains

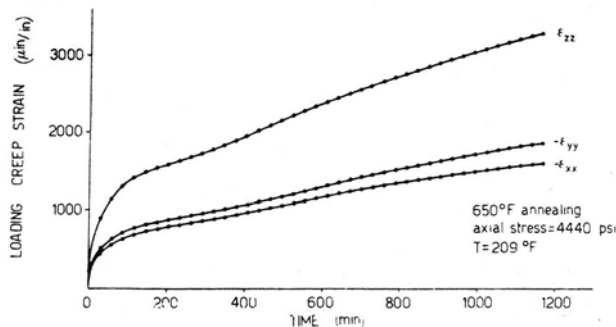


Fig. 14

while the stress remains at 4440 psi. Now there develops some anisotropy since  $e_y^{cr}$  is becoming larger than  $e_x^{cr}$ . At the end of the test we have a total value of axial creep strain of 3350  $\mu\text{in/in}$  while  $e_x^{cr} = 1680 \mu\text{in/in}$  and  $e_y = 1920 \mu\text{in/in}$ . The ratios  $v = -e_x^{cr}/e_z^{cr}$  and  $v = -e_y^{cr}/e_z^{cr}$  are now .50 and .57 with the average  $v$  equal to .54. It follows, that there is a change in volume during creep. In this particular case, however, there is a decrease in volume. It is, of course, to be assumed that if the creep experiment would have been allowed to continue this decrease in volume would have gradually stopped.

Figures 15 and 16 show the experimental results for another specimen annealed at  $1000^{\circ}\text{F}$  and tested at  $70^{\circ}\text{F}$ . The specimen in Figures 15 and 16 was

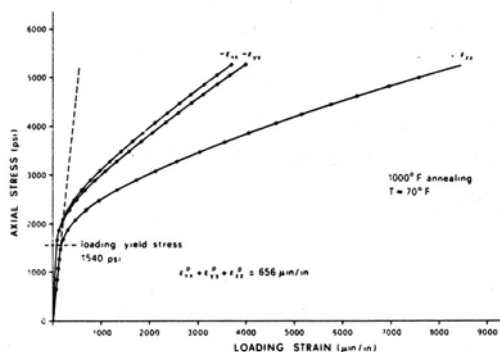


Fig. 15

loaded axially to 5240 psi with an axial strain of 8500  $\mu\text{in/in}$ . Then the specimen remained at that stress level for 1200 minutes while creep strains were occurring. Figure 15 shows the development of the axial strain  $e_z$  and of the two lateral strains  $e_x$  and  $e_y$  while the specimen was loaded. The specimen remains practically isotropic since  $e_x^{pl} \approx e_y^{pl}$  and the value of  $v^{pl} = -e_x^{pl}/e_z^{pl}$  is equal to .44. This means that there is an increase in the volume. However, if we follow the development of the plastic strains we shall observe that up to approximately 400 psi the value of  $v$  remains .50 but it changes rapidly to the final value of .44 between the values 4000 psi and 5240 psi. Therefore the increase in volume of approximately 656  $\mu\text{in/in}$  occurs at that stage.

Figure 16 shows the development of the creep strain while the stress remains at 5240 psi. We observe that  $e_x^{cr} = e_y^{cr}$ . At the end of the test we have a total axis creep strain of 350  $\mu\text{in/in}$  while the lateral creep strains were  $e_x = e_y \approx 100 \mu\text{in/in}$ . The ratio  $v = -e_y/e_z = .29$  shows a considerable increase in volume due to creep.

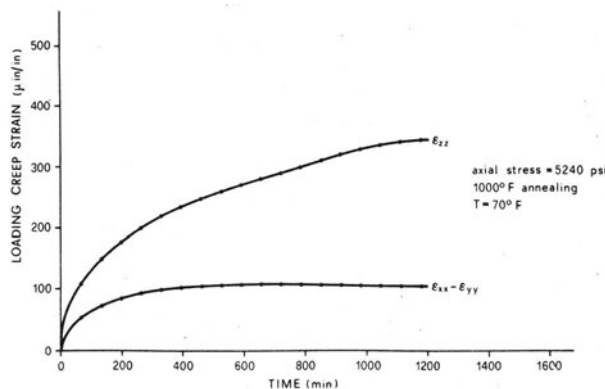


Fig. 16

From our experiments we can conclude, therefore, that for the plastic strain there is no change in volume but that for creep there is some change in volume. These conclusions will be used in the development of the theory.

We conclude this section by clarifying the concepts of plasticity, creep, and viscoplasticity. Let us consider in Fig. 17 the equilibrium stress-strain curve OA and the non-equilibrium stress-strain curve OB obtained with a constant stress rate  $\dot{s}$ . While the stress is increasing with the stress rate  $\dot{s}$  plastic strain develops. If at the stress  $s_A$ , point M, we unload abruptly below the equilibrium stress-strain line the plastic strain is frozen to some value  $e_A^{pl}$ , and the corresponding stress at the equilibrium stress-strain line is  $s'_A$ , point M'. If instead of decreasing the stress we keep the stress at  $s_A$  the creep strain will occur under the constant stress  $s_A$ . The total creep strain  $e_A^{cr}$  is equal to the segment MN of the line parallel to the strain axis but between the two stress-strain curves OA and OB at the stress level  $s_A$ . This creep strain which develops gradually, stops at N, and it can be assumed to develop with a rate which is a function of the distance between the line MN and the equilibrium stress-strain line OA. It will be called the limited creep strain and its development follows a strain-time diagram of the type shown in Fig. 18a.

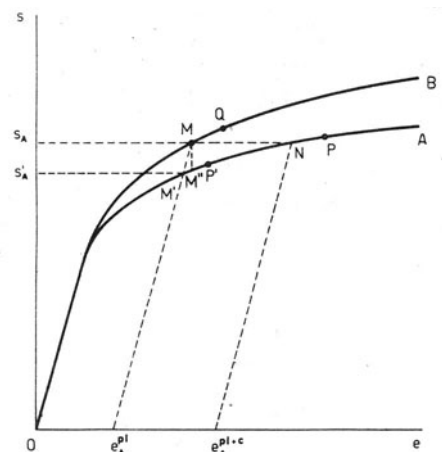


Fig. 17

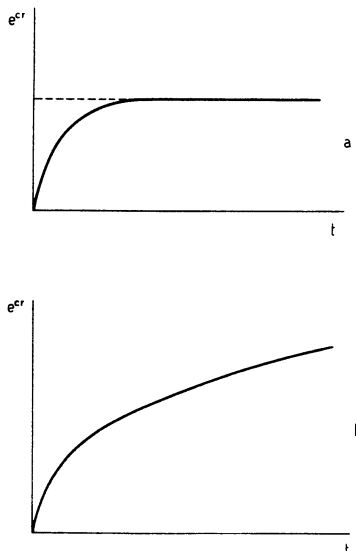


Fig. 18

If the stress  $s_A$  is so high that there is no intersection between the line parallel to the strain axis but intersecting the stress axis at  $s_A$ , and the equilibrium stress-strain line OA then creep strain develops without limit and such a creep strain will be called **unlimited creep strain**. The development of unlimited creep follows a strain-time diagram of the type shown in Fig. 18b. Unlimited creep will occur also when the temperature is sufficiently high since the equilibrium stress-strain line becomes the flatter the higher the temperature, and therefore no intersection N, Fig. 17 will occur at higher temperatures. In one of the sections of these lectures we shall consider limited and unlimited creep.

Now suppose that at the stress point N, Fig. 17, we increase the stress by a small amount  $ds$  to obtain the stress point P. The relation between the stress increment  $ds$  and the sum of plastic and creep strain due to  $ds$  is discussed in the **theory of plasticity**. Similarly, we may be at M' and increase the stress by  $ds$  to P'. Plasticity discusses the relation between  $ds$  at M'P' and the sum of plastic and creep strain due to  $ds$ . Thus, the theory of plasticity considers the relation between the stress increment  $ds$  and the resulting sum of plastic and creep strain increments, when the material is in the equilibrium stress-strain line. The theory of plasticity will be discussed in one of the sections of these lectures.

Now, suppose that instead of unloading from M to M' we continue loading from M to Q with a stress rate  $\dot{s}$ . The theory discussing the relation between stress and strain while loading from M to Q is the **theory of viscoplasticity**. When acceleration effects are neglected we have problems of **static viscoplasticity**, when however, acceleration effects are considered as in wave propagation we have **dynamic viscoplasticity**. In sections of these lectures we shall consider both static and dynamic viscoplasticity. It is seen that there exists a unifying thread connecting plasticity, viscoplasticity, and creep.

A final point should be made concerning the concept of **stress relaxation**. Suppose that at the stress point M the material is forced to keep the same total strain  $e_A^{pl} + e_A^{el}$  but that the stress is allowed to change. The only way the stress can move under these circumstances is in a direction parallel to the stress axis, line

MM''. Creep can develop since MM'' is not the same as MM' but for creep to develop it is necessary for the stress to decrease so that the creep strain will take the place of the disappearing elastic strain. The decrease in the stress is called **stress relaxation** and the limiting value of stress is given by the stress which corresponds to the point M''. This stress relaxation takes time to develop and the rate of its development is a function of the distance between the actual stress and the limiting stress at M''.

#### 4. The Initial Yield Surface

A fundamental assumption of the theory of plasticity is the existence of a yield surface in the seven-dimensional stress-temperature space. This surface represents the locus of all points enclosing the region in the stress-temperature space in which the motion of the generic stress point produces only elastic strains. It is assumed that any excursion of the generic stress point outside the yield surface will produce permanent strain.

In some recent accounts of the theory of plasticity [ 7, 8 ] the attempt was made to avoid having to make the assumption that a yield surface exists. The authors of these papers prefer the theory to predict the existence of a yield surface instead of assuming its existence in the first instance. To this author, such an attempt seems to be of academic interest. We do know from experiments that yield surfaces exist and it is immaterial whether the yield surface is a primary or a derived quantity. Only the simplicity of a particular theory will decide whether the yield surface should be an assumed or a derived concept. Of course, any proposed theory, simple or not, should agree with the available experimental results. In addition its validity will be the more secure the larger the number of predictions which are experimentally verified.

The concept of the yield surface is intrinsically connected with the definition of yielding and with the first appearance of plastic strain. To determine the yield surface it is necessary to define yielding as an equivalent to the proportional limit if the yield surface is to be the region in stress space in which for any motion of the stress point only elastic strains appear.

The definition of yielding by means of the proof strain implies that part of the region enclosed by the yield surface will be such that the motion of the stress point within this region will produce plastic strains in addition to the elastic strains. The maximum plastic strain permissible within the region enclosed by the yield surface is equal to the proof strain. However, once an amount of permissible proof

strain for a simple extension is accepted in the definition the question is raised about the amount of proof strain permissible when combined plastic strain appears. Hence, it is then necessary to adopt a criterion of equivalence between proof strain in simple extension and proof strain in combined strain. The adoption of such a criterion of equivalence means implicitly that a theory of plasticity has been adopted, the theory which we are trying to prove or disprove in the first place. Thus a bias is introduced in favor of the theory adopted.

A similar problem occurs when we define yielding by means of the backward linear extrapolation procedure.

In the experimental determination of the yield surface the use of more than one specimen for obtaining the complete yield surface (and the subsequent yield surfaces) inevitably introduces scattering of the results. Consequently in our experiments for the determination of initial and subsequent yield surfaces we always used one specimen only for the entire sequence of yield surfaces.

The use of one specimen only for the entire series of yield surfaces necessitates, of course, the use of the definition of yielding by means of our definition of the proportional limit. The proof strain definition as well as the backward linear extrapolation definition introduce plastic strains while the surface is obtained and this fact makes it impossible to obtain more than one point of the yield surface with each specimen; the plastic strain distorts the yield surface.

The initial yield surface for commercially pure aluminum has been obtained by the author and his students repeatedly for the temperature range of  $70^{\circ}\text{F}$  –  $305^{\circ}\text{F}$ . It has been obtained for combined tension and torsion as well as for combined tension, torsion, and internal pressure. In [10] we give some information concerning the experimental procedure used.

Fig. 19 from [9] shows the initial yield surface in the tension-torsion space for commercially pure aluminum annealed at  $650^{\circ}\text{F}$ . In this figure the yield surface is given in terms of its isothermals at the temperature of  $70^{\circ}\text{F}$ ,  $151^{\circ}\text{F}$ ,  $227^{\circ}\text{F}$ , and  $305^{\circ}\text{F}$ . The same specimen was used to obtain all data points at all temperatures. All the data on the  $70^{\circ}\text{F}$  isothermal was determined before raising the temperature to  $151^{\circ}\text{F}$  and the same procedure was followed for the higher temperatures until all the data at the highest temperature were obtained.

From the experiments it is shown that the yield surface lies between the Mises and Tresca surfaces. Other experiments by us [10] show that even the order in the temperature does not affect the yield curves, at least when the temperature change is slow.

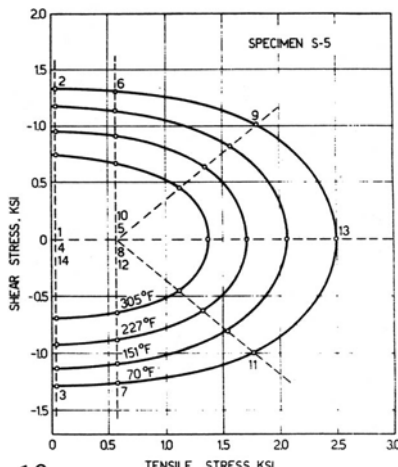


Fig. 19

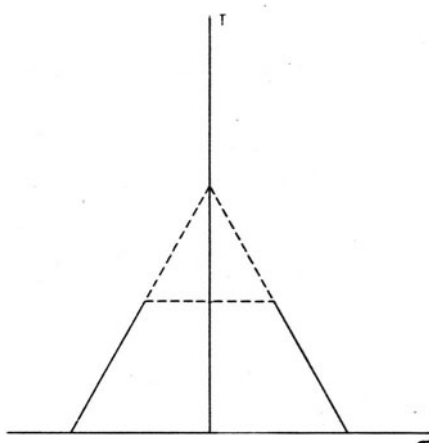


Fig. 20

The virgin equilibrium yield surface is a truncated elliptical cone in the  $\sigma$ ,  $\tau$ ,  $T$  space. The extrapolated apex of this cone is on the temperature axis at  $T = 600^{\circ}\text{F}$  and the basis of the cone is at  $70^{\circ}\text{F}$ . The cone is truncated at  $305^{\circ}\text{F}$  since no data are available at higher temperatures. The intersection between this cone and the  $\tau - T$  plane is shown in the Fig. 20 which consists of two straight lines. In this figure it is shown the obvious fact that as the temperature increases the yield surface decreases in size in the stress direction. It is seen that plastic deformation will occur when the stress does not change or even when it decreases, provided that the temperature increases appropriately.

For the determination of the yield surface we can also use thermal loading paths. This was done by the author for pure aluminum [11] and Fig. 21 shows the type of loading paths used. No difference in the results has been found between the isothermal tests and the thermal loading tests.

Figure 22 from [12] shows the yield surface in the  $\sigma_y$ ,  $\sigma_z$  space for pure aluminium. The similarity with the Mises surface is striking. Fig. 23 from [12] gives the threedimensional yield surface for aluminium in the  $\sigma_y$ ,  $\sigma_z$ ,  $\tau$  space at room temperature.

Experiments were also performed with copper and brass. Figure 24 from some unpublished work in our laboratory [13] shows the initial yield surface at room temperature in the  $\sigma$ ,  $\tau$  space for oxygen free high conductivity copper annealed for one hour at  $750^{\circ}\text{F}$  in a vacuum furnace. Figure 25 shows the initial yield surface at room temperature in the  $\sigma_y$ ,  $\sigma_z$  space for the same material as above. From Figures 24 and 25 we conclude that copper follows nearly the Tresca

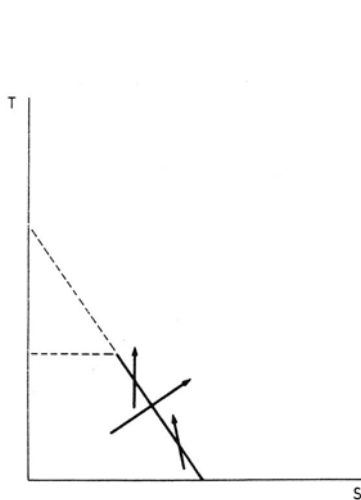


Fig. 21

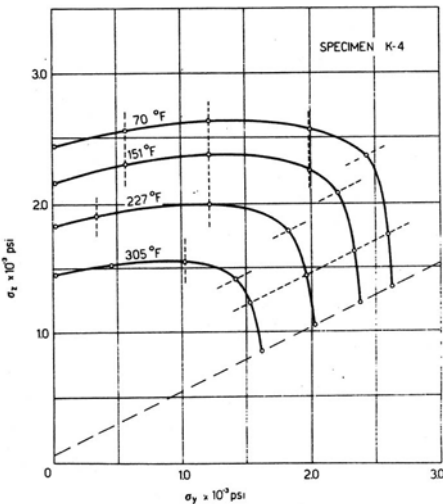


Fig. 22

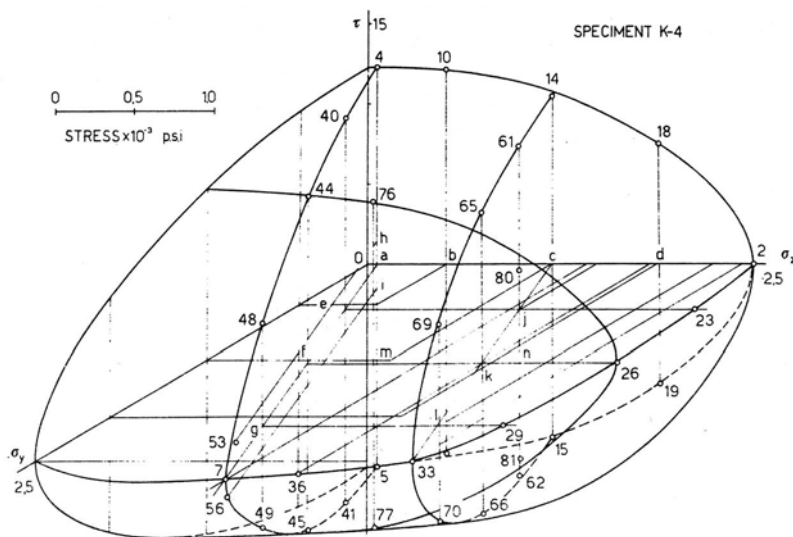


Fig. 23

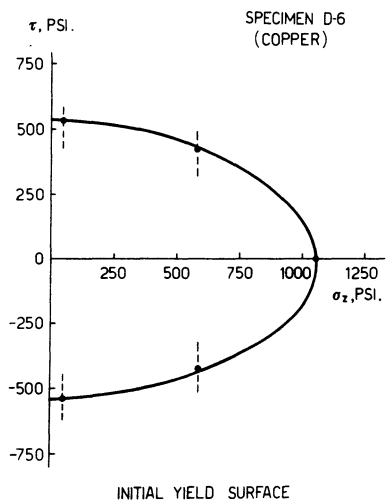


Fig. 24

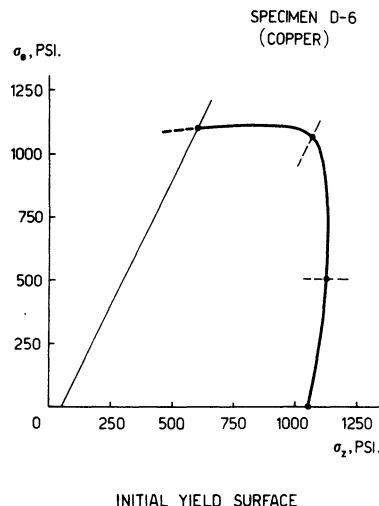


Fig. 25

surface.

Figure 26 from [13] shows the initial yield surface for brass annealed at  $1080^{\circ}\text{F}$  for one hour. The yield surface is shown in the  $\sigma$ ,  $\tau$  plane and it was obtained by means of the isothermals at  $75^{\circ}\text{F}$  and  $200^{\circ}\text{F}$ . It agrees very nearly with the Tresca condition.

In all our experiments we used thin-walled tubes which were loaded in either tension, or torsion, or internal pressure, or in some combination of these three modes of loading. In these experiments the most general stress state applied on an element of the wall of the tube is given by the plane state of stress  $s_z$ ,  $s_x$ ,  $\tau_{xz}$  where  $s_z$  is the axial stress,  $s_x$  is the hoop stress and  $\tau_{xz}$  is the shear stress between the  $x$  and  $z$  directions. The radial stress  $s_y$  is a very small one compared to the hoop stress  $s_x$  to that it can be neglected.

Yield surfaces were also obtained in the literature on the basis of a proof strain as well as of the Lode backwards extrapolation. In both cases the so

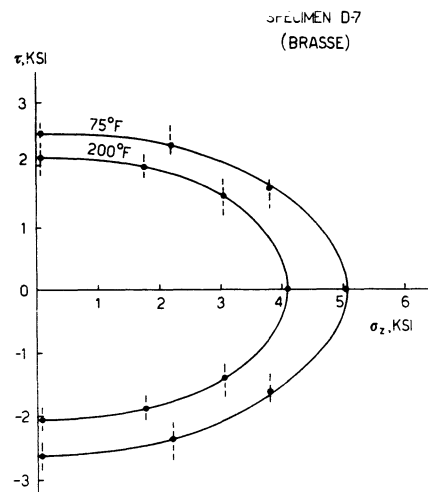


Fig. 26

determined yield surfaces include a region where the motion of the stress point will produce some plastic deformation. In addition any so determined yield surface presupposes some theory of equivalent stress or equivalent strain in order to facilitate the determination of the combined stress points. Fig. 27 shows the results

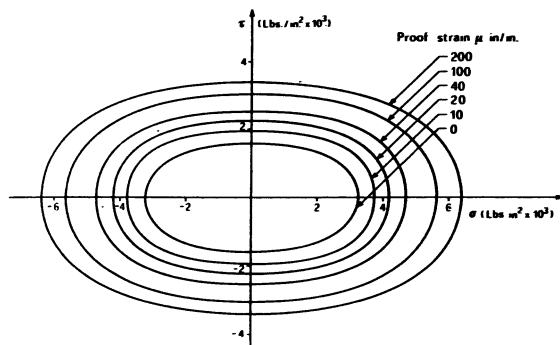


Fig. 27

of Williams and Svensson [14] for yield surfaces under combined tension and torsion for different values of proof strain. There is a nearly proportional growth of the yield surface with the increasing equivalent permanent set.

It is generally assumed that the first experimenter to determine the initial yield surface

was Guest [15]. This is, however, not correct since more appropriately it can be said that Guest determined a subsequent yield surface. We shall return to Guest's work in the next section.

In the previous section we observed that plastic strain does not change the volume. Consider the six-dimensional plastic strain space. In this space the plastic strain increment will be a strain increment vector with its origin at some point in the plastic strain space. Figure 28 illustrates a three-dimensional principal plastic strain space,

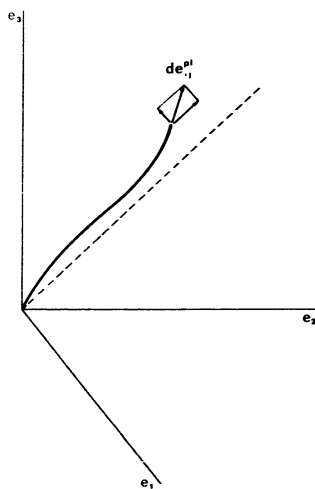


Fig. 28

and the strain increment vector  $de_{ij}^{p\ell}$  is shown at the end of a plastic strain path. The vector  $de_{ij}^{p\ell}$  can be resolved in two directions normal to each other. The first is the direction making equal angles with the three principal plastic strain axes and the other lies on the plane perpendicular to the first direction, the octahedral plane. The direction making equal angles with the principal axes has the direction cosines  $1/\sqrt{3}, 1/\sqrt{3}, 1/\sqrt{3}$ . The component of  $de_{ij}^{p\ell}$  in the direction parallel to the direction  $(1/\sqrt{3}, 1/\sqrt{3}, 1/\sqrt{3})$  has the magnitude  $de_{kk}^{p\ell}/\sqrt{3}$  and the components  $de_{ij}^{p\ell}/3$ . It follows that this vector is proportional to the change in volume due to the plastic strain. Since there is no plastic change in volume it follows that  $de_{ij}^{p\ell}$  will always be parallel to the

octahedral plane. The above conclusion is also valid for the six-dimensional plastic strain space.

We now consider the six-dimensional stress space. As a representative of this space consider the three-dimensional principal stress space and consider also the stress vector  $s_{ij}$ . The stress vector can be resolved in two directions one making equal angles with the three principal axes of stress and the other perpendicular to the first one, that is parallel to the octahedral plane. We again obtain the result that the component of  $s_{ij}$  in the direction of  $1/\sqrt{3}, 1/\sqrt{3}, 1/\sqrt{3}$  has the magnitude  $s_k k / \sqrt{3}$  and the components  $s_{ij} / 3$ . Therefore, this vector is proportional to the average normal stress. The other component of  $s_{ij}$  which is equal to

$$s'_{ij} = s_{ij} - \frac{1}{3} \delta_{ij} s_k k \quad (2)$$

lies on the octahedral plane.

Experiments by Bridgman [16] as well as by Crossland [17] indicate that essentially the plastic deformation of metals is independent of hydrostatic pressure or of the mean normal stress. Whether this assumption is exactly true or not is not known but we shall assume the correctness of this assumption and in particular we shall assume that the yield surface is unaffected by the mean normal stress. Experiments, however, in which the yield surface as we defined it is obtained before and after the application of a mean normal stress are lacking to the authors knowledge and they are essential in order to clarify the above question.

The assumption that the yield surface is unaffected by the mean normal stress means that in the principal stress space the yield surface takes the form of a cylinder whose generators are perpendicular to the octahedral plane. The yield surface can then be adequately represented by the curve of intersection of the cylindrical yield surface with the octahedral plane.

If we superpose the plastic strain space on the stress space we find that the two octahedral planes coincide. The plastic strain increment vector has been found to be parallel to the octahedral plane. However, it cannot be assumed to be always normal to the cylindrical yield surface. The only conclusion we can draw is that the yield curve and the plastic strain increment vector are on parallel planes.

The analytical expression of the initial yield surface is given by

$$f(s_k k, T) = \kappa \quad (3)$$

where  $s_{ij}$  represents the components of the stress tensor,  $T$  is the temperature, and  $\kappa$  is a constant. Equation (3) can be considered as the equation of a hypersurface in

the seven-dimensional stress-temperature space.

For an isotropic material the yield function  $f$  is an isotropic function of the stress so that we can write equation (3) in the form

$$(4) \quad f(J_1, J_2, J_3, T) = \kappa$$

where  $J_1, J_2, J_3$  are the three invariants of the stress tensor  $s_{ij}$ .

Since the yield surface is supposed to be independent of the mean normal stress we should express (4) in terms of the stress deviation components  $s'_{ij}$  given by (2). The invariants of the stress deviator are  $J'_1, J'_2$ , and  $J'_3$  where

$$(5) \quad J'_1 = s'_{kk} = s'_1 + s'_2 + s'_3 = 0$$

The two invariants  $J'_2$  and  $J'_3$  are given by

$$(6) \quad J'_2 = \frac{1}{2} s'_{ij} s'_{ij}$$

$$(7) \quad J'_3 = \frac{1}{2} s'_{ij} s'_{ik} s'_{ki}$$

Equation (4) becomes now

$$(8) \quad f(J'_2, J'_3, T) = \kappa$$

The Mises yield surface has the expression

$$(9) \quad f(J'_2, T) = \kappa$$

while the Tresca yield surface is given by a function of both  $J'_2$  and  $J'_3$  as well as of  $T$ :

$$(10) \quad f(J'_2, J'_3, T) = \kappa$$

Of interest are the representations of the Mises and Tresca yield surfaces in the octahedral plane, Fig. 29, in the  $\sigma, \tau$  plane, Fig. 30, and in the  $\sigma_1, \sigma_2$  plane, Fig. 31. We observe that in the octahedral plane for given  $T$  and  $\kappa$  the Mises condition is a circle while the Tresca condition is the hexagon inscribed in the Mises circle.

The function  $f$  expressing the initial yield surface should be of such a form that for some value  $T^*$ , at present unknown but definitely less than the annealing temperature of the material, equation (3) should be satisfied only at the origin of the stress space.

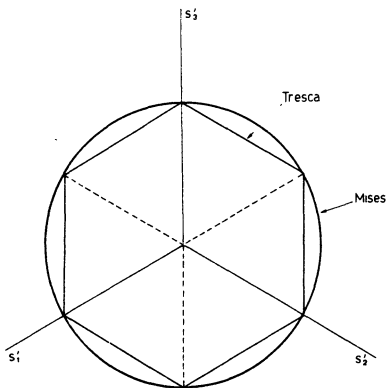


Fig. 29

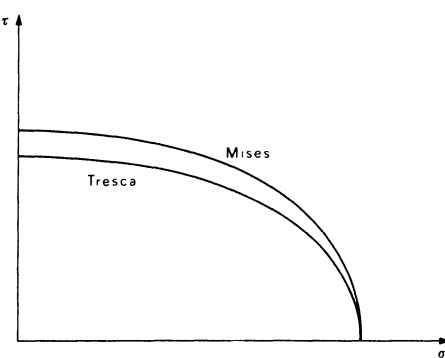


Fig. 30

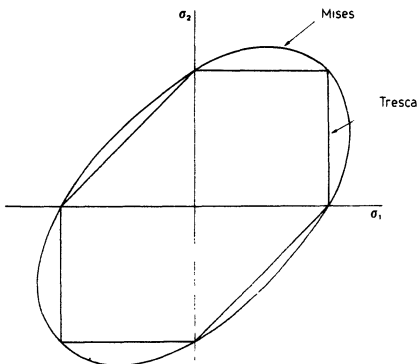


Fig. 31

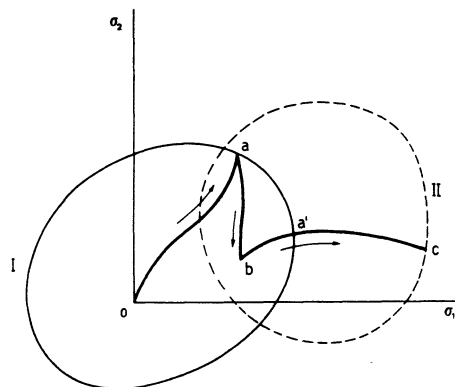


Fig. 32

## 5. The Subsequent Yield Surfaces

Loading beyond the initial yield surface produces plastic deformation and changes in the yield surface so that new subsequent yield surfaces appear.

The change of the yield surface can be illustrated in Fig. 32 and 33. In Figure 32 we illustrate the generalization in the two-dimensional stress space of the stress-strain curve, Fig. 7, used in plasticity. We see that the initial yield surface I becomes a subsequent yield surface II when the stress path moves outside the yield surface I (line a'b'c). As long as the stress path remains within the initial yield surface there is no change in the yield surface I.

In Figure 33 we illustrate the generalization in the two-dimensional stress space of the stress-strain curve, Fig. 9, which is used in these lectures. The initial

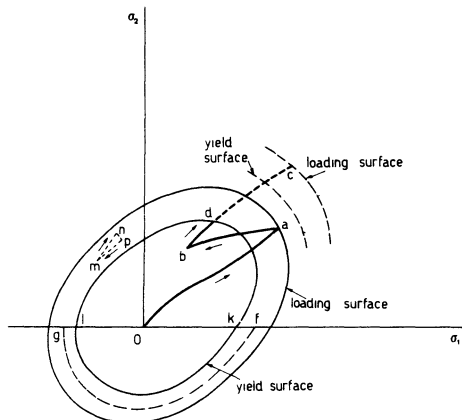


Fig. 33

yield surface is replaced by two surfaces, the subsequent yield surface and the loading surface. The loading surface corresponds to the stress  $a$  in Figure 9, while the yield surface corresponds to the stress  $d$ . The stress space is divided into three regions. An inner region enclosed by the yield surface where only elastic strains appear. An intermediate region between the two surfaces where small plastic strains appear, and an exterior region outside of the loading surface where full plastic strains appear. As long

as the stress point moves within the inner region there are no plastic strains and both the yield surface and the loading surface remain unchanged. When the stress point moves from  $a$  towards the yield surface very fast there will be no plastic strains developed and the two surfaces will remain intact. The same happens if the stress point moves very fast from a position on the yield surface to some position on the loading surface. If, however, the motion of the stress point between the two surfaces is slow enough to allow for plastic strains to be developed there will be a change in both the yield surface and the loading surface except that the loading surface will continue to pass through the point  $a$  even after the change.

When the stress point moves outside the loading surface there will be plastic strain developed and both surfaces will change. In this section we shall consider only the change of the yield surface, that is the development of subsequent yield surfaces.

We obtained experimentally a large number of subsequent yield surfaces due to prestressing. Most of these surfaces were for aluminum specimens and a smaller number were for copper and brass. Figure 34 from [18] gives a sequence of two prestressings for aluminum. The initial yield surface has been obtained first, then the specimen was prestressed to the point A and the first subsequent yield surface was obtained. Subsequently, the loading path starting from inside the first subsequent yield surface proceeded to prestress the same initial specimen to the point B and then the second subsequent yield surface was obtained. All prestressing were at room temperature. The isothermals at four temperatures were obtained for the initial yield surface and for the first subsequent yield surface. For the second

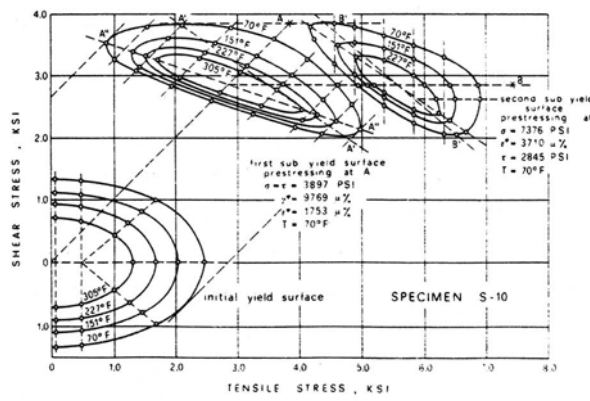


Fig. 34

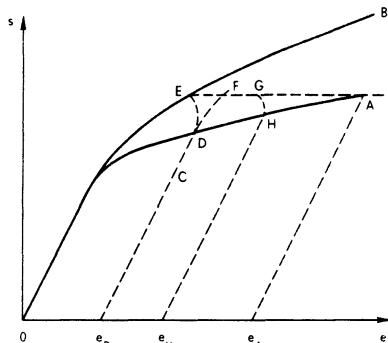


Fig. 35

DF does not coincide with ED. Thus, the point D of the equilibrium line corresponds to the prestress point E and the plastic strain  $\epsilon_E$ . If unloading would have been started at  $e_D$  but after some additional plastic strain has appeared, for example at G, and the equilibrium line had been crossed at H the plastic strain would have been frozen at H, with the plastic strain value  $\epsilon_H$  which is obviously different from  $\epsilon_D$ .

In combined stress the axis  $\sigma$  of

the figure 35 is replaced by the stress space and we observe that the points D and E in figure 36 do not coincide. Hence, the prestressing point lies outside the yield surface which corresponds to that pre-

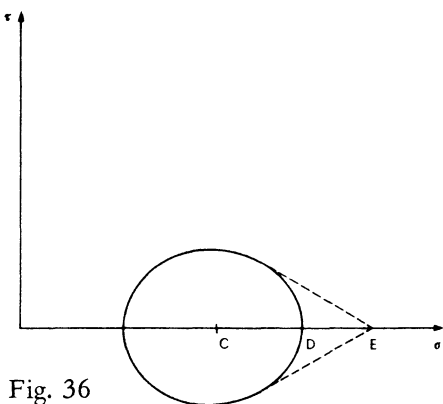


Fig. 36

stressing point. Our experiments have shown that for even a very slow rate of stressing as applied by dead load testing of the order of 50 lb/sq. in. every 2 minutes, for commercially pure aluminum at room temperature, the equilibrium yield surface does not pass through the prestressing point. The experiments have also shown that the yield surface does not change even if several days pass,

while the stress point lies within the elastic region; the yield surface is frozen. On the other hand by waiting at the prestressing point before unloading we succeed to have the yield surface move gradually towards the prestressing point and finally pass through the prestressing point as predicted by the model of the time development of plastic strain introduced earlier. It follows that hardening is due to both the prestressing and to the amount of plastic strain developed during prestressing.

The above comments are substantiated by Fig.s 37 and 38. In the experiment illustrated in Figure 37 from [12] once the subsequent yield surface has been determined, the prestressing point A has been reached again and the new subsequent yield surface was determined. We see that the second subsequent yield surface, due to prestressing to the same point A as the first subsequent yield surface, lies in a position closer to the prestressing point than the first subsequent yield

surface, since additional plastic strain has been developed. The amount of plastic strain developed while the loading point is outside the yield surface determines the proximity of the yield surface to the prestressing point.

In the experiment illustrated in Figure 38 the stress point remained at the prestressing location for a considerable time before it was attempted to obtain the corresponding yield surface. As a consequence the yield surface passes through the prestressing point. Thus, our comments above are substantiated by these experimental observations.

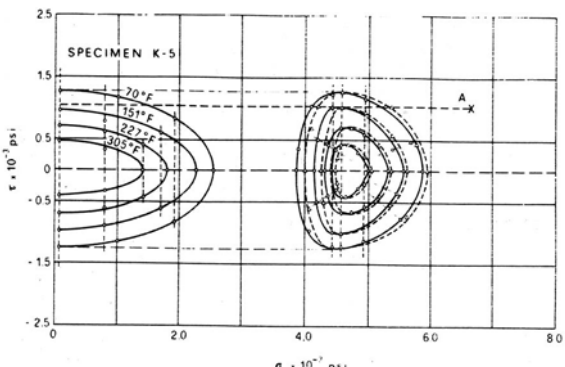


Fig. 37

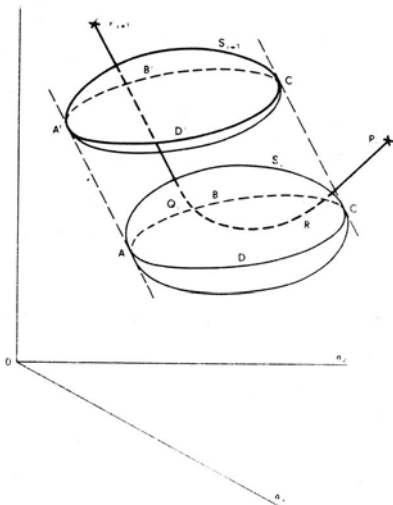


Fig. 39

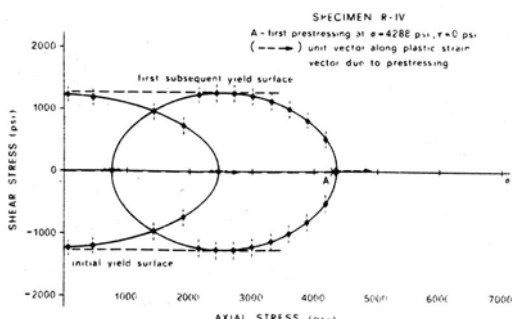


Fig. 38

Experimental work by Naghdi, Essenburg and Koff [19] and by Ivey [20] has shown that in torsion there is absence of cross effect. This means that if the prestressing or prestraining is in torsion the yield surface does not change its diameter in the tension direction. In [18] and [12] we have shown that for the yield surface lack of cross effect is a universal law at every tested temperature and every direction of prestressing provided the definition of yielding is that of the proportional limit. Figure 39 shows the law of hardening as discovered by us. It is explained below.

Suppose that the yield surface in the  $\sigma_y$ ,  $\sigma_z$ ,  $\tau$  stress space at some

constant temperature and at some level of prestressing is given by  $S_i$  and that the stress path which is responsible for the surface  $S_i$  terminates at the stress point  $P_i$ . Note that the point  $P_i$  does not necessarily lie on the surface  $S_i$  but it may lie outside  $S_i$ . We retrace the stress path leading to  $P_i$  backwards until we reach some arbitrary position  $R_i$  inside  $S_i$ . Since any motion of the stress point inside or on  $S_i$  will not alter  $S_i$  let us select a new arbitrary position  $Q_i$  inside or on  $S_i$  not necessarily on the stress path leading to  $P_i$ . Suppose now that additional prestressing is generated by arbitrary rectilinear motion of the stress point from  $Q_i$  inside  $S_i$  to a position  $P_{i+1}$  outside  $S_i$ . The position  $P_{i+1}$  may of course be the same as  $P_i$ . Then the new yield surface  $S_{i+1}$  corresponding to the stress path terminating at  $P_{i+1}$ , is generated from the surface  $S_i$  by a superposition of a rigid body translation in the direction of prestressing  $Q_i P_{i+1}$  and of a deformation in the same direction  $Q_i P_{i+1}$ , independent of the direction of the normal to the yield surface at the intersection between the yield surface and path  $Q_i P_{i+1}$ . The effect of the deformation is that the width of the yield surface in the direction of prestressing will be decreasing when the motion is away from the origin, and be increasing when the motion is towards the origin. Rigid body translation is determined by the motion of the curve ABCD to its new position A'B'C'D'. The motion of this curve generates a cylinder with its axis in the direction of prestressing. This cylinder is tangential to both the original and to the new yield surface at the curves ABCD and A'B'C'D', respectively. This new law of hardening is valid for pure aluminum, copper and brass for every temperature within the ranges tested.

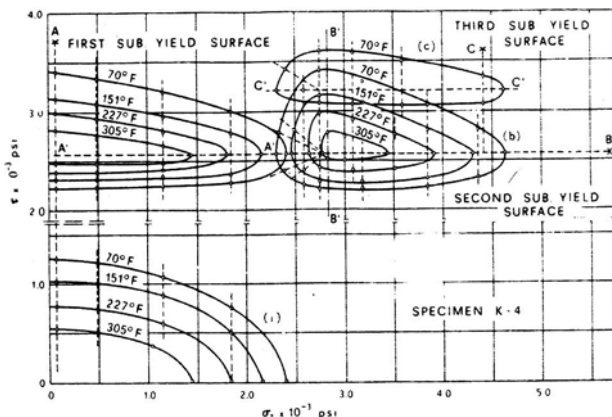


Fig. 40

As illustrations of the validity of our law of hardening we shall consider Figures 40 to 42. In Fig. 40 from [12] we see the  $\sigma$ ,  $\tau$  plane for an experiment in which the three-dimensional yield surfaces for an aluminum specimen were obtained after three successive prestressings at room temperature in torsion, tension, and torsion, respectively. The

prestressing were all in the  $\sigma$ ,  $\tau$  plane. Figure 41 from [12] gives the projections of these three-dimensional yield surfaces on the  $\sigma_y$ ,  $\sigma_x$  plane. From both figures we see that our hardening law is valid.

Figure 42 from [18] gives the initial and four subsequent yield surfaces for an aluminum specimen in which the first prestressing was in torsion and the three subsequent ones were in tension. All prestressings were at room temperature.

Figure 43 from [12] shows the three-dimensional form of the first subsequent yield surface of the specimen referred to in Figures 40 and 41. It is remarkable that our law of hardening is valid for all yield surfaces at all tested temperatures.

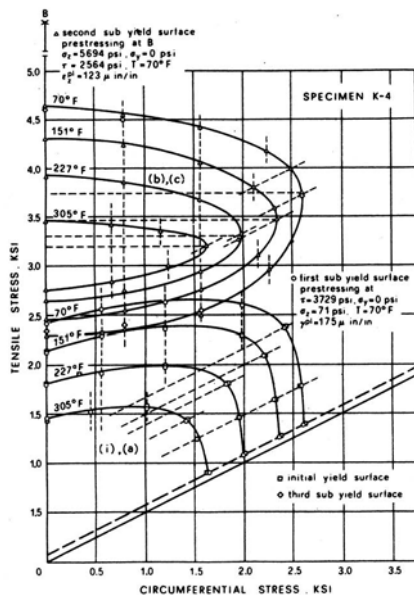


Fig. 41

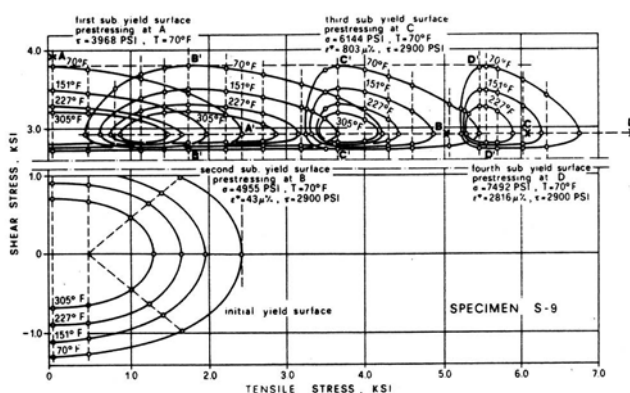


Fig. 42

In Figures 40 to 43 we have shown the results of experiments in which three-dimensional yield surfaces for pure aluminum were determined but the prestressings were in the  $\sigma$ ,  $\tau$  plane. We shall discuss now experiments in which three-dimensional yield surfaces for pure aluminum were determined but the prestressings were three-dimensional.

Figure 44 from [13] shows the first prestressing path at room temperature. This path was in a three-dimensional direction ( $\sigma_z$ ,  $\sigma_x$ ,  $\tau$ ). Fig. 45

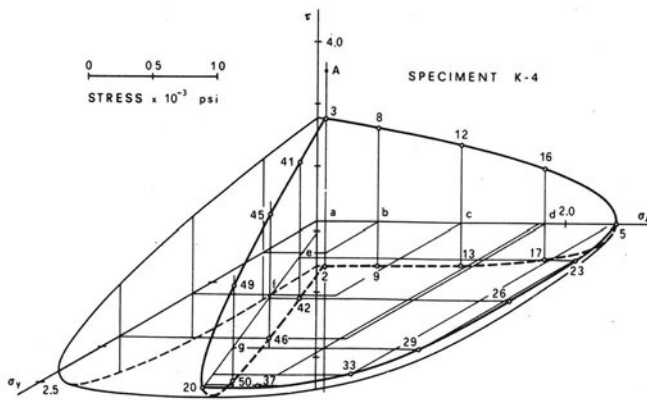
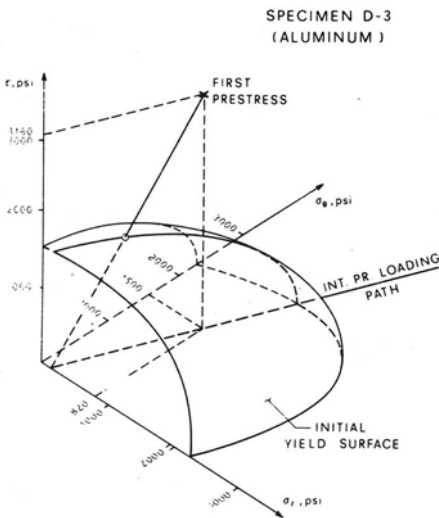


Fig. 43



THE FIRST PRESTRESS PATH

Fig. 44

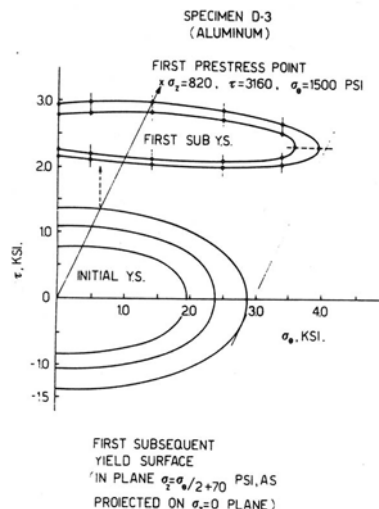


Fig. 45

shows the projection on the  $\sigma_x$ ,  $\tau$  plane of the intersections of the initial and first subsequent yield surfaces with the plane which is parallel to the  $\tau$ -axis but which includes the prestressing path. We observe that our law of hardening remains valid.

Figure 46 shows the second and third prestressing paths for the same specimen as above. From A the specimen was unloaded to B then loaded to C and unloaded to D at which time the second subsequent yield surface was obtained. Then it was loaded to E and F at which time the third subsequent yield surface was obtained. Our law of hardening continued to be valid during these two additional

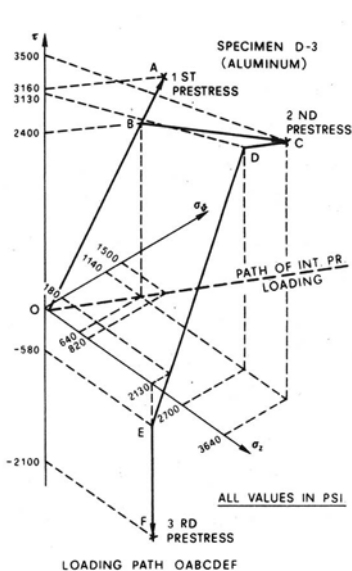


Fig. 46

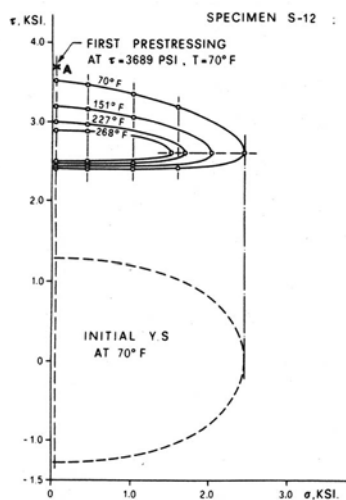


Fig. 47

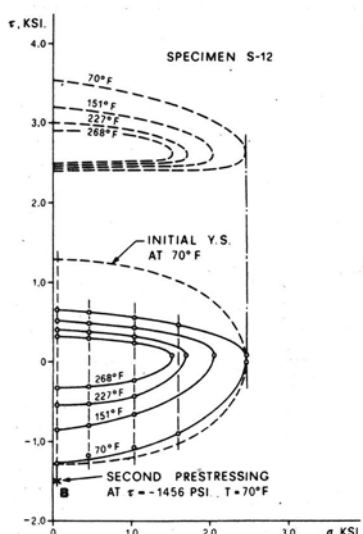


Fig. 48

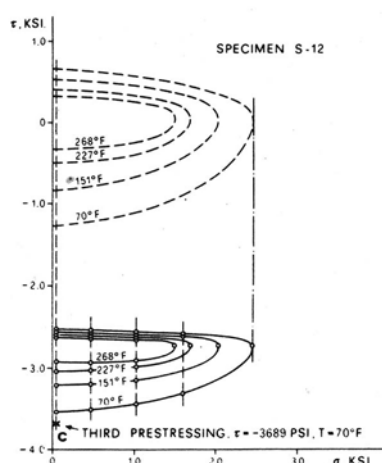


Fig. 49

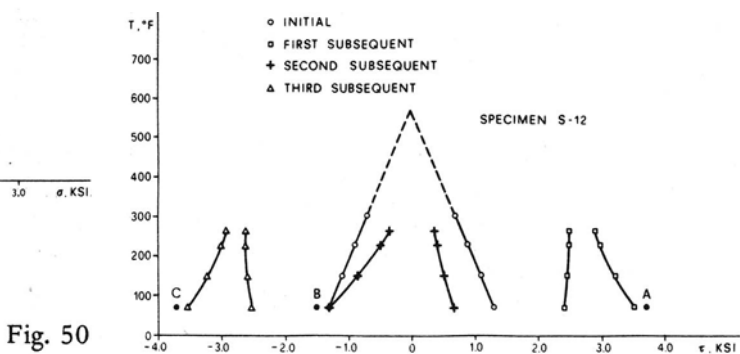


Fig. 50

prestressing.

Figures 47, 48, and 49 from [11] present the case of an aluminum specimen in which the prestressing was of a cyclic nature. The specimen was prestressed first to A, Fig. 47, then to B, Fig. 48, and finally to C, Fig. 49. We observe that not only the hardening law is valid but also that the width of the yield surface in the direction of prestressing first decreases, then increases, and finally decreases again. Figure 50 illustrates this phenomenon.

Figures 51 and 52 from [11] show that the phenomenon just described is not limited to torsion but it is valid also for tension. Indeed, Figure 51 shows the initial and the first subsequent yield surface for prestressing in tension for pure aluminum, whereas Figure 52 shows the second and third prestressing of the same specimen first in tension towards the origin and then in torsion. We observe that the width of the yield surface in the direction of prestressing, first decreases, then increases, and finally decreases again.

Figure 53 from [23] shows the continuation of this experiment. The

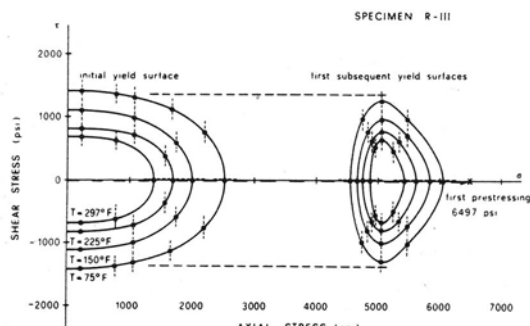


Fig. 51

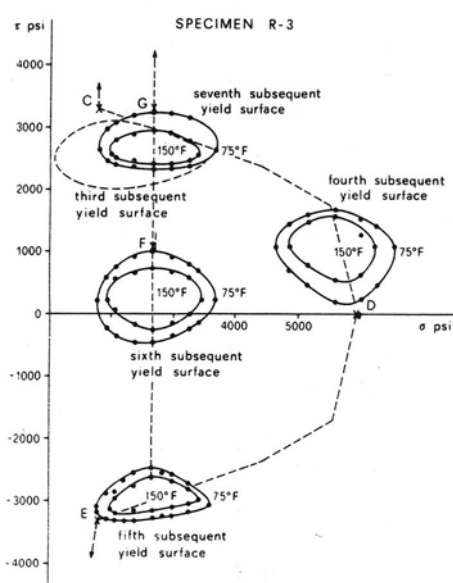


Fig. 53

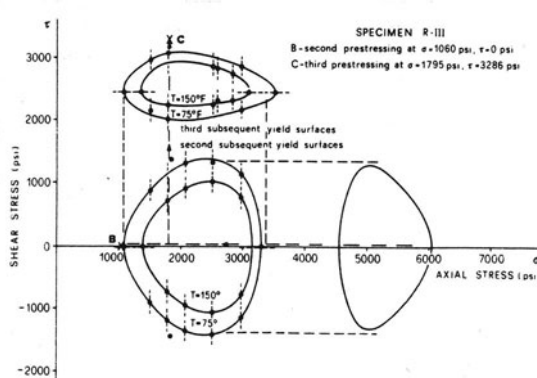


Fig. 52

third to seventh subsequent yield surfaces have been obtained and they are illustrated in this figure. The path of loading is from C to D to E to F and finally to G. The validity of our law of hardening and the changes in the width of the yield surfaces as outlined above are always valid whenever they could be obtained.

We see that the width of the yield curve in the direction of prestressing decreases the farther we move from the origin. If the prestressing point starts moving towards the origin the width of the yield surface in the direction of prestressing increases until the origin is reached and then it starts again decreasing as soon as the prestressing point has passed the origin. It is to be expected that when a yield surface has been obtained, due to a particular prestressing point, there must be limiting directions in stress space which separate the directions of prestressing of yield surfaces with decreasing width from the directions of increasing width yield surfaces. Figure 54 illustrates this concept.

Figure 55 from [13] shows the motion of the yield surface for a copper specimen for five consecutive prestressings. It is obvious that our law of hardening is valid also for copper and it was also shown to be valid for brass [13].

An important observation is that the subsequent yield surfaces may and usually do not include the origin. For torsional loading only this phenomenon has first been observed by Ivey [20].

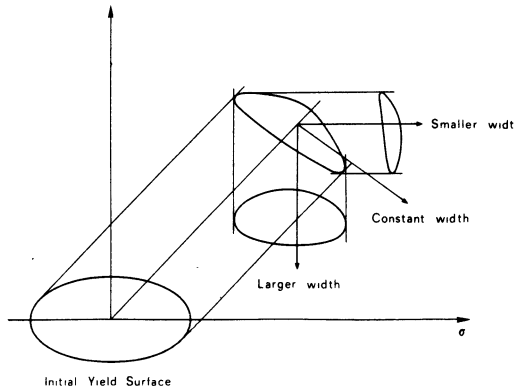


Fig. 54

We already mentioned that if the prestressing point remains at the prestressing location for considerable time the yield surface passes through the prestressing point. Figure 56 from [23] shows three subsequent yield surfaces passing through their prestressing points

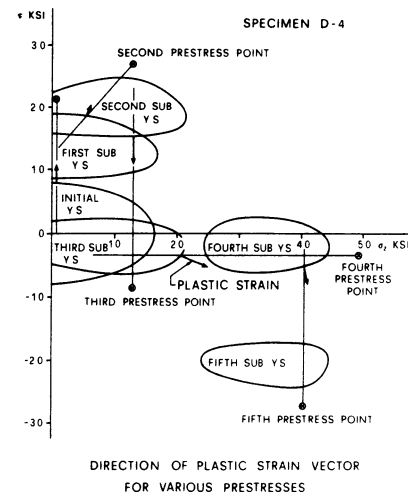


Fig. 55

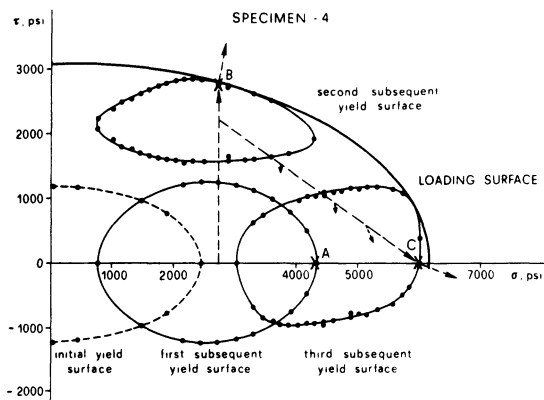


Fig. 56

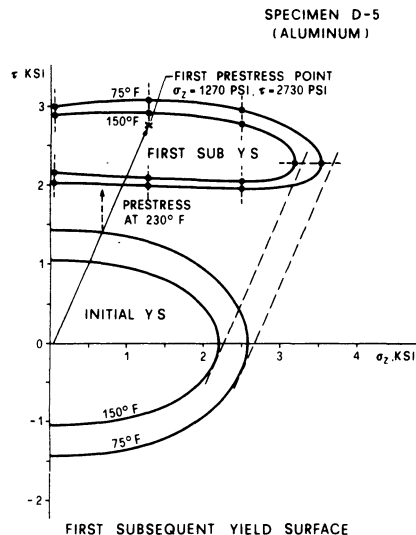


Fig. 57

because the stress point remained at these points for considerable time. We shall return to this figure in the next section.

In the previous discussion we considered prestressings at room temperature. At this stage we shall consider prestressings at elevated temperature.

Figures 57 from [13] show the results of an experiment with pure aluminum in which the

prestressing paths was at 230°F. The initial and first subsequent yield surfaces are illustrated in Fig. 57 by means of their 75°F and 150°F yield curves. We observe that our law of hardening is valid. Figure 58 shows the first and second subsequent yield surfaces and again our law of hardening is valid.

A critical evaluation of the experiments of other investigators and a comparison of their findings to ours is a very difficult task since the experimental technique of other investigators was not the same as ours and in many cases a complete description of the experimental technique is not given in their publications. Consequently, we shall be very selective in the choice of the work of

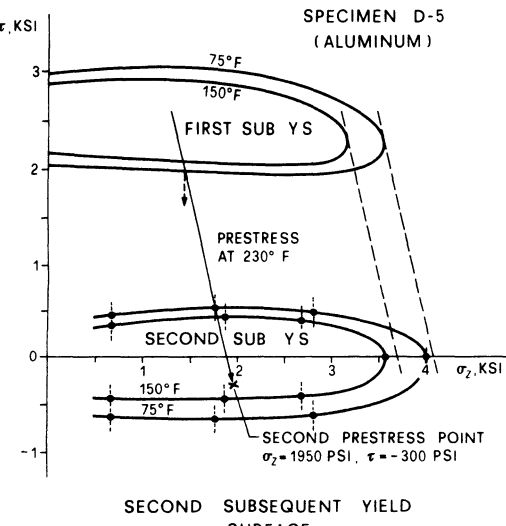


Fig. 58

others which will be discussed.

The first systematic experiment to obtain a subsequent yield surface was that of Guest [15]. Although it is usually stated that this experiment has to do with the initial surface this is not the case since Guest before obtaining the yield surface he prestressed his specimen deeply in torsion. He simply failed to obtain the initial yield surface. He used tubes of steel, copper, and brass, which he first loaded in pure torsion until the torquetwist curve became practically parallel to the twist axes. Then, the corresponding shearing stress was the prestress in torsion. Next the specimen was unloaded completely and then reloaded in torsion but only to a fraction of the prestressing shearing stress. Next the shearing stress was held constant while the axial tension was applied until it was observed that the elongation was no longer proportional to the axial tension. Next the specimen was unloaded and reloaded in combined stress again. A typical loading sequence was : pure torsion, combined torsion and tension, pure tension, combined tension and internal pressure, and finally internal pressure alone.

Guest observed that the influence of the intermediate principal stress was small and he concluded that the Tresca yield condition was valid. He did not construct a yield surface.

Morrison [ 21] plotted Guest's data in the  $\sigma$ ,  $\tau$  stress space and found such a scatter that it was not possible to find whether the Mises or the Tresca condition was correct.

Taylor and Quinney [ 4] obtained the subsequent yield surface in the  $\sigma$ ,  $\tau$  plane after prestressing in tension. They used aluminum, copper and steel tubes and their definition of yielding was the Lode backward extrapolation one. They found that the Mises condition agreed very well with the experiments for copper and aluminum but less well for the steel tubes. We shall return to these experiments in the next section.

Of considerable interest are the experiments with combined tension and torsion of Williams and Svensson [ 14], [22] with thin-walled tubes of commercially pure aluminum. These investigators determined the effect of prestrain on the yield surface. While determining the yield surface they used the proof strain definition and in addition they determined the effect of the amount of proof strain on the yield surface. Their testing machine was not a dead load one and each point on the yield surface was determined by a separate specimen. Their technique, therefore, was different from ours. Figures 59 and 60 show two of their results. Figure 59 shows the effect of tensile prestrain of 1% . Figure 60 shows the effect of torsional

prestrain of 1 %. The proportional limit yield surfaces are not shown since the smallest proof strain was 20  $\mu\text{in/in}$ . The effect of the amount of proof strain on the yield surface is very large. It should also be remarked that the corner indicated by the 20  $\mu\text{in/in}$  yield surface in Fig. 59 is not a real one since the measurement in the corner represents only the prestrain to that corner and not a subsequent yield.

Another set of experiments of interest is that of Miastkowski and Szczepinski [23] which also have used thin-walled tubes. The material tested was brass and the tubes were tested in combined axial and circumferential stress. In this case the proportional limit yield surface was determined and in addition the effect of the proof strain amount on the yield surface was obtained. The testing machine was not a dead load machine and each point on the yield surface was determined by a separate specimen. Figure 61 gives the yield curves before and after prestressing.

An interesting discussion on the effect of the definition of yielding on the determination of the yield surface has been given by Mair and Pugh [24].

From the experiments discussed in this section we can draw certain conclusions concerning the analytical representation of the subsequent yield surface.

We shall consider first the case when the subsequent yield surface passes through the prestress point. This case occurs when we wait at the prestress point for sufficient time until practically all plastic (and creep) strain associated with that

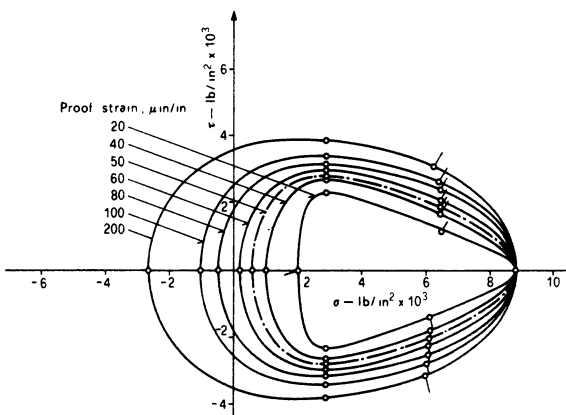


Fig. 59

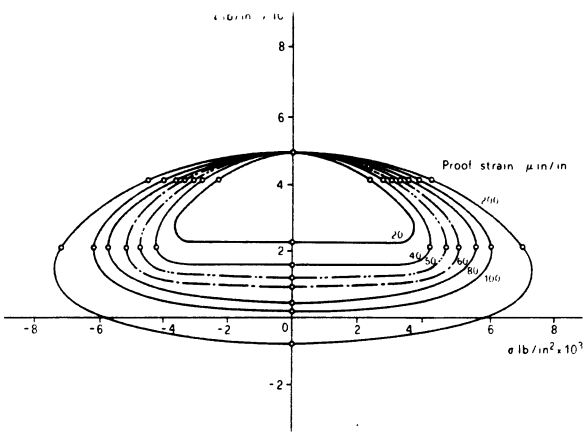


Fig. 60

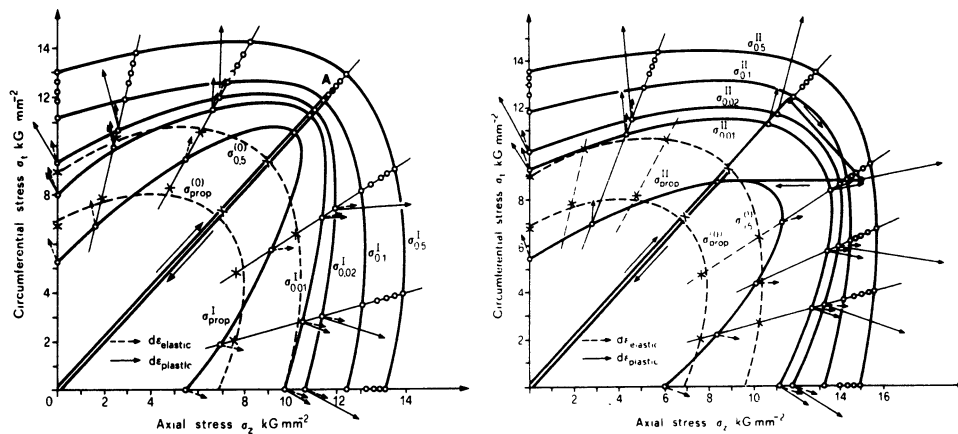


Fig. 61

prestress point at the equilibrium stage had the time to appear. The subsequent yield surface will depend on the total plastic strain  $e_{k\ell}^{p\ell}$  developed while the stress point is at the prestress stage. The subsequent yield surface will then be of the form

$$f \left( s_{k\ell}, T, e_{k\ell}^{p\ell} \right) = \kappa \quad (11)$$

We may assume that  $\kappa$  is a function of the history of plastic strain and of some additional as yet unknown variables. Similarly we can assume that the function  $f$  may include some additional as yet unknown variables.

Since the yield surface does not need to include the origin, and in fact in most cases does not include the origin we shall have in most cases

$$f \left( 0, T, e_{k\ell}^{p\ell} \right) > \kappa \quad (12)$$

where of course it is implied that  $f > \kappa$  denotes the region outside of the yield surface.

As the temperature increases the yield surface tends to decrease in size and at some value  $T^*$  which is less than the annealing temperature the surface will shrink to a small straight line segment. Therefore at  $T^*$  the yield surface will reduce to a linear form. The value of  $T^*$  may of course depend on  $e_{k\ell}^{p\ell}$  and on  $\kappa$ .

Since the yield surface passes through the prestress point we must have

$$f \left( s_{ij}^o, T^o, e_{ij}^{p\ell} \right) = \kappa \quad (13)$$

where  $s_{ij}^o$  is the prestress point and  $T^o$  is the temperature at which the prestressing occurred. If the subsequent yield surface does not pass through the prestress point because we did not wait at that point sufficiently long then equation (13) will be replaced by

$$(14) \quad f \left( s_{ij}^o, T^o, e_{ij}^{pl} \right) > \kappa$$

where of course  $\kappa$  and  $e_{ij}^{pl}$  have now different values than in (13). The rest of the previous discussion remains valid. The question of the law of motion of the yield surface will be considered in one of the next sections.

## 6. The Loading Surface

The concept of the loading surface has been introduced, in a rather imprecise manner, as the generalization of the loading point in Fig. 9 in the seven-dimensional stress-temperature space. We shall now proceed to introduce a more precise definition of this surface.

We remark that the loading point a in Fig. 9 has been reached by means of a certain stress rate. Suppose that we would have increased the stress at the same stress rate beyond "a", then in the immediate neighborhood of "a" the plastic strain rate would have remained the same. Unloading from "a" will produce either a zero plastic strain rate for very fast unloading stress rate or finite plastic strain rates for slower unloading stress rate. However these unloading plastic strain rates will be much smaller than the ones prevailing during loading. In effect, for  $\dot{s} > 0$  we obtain an  $\dot{e}^{pl}$  which is much larger than the one valid for  $\dot{s} < 0$ .

Consider now Fig. 33. We remark that from the point "a" we can move either in a loading direction or in an unloading direction. The difference between these two direction types is that they produce plastic strain rates  $\dot{e}^{pl}$  of very different magnitudes, irrespective of the stress rates  $\dot{s}$  applied. For some intermediate direction we must therefore have a discontinuity in the plastic strain rate. Such an intermediate direction is assumed to be tangential to the loading surface. We can, therefore, obtain in principle a surface of discontinuity in the plastic strain rates and this surface we call the loading surface.

For the special case when we consider the model in which unloading produces only elastic strains the loading surface can be defined as follows. From the point "a" in Fig. 33 we can move either in a direction of loading producing

additional plastic strain or in a direction of unloading without additional plastic strain. It follows that there must exist, intermediate limiting directions for which no plastic strain will be produced. Motions along these directions will produce no additional plastic strains and as a consequence they will not produce changes in the yield surface or in the loading surface. Such directions may be termed neutral. Continuing from point to point along neutral directions we obtain the loading surface passing through "a" associated with the history of plastic strain at "a" and with the amount of total plastic strain accumulated at "a".

At this stage it is important to consider Figure 9 again. We recall that if the stress point stays at the stress level of A for sufficient time the point D will reach the stress value of A. This is seen clearly from Figure 35. Now it may seem then that in this case the yield surface will coincide with the loading surface. We shall see later on that this is not so, although there is one point in stress space where this coincidence will be valid. The region between the yield surface and the loading surface does not become zero by the stress point remaining at A.

Consider now the case of partial unloading from "a" to some point "f" between the loading surface and the yield surface, Fig. 33, always considering our model in which unloading produces no plastic strains. From the point "f" we can again proceed in a loading direction, an unloading direction, or a neutral direction. Hence, we can define an intermediate loading surface passing through "f". More generally, we can define a family of intermediate loading surfaces lying between the outer loading surface and the yield surface. Through each point in the region between the yield surface and the outer loading surface passes an intermediate loading surface. The family of the intermediate loading surfaces is determined by the total amount of plastic strain and by the history of plastic strain.

We can show that the intermediate loading surfaces cannot intersect each other. Indeed, suppose they intersect each other as shown in Fig. 33 where surface  $m_p$  intersects surface  $m$ . Then the path  $p m n$  will allow a motion from  $p$  to  $n - p m n$  – without additional plastic strain. This means that we will then have, in the region between yield surface and loading surface, reloading without the production of additional plastic strain. Such a situation is clearly not admissible. We conclude that the intermediate loading surfaces cannot intersect one another, and therefore that through each point of the region between the yield surface and the outer loading surface passes one and only one intermediate loading surface. This result is of course based on a simplified model. In reality we shall see that the yield surface and the loading surface can be tangent to each other at one point in stress space. This, of

course, may be due to the fact that in reality we have plastic deformation upon unloading.

A direct determination of the loading surface is impossible. We were fortunate, however to obtain the loading surface as the envelope of the different positions which the yield surface can take. We shall concentrate our attention now to this problem.

In Fig. 56 we observe that the Tresca surface passing through the point B is tangential to both the second and third subsequent yield surfaces and that for the same specimen the initial yield surface was the Tresca surface. We can tentatively conclude that the loading surface has the form of the initial yield surface, only extended proportionally, and that the yield surface tends to be tangential to the loading surface unless the loading point moves outside the loading surface, in which case a new loading surface is established by means of proportional expansion of the initial yield surface. If the loading point moves to a considerable distance inside the loading surface the yield surface moves away from the loading surface. The region between yield and loading surface is the region of very small plastic strains. On the other hand the region outside the loading surface is the one in which larger plastic strains occur.

An explanation of the fact that the yield surface is tangential to the loading surface in stress space follows from a consideration of Figures 7 and 9. Figure 7 can be considered as the special case of Figure 9 in which the point D has reached the point A. Now, since the point D represents the yield surface and the point A represents the loading surface, it follows that in the stress space the two surfaces must be tangential to each other.

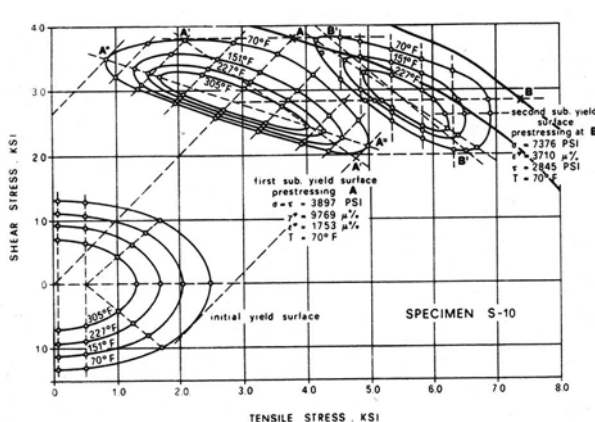


Fig. 62

Our previous conclusion is strengthened by considering the experiment described in Fig. 34. In Figure 62 we reproduce the experimental results but with the addition of two successive loading surfaces passing through A and B respectively. We see that the yield surfaces tend to be parallel to the loading surfaces near A and B.

A similar conclusion can be drawn for the other experiments described in the previous section. It is conceivable that if we had waited at A or B before unloading the yield surfaces would have passed by A and B and would have been tangential to the loading surfaces. In the next section we shall consider the plastic strain increment vectors and we shall see that our conclusion concerning the relationship between yield surface and loading surface is indeed correct.

As a final point we should remark that the experiments in which the Lode extrapolation technique has been used, it was always seen that proportional expansion agrees with the experimental results. The reason for this finding is that when the Lode extrapolation technique is used the experimentalist is obtaining a loading surface instead of a yield surface, and as we have seen the loading surface is the initial yield surface expanded proportionally.

The analytical expression of the loading surface is given by

$$F(s_k \ell, T) = K \quad (15)$$

We know that the loading surface (1) follows from the initial yield surface (3) by a proportional increase in all radial directions. Hence, there must be a relation between equation (15) and equation (3). This question will be discussed in section 9.

## 7. The Plastic Strain Increment Vector and the Creep Strain Vector

In order to develop a theory of plasticity it is, of course, not sufficient to know the yield and loading surfaces. It is equally important to know the direction of the plastic strain increment vector and its magnitude as a function of the direction and magnitude of the stress increment vector.

In our experiments for the determination of the subsequent yield surfaces the loading point had to proceed from one position to the next by crossing the yield surface and thus plastic strains were generated. We were therefore able to obtain the directions of the plastic strain increment vectors as well as the magnitudes of these plastic strain increment vectors for a variety of prestressings.

Fig. 63 shows the  $e^{pl} - \gamma^{pl}$  line during the first prestressing in the experiment S - 10 described in Fig. 34. A superposition of the  $e^{pl} - \gamma^{pl}$  diagram on the  $\sigma - \tau$  diagram will show that the  $e^{pl} - \gamma^{pl}$  curve is normal to the initial yield curve at the point where the stress path enters the plastic region. We also observe that the first subsequent yield surface is normal to the direction of the  $e^{pl} - \gamma^{pl}$  curve near the prestressing point A.

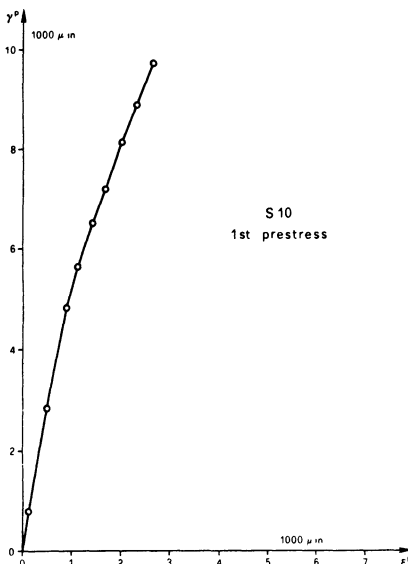


Fig. 63

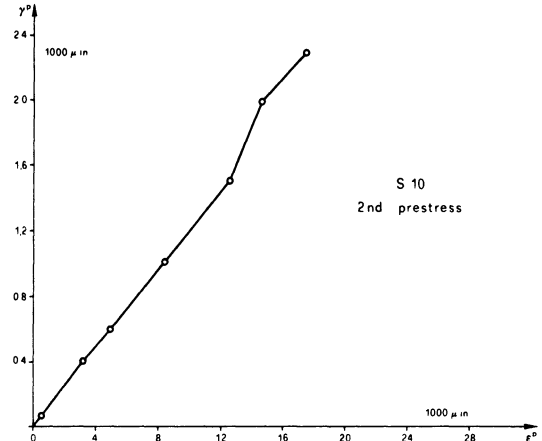


Fig. 64

Fig. 64 shows the  $\epsilon_p^{\text{pl}} - \gamma_p^{\text{pl}}$  line during the second prestressing in experiment S - 10, Fig. 34. Again a superposition of the  $\epsilon_p^{\text{pl}} - \gamma_p^{\text{pl}}$  diagram on the  $\sigma - \tau$  diagram shows that the  $\epsilon_p^{\text{pl}} - \gamma_p^{\text{pl}}$  curve is normal to the first and second subsequent yield surface at the beginning and at the end of the prestressing respectively.

In these results it is important to observe that the directions of the plastic strain increment vectors coincide also with the normals to the appropriate Mises surfaces passing through the loading points as prestressings proceed. Hence the plastic strain increment vectors are normal to the appropriate loading surfaces. In effect the loading surfaces and the yield surfaces are parallel to one another at the prestressing points.

Figure 65 shows the  $\epsilon_p^{\text{pl}} - \gamma_p^{\text{pl}}$  line during the second prestressing in experiment S - 9, Fig. 42. We again observe that the directions of the plastic strain increment vectors are normal to both the yield surface and the loading surface since both surfaces are parallel at the appropriate points.

Fig. 55, discussed previously, shows the directions of the plastic strain increment vectors as the stress path intersects the appropriate yield surfaces. It is seen that when the stress path is establishing a new loading surface as for example when crossing the first subsequent yield surface towards the second subsequent yield surface the plastic strain rate vector is normal to both the yield surface and the

loading surface. When, however, the stress path is within the loading surface but it is crossing a yield surface then the direction of the plastic strain rate vector is normal only to the appropriate yield surface without regard to the loading surface.

Figure 53 shows the directions of the plastic strain increment vectors at the prestressing points C, D, E, F, and G. We observe that at C, E, and G these directions are normal to the loading surfaces and to the subsequent yield surfaces when they are parallel to the loading surfaces at these points. On the other hand at the points D, and F where the prestressing points are inside the loading surfaces the directions of  $\delta_{ij}^{pl}$  are normal to the yield surfaces only, without regard to the loading surfaces.

In a number of experiments after the stress point has reached the prestressing level we waited for a considerable time until the yield surface has reached the prestressing point. Thus, we obtained both the plastic strain when the prestressing point was reached and the creep strain while waiting at the prestressing point. Some interesting results can be reported.

Figure 56 shows the directions of the plastic strain increment vectors at the prestressing points B and C as well as intermediate directions while the stress path moves from B to C. We observe that the direction of the plastic strain increment vector at B is normal to both the loading surface through B and to the yield surface since both the loading surface tangent to each other at B. On the other hand the point C is inside the region established by the loading surface through B. Therefore, the direction of the plastic strain vector increment at C is normal to the yield surface through C and not to the loading surface.

In addition the sequence of directions of plastic strain increment vectors between B and C shows clearly how the direction changes gradually and therefore how the yield surface in the neighborhood of the stress path is changing as the stress changes. In addition, as the path proceeds from B to C the direction changes in such a manner that if it would have continued beyond C it would have become normal to the loading surface.

Figure 66 shows the  $e^{px} - \gamma^{pl}$  diagram for the second and third prestressings for the experiment Fig. 56. The portion labeled plastic strain represents

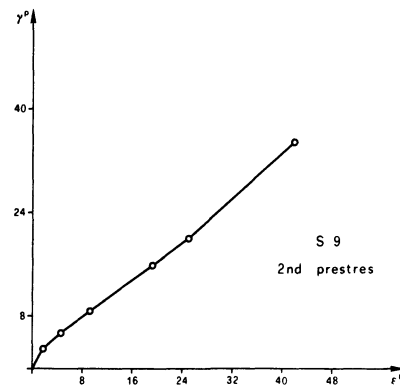


Fig. 65

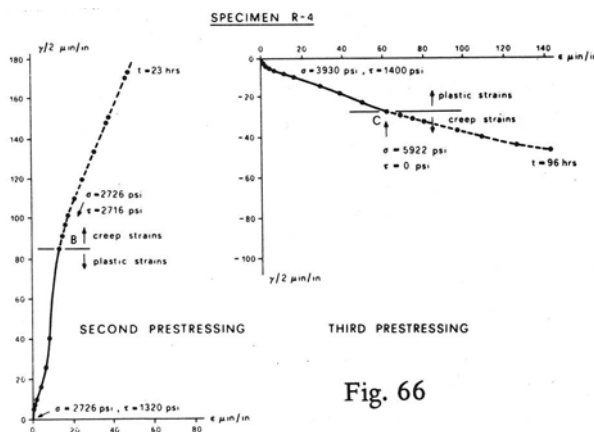


Fig. 66

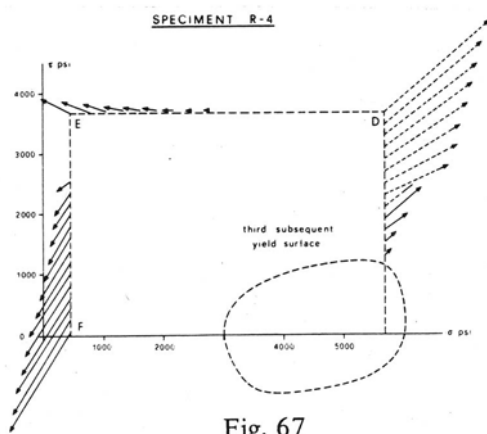


Fig. 67

Fig. 67 shows a continuation of the prestressing in the experiment described by Fig. 56. The specimen, after the third subsequent yield surface was obtained, was prestressed to the point D, E, and F, successively. While prestressing occurs, the plastic strain increment vectors were obtained and they are shown in Fig. 67. We observe that while prestressing proceeds to D new loading surfaces are produced and the directions of the plastic strain increment vectors are normal to the loading surfaces. While prestressing from D to E and then to F the stress point moves within the area established by the loading surface at D and therefore the plastic strain rate vector is normal to the moving yield surface.

As a conclusion from the experiments described above we can state that the plastic strain increment vector is normal to the yield surface when the stress point is within the area established by the loading surface previously. The plastic

the strains developed until the prestressing points B or C were reached. The portion labeled creep strains represents the strains developed during the period of time the stress point remained at the prestressing points before it would retreat into the elastic region. This period of time was 23 hours for B and 96 hours for C. We observe that there is some change in the direction of the strain increment vector when a transition occurs from the plastic region to the creep region.

strain increment vector is normal to the loading surface when the stress point is moving in a manner which establishes a new loading surface ; in this case the loading surface and the yield surface are parallel to each other in the region where the stress point is located.

## 8. Corners and Normality. Plastic Stability

After the discussion of the loading surfaces and the plastic strain increment vector we shall now consider two major questions in plasticity : the existence of corners in the loading surface and the normality between the plastic strain increment vector and the yield or loading surface.

We have seen from our experiments that the plastic strain increment vector is indeed normal to the yield and loading surface. Thus, the question of normality is no longer a question to be solved by additional experiments, but a problem to be discussed within a theoretical framework.

Since the yield surface is given by a function

$$f(s_k \lambda, T) = \kappa \quad (16)$$

and the loading surface by a function

$$F(s_k \lambda, T) = K \quad (17)$$

we should express the fact of normality by writing

$$d\epsilon_{ij}^p \lambda = d\lambda \cdot \frac{\partial f}{\partial s_{ij}} \quad (18)$$

or

$$d\epsilon_{ij}^p \lambda = d\lambda \cdot \frac{\partial F}{\partial s_{ij}} \quad (19)$$

Here  $d\lambda$  must be positive in order for  $d\epsilon_{ij}^p \lambda$  to be directed towards the exterior of the yield and loading surfaces.

Equations (18) and (19) are experimental facts which should be at the beginning of the theory. In our discussion we shall first assume that  $f$  and  $F$  are smooth functions in the neighborhood of the loading or stress point, so that there is only a unique normal to the yield or loading surface.

We already discussed the assumption that in the principal stress space the yield surface can be represented by a cylinder with the axis parallel to the line

making equal angles with the three principal axes. It follows therefore, that in the principal stress space the yield surface is not a closed surface but an infinite one in one direction. In the six-dimensional stress space we have the same conclusion, since then the yield surface will be a hypercylinder the generators of which are parallel to the line making equal angles with the three normal stress axes  $\sigma_x$ ,  $\sigma_y$ ,  $\sigma_z$ . It follows again that the yield surface is not a closed surface in the direction making equal angles with the three normal stress axes.

A large number of experiments have shown without exception that for the three-dimensional stress space yield surfaces are convex closed surfaces. We can assume the same to be the case for the six-dimensional stress space with the single exception presented by the hydrostatic pressure or hydrostatic tension, as far as the yield surface being a closed one. The convexity of the yield surface should not be affected by the fact that the yield surface is not a closed surface in the direction of hydrostatic stress. Although based on the results of fewer experiments the same conclusions can be drawn for the loading surface.

Convexity is therefore a physical property of the yield – and loading surfaces which has been experimentally verified. It can be expressed by means of the two inequalities

$$(20) \quad (s_{k\ell} - s_{k\ell}^*) \frac{\partial f}{\partial s_{k\ell}} \geq 0$$

$$(21) \quad (s_{k\ell} - s_{k\ell}^*) \frac{\partial F}{\partial s_{k\ell}} \geq 0$$

where  $s_{k\ell}^*$  is any point within or on the yield – or loading surface, respectively. Since we already obtained from the normality axiom that

$$(22) \quad d\epsilon_{k\ell}^{p\ell} = d\lambda \cdot \frac{\partial f}{\partial s_{k\ell}}$$

and

$$(23) \quad d\epsilon_{k\ell}^{p\ell} = d\lambda \cdot \frac{\partial F}{\partial s_{k\ell}}$$

where  $d\lambda > 0$ , we can write

$$(24) \quad (s_{k\ell} - s_{k\ell}^*) d\epsilon_{k\ell}^{p\ell} \geq 0.$$

Equation (22) is the postulate of maximum plastic work which, as we have seen, follows from the two postulates of convexity and normality. At this stage we shall now consider the concepts of loading, neutral loading, and unloading.

When the stress point is on the yield surface the stress increment  $ds_{k\ell}$  may be directed towards the outside of the yield surface or tangentially to the yield surface. In the first case plastic strain will be produced, in the second case no plastic strain will be produced, and in the third case, because of continuity requirements, no plastic strain will be produced. The analytical expression of the three cases is the following

$$\text{When } ds_{ij} \frac{\partial f}{\partial s_{ij}} > 0 \quad \text{we have } de_{ij}^{pl} \neq 0 \quad (25)$$

$$\text{When } ds_{ij} \frac{\partial f}{\partial s_{ij}} \leq 0 \quad \text{we have } de_{ij}^{pl} = 0. \quad (26)$$

The first case is called loading, the second is the unloading case, and the third is the case of neutral loading.

For loading we have

$$ds_{ij} \cdot de_{ij}^{pl} > 0 \quad (27)$$

since  $de_{ij}^{pl}$  is always normal to the yield surface. Inequality (27) expresses the so-called Drucker's stability in the small. It follows from the normality and from experimental evidence.

We may now express  $de_{ij}^{pl}$  as a function of  $ds_{ij}$  and expand this function in a Taylor series in terms of the powers of  $ds_{ij}$ . Since  $ds_{ij}$  is very small, we can neglect all the higher power terms so that we can write

$$de_{ij}^{pl} = \alpha_{ijk\ell} ds_{k\ell} \quad (28)$$

Equation (28) express the linearity relation between  $de_{ij}^{pl}$  and  $ds_{k\ell}$ .

When the stress point is on the loading surface the yield surface is tangential to the loading surface at the stress point. Hence, it is impossible to have an infinitely small unloading which will produce plastic strains. Therefore, the previous considerations concerning loading, unloading, and neutral loading, as well as equations (25) to (28) continue to be valid.

Up to now we assumed that the yield and loading surface are smooth.

Sharply pointed vertices, however, may exist. One example is given by the Tresca surface in the octahedral plane or in the  $\sigma_x$ ,  $\sigma_y$  plane. It is therefore important to discuss the question of vertices or corners.

The first question to be raised is whether the corners apparent in the Tresca surface are indeed existing. No experimental verification of a corner has ever been obtained, although a region of a very large curvature, i.e. sharply rounded vertices have been observed in our experiments, where the Tresca corner is supposed to appear, Fig. 25. In addition it should be remarked that sharply rounded vertices appear in most subsequent yield surfaces in directions conjugate to the direction of prestressing and they are the sharper the higher the temperature and the greater the prestressing away from the origin.

The above remarks refer to the yield surfaces. Another important question has to do with the existence of a pointex vertex in the loading surface at the loading point. An attempt to observe corners at the loading point has been made in [25] by sharply changing the direction of the stress increment  $ds_{ij}$  when proceeding from one stress increment to the next one. The essential observation is whether or not the direction of  $de_{ij}^{pl}$  will change significantly when the direction of  $ds_{ij}$  changes significantly. If such a change occurs then we have circumstantial evidence of the existence of a corner in the loading surface at the loading point. Such an evidence is, however, not conclusive since the theory of this experimental procedure is based on certain assumptions which must be shown correct in the first instance. The results of the experiments in [25] show that there is some probability in corners in the loading surface at the loading point, but no other conclusion can be drawn concerning the magnitude of the opening of the corner except that if the corner is real then it must be rather blunt. Another question which should be asked is whether the corner, if it exists, does not disappear when we wait at the loading point for all the strains to develop.

Experimentally it is impossible to observe actual corners or sharply pointed vertices, as this author stated in [26]. We can only observe regions with very large curvatures i.e. sharply rounded vertices. Only if it were possible to apply experimentally infinitely small stress increments would we be able to conclude whether the loading point lies at a pointed vertex or whether it lies at a sharply rounded vertex. Indeed, in the case of a pointed vertex, the plastic strain increments corresponding to two properly directed stress increments have different directions; in the case of a sharply rounded vertex the plastic strain increments have the same direction irrespective of the directions of the stress increments. We can, however,

apply only finite stress increments and because of the path dependence of the plastic strain, sharply rounded vertices will give the same results as pointed vertices.

The problem of plastic stability of plates and shells is connected with the question of the existence of corners in the loading surface. Sewell [27] discussed theoretically the connection between corners and plastic stability. In a recent experimental investigation Dr. Dietrich and I [28] discussed the same problem from the experimentalist point of view.

The basic question is that in comparing experimental results with the theory of plasticity investigators found that the fundamentally incorrect total deformation theory of plasticity agrees with the experimental results quite well, while the simplest incremental theory of plasticity disagrees with the experimental results. Sewell [27] investigated whether the existence of a corner at the loading point can be the reason for the discrepancy. It seems, however, that the discrepancy cannot be eliminated by the assumption of a corner at the loading point. In another paper [27] this author speculated that the radical change in the yield surface due to prestressing may be the reason for the discrepancy. At this time the problem is still unanswered but this author believes that theoretical results based on the simplest incremental theory of plasticity, cannot possibly agree with the experimental results because the simplest theory is not correct in the first place. Only after the correct incremental theory of plasticity will be introduced in the theoretical calculations will it be possible to reconcile theory and experiment. The axiomatic procedure will be of genuine advantage in this problem.

## 9. Analytical Expressions of the Motion of the Yield – and Loading Surfaces.

### 9.1. Hardening Rules .

The change in the yield surface or in the loading surface, which is due to prestressing, has been described analytically in the literature by a number of expressions. The simplest expression is the one due to proportional expansion and it is called isotropic hardening. According to this expression the surface depends on a scalar parameter which increases monotonically with plastic deformation. Hence we have

$$f(s_{ij}, \kappa) = 0 \quad (29)$$

for the yield surface, and

$$F(s_{ij}, K) = 0 \quad (30)$$

for the loading surface. In this section we consider the isothermal case only, so that the effect of the temperature  $T$  is not considered.

For this scalar parameters  $\kappa$  or  $K$  the following two expressions have been proposed.

$$(31) \quad \kappa = \int s_{ij} d\epsilon_{ij}^{pl}$$

and

$$(32) \quad \kappa = \left( \frac{2}{3} \int d\epsilon_{ij}^{pl} d\epsilon_{ij}^{pl} \right)^{1/2}$$

It is obvious that the expression (31) represents the plastic work done in the deformation process while the expression (32) represents the integral of the square root of the second invariant of the plastic strain increments. As the plastic strain increases the yield – and loading surfaces expand according to (29), (30), (31), and (32) uniformly; thus the name isotropic hardening.

From our experiments we know that only the loading surface expands according to the rule of isotropic hardening. Hence, equation (30) is correct for the loading surface. However, neither equation (31) nor equation (32) are appropriate since the loading surface expands according to the amount of maximum prestressing as measured by the greatest distance of the prestressing point from the origin during the entire stressing path (loading, unloading, and neutral loading). This distance can be expressed by

$$\max \left[ (s_{ij}^o, s_{ij}^o)^{1/2} \right]$$

where  $s_{ij}^o$  is the loading point. The loading surface will pass by the prestressing point. It follows that we can write

$$(33) \quad K = \max \left[ (s_{ij}^o, s_{ij}^o)^{1/2} \right]$$

We also know from our experiments that the loading surface is an isotropic expansion of the initial yield surface. Hence, the loading surface could also be expressed by

$$(34) \quad f(s_{ij}, \kappa) = 0$$

with

$$\kappa = \max \left[ \left( s_{ij}^o - \alpha_{ij}^o \right)^{\frac{1}{2}} \right] \quad (35)$$

We prefer to use equations (30) and (33) instead of (34) and (35) since equation (34) will also be used when the plastic strain is an independent variable.

We now consider the yield surface exclusively. The yield surface motion cannot be expressed by isotropic hardening. The next simple expression for the motion of the yield surface is the one in which the surface depends on two parameters, a scalar  $\kappa$ , and a second order tensorial one  $\alpha_{ij}$ . We write

$$f(s_{ij} - \alpha_{ij}, \kappa) = 0 \quad (36)$$

The first possibility is that  $\kappa$  remains a constant and  $f$  is a homogeneous function of even order of  $s_{ij} - \alpha_{ij}$ . Then equation (36) represents a rigid body translation in which the change in  $\alpha_{ij}$  represents the motion of the center of the yield surface. This case is called kinematic hardening.

A number of writers starting with Melan [30] and including Ishlinskii [31], Prager [32], and Kadashevitch and Novozhilov [33] have proposed that in equation (36) the change in the yield surface is associated with a change in  $\alpha_{ij}$  by means of equation

$$d\alpha_{ij} = c d e_{ij}^{pl} \quad (37)$$

This means that the yield surface translates in the direction of the increment of plastic strain. As Shield and Ziegler [34] have shown the assumption (37) is not invariant when we pass from the six-dimensional stress space to a space with fewer dimensions, for example, to the three-dimensional space  $\sigma_x, \sigma_z, \tau$  so often used by experimentalists. The coefficient  $c$  in (37) is assumed to be a function of the stress or strain state since the amount of translation may vary with the position in the stress or strain path independently of the value of  $d e_{ij}^{pl}$ .

The proposal of Ziegler [35] :

$$d\alpha_{ij} = c(s_{ij} - \alpha_{ij}) / d e_{ij}^{pl} / \quad (38)$$

is free from the drawback above concerning the change of space. Equation (38) means that the yield surface translates in the direction of  $s_{ij} - \alpha_{ij}$ , that is in the direction of the radius vector that joins  $\alpha_{ij}$  with the stress point  $s_{ij}$ . The coefficient  $c$  in (38) is again assumed to be a function of the stress or strain state.

When  $\kappa$  is variable, the yield surface change represented by (36) includes not only a rigid body motion but a uniform expansion as well. In this case we may take

$$(39) \quad \kappa = \int (s_{ij} - \alpha_{ij}) de_{ij}^{pl}$$

or

$$(40) \quad \kappa = \int \left( \frac{2}{3} de_{ij}^{pl} de_{ij}^{pl} \right)^{\frac{1}{2}}$$

Equation (39) differs from equation (31) since the surface may now not include the origin.

Baltov and Sawczuk [36] introduced the hardening rule

$$(41) \quad \begin{aligned} f(s_{ij}, \alpha_{ij}, \kappa) &= \frac{1}{2} (s_{ij} - c e_{ij}^{pl})(s_{ij} - c e_{ij}^{pl}) + \\ &+ A_1 c^2 e_{ij}^{pl} e_{kl}^{pl} (s_{ij} - c e_{ij}^{pl})(s_{kl} - c e_{kl}^{pl}) - 2\phi(\kappa) = 0. \end{aligned}$$

In this equation  $A_1$ , and  $c$  are constants. This hardening rule which is one of many proposed by several authors, introduces rigid body translation, rotation, and expansion of the yield surface. We shall use equation (41) later in this article.

## 9.2. A New Hardening Rule .

We shall now consider the results of our own experiments. We shall follow the discussion in [ 37 ]. Figure 68 illustrates the rule of motion of the yield surface introduced by us. In Fig. 68 the amount of the rigid body translation is determined by the motion of the line  $A^{(1)}C^{(1)}$  to the new position  $A^{(2)}C^{(2)}$ . In the six-dimensional space this motion generates a five-dimensional hypercylinder with its axis in the direction of prestressing  $\Delta s_{ij}$ . This hypercylinder is tangential to both the original and to the new yield surface at the four-dimensional hypersurfaces ABCD and A'B'C'D', respectively.

The locus of the tangent subspace of the five-dimensional first yield surface and the five-dimensional hypercylinder is given by solving the two simultaneous equations

$$(42) \quad f^{(1)}(s_{ij}) = 0$$

$$(43) \quad (\partial f^{(1)}(s_{ij}) / \partial s_{ij}) \Delta s_{ij} = 0.$$

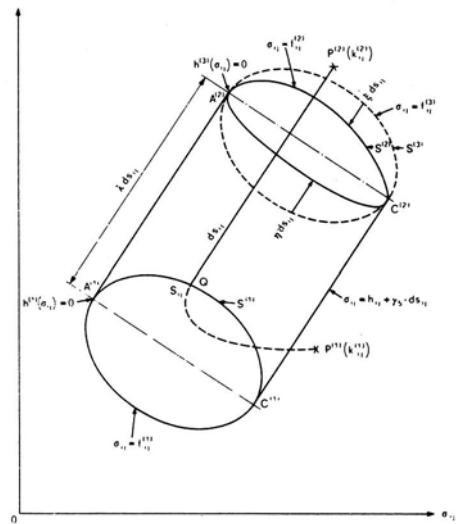


**Fig. 68**

functions  $\xi(s_{ij})$  and  $\eta(s_{ij})$ . The first one is valid for those stress points for which inequality (47) is valid; the second one for the points for which inequality (48) is valid. Referring to Fig. 68 we can then write that the final yield surface, after the rigid body translation  $\lambda \cdot \Delta s_{ij}$  and the non-uniform deformation represented by  $\xi$  and  $\eta$ , is given by

$$(49) \quad f^{(2)}(s_{ij}) = f^{(1)}(s_{ij} - (\lambda + \xi)\Delta s_{ij})$$

$$(50) \quad f^{(2)}(s_{ij}) = f^{(1)}(s_{ij} - (\lambda + \eta)\Delta s_{ij})$$

for points satisfying equations (47) and (48) respectively. Equations (49) and (50) give the expression of our rule of hardening. This rule must be supplemented by appropriate expressions for  $\lambda$ ,  $\xi$ , and  $\eta$ . Additional experimentation is necessary to discover the laws governing these expressions.

At present we can say that  $\lambda$  is generally close to one, and that depending on whether the vector  $\Delta s_{ij}$  is pointing away from or towards the origin of the stress space we have

$$(51) \quad 1 > \eta > -\xi > 0$$

or

$$(52) \quad 1 > \xi > -\eta > 0.$$

Indeed, from Fig. 68 we see that the yield surface tends to shrink in the direction of incremental loading when this loading points away from the origin.

Up to now all experiments were performed with the vector  $\Delta s_{ij}$  originating from a point Q of the yield surface, Fig. 68, which was located at some distance from the limiting subspace  $h^{(1)}(s_{ij})$ . The important role which this subspace plays in the formulation of our hardening law leads one to ask whether for points of the yield surface very near to  $h^{(1)}(s_{ij})$  our hardening law still holds without modifications. Experimentation is now under way to explore this question.

### 9.3. Application.

We shall now apply the rule presented above to our experiments. We select the set of experimental results shown in Fig. 69 by broken lines [18]. The purpose of applying this rule to our experiments is not to prove the validity of the rule which after all is modeled on our experimental results. Our purpose is to give an example of application of our formulas so that the reader will be facilitated to use these formulas for expressing additional experimental results. Consequently a liberal amount of curve fitting will be used. In Fig. 69 the solid lines represent the results from our rule. It is seen that for the initial yield surface the solid line coincides with

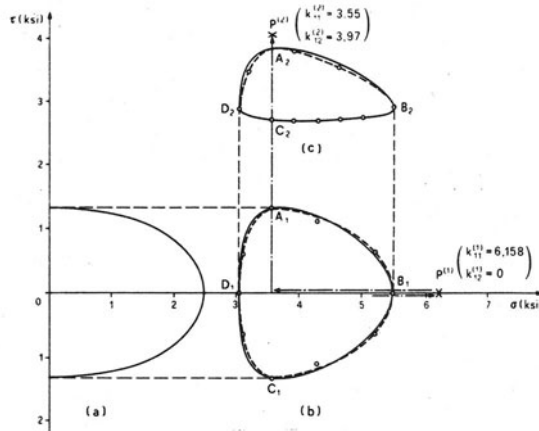


Fig. 69

the broken line and that for the first and second subsequent yield surfaces the solid lines are very close to the appropriate experimentally determined broken lines. This result is due, of course, to the selection of the values of  $\lambda$ ,  $\xi$ , and  $\eta$ .

The initial yield surface, Fig. 69(a) according to the data in [18] could be represented by an ellipse in  $\sigma - \tau$  space as

$$f^{(1)}(\sigma_{ij}) = \frac{\sigma^2}{2.50^2} + \frac{\tau^2}{1.33^2} - 1 = 0 \quad (53)$$

To obtain the first subsequent yield surface prestressing proceeds to  $K_{11}^{(1)} = 6.158$  ksi. The unloading occurs to the elastic state at  $\sigma = 3.55$  ksi,  $\tau = 0$ . To obtain the second subsequent yield surface reloading occurs in torsion to  $K_{11}^{(2)} = 3.55$  ksi and  $K_{12}^{(2)} = 3.97$  ksi. Our task is to find the corresponding subsequent yield surfaces according to our law and compare then with experimental results.

To obtain the first subsequent yield surface associated with the prestress in pure tension we note that

$$\Delta s_{11} = 3.658, \quad \Delta s_{12} = \Delta s_{13} = \dots = 0 \quad (54a,b)$$

It is easily seen that, in this special case, the stress hypercylinder is reduced to the two lines:  $\tau = \pm 1.33$  ksi.

The proper value of  $\lambda$  is assumed here to be 0.945. The intermediate yield surface, which is obtained by a rigid body translation along the direction of prestress, could then be represented by

$$f^{(3)}(\sigma_{ij}) = (\sigma - (0.945)(3.658))^2 / (2.50)^2 + (\tau^2 / (1.33)^2) - 1 = 0. \quad (55)$$

The functions of  $\xi$  and  $\eta$ , which describe the change from the intermediate yield surface to the final one, change along the yield surface, and take the forms:

$$(56a,b) \quad \xi = -0.18 + 0.0585 \tau^4, \quad \eta = 0.564 - 0.183 \tau^4.$$

Consequently the first subsequent yield surface can be written in the following form for  $A_1 B_1 C_1$ , and  $A_1 D_1 C_1$ , respectively:

$$(57) \quad f^2(\sigma_{ij}) = [\sigma - (0.765 + 0.058\tau^4) \cdot 3,658]^2 / 2,50^2 + [\tau^2 / 1.33^2] - 1 = 0$$

$$f^2(\sigma_{ij}) = [\sigma - (0.381 - 0.183\tau^4) \cdot 3,658]^2 / 2,50^2 + [\tau^2 / 1.33^2] - 1 = 0.$$

This yield surface is shown by the solid line in Fig. (69b). It is very close to the experimentally determined one.

The second subsequent yield surface associated with the prestress  $K_{11}^{(2)} = 3.55$  ksi and  $K_{12}^{(2)} = 3.97$  ksi can be obtained by following the same procedure.  $\lambda$  is equal to 1.1. Since  $A_1 B_1$  and  $A_1 D_1$  are not represented by a single equation, it is necessary that the corresponding  $\xi$  assume different functions for these two portions. This is also true for  $\eta$  as  $B_1 C_1$  and  $C_1 D_1$  are considered.

Under the present prestressing we find that for  $A_1 B_1$  and  $A_1 D_1$ , respectively, we have

$$(58) \quad \xi = -0.15 + 0.0104 (\sigma - 3.55)^4, \quad \xi = -0.15 + 2.4 (\sigma - 3.55)^4$$

and for  $B_1 C_1$  and  $C_1 D_1$ , respectively, we have

$$(59) \quad \eta = 0.44 - 0.0311 (\sigma - 3.55)^4, \quad \eta = 0.44 - 7.1 (\sigma - 3.55)^4.$$

The second subsequent yield surface, by noting that  $ds_{12} = 2.64$  ksi and  $ds_{11} = ds_{22} = ds_{13} = \dots = 0$ , is given by analogous expressions and it is shown in Fig. (69c) by the solid curve  $A_2 B_2 C_2 D_2 A_2$ , which is obviously very close to the experimentally determined one.

#### 9.4. Comparison of Rules.

In this section three previously proposed hardening rules will be compared with our rule. All three previous rules have the common features that 1) the yield surface throughout its motion has a center, and 2) the prestressing point always lies on the yield surface. Both these features are not necessary for our rule. In both the kinematic hardening rule and its modification the yield surface moves in

translation without deformation. For kinematic hardening the direction of translation follows the normal to the yield surface at the stress point where incremental loading takes place. For Ziegler's modification the direction of translation is given by connecting the center of the yield surface,  $\alpha_{ij}$ , to the current stress state. For finite loading, the direction of translation for both laws is determined by a process of integration along the loading path.

A comparison to our rule shows that 1) deformation of the yield surface inherent to our case is neglected by both previously mentioned rules; 2) in the kinematic hardening rule the direction of translation is given by the normal to the yield surface ( $de_{ij}^P$ ) while in our case it is given by the prestress direction ( $ds_{ij}$ ); and 3) in Ziegler's modification, the direction of translation is given by connecting the center of the yield surface,  $\alpha_{ij}$ , to the current state of stress  $s_{ij}$ . This direction in Ziegler's modification is different from the prestress direction ( $ds_{ij}$ ). However, in the special case that the extension of the incremental loading  $ds_{ij}$  passes through the center  $\alpha_{ij}$  these two directions coincide. Note, however, that due to the deformation process inherent in our law, the subsequent yield surfaces corresponding to Ziegler's modification and to our rule are by no means coincident.

Baltov and Sawczuk's [36] anisotropic hardening rule is essentially a combination of kinematic hardening, a certain amount of rigid body rotation, and a symmetric deformation of the yield surface with respect to the center of the yield surface. The rigid body translation of the yield surface is in the direction of the normal to the yield surface at the loading point.

The independency of deformation of the yield surface from the loading path in Baltov and Sawczuk's rule deviates radically from our hardening rule. On the other hand Baltov and Sawczuk's rule consists also of two processes of operation, a rigid body motion and a deformation. However, the contents of these two processes are quite different from the two comparative processes in our rule. In our case the translation is not in the direction of the normal to the yield surface and the deformation is not symmetric.

In addition, the rule of Baltov and Sawczuk presupposes a yield surface which is an ellipsoidal one at any stage of the loading and which at the origin of the stress space is the Mises yield surface. In our case, the yield surface, at any stage of loading, is arbitrary. Finally, Baltov and Sawczuk's rule does not provide for a general validity of the phenomenon of lack of cross effect.

To provide illustrative examples of comparison of our rule with the other three previously proposed laws, we give in Figures 70 and 71 the first and second

subsequent yield surfaces in each of the four cases. The initial yield surface is assumed to be a Mises Surface. The differences between the predictions of the different laws is clear.

9.5. We shall consider now briefly the relationship between the loading surface and the yield surface. At the outset it should be understood that the loading surface cannot grow beyond a maximum limit given by the maximum stress in a tension test. This maximum limit may be a function of the path of loading. It can be called the limiting loading surface.

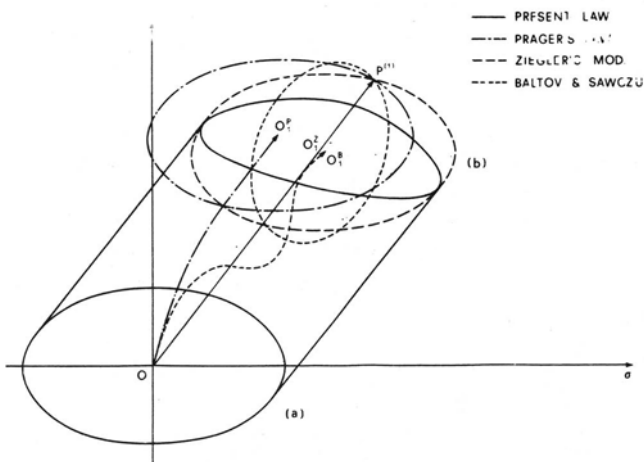


Fig. 70

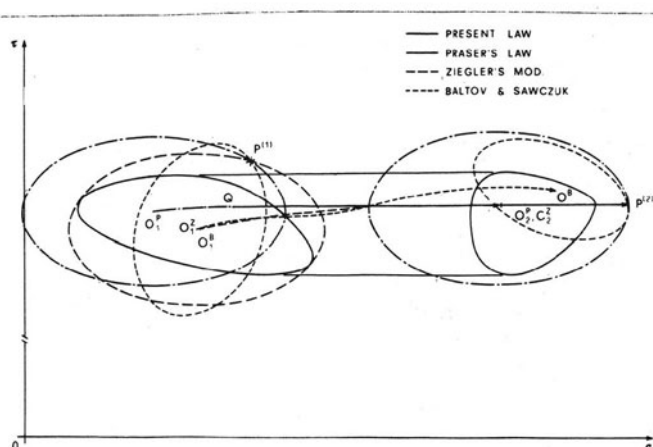


Fig. 71

Suppose we have a stress path consisting of any combination of loading, unloading, and neutral loading. Then the loading surface will continuously or intermittently expand but it will never shrink and it will never move beyond the limiting loading surface. The yield surface will always be inside the instantaneous loading surface, it may at time be tangential to it or it may move away from it. As the yield surface moves it will simultaneously change its size and shape, always following our hardening rule and becoming smaller in size in the direction of

prestressing, when the prestressing is away from the origin, and becoming larger in size in the prestressing direction, when prestressing is towards the origin.

An analytical expression of the interaction between yield surface and loading surface is now in preparation in combination with currently performed additional very much needed experimentation. This interaction seems to be the key to the explanation of phenomena of repeated loading and low cycle fatigue.

## 10. The Theory of Plasticity

At this stage, after having discussed experimental evidence concerning the initial and subsequent yield surfaces, the loading surface, and the strain rate vector, as well as some analytical expressions concerning the motion of the yield – and loading surfaces we shall consider the basic stress-strain relations of plasticity. It is obvious that it is not possible to present a complete theory since much additional experimental evidence is necessary. It will be necessary to make assumptions which will need to be verified by experiments and the theory may have to be modified in the future if the assumptions made will be shown to be incorrect. With this fact in mind we shall proceed to develop the theory with the minimum number of assumptions.

We shall assume that the strain rate  $\dot{\epsilon}_{ij}^{pl}$  is a linear function of  $\dot{s}_{ij}$  and  $\dot{T}$ :

$$\dot{\epsilon}_{ij}^{pl} = \alpha_{ijmn} \dot{s}_{mn} + \alpha_{ij} \dot{T} \quad (60)$$

where  $\alpha_{ijmn}$  and  $\alpha_{mn}$  and tensor functions of several variables, probably of  $s_{mn}$ ,  $e_{mn}^{pl}$ , and  $T$ . Equation (60) is a generalization of the formula

$$\dot{\epsilon}_{ij}^{pl} = \alpha_{ijmn} \dot{s}_{mn} \quad (61)$$

we derived in section 8.

During neutral loading, that is whenever

$$\frac{\partial f}{\partial s_{mn}} \dot{s}_{mn} + \frac{\partial f}{\partial T} \dot{T} = 0 \quad (62)$$

we must have

$$\alpha_{ijmn} \dot{s}_{mn} + \alpha_{ij} \dot{T} = 0. \quad (63)$$

Therefore

$$(64) \quad \left( \alpha_{ijmn} - \lambda \beta_{ij} \frac{\partial f}{\partial s_{mn}} \right) \dot{s}_{mn} + \left( \alpha_{ij} - \lambda \beta_{ij} \frac{\partial f}{\partial T} \right) \dot{T} = 0.$$

In (64)  $\beta_{ij}$  is a symmetric tensor function and  $\lambda$  is a scalar function of  $s_{mn}$ ,  $e_{mn}^{pl}$ , and  $T$ , conceivably. Let us choose now each value of  $\lambda \beta_{ij}$  so that the coefficient of  $\dot{T}$  vanishes. The remaining equations are valid for arbitrary values of  $\dot{s}_{mn}$  and because the function in the parentheses are independent of  $\dot{s}_{mn}$  and  $\dot{T}$  we conclude that

$$(65) \quad \alpha_{ij} = \lambda \beta_{ij} \frac{\partial f}{\partial T}$$

and

$$(66) \quad \alpha_{ijmn} = \lambda \beta_{ij} \frac{\partial f}{\partial s_{mn}}.$$

Equation (61) becomes now

$$(67) \quad \dot{e}_{ij}^{pl} = \lambda \beta_{ij} \left( \frac{\partial f}{\partial s_{mn}} \dot{s}_{mn} + \frac{\partial f}{\partial T} \dot{T} \right)$$

Equation (67) holds during loading and during neutral loading. For any values of  $\dot{s}_{mn}$  and  $\dot{T}$  the direction of the vector  $\dot{e}_{ij}^{pl}$  is given by the direction of  $\lambda \beta_{ij}$  which is independent of  $\dot{s}_{mn}$  and  $\dot{T}$ .

In the previous equations we use the function  $f$  in which case we consider the yield surface within the loading surface. We could equally well use the function  $F$  thus considering the loading surface. In both cases we know from experiments that  $\dot{e}_{ij}^{pl}$  is normal to the yield – or loading surface. Consequently we can write

$$(68) \quad \beta_{ij} = \frac{\partial f}{\partial s_{ij}}$$

or

$$(69) \quad \beta_{ij} = \frac{\partial F}{\partial s_{ij}}$$

Consequently we finally have

$$\dot{e}_{ij}^{pl} = \lambda \frac{\partial F}{\partial s_{ij}} \left( \frac{\partial F}{\partial s_{mn}} \dot{s}_{mn} + \frac{\partial F}{\partial T} \dot{T} \right) \quad (70)$$

or

$$\dot{e}_{ij}^{pl} = \lambda \frac{\partial f}{\partial s_{ij}} \left( \frac{\partial f}{\partial s_{mn}} \dot{s}_{mn} + \frac{\partial f}{\partial T} \dot{T} \right) \quad (71)$$

To complete the theory it is necessary to introduce a relation for the growth of the variables  $\kappa$  etc. within  $f$  or  $F$  and a consistency relation. Since not much is known experimentally concerning these expressions we shall stop our considerations at this stage.

An interesting attempt towards a theory is given in [38]. Extensions to the case when there is no yield surface are given in [39] and [40]. A problem of nonlinear hardening is discussed in [41].

## 11. Thermodynamic Considerations

The first law of thermodynamics gives the energy equation

$$\dot{U} = \frac{1}{\rho} s_{kl} \dot{e}_{kl} - \frac{1}{\rho} Q_{k,k} + r \quad (72)$$

where  $s_{kl}$  is the stress,  $e_{kl}$  is the strain,  $r$  is the heat supply function per unit mass,  $Q_k$  is the heat flux per unit area per unit time, and  $U$  is the internal energy per unit mass. We introduce the free energy  $A$

$$A = U - T S \quad (73)$$

and equation (72) becomes

$$\rho r - \rho (\dot{A} + \dot{T} S + T \dot{S}) - Q_{k,k} + s_{kl} \dot{e}_{kl} = 0. \quad (74)$$

The second law of thermodynamics has the form

$$\rho TS - \rho r + Q_{k,k} - \frac{Q_k T_{,k}}{T} \geq 0. \quad (75)$$

Substituting for  $\rho r$  from (74), into (75) we obtain

$$(76) \quad -\rho(\dot{A} + \dot{ST}) + s_{k\ell}\dot{e}_{k\ell} - \frac{Q_k T_{,k}}{T} \geq 0.$$

Assume now that

$$(77) \quad e_{k\ell} = e_{k\ell}^{el} + e_{k\ell}^{pl}$$

and that

$$(78) \quad A = A\left(e_{k\ell}^{el}, e_{k\ell}^{pl}, \kappa, T\right)$$

$$(79) \quad S = S\left(e_{k\ell}^{el}, e_{k\ell}^{pl}, \kappa, T\right)$$

$$(80) \quad Q_k = Q_k\left(T, T_{,m}, \kappa, e_{mn}^{el}, e_{mn}^{pl}\right)$$

hold throughout loading and unloading. In these equations  $\kappa$  is a scalar variable which appears in the expression for the yield – or loading surfaces. Then, equations (74) and (75) become

$$(81) \quad \begin{aligned} \rho r - \rho \left( S + \frac{\partial A}{\partial T} \right) \dot{T} + \left( s_{k\ell} - \rho \frac{\partial A}{\partial e_{k\ell}^{el}} \right) \dot{e}_{k\ell}^{el} + \left( s_{k\ell} - \rho \frac{\partial A}{\partial e_{k\ell}^{pl}} \right) \dot{e}_{k\ell}^{pl} \\ - \rho \dot{ST} - Q_{k,k} - \rho \frac{\partial A}{\partial \kappa} \dot{\kappa} = 0 \end{aligned}$$

and

$$(82) \quad \begin{aligned} -\rho \left( S + \frac{\partial A}{\partial T} \right) \dot{T} + \left( s_{k\ell} - \rho \frac{\partial A}{\partial e_{k\ell}^{el}} \right) \dot{e}_{k\ell}^{el} - \rho \frac{\partial A}{\partial \kappa} \dot{\kappa} \\ + \left( s_{k\ell} - \rho \frac{\partial A}{\partial e_{k\ell}^{pl}} \right) \dot{e}_{k\ell}^{pl} - \frac{Q_k T_{,k}}{T} \geq 0 \end{aligned}$$

which both hold during loading and unloading.

Considering unloading during which  $\dot{e}_{k\ell}^{pl} = 0$ ,  $\kappa = 0$  and  $f < 0$  we obtain from (82)

$$-\rho \left( S + \frac{\partial A}{\partial T} \right) \dot{T} + \left( s_{k\ell} - \rho \frac{\partial A}{\partial e_{k\ell}^e} \right) \dot{e}_{k\ell}^e - \frac{Q_k T_{,k}}{T} \geq 0 \quad (83)$$

for all arbitrary values of  $\dot{T}$ ,  $\dot{e}_{k\ell}^e$  and for given values of  $T$ ,  $e_{k\ell}^e$ , and  $e_{k\ell}^{pl}$ . For an arbitrary homogeneous temperature distribution  $T_{,k} = 0$  so that (83) becomes

$$-\rho \left( S + \frac{\partial A}{\partial T} \right) \dot{T} + \left( s_{k\ell} - \rho \frac{\partial A}{\partial e_{k\ell}^e} \right) \dot{e}_{k\ell}^e \geq 0 \quad (84)$$

for arbitrary  $T$  and  $\dot{e}_{k\ell}^e$ . The coefficients in (84) are independent of the rates. Hence

$$S = - \frac{\partial A}{\partial T} \quad (85)$$

$$s_{k\ell} = \rho \frac{\partial A}{\partial e_{k\ell}^e} . \quad (86)$$

Hence, equations (81) and (82) become now

$$\rho r + \left( s_{k\ell} - \rho \frac{\partial A}{\partial e_{k\ell}^{pl}} \right) \dot{e}_{k\ell}^{pl} - \rho \frac{\partial A}{\partial \kappa} \dot{\kappa} - \rho \dot{S} T - Q_{k,k} = 0 \quad (87)$$

and

$$\left( s_{k\ell} - \rho \frac{\partial A}{\partial e_{k\ell}^{pl}} \right) \dot{e}_{k\ell}^{pl} - \rho \frac{\partial A}{\partial \kappa} \dot{\kappa} - \frac{Q_k T_{,k}}{T} \geq 0 . \quad (88)$$

In equation (86) the left hand member can be determined from the elastic strain and the temperature. Hence  $s_{k\ell}$  is not a function of the plastic strain or of the history of plastic strain and  $\partial A / \partial e_{k\ell}^e$  must also be independent of  $\kappa$  and  $e_{k\ell}^{pl}$ . Hence we can write

$$A = A'(e_{k\ell}^e, T) + A''(e_{k\ell}^{pl}, \kappa, T) . \quad (89)$$

Then equation (85) gives

$$S = S'(e_{k\ell}^e, T) + S''(e_{k\ell}^{pl}, \kappa, T) . \quad (90)$$

where

$$(91) \quad S'(e_k^{\epsilon\ell}, T) = \frac{\partial A'(e_k^{\epsilon\ell}, T)}{\partial T}$$

$$(92) \quad S''(e_k^{\epsilon\ell}, \kappa, T) = - \frac{\partial A''(e_k^{\epsilon\ell}, \kappa, T)}{\partial T} .$$

During unloading, when  $de_k^{\epsilon\ell} = 0$ ,  $d\kappa = 0$ ,  $dS$  should be independent of the particular value of  $e_k^{\epsilon\ell}$  and  $\kappa$ . Hence

$$(93) \quad dS = \frac{\partial S'}{\partial e_k^{\epsilon\ell}} de_k^{\epsilon\ell} + \frac{\partial S'}{\partial T} dT + \frac{\partial S''}{\partial T} dT .$$

It follows that  $\partial S''/\partial T = c = \text{constant independent of } e_k^{\epsilon\ell}, \kappa$ , and

$$(94) \quad S'' = cT + c_1(e_k^{\epsilon\ell}, \kappa) .$$

Now, in

$$(95) \quad S = S'(e_k^{\epsilon\ell}, T) + cT + c_1(e_k^{\epsilon\ell}, \kappa)$$

we can incorporate  $cT$  into  $S'(e_k^{\epsilon\ell}, T)$  and thus write

$$(96) \quad S'' = c_1(e_k^{\epsilon\ell}, \kappa) = S''(e_k^{\epsilon\ell}, \kappa)$$

and from (92), we obtain

$$(97) \quad \frac{\partial A''}{\partial T} = - S''(e_k^{\epsilon\ell}, \kappa)$$

It follows

$$(98) \quad A''' = - TS''(e_k^{\epsilon\ell}, \kappa) + A'''(e_k^{\epsilon\ell}, \kappa)$$

from which we obtain

$$(99) \quad A = A'(e_k^{\epsilon\ell}, T) - TS''(e_k^{\epsilon\ell}, \kappa) + A'''(e_k^{\epsilon\ell}, \kappa) .$$

At this stage consider a homogeneous temperature distribution. From (88) we obtain

$$(100) \quad \left( s_k \ell - \rho \frac{\partial A}{\partial e^{\epsilon\ell}} \right) \dot{e}_k^{\epsilon\ell} - \rho \frac{\partial A}{\partial \kappa} \dot{\kappa} \geq 0 .$$

Suppose that  $\kappa$  is a function of the plastic strain rate, as is usually assumed. Then we can write that  $\kappa$  is a linear function of  $\dot{e}_{kl}^{pl}$  so that

$$\dot{\kappa} = h_{kl} \left( s_{mn}, e_{mn}^{pl}, T \right) \dot{e}_{kl}^{pl}. \quad (101)$$

Here  $h_{kl}$  is a tensorial function of several variables, the choice of which is not important except that they should not include  $\dot{e}_{kl}^{pl}$ . Then we obtain from (100)

$$\left( s_{kl} - \rho \frac{\partial A}{\partial e^{pl}} - \rho \frac{\partial A}{\partial \kappa} h_{kl} \right) \dot{e}_{kl}^{pl} \geq 0. \quad (102)$$

From equation (102) we observe that the quantity

$$\rho \left( \frac{\partial A}{\partial e^{pl}} + \frac{\partial A}{\partial \kappa} h_{kl} \right) = S_{kl}^o \quad (103)$$

has the dimensions of stress. We can then write equation (102) as

$$\left( s_{kl} - S_{kl}^o \right) \dot{e}_{kl}^{pl} \geq 0 \quad (104)$$

where  $s_{kl}$  is any arbitrary point of the yield surface and  $S_{kl}^o$  is the "thermodynamic reference stress". By using equation (99) we can write equation (107) in the form

$$S_{kl}^o = \rho \left( \frac{\partial A'''}{\partial e_{kl}^{pl}} + \frac{\partial A'''}{\partial \kappa} \cdot h_{kl} - T \left( \frac{\partial S''}{\partial e_{kl}^{pl}} + \frac{\partial S''}{\partial \kappa} h_{kl} \right) \right) \quad (105)$$

where all the terms

$$\rho \frac{\partial A'''}{\partial e_{kl}^{pl}}, \quad \rho \frac{\partial A'''}{\partial \kappa} h_{kl}, \quad \rho T \frac{\partial S''}{\partial e_{kl}^{pl}}, \quad \rho T h_{kl} \frac{\partial S''}{\partial \kappa}$$

represent stresses.

At any particular values of  $e_{kl}^{pl}$  and  $\kappa$  the yield surface is determined, and at an arbitrary but particular value of the temperature, inequality (103) together with the normality rule mean that  $S_{kl}^o$  corresponding to that particular temperature must lie within the corresponding isothermal yield curve. The higher the temperature becomes the smaller will be the area enclosed by the isothermal yield curve and the stress  $S_{kl}^o$  will tend to be restricted towards the center of the cluster of isothermals.

An interesting remark is that we must always have the inequality

$$(106) \quad F(s_{k\ell}^o, e_{k\ell}^{p\ell}, T, \kappa) < 0$$

which shows that we should be careful when selecting the functions  $F$ ,  $\kappa$ ,  $e_{k\ell}^{p\ell}$ ,  $A''$ ,  $A'''$ , and  $S''$  so that inequality (106) will not be violated for any possible path of loading.

An interesting case in which a violation of (106) occurs is given in [42].

## 12. Creep and Viscoplasticity

The concepts of limited and unlimited creep were introduced in section 3. We considered the equilibrium stress-strain curve OA and the non-equilibrium stress-strain curve OB obtained with a constant stress rate  $\dot{s}$ , Fig. 17. If at the value  $s_A$  we keep the stress constant, the creep strain will increase with time. Its rate  $\dot{e}^{cr}$  can be assumed to be a function of the distance in the stress direction between the lines MN and OA at the corresponding strain. The rate  $\dot{e}^{cr}$  will be a function of other variables also. The distinction between limited and unlimited creep follows from the two cases in which the line parallel to the strain axis at  $s = s_A$  intersects the equilibrium stress-strain line OA or not. Proper experimental information under a variety of conditions is necessary to show whether our assumption is correct or not and to find the other variables upon which  $\dot{e}^{cr}$  depends. Such experimental information is still lacking to a large extent.

Analytically our assumption can be expressed as

$$(107) \quad e^{cr} = \Phi(s^* - \phi(e^{p\ell} + e^{cr}), \dots)$$

where  $s^*$  is the actual stress and

$$(108) \quad s = \phi(e^{p\ell} + e^{cr})$$

is the equation of the equilibrium stress-strain line. For the case of limited creep we have ultimately  $\dot{e}^{cr} = 0$  since  $\phi(e^{p\ell} + e^{cr})$  becomes finally equal to  $s^*$ . In the case of unlimited creep  $\phi(e^{p\ell} + e^{cr})$  cannot reach the value  $s^*$  so that  $\dot{e}^{cr}$  never becomes zero. We obtain  $\phi(e^{p\ell} + e^{cr}) \rightarrow \text{const.}$  so that  $(s^* - \phi(e^{p\ell} + e^{cr})) \rightarrow \text{const.}$

If  $h$  denotes the distance between the value  $s^*$  and the equilibrium stress strain line at a given  $e^{p\ell} + e^{cr}$ , we have

$$\dot{\epsilon}^{cr} = \Phi(h) = \Phi(s^* - s) = \Phi(s^* - \phi(e^{cr} + e^{pl})) \quad (109)$$

We obviously have

$$s^* = s + h = \text{const} \quad (110)$$

so that as  $s$  increases  $h$  decreases and therefore  $\dot{\epsilon}^{cr}$  decreases.

Solving equation (109) for  $h$  we obtain

$$h = f(\dot{\epsilon}^{cr}) \quad (111)$$

or

$$\begin{aligned} s^* &= s + f(\dot{\epsilon}^{cr}) = \\ &= \phi(e^{cr} + e^{pl}) + f(\dot{\epsilon}^{cr}) . \end{aligned} \quad (112)$$

In the combined stress case we have a yield surface which takes the place of the equilibrium stress-strain curve and which moves in space, and the value  $s^* - \phi(e^{pl} + e^{cr})$  is being replaced by the excess stress  $h_{ij}$ , that is the normal distance from the stress point  $s_{ij}^*$  to the yield surface. The foot of the normal upon the yield surface could be denoted by  $k_{ij}$ .

As the yield surface moves and the plastic and creep strains increase the yield surface for the case of limited creep will ultimately pass through  $s_{ij}^*$  so that  $s_{ij}^* = k_{ij}$ . On the other hand, for the unlimited creep the yield surface will never succeed to pass through  $s_{ij}^*$  so that  $(s_{ij}^* - k_{ij}) \rightarrow \text{const}$ .

In addition, as the strain increases, and in particular as the stress increases, the yield surface will decrease in size and finally become a straight line segment normal to the direction of motion of  $s_{ij}^*$ . A similar conclusion can be drawn for higher temperatures.

We have seen already that the creep strain  $\dot{\epsilon}_{ij}^{cr}$  is normal to the yield surface. We have also seen that as creep develops the creep strain changes its direction and also that during creep there is some change in volume.

We can write

$$\sigma_{ij}^* = k_{ij} + h_{ij} = \text{const.} \quad (113)$$

which is a generalization of equation (110) in the nine dimensional stress space. We also know that the excess stress tensor  $h$  is normal to the yield surface.

Thus we can write

$$(114) \quad h_{ij} = hn_{ij}$$

where  $h$  is the magnitude of the excess stress tensor and  $n_{ij}$  is the unit normal vector to the yield surface. Suppose that  $f = 0$  is the equation of the yield surface. Then

$$(115) \quad n_{ij} = \frac{\partial f / \partial \sigma_{ij}}{[(\partial f / \partial \sigma_{\ell_m}) (\partial f / \partial \sigma_{\ell_m})]^{1/2}} \quad \text{at } \sigma_{ij} = k_{ij}$$

is the unit normal vector to the yield surface at  $k_{ij}$ . The creep strain is equal to

$$(116) \quad \dot{\epsilon}_{ij}^{cr} = \Phi(h) n_{ij} = \Phi(h) \frac{\partial f / \partial \sigma_{ij}}{[(\partial f / \partial \sigma_{\ell_m}) (\partial f / \partial \sigma_{\ell_m})]^{1/2}}$$

Multiplying both sides of equation (116) by itself and taking the square root of the resulting expression we obtain

$$(117) \quad (I_2^{cr})^{1/2} = \Phi(h)$$

where  $I_2^{cr}$  is the product of  $\dot{\epsilon}_{ij}^{cr}$  by itself, which is an invariant. Inverting equation (117) we obtain

$$(118) \quad h = \Phi^{-1} [(I_2^{cr})]^{1/2}.$$

A theory of viscoplasticity can be obtained by considering Fig. 17 where we have the equilibrium stress strain curve OA and the non-equilibrium stress-strain curve OB obtained with a constant stress rate  $\dot{s}$ . Suppose after reaching the stress  $s_A$  at M we continue loading from M to Q with the stress rate  $\dot{s}$ . Then, the stress will increase, the plastic and creep strains which now we can call  $e^{vp}$  will increase with a rate  $\dot{e}^{vp}$  which can be assumed to be a function of the distance in the stress direction between the lines MQ and OA at the corresponding strain. The rate  $\dot{e}^{vp}$  will be a function of other variables also.

Analytically we can write

$$(119) \quad \dot{e}^{vp} = \Phi(s^* - \phi(e^{vp}), \dots)$$

where  $s^*$  is the actual stress and

$$(120) \quad s = \phi(e^{vp})$$

is the equation of the equilibrium stress-strain line.

In the combined stress case the yield surface takes the place of the equilibrium stress strain curve and it moves in space. The value  $s^* - \phi(e^{vp})$  is replaced by the excess stress  $h_{ij}$ , that is the normal distance from the stress point  $s_{ij}^*$  to the yield surface.

In the case of viscoplasticity the stress point is moving and consequently the moving yield surface tries to reach a moving stress point. On the other hand in creep the stress point was stationary. The equations developed for creep are also valid for viscoplasticity.

When the motion of the loading point occurs slowly so that acceleration effects can be neglected we have static viscoplasticity examples of which are given in [43], [44], and [45]. When acceleration effects are taken into account we have dynamic viscoplasticity, examples of which are given in [45], [46], [47], [48], [49].

## BIBLIOGRAPHY

- [1] Morrison, J.L.M. and W.M. Shepherd: Proceedings of the Institution of Mechanical Engineers, **163**, p. 1 (1950).
- [2] Baushinger, J: Mitteilungen aus dem mechanischtechnischen Laboratorium der k. polytechnischen Schule, München, Hefte 7-14 (1877-1886); Heft 13, pp. 1-115 (1886).
- [3] Phillips, A. and M. Ricciuti: Int. J. Solids Structures, **12**, 159-171 (1976).
- [4] Taylor, G. I. and H. Quinney: Phil. Trans. Roy. Soc. London Ser. A **230**, 323-362, (1931).
- [5] Lode, W.: Z. Physik 36, 913-939, (1926).
- [6] Lubahn, J.D.: Journal of Metals, pp. 1031, (1955)
- [7] Valanis, K.C.: Archives of Mechanics, **23**, 517-551, (1971).
- [8] Fox, N.: Acta Mechanica **7**, 248-252 (1969).
- [9] Phillips, A.: International Symposium on Foundations of Plasticity. Vol. II, Problems of Plasticity pp. 193-233 (1974). Noordhoff.
- [10] Phillips, A., Liu, C.S. and Justusson, J.W.: Acta Mechanica, **14**, 119-146 (1972).
- [11] Phillips, A., Tang, J.L. and Ricciuti, M.: Acta Mechanica **20**, 23-40 (1974).
- [12] Phillips, A. and Kasper, R.: Journal of Applied Mechanics **40**, pp. 891-896 (1973).
- [13] Phillips, A. and Das, P.: to be published.
- [14] Williams, J.F. and Svensson, N.L.: Journal of Strain Analysis, **5**, 128-139 (1970).
- [15] Guest, J.J.: Phil. Mag. **50**, 69-132 (1900).
- [16] Bridgman, P.W.: Collected Experimental Papers (1964). 17
- [17] Crossland, B.: Proc. Inst. Mech. Engr. **169**, 935-944 (1954).
- [18] Phillips, A., and Tang, J.L.: Intern Journal Solids and Structures **8**, 463-474 (1972).
- [19] Naghdi, P.M., F. Essenburg, W. Koff: J. Appl. Mech. **25**, 201-209 (1958).

- [ 20 ] Ivey, H.J.: J. Mech. Eng. Sciences **3**, 15-37 (1961).
- [ 21 ] Morrison, J.L.M.: Proc. Instn. Mech. Engrs. **142**, 193-223 (1940).
- [ 22 ] Williams, J.F. and Svensson, N.L.: Journal Strain Analysis **5**, 263-272 (1971).
- [ 23 ] Miastkowski, J. and Szczepinski, W.: Int. Journal Solids Structures **1**, 189-194 (1965).
- [ 24 ] Mair, W.M. and Pugh, H. L .D.: Journ. Mech. Eng. Sci. **6**, 150-163 (1964).
- [ 25 ] Phillips, A. and Gray G.: Journal of Basic Eng. **83**, 275-289 (1961).
- [ 26 ] Phillips, A.: Proc. 2nd Symp. Naval Struct. Mech. 202-214 (1960).
- [ 27 ] Sewell, M.J.: J. Mech. and Phys. of Solids, **21**, 19-45 (1973).
- [ 28 ] Dietrich, L., Kawahara, W., and A. Phillips, Acta Mechanica. **29**, 257-267 (1978).
- [ 29 ] Phillips, A.: AIAA Journal 10, 951-953 (1972).
- [ 30 ] Melan, E.: Ing. Archiv, 116-126 (1938).
- [ 31 ] Ishlinskii, Yu.: Uklz. Math. Jour. **6**, (1954).
- [ 32 ] Prager, W.: Journ. Appl. Mech. **23**, 493, (1956).
- [ 33 ] Kadashevitch, I. and Novoshilov, V.V.: Prikl. Math. un Mekch. **22**, 104 (1959).
- [ 34 ] Shield, R.T. and Ziegler, H.: ZAMP, **9a**, 260 (1958).
- [ 35 ] Ziegler, H.: Quart. Appl. Math. **17**, 55-60 (1959).
- [ 36 ] Baltov, A. and Sawczuk, A.: Acta Mechanica **1**, 81-92 (1965).
- [ 37 ] Phillips, A. and Weng, G.: J. Appl. Mechanics **42**, 375-378, 1975.
- [ 38 ] Eisenberg, M.A. and A. Phillips: Acta Mechanica **11**, 247-260, (1971).
- [ 39 ] Greenstreet, W.L. and A. Phillips: Acta Mechanica **16**, 143-156, (1973).
- [ 40 ] Phillips, A.: Nuclear Engineering and Design **18**, 203-211, (1972).
- [ 41 ] Eisenberg, M.A. and A. Phillips: Acta Mechanica **5**, 1-13, (1968).

- [ 42 ] Phillips, A. and M. Eisenberg: Int. Journal Nonlinear Mechanics, **1**, 247-256 (1966).
- [ 43 ] Phillips, A. and H.C. Wu: Int. Journal Solids and Structures **9**, 15-30 (1973).
- [ 44 ] Phillips, A. and H.C. Wu: Acta Mechanica **17**, 121-136 (1973).
- [ 45 ] Nicholson, D.W. and A. Phillips: Int. Journal Solids and Structures **10**, 149-160 (1974).
- [ 46 ] Wood, E.R. and A. Phillips: J. Mech. and Physics of Solids **15**, 241-254, (1967).
- [ 47 ] Phillips, A., Wood, E.R., Zabinski, M.P. and Zannis, P.: Int. J. Nonlinear Mechanics **8**, 1-16 (1973).
- [ 48 ] Phillips, A. and Zabinski, M.P.: Ing. Archiv. **41**, 367-376 (1972).
- [ 49 ] Phillips, A. and Zannis, P.: Int. J. Nonlinear Mechanics **8**, 89-108 (1973).

## APPENDIX

Five years have elapsed from the time of preparation of these lectures (Summer 1974). During this time considerable progress both in theoretical and experimental research was done by the author and his associates. The purpose of this appendix is to indicate some of this progress which enhances the results presented in these lectures. This appendix is divided into two parts. The first one discusses new experimental findings, the second one discusses new theoretical findings.

**A-1 Experimental.** Here we shall report on some new experimental results obtained with H. Moon [50] and with C.W. Lee [51]. These experimental results give a firm foundation to the concept of the loading surface and to the interaction between loading surface and yield surface. In Fig. A-1 we represent schematically the essence of our findings. Let the stress path in stress space be given by the line OA. Then, the loading surface I passes through A and is generated from the initial yield surface by means of isotropic expansion.

Suppose the stress point remains at A until all plastic and creep strains had time to develop; then the yield surface II will pass through the same point A, it will be tangential to I at A, it will be enclosed by I, and it will be much smaller than the loading surface through A. If the stress point does not remain at A until all plastic and creep strains had time to develop, then the yield surface II will not pass through A, but it will be enclosed by I; it will have such a focus that a relatively small rigid body motion of this yield surface in the direction of A will make it pass through A and simultaneously to become tangential to I at A.

Suppose we continue the stress path from A to B within I. Then, the loading surface I will remain unchanged while the yield surface will move and pass through B, if of course again all plastic and creep strains had time to develop while the stress point was stationary at B at the end of the path. The new yield surface II' will be tangential to I if B is on I or very near I. On the other hand, if the point B is sufficiently far from I, as is the case with the point C at the end of the path AC, then the new yield surface II'' which passes through C will be completely inside I and will not be tangent to I.

Suppose now that we continue our stress path from B to D (or from C to D) where D is outside I. Then the loading surface I changes to the new loading

surface  $I'$  which passes through D. If again, while the stress point is stationary at D, all plastic and creep strains had time to develop, the new yield surface  $II'''$  will pass through D, will be tangential to  $I'$  at D and will be completely inside  $I'$ . During the motion of the stress point which generated a new loading surface,  $I \rightarrow I'$ , the plastic and the creep strain rates generated are much larger than those strain rates generated by a motion of the stress point which keeps the loading surface unchanged. The plastic strain rate vector is normal to the moving yield surface and since at the intersection of the stress path with the loading surface, the yield surface is tangential to the loading surface, the plastic strain rate vector is also ultimately normal to the loading surface.

Fig. A-2 illustrates the results of experiments for specimen M-4 from [50]. The loading path is PR-ST-TU.

Fig. A-3 illustrates the results of experiments for specimen L-2 from [51]. The loading path is AB-CDEF. Fig. A-4 illustrates the continuation of the experiments for specimen L-2. The path is now FGKL.

We observe that the behavior discussed on the basis of Fig. A-1 is indeed experimentally verified.

**A-2 Theoretical.** In [52] the author discusses some thermodynamic consequences of his experimental work and he shows that the cluster of isothermal yield surfaces in the stress-temperature space, for increasing temperature reduces to a limiting straight line associated with thermodynamic quantities. In [53] the author and his colleagues, M. Eisenberg and C.W. Lee, continued the previous work and set the concept of the thermodynamic reference stress on a firm foundation. Then the stress-strain response is represented in a two-dimensional stress-plastic strain space and the concepts of the upper and lower quasistatic stress-strain curve for a given temperature is introduced, Fig. A-5. Here  $\bar{\sigma}$  is the stress magnitude in the six dimensional stress space and  $\varepsilon^P$  is the plastic strain magnitude in the six dimensional plastic strain space. Curve AC is the quasistatic stress-strain curve for a given temperature  $\theta$  if loading with increasing  $\bar{\sigma}$ , while  $\bar{AC}$  is the quasistatic stress-strain curve for a given temperature  $\theta$  if loading with decreasing  $\bar{\sigma}$ . The two curves AC and  $\bar{AC}$  intersect at a value of  $\bar{\sigma}$  which corresponds to the thermodynamic reference stress. Figure A-6 shows a sequence of equilibrium stress-strain curves for increasing temperature  $\theta$ . The locus of intersections of each pair of equilibrium stress-strain curves defines an equilibrium boundary line.

Next the experimental results of [18] are evaluated and in Fig. A-7 we see

the limiting straight line yield surface of one of the tests in this series. For the series of tests in [18] Fig. A-8 shows in a double logarithmic scale the upper and lower equilibrium stress-strain line at 70° F. The lower equilibrium stress-strain line approaches the upper equilibrium stress-strain line as  $\epsilon^{-P}$  increases. These two experimentally determined lines should be compared with lines AC and  $\bar{A}\bar{C}$  of Fig. A-5. The width of the yield surface in the direction of prestressing decreases as the plastic strain increases. The widths of the yield surfaces in the direction of prestressing as a function of  $\epsilon^{-P}$  are given in Fig. A-8 for each testing temperature. It is seen that the slope of the change in width decreases as the temperature increases with the plastic strain remaining constant. Hence, the rate of decrease in width is higher at high temperature than at lower temperatures. At some maximum allowable temperature  $\theta_{\max}$  (°F) the yield surface becomes a straight line. From Fig. A-8 we see that  $\theta_{\max}$  (°F) starts from approximately 650° F at  $\epsilon^{-P} = 0$  which is the annealing temperature and decreases as shown. The size of the limiting yield surface, that is, the length of the straight line to which the yield surface degenerates at  $\theta_{\max}$ , increases with  $\epsilon^{-P}$ .

We mention also briefly that in three additional papers [54,55,56] by using the theory of dislocations, G. Weng and this author succeeded in obtaining subsequent yield surfaces of aluminium which exhibit most features shown in our experimental results.

Fig. A-3

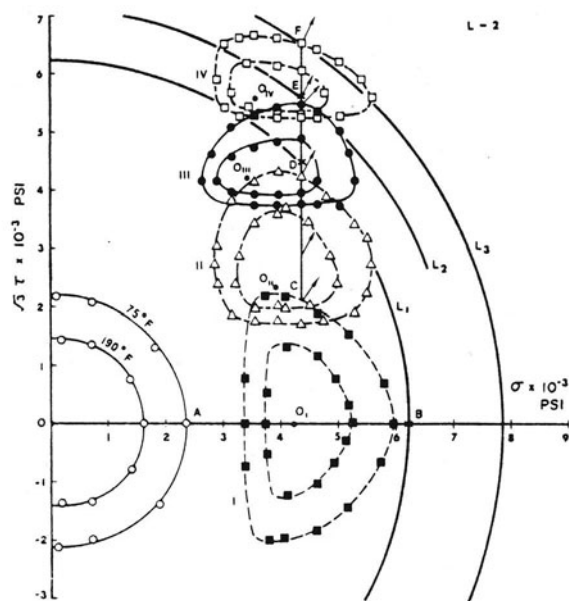
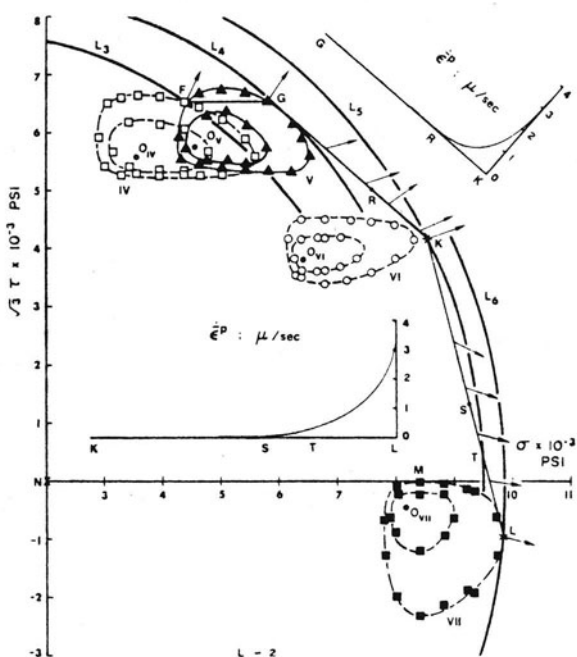


Fig. A-4



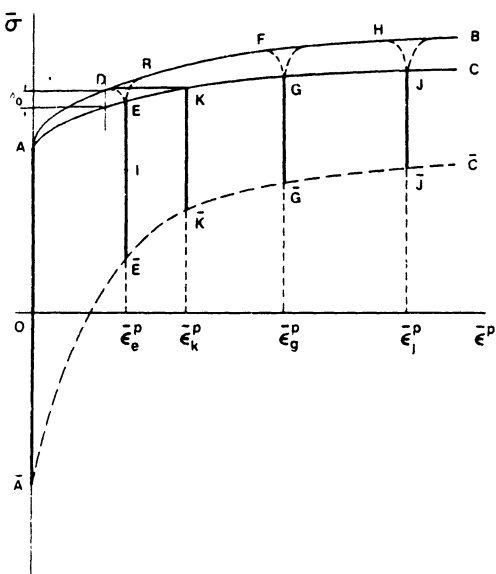


Fig. A-5

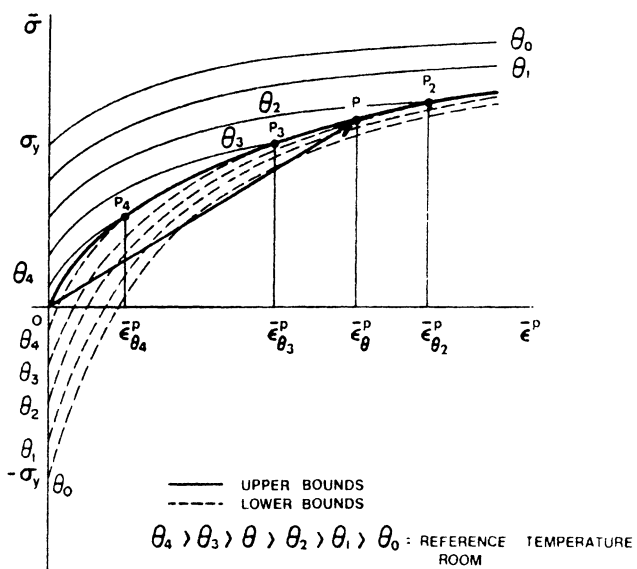


Fig. A-6

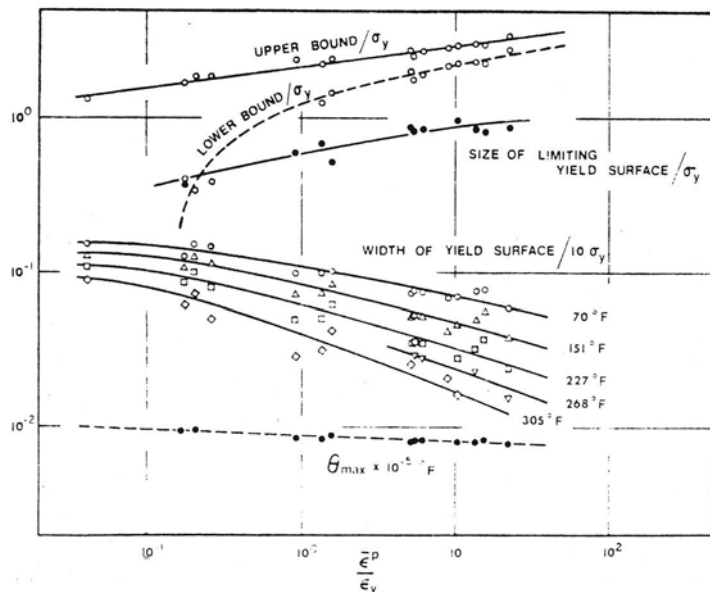


Fig. A-7

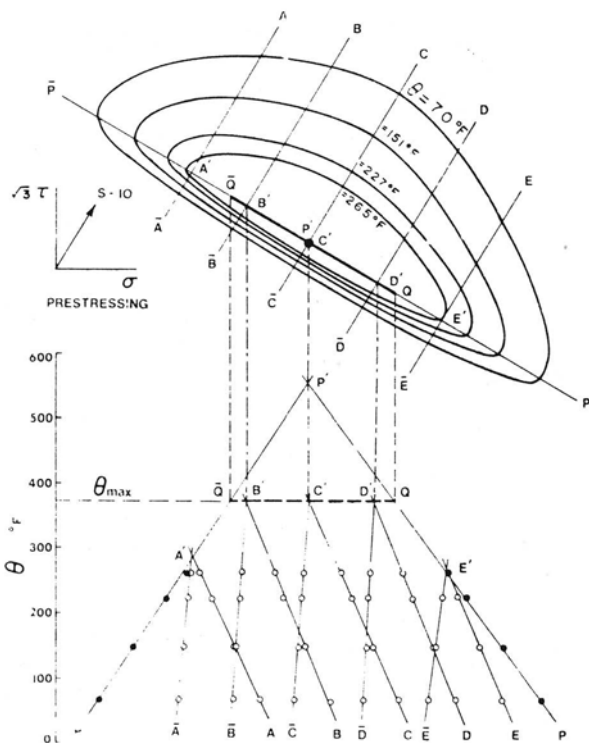


Fig. A-8

## REFERENCES

- [ 50] Phillips, A. and H. Moon: *Acta Mechanica* 27, 91-102 (1977).
- [ 51] Phillips, A. and C.W. Lee: *Int. J. Solids Structures* (in press) 1979.
- [ 52] Phillips, A.: Topics in Applied Continuum Mechanics. (Z.L. Zeman and F. Ziegler, Editors), pp. 1-21, Springer Wien, 1974.
- [ 53] Eisenberg, M.A., Lee, C.W., and A. Phillips: *Int. J. Solids Structures*, 13, 1239-1255 (1977).
- [ 54] Weng, G.J. and A. Phillips: *Int. J. Engng. Sci.* 15, 45-60 (1977).
- [ 55] Weng, G.J. and A. Phillips: *Int. J. Engng. Sci.* 15, 61-70 (1977).
- [ 56] Weng, G.J. and A. Phillips: *Int. J. Solids Structures* 14, 535-544 (1978).

**GENERALIZED YIELD CRITERIA  
FOR ADVANCED MODELS OF MATERIAL RESPONSE**

by W. Olszak

Polish Academy of Sciences

International Centre for Mechanical Sciences

Udine

### Summary

When formulating the yield criterion, we as a rule, adopt the well known classical approach which refers to homogeneous and isotropic bodies. The physical reality is, however, more complex and has to be accounted for: more general and realistic models have to be analysed. Thus we successively take into consideration new mechanical phenomena which originally were disregarded:

- the anisotropic and nonhomogeneous material structure;
- the rheological material response in both its aspects, i. e. when it occurs after having exceeded the plastic limit or else when it accompanies the deformation process from its very beginning;
- the next step consists in investigating the consequences of a nonstationary character of the yield criterion which may be induced, e.g., by artificial irradiation processes of solids or may occur in elasto-visco-plastic soils with time-variable humidity;
- finally, in a rather general approach, the original states of strain and stress are supposed to be nonuniform (nonhomogeneous) in space and time.

### I. Introductory Remarks

The evolution of the notion of the yield criterion (yield condition) presents many interesting aspects. In this respect, the last two decades are particularly characteristic. This is closely related to the rapid development of the theory of plasticity as well as of our continuously increasing understanding of its physical background.

It is well known that, for analyzing the behaviour of elastic-plastic solids, we have to define the following three ingredients: (a) the law governing their behaviour in the elastic range; (b) the yield criterion which indicates when the plastic deformations set in (active process) or else when they cease (passive process); (c) the law of the material behaviour in the plastic range. An interrelation between (b) and (c) may be envisaged; this often is physically justified and, moreover, may facilitate the solution of effective problems, is, however, not necessary.

The basic theoretical and experimental research on plasticity has successively been extended to phenomena which originally were disregarded. This also holds true for the approach to formulating the relevant yield criteria. Thus we proceed, in a quite natural way, from physically simpler to more complicated situations.

Thus the first attempts were related to mechanically isotropic and homogeneous media.

The next step consisted in taking into account the material anisotropy and (macro) nonhomogeneity.

Afterwards the rheological material response has been considered in both its aspects: first, the one which reflects time-dependent phenomena only after the plastic limit has been exceeded; and, second, also that—considerably more difficult to be accounted for—which is related to rheological phenomena accompanying the deformation process right from its very beginning.

The further stage of evolution consisted in investigating the consequences of a time-variable plasticity criterion which, quite independently of the loading programme, may undergo changes when, e.g., artificial irradiation effects in metals or a time variable humidity content of elasto-visco-plastic soils are being examined.

For either of the above mentioned types of material response, the corresponding yield criteria have to be formulated in an appropriate way. But even if, for this purpose, we successively account for the more and more complex physical material behaviour, we as a rule tacitly accept a very restrictive limitation: the deformation and stress fields are considered to be uniform (homogeneous). This particular assumption, however, only very rarely (if at all) corresponds to physical reality. So the next step to be taken consisted in introducing (space and time dependent) variability of these fields. The ensuing consequences are of considerable importance. They may result, e.g., under certain conditions, in a remarkable increase of the plastic limit. It is interesting to note that this fact has already been known for many years from experimental evidence.

In what follows we shall briefly discuss some characteristic results when the yield criteria are successively developed and formulated for more and more general physical assumptions.

## II. The Classical Approach

For obvious — theoretical and practical — reasons, the frontiers between the domains of the different types of material response have ever since attracted a vivid interest. Thus efforts have always been undertaken to find the conditions marking off these domains (elastic, plastic, fracture,...) as well as those to pass from one domain to the other. Historically, an interesting evolution of conceptions and approaches can be observed whereby one may note that preference was given to criteria having a physical significance. The main proposals can thus be connected with the notion of limit values (or certain functions) (a) of stress  $\sigma$ , (b) of strain  $\epsilon$ , (c) of energy  $\phi$ .

The first attempts date back to Galileo Galilei (1638) [8] who vaguely suggested to consider the maximum [principal] stress to constitute such a demarcation. In this he was later followed by many other scientists.

The strain conditions were inspired by the ideas of F. Mariotte (1686) [15] and lead to the conception (and its later generalizations) that the maximum [principal] strain has, as an appropriate limit criterion, to be taken into consideration.

These two approaches [of the types (a) and (b)] were afterwards developed and generalized in various ways for combined states of stress and strain by numerous researchers who proposed certain functions of  $\sigma_{ij}$  or  $\epsilon_{ij}$  to represent the frontier of the elastic domain. These functions were as a rule adapted to appropriately reflect physical reality. For this, often special experimental research programmes have been conceived.

The energy approach [of type (c)] is of younger origin. E. Beltrami (1885) [1] formulated a criterion based on the notion of the critical value of the (total) energy of deformation

$$\phi = \phi_v + \phi_f , \quad (II,1)$$

whereas M. T. Huber (1904) [12] , in view of the experimental results invalidating the above idea, assumed that only part of this energy, the distortion energy  $\Phi_f$  , be responsible for attaining the critical (limit) state. This form of yield condition was also, independently, proposed by R. von Mises (1913) [16 a] and H. Hencky (1924) [9] . [  $\Phi_v$  in the expression (II.1) stands for the energy of volume change] .

Interesting comprehensive surveys of the numerous attempts aiming at separating the different ranges of material response and, especially, at defining the demarcation of the elastic behaviour, are to be found in the monographic studies by W. Burzyński [3] and by W. Prager [26a].

In the classical case, the approach to formulating the yield criterion is based on the assumption of mechanical material isotropy and (macro) homogeneity. Moreover, the stress and strain fields are considered to be uniform (homogeneous) [27] . Then, as a matter of fact, any expression formed by use of the principle values of the stress tensor or of the strain tensor, is independent of the orientation of the principal axes of these tensors, and thus may be envisaged for the condition required to mark off the ranges of mechanical behaviour of solids. Under such conditions, the known relation

$$f(I_1, I_2, I_3) = 0 \quad (\text{II.2})$$

generally adopted, has been investigated in detail and specified by numerous researchers,  $I_i$  ( $i = 1, 2, 3$ ) standing for the three invariants of the stress tensor. The geometrical representation of the plastic frontier (the flow surface) in the stress space varies according to the choice of the function  $f$  ; for this choice, the authors refer to the relevant experimental results.

So, e.g., a simple possible form of Eq. (II.2), leads to

$$I_2 - k^2 = 0 , \quad (\text{II.3})$$

which represents the Huber-von Mises yield condition (yield cylinder) and is, to-day, the normally used classical criterion [of the energy type (c)].

Another frequently used criterion [of the stress type (a)], due to H. Tresca (1868) [33] is based on the notion of the critical value of the greatest shear stress; in such a case, the criterion in an invariant presentation according to Eq. (II. 2) can be written in the form

$$4l_2^3 - 27l_3^2 - 36k^2l_2^2 + 96k^4l_2 - 64k^6 = 0, \quad (\text{II. 4})$$

which is due to B. de Saint-Venant [31], [27]

The Tresca condition constitutes a particular case of a more general condition proposed by Ch. A. Coulomb (1778) [6], in which the limit value depends on the greatest shear stress as well as on the mean stress.

### III. Anisotropy. Nonhomogeneity

The effects of anisotropic material structure have been explored by numerous authors, e.g. [16b], [10] [21a, b], etc. But simultaneously, the solids are, as a rule, on the "macro" and/or "micro" scale mechanically nonhomogeneous. The influence of the (elastic and plastic) mechanical nonhomogeneity has been analyzed by the author [18a, b] and his co-workers [20], [21], ..., the elastic and plastic "moduli",  $M_p^{el}$  and  $M_p^{pl}$ , respectively, being supposed to depend on the coordinates of the generic point  $P(x_i)$ , ( $i = 1, 2, 3$ ). New interesting qualitative and quantitative results and solutions have been obtained.

The investigations concern the general case of material nonhomogeneity coupled with its anisotropy. Here, immediately, a fundamental question has to be answered, viz. whether and under which conditions the strain energy  $\phi$ , given by

$$\phi = \frac{1}{2}\sigma_{kl}\epsilon_{kl} = \frac{1}{2}E_{kl\mu\nu}(P)\cdot\epsilon_{kl}\epsilon_{\mu\nu} = \frac{1}{2}\tilde{E}_{kl\mu\nu}(P)\cdot\sigma_{kl}\sigma_{\mu\nu} \quad (\text{III. 1})$$

can be decomposed into two terms in a similar way as indicated in Eq. (II.1), for isotropic bodies. In Eq. (III, 1), the components of the tensor of moduli of elasticity  $E_{klmn}(P)$  and those of the tensor of coefficients of deformation  $\tilde{E}_{klmn}(P)$  satisfy equations of the type

$$H_{klmn} = H_{lkmn}, \quad H_{klmn} = H_{klnm}, \quad H_{klmn} = H_{mnkl} \quad (\text{III.2})$$

and, in addition, the following equation

$$E_{klpq} \cdot \tilde{E}_{klrs} = \delta_{pr} \delta_{qs}. \quad (\text{III.3})$$

It can be proved that in the most general case of anisotropy (characterized by 21 different elastic moduli  $E_{klmn}$ ), the strain energy  $\Phi$  cannot, for an arbitrary load, be decomposed into two such terms.

A decomposition of this kind is found to be possible only in cases of certain particular types of symmetry of the anisotropic structure of the bodies considered and, of course, in the case of total symmetry, i.e. in the case of isotropy.

If, therefore, in the general case of an anisotropic body the notion of the distortion energy  $\Phi_f$  proves to be devoid of physical sense, it follows that it cannot be used in its hitherto existing form as a criterion for the attainment of the critical state (yield limit).

However, it can be proved [21] that by introducing certain generalized notions, we shall be able to split the quantity  $\Phi$  into two terms, the significance of which is analogous to that of  $\Phi_v$  and  $\Phi_f$ .

For this purpose, we introduce certain generalized invariants of the stress tensor,  $I_1^*$ ,  $I_2^*$ , and of the stress deviation,  $I_2^{**}$ , as well as of the strain tensor  $J_1^*$ ,  $J_2^*$ , and of the strain deviation  $J_2^{**}$ , which are denoted by asterisks in order to distinguish them from the corresponding classical invariants  $I_1$ ,  $I_2$ ,  $I_2'$ ;  $J_1$ ,  $J_2$ ,  $J_2'$ . The expressions for these invariants are given in our paper [20].

Then, the generalized expressions  $\phi_v^*$  and  $\phi_f^*$  are constructed in a suitable way, and it can be shown that, now, such a decomposition of the strain energy  $\phi$  into two parts is possible. These two generalized quantities,  $\phi_v^*$  and  $\phi_f^*$ , preserve some of the properties of the classical energy of volume change  $\phi_v$  and of the classical energy of distortion  $\phi_f$ .

But this decomposition is not unique.

It is unique for some particular classes of bodies only for which certain conditions are satisfied. These conditions are formulated in our paper [ 21 ]. It should be stressed that the class of bodies for which the above conditions are fulfilled is physically not void. It covers all bodies crystallizing in regular systems and, in particular, also isotropic bodies.

For the other types of anisotropy, for which this decomposition is not unique, it can be shown that there are two possible manners of splitting the strain energy into two parts. So we have

$$\phi = \begin{cases} \phi_v^* + \phi_f^* ; \\ \tilde{\phi}_v^* + \tilde{\phi}_f^* . \end{cases} \quad (\text{III. 4})$$

We have called the quantities  $\phi_f^*$  and  $\tilde{\phi}_f^*$  the generalized distortion energies of the first kind and of the second kind, respectively.

It is interesting to show that:

- (1) the value of  $\phi_f^*$  does not change if the element undergoes a specific elongation  $\epsilon$  which is the same in all three orthogonal directions;
- (2) the value of  $\tilde{\phi}_f^*$  does not change if the element is subjected to a uniform pressure (or traction)  $\sigma$  in all directions (of the hydrostatic type).

Now, the above statements allow the generalization of the yield condition, based on the limit value of the generalized distortion energy to anisotropic nonhomogeneous bodies.

According to the above, there are two alternative manners of procedure. These conditions can be written in the form

$$\phi_f^* = [K(P)]^2 \quad (\text{III. 5.1})$$

or

$$\tilde{\phi}_f^* = [\tilde{K}(P)]^2 \quad (\text{III. 5.2})$$

where in general  $K(P)$  and  $\tilde{K}(P)$  are certain functions of the coordinates of the considered point  $P$ . They are related to the plastic nonhomogeneity of the body.

The ensuing physical and theoretical conclusions to be drawn are given in [21].

If the above yield conditions are supposed to constitute the plastic potential, we immediately can derive the associated flow rules for materials of various types of anisotropy and nonhomogeneity.

#### IV. Rheological Effects

When passing to rheologically reacting bodies, we immediately find two new notions: that of the static yield criterion and that of the dynamic yield criterion, these two notions marking in their evolution a considerable step.

Before discussing them in more detail, let us first briefly mention the work-hardening effects which are of great importance in both the theory of inviscid plasticity and that of rheological approach. As a matter of fact, experimental results clearly show that time-dependent phenomena, like, e.g., elastic-visco-plastic deformation processes in metals and soils, occur as a rule in the presence of work-hardening effects. The latter, very complex from the physical point of view, also present serious difficulties for their formal assessment. The methods of research, experimental and theoretical, are ingenious, the literature rich and abundant. In this brief survey, we cannot enter into details. It may at least suffice to refer to the perspicaceous gener-

alizations advanced by Z. Mroz [17] and to the interesting research work by A. Phillips [24], [25].

The essential feature of rheological material behaviour is the time-dependence of the deformation process occurring even for time-independent external loads (and vice versa). Still more sensible may be in this respect the dynamic response. For materials of this class, the inelastic strain tensor turns out to depend not only on the path stress history but also on the time stress history. In inviscid plasticity, as we know, it is only path dependent.

(1) For simplicity, we shall first introduce the notion of an elastic/viscoplastic body [11], [32], [22]. For this, we assume that the body is purely elastic before the plastic state is reached, and becomes elastic/viscoplastic after this limit has been exceeded. Owing to this assumption, the original yield criterion, called in what follows, the static yield criterion, will not differ from the normally used criterion of the inviscid plasticity theory. (Its counterpart, the dynamic yield criterion, will be given below).

Only later [Sec. IV.(3)] we shall consider the more general case when the rheological effects are being taken into account right from the very beginning of the deformation process (elastic-visco-plastic response).

When assuming that the strain-rate tensor can be decomposed into its elastic and inelastic parts

$$\dot{\epsilon}_{ij} = \dot{\epsilon}_{ij}^e + \dot{\epsilon}_{ij}^p$$

with the term  $\dot{\epsilon}_{ij}^p$  representing both the viscous and plastic responses of the material, and when taking into account the work-hardening effects, we can formulate the static yield condition in the form

$$F(\sigma_{ij}, \dot{\epsilon}_{ij}^p) = \frac{f(\sigma_{ij}, \dot{\epsilon}_{ij}^p)}{\alpha} - 1$$

where

is the work-hardening parameter. We shall assume that the yield surface  $F = 0$  considered in the stress space is regular and convex.

An elastic/viscoplastic material may be described by the following constitutive equation

$$\dot{\epsilon}_{ij} = \frac{\dot{s}_{ij}}{2\mu} - \frac{1-2\nu}{E} \delta_m \delta_{ij} + \gamma \langle \Omega(F) \rangle \frac{\partial F}{\partial \delta_{ij}},$$

where  $E$ ,  $\mu$  and  $\nu$  are the elastic constants,  $\gamma$  being the viscosity coefficient (for the simple case of Maxwell's viscosity law) and, as usual,  $\delta_m = \frac{1}{3} \delta_{ii}$ , and  $s_{ij} = \delta_{ij} - \delta_m \delta_{ij}$ , the dot denoting differentiation with respect to time.

The symbol  $\langle \Omega(F) \rangle$  is defined in the following way

$$\langle \Omega(F) \rangle = \begin{cases} 0 & \text{for } F \leq 0, \\ \Omega(F) & \text{for } F > 0, \end{cases}$$

the function  $\Omega(F)$  being based on experimental results of dynamic properties of materials. This approach has been discussed in detail by P. Perzyna [22] and various forms of  $\Omega$  were proposed by him and his co-workers for incompressible materials [23]. When dealing with compressible materials, we should refer to paper [19a].

It is seen from the constitutive equation (IV.4) that the inelastic components of the strain-rate tensor  $\dot{\epsilon}_{ij}^p$  depend on the difference between the actual state of stress and the state corresponding to the static yield criterion. Thus the plastic and viscous effects are seen to be generated by the function  $\Omega(F)$  of this stress difference, i.e. the function of the excess stress  $\delta_{ij}^*$  above the static yield condition. The static part of the strain rate tensor is, in this first approach (1), considered to be independent of time effects.

When considering the inelastic part of the strain rate  $\dot{\epsilon}_{ij}^p$  represented by the third term of Eq. (IV.4) and bearing in mind that its second invariant is given by  $I_2^p = \frac{1}{2} \dot{\epsilon}_{ij}^p \dot{\epsilon}_{ij}^p$ , we obtain

$$I_2^P = \frac{1}{2} \gamma^2 <\Omega(F)> \frac{\partial F}{\partial \sigma_{kl}} \frac{\partial F}{\partial \sigma_{kl}} , \quad (IV.6)$$

from which, in view of Eq. (IV.2), we readily find the following dynamic yield condition

$$f(\sigma_{ij}, \epsilon_{ij}^P) = \alpha \left\{ 1 + \Omega^{-1} \left[ \frac{(I_2^P)^{1/2}}{\gamma} \left( \frac{1}{2} \frac{\partial F}{\partial \sigma_{kl}} \frac{\partial F}{\partial \sigma_{kl}} \right)^{-1/2} \right] \right\} , \quad (IV.7)$$

where  $\Omega^{-1}$  denotes the inverse function of  $\Omega$ .

The relation (IV.7) represents the actual evolution of the yield surface during the process of inelastic deformation. Its changes are seen to be a function of the state of stress  $\sigma_{ij}$ , of the state of inelastic strain  $\epsilon_{ij}^P$ , of the (isotropic and anisotropic) work-hardening of the material, its rheological properties  $\gamma$ , and, explicitly, of the strain-rate  $I_2^P$ .

Various particular cases of this rather general approach have been discussed in [22], [19a].

(2) So far, we have assumed that the excess stress  $\sigma_{ij}^*$  above the static yield surface was responsible for generating the inelastic strain-rates  $\epsilon_{ij}^P$  according to a simple possible assumption: Maxwell's viscosity law. A more general treatment in order to include a wider class of response phenomena, is possible when relating these quantities by the relation

$$P \epsilon_{ij}^P = Q \sigma_{ij}^* \quad (IV.8)$$

where the differential operators  $P$  and  $Q$ , respectively, are given in the usual form

$$P = a_0 + \sum_{k=1}^m a_k \frac{\partial^k}{\partial t^k} , \quad Q = b_0 + \sum_{k=1}^n b_k \frac{\partial^k}{\partial t^k} . \quad (IV.9)$$

(Maxwell's relation of Sec. IV.(1) was limited to solely retaining  $a_1, b_0, b_1$ ), and the constitutive equation (IV.4) is seen to represent a particular case of the more general approach (2) only. The basic relationships for conditions referred to in (2) are again as readily seen nonlinear. The ensuing conclu-

sions will be discussed separately.

3) In the simplified elastic/viscoplastic physical model from Sec. IV (1) and Sec. IV (2), the material is supposed, as we may recall, to be purely elastic before the plastic state is attained and reacts by elastic and inelastic (i.e. plastic as well as viscous) deformations only after this limit has been exceeded. We have seen that, owing to this assumption, the original yield criterion (called the static yield criterion) does not differ from the known criteria of the inviscid plasticity theory [Sec. IV (1)]. Their most appropriate form may be based on the energy approach (Huber-von Mises), a critical value of the conserved (accumulated) distortion energy marking the transition from the elastic to the inelastic state.

In the more general model of an elastic-visco-plastic material, the rheological response is supposed to occur right from the very beginning of the loading process. Under such conditions it seems appropriate to take into account the accumulated energy  $\phi_E$  as well as the dissipated power  $\dot{\phi}_D$ , both quantities being now regarded to be responsible for the behaviour of the visco-elastic material. The yield condition is then given by a certain function of these two arguments

$$f(\phi_E, \dot{\phi}_D) = 0; \quad (\text{IV.10})$$

its form should, of course, be based on experimental evidence. The simplest possible form is a linear combination

$$\xi_E \phi_E + \xi_D c \dot{\phi}_D = k^2 \quad (\text{IV.11})$$

with

$$0 \leq \{\xi_E, \xi_D\} \leq 1. \quad (\text{IV.12})$$

With  $\xi_E = 0$  or  $\xi_D = 0$  we assume that the accumulated energy or the dissipated power, respectively, have no effect on the yield criterion. The second case corresponds, e.g., to M. Reiner and K. Weissenberg's point of view [29] who disregard, when formulating the yield condition, the influence of  $\dot{\phi}_D$ . Other particular cases contained in Eq. (IV.10), are also possible. This problem is discussed in more detail in [18c].

### V. Nonstationary Yield Criteria

So far, the changes of the yield surface considered were assumed to depend on the relevant physical parameters and the loading programme only. However, numerous experimental investigations prove that, under certain circumstances, the yield criterion may essentially depend on time (or a time-dependent parameter). For such phenomena, the nonstationary character of the relevant yield criterion has to be taken into account.

Such situations may occur if, e.g., materials, especially metals, are exposed to artificial irradiation. As a matter of fact, it has been experimentally found that the flow of elementary particles may induce very pronounced changes in the mechanical material response and that, particularly, the yield limit of metals (like mild steel, copper, nickel, etc.) is most sensitive to the quantity of neutron irradiation  $nvt$  ( $n$  denoting the number of neutrons per unit volume of the flow and  $v$  its average velocity) and, as a result, may exhibit great variations. (In most cases, the yield limit increases with increasing  $nvt$ ). These, in turn, can essentially influence the behaviour of the material in the plastic range. This sensitivity of the material is observed for specimens loaded dynamically as well as statically.

The quantity of neutron irradiation  $nvt$  is, as a rule, time-variable; as a consequence, the time-dependent change of the plastic limit involves a nonstationary form of the yield surface. (This will, in the stress space, with increasing time  $t$ , in most cases expand). Some of the ensuing consequences were discussed in more detail in one of our previous papers [19b]. Cf. Fig. 1, Fig. 2, and Fig. 3.

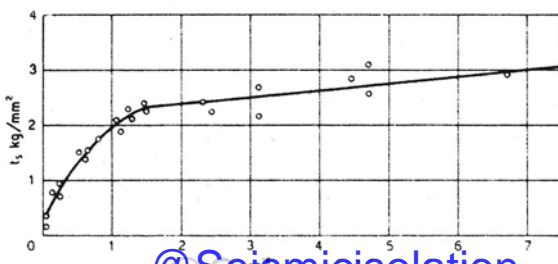


Fig. 1 : Monocrystal of copper (Jamiston and Blewitt, [19d]<sup>17</sup>)

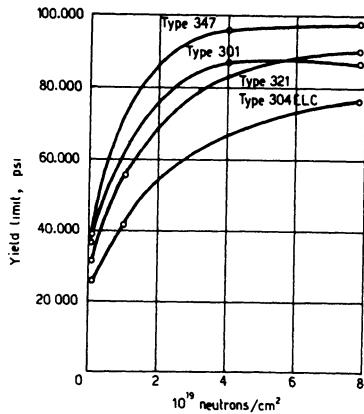


Fig. 2 : Stainless steel (Wilson and Berggren, [19d]<sup>18</sup>)

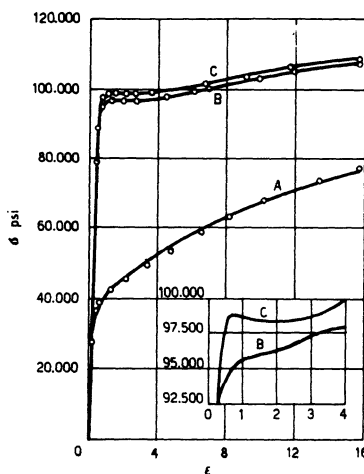


Fig. 3 : Stainless austenite steel (Wilson and Berggren [19d]<sup>18</sup>)

Another analogous example is given by a time-variable humidity contained in soils. It is known that the angle  $\psi$  of interior friction in soils and granular media depends on their humidity content, the yield condition itself being a function of  $\psi$ . Hence the time variability of the yield condition

itself. Since the yield limit will, with an increasing or decreasing angle  $\psi$ , as a rule increase or drop, respectively, the yield surface (in the stress space) will, in consequence, expand or shrink, again, quite independently of the loading programme. Cf. Fig. 4.

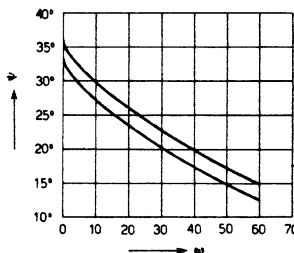


Fig. 4 : Humid soils (Koehler and Scheidig, [19d]<sup>19</sup>)

Similar phenomena may also be observed when the effects of nonstationary temperature fields are considered. As it is known, the yield limit of some metals (e.g. steel) may vary with the temperature in a quite pronounced way, whereas their elastic properties are hardly affected (at least, within certain limits).<sup>1)</sup>

In order to assess the influence of these phenomena in our theoretical approach, the following static criterion for an elastic-viscoplastic solid (of the Maxwell type) has been proposed [19b]

$$F(\sigma_{ij}, \epsilon_{ij}^P, \eta) = \frac{f(\sigma_{ij}, \epsilon_{ij}^P)}{\alpha(\epsilon_{ij}^P, \eta)} - 1, \quad (V.1)$$

whereas an appropriate analysis, analogous to that of Sec. IV(1), leads, under certain conditions, to the dynamic criterion in the form

$$f(\sigma_{ij}, \epsilon_{ij}^P) = \alpha(\epsilon_{ij}^P, \eta) \left\{ 1 + \Omega^{-1} \left[ \frac{(\epsilon_2^P)^{1/2}}{\gamma(\eta)} \left( \frac{1}{2} \frac{\partial f}{\partial \sigma_{kl}} \frac{\partial f}{\partial \sigma_{kl}} \right)^{-1/2} \right] \right\} \quad (V.2)$$

where

$$\alpha = \alpha \left( \int_0^{\epsilon_{ij}^P} \sigma_{ij} d\epsilon_{ij}^P, \eta \right). \quad (V.3)$$

When comparing the above expressions with (IV.2), (IV.7), (IV.3), we note the influence of the variables of the preceding problem including again, explicitly, the strain-rate [cf. Sec. IV. (1)], but also the influence of the time-variable parameter  $\eta = \eta(t)$  which, as pointed out, may express the time-vari-

1) The influence of the temperature has already been taken into account by W.

able irradiation quantity, or time-variable humidity, temperature, etc.

Under such conditions, when the yield surface is moving independently of the loading programme, a particularly important problem is to appropriately define the active (loading), the neutral, and the passive (unloading) processes. The following criteria are readily found to hold:

$$\frac{\partial F}{\partial \sigma_{ij}} \dot{\sigma}_{ij} + \frac{\partial F}{\partial \eta} \frac{d\eta}{dt} \left\{ \begin{array}{ll} > 0 & \text{for loading processes;} \\ = 0 & \text{for neutral processes, (V.4)} \\ < 0 & \text{for unloading processes.} \end{array} \right.$$

For an appropriate geometrical interpretation in a nine-dimensional space of stresses, let us denote by  $\psi$  the angle between the normal to the yield surface at a point  $P$  and by  $\dot{\sigma}_{ij}$  the vector of stress-rate (see Fig. 5).

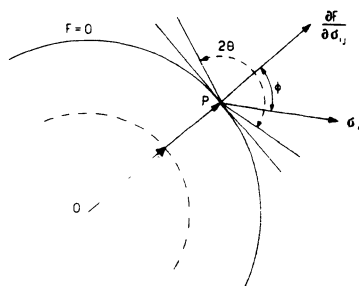


Fig. 5 : Time-variable yield surface [19b]

Then, after some transformations, the conditions (V.4) may be visualized, in the chosen stress space, by a hypercone with the opening angle  $2\delta$  and the relevant position of the vector  $\dot{\sigma}_{ij}$  :

$$\begin{aligned} \psi &< \delta && \text{for loading processes;} \\ \psi &= \delta && \text{for neutral processes;} \\ \psi &> \delta && \text{for unloading processes.} \end{aligned} \quad (\text{V.5})$$

The difference between stationary and nonstationary processes is clearly visible. The ensuing geometrical interpretation presents no difficulty.

## VI. Space and Time Variable Stress and Strain Fields

In the preceding Sections we showed how the treatment has successively been generalized by taking into consideration new physical phenomena which were originally disregarded. All these investigations and results, completed by variational and uniqueness theorems, enable us to closer approach the physical reality, to widen the basic knowledge and to tackle effective problems of engineering importance. All of them, however, are handicapped by a severe limitation: they start, for the formulation of the yield criteria, from a very restrictive assumption which supposes the considered elastic stress and strain states to be uniform (homogeneous). This, of course, constitutes a hypothesis which only very seldom (if at all) corresponds to reality.

A further step in realistically generalizing the approach can therefore be accomplished if we realize that the transition of a material from the elastic to the plastic state is connected with a change of its structure. It is obvious that, even within the framework of a continuum theory, one has to take into account the fact that the notion of structure does make sense only if it is related to a finite region (and not to a single point), and also, in an analogous way, to a finite interval of time.

Thus, if the behaviour of the considered body at a given instant and in a given point has to be described, one has to assume that the behaviour will explicitly depend also on prior states (in time) as well as on states of neighbouring points (in space).

As the notions of spatial and time neighbourhood are not precise, it seems to be justified to introduce, as a first approximation, the dependence on the corresponding gradients; hence, in our case, the dependence on the gradients of the stress and the strain tensors with respect to their space and time coordinates, as these gradients characterize the changes of state in the spatial neighbourhood of the point as well as in neighbouring instants.

That such influences actually do exist has been proved by experimental evidence. The corresponding observed facts are:

(a) the phenomenon of the so called "overelasticity" (see, e.g., [4], [5], [7])<sup>2)</sup>, resulting in an increase of the yield limit if the state of stress is spatially nonhomogeneous;

(b) the phenomenon of a pronounced dependence of the yield limit on the rate of loading and deformation (cf. Sections IV and V as well as, e.g., [14]), usually explained by the viscous material properties.

The present-time intense research activities in the field of viscoplasticity proceed from the facts mentioned under (b), whereas it seems that the influence of spatial nonhomogeneity of stress and strain fields on the formulation of the yield criterion has not been considered up to now.

The first engineering attempts to assess the phenomena mentioned under (a) date back to the years before World War II. The relevant results are incomplete and difficult to be found. Instructive coherent experimental research programmes have been conceived and implemented, as far as we know, only in the last decades by F. Campus and his Belgian co-workers. They will be referred to later on.

Incidentally, it may be mentioned that phenomenologically apparently homogeneous states of stress cannot be considered to be strictly such in reality, in view of the granular structure of materials. The well known "region of instability" in the classical stress-strain diagramme when reaching the yield limit can be attributed to similar reasons, although uniaxial tension of a rod is usually considered as a particularly characteristic example of a homogeneous state of stress. These facts have been known for a long time; Fig. 6, taken from L. Prandtl's paper [28c], allows for this phenomenon

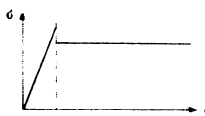


Fig. 6 : Prandtl's diagram [28b]

2) In French "surélasticité". Purposly we avoid other expressions (like, e.g., combinations with "hyper...", "super...", etc.), which are already in current use to designate other phenomena.

in an idealized manner.

Most of these experimentally observed results can theoretically be represented with relative ease if the yield criterion is assumed to depend also on the changes (nonuniformities) of initial (elastic) stress and strain fields. We shall consider these changes to be quite general, i. e. as changes with respect to spatial coordinates as well as with respect to time.

In our approach [13] , for simplicity of presentation, a four-dimensional time-space system has been introduced, this being, however, to be understood in the sense of classical Mechanics. Consequently, the (absolute) time  $t$  becomes a privileged coordinate.

Now, we shall assume that the transition of the material from the elastic into the plastic state depends not only on the tensors  $\sigma_{ij}$ ,  $\epsilon_{ij}$  themselves as usually supposed, but also on the gradients mentioned above. This dependence may be of various types and we have especially considered the following ones:

- (1) an explicit dependence on the components of the gradients;
- (2) a dependence on the invariants of the system of tensors  
 $\sigma_{ij}$ ,  $\epsilon_{ij}$ ;  $\sigma_{ijk}$ ,  $\epsilon_{ijk}$  ( $k = 1, 2, 3, 4$ );
- (3) a dependence on the gradients of some quantities which are scalar functions with respect to the components of the tensors  
 $\sigma_{ij}$ ,  $\epsilon_{ij}$  ;
- (4) a dependence on the derivatives of these scalar functions with respect to the components of the tensors  $\sigma_{ij}$ ,  $\epsilon_{ij}$  .

It can quite easily be shown [13] that, for isotropic bodies, (1) and (2) are equivalent. Furthermore, (3) is a special case of (2). Finally, case (4) leads back to the classical theory, i. e. to the yield criterion of the form

$$F(\sigma_{ij}, \epsilon_{ij}) = 0. \quad (\text{VI.1})$$

Following the pattern of these considerations, the general form of the yield criterion has been assumed to have the form

$$F(\sigma_{ij}, \epsilon_{ij}, \alpha_{ijk}, \beta_{ijk}) = 0, \quad (\text{VI.2})$$

where  $\alpha_{ijk} = \sigma_{ijk,k}$ ,  $\beta_{ijk} = \epsilon_{ijk,k}$  are tensors of rank three, each having 64 components.

Because of formal as well as physical relations, this number reduces to 18. Thus, for an isotropic material, the function  $F$  of Eq. (VI.2) will in general depend on 42 variables.

In view of this complicated form and, especially, with reference to real applications, it seemed to be appropriate to introduce and analyze expressions of simpler form. This turned out to be all the more justified as the influence of all the various variables, occurring in the function  $F$ , is not of equal importance, and thus for practical purposes a good approximation of  $F$  may contain much less of them.

The first approximation refers to the notion of ideal plasticity; then the function  $F$  reduces to

$$F(\sigma_{ij}, \alpha_{ijk}) = 0. \quad (\text{VI.3})$$

Furthermore, in agreement with our previous considerations, we will investigate the following form of the function :

$$F(l_1, l_2, l_3; g_1, \dots, g_n) = 0; \quad (\text{VI.4})$$

here,  $l_1, l_2, l_3$  denote, as usual, the invariants of the stress tensor, whereas in the invariants  $g_1, \dots, g_n$  also the components of the gradient tensor shall occur.

The reasons explained in [13] permit to consider the invariant criterion (VI.4) for  $n = 1$ , where  $g_i = g$  shall depend solely on  $l_i$  ( $i = 1, 2, 3$ ) and their derivatives with respect to  $x_i$  ( $i = 1, 2, 3, 4$ ) .

Even this relatively simple form already allows to describe phenomena reflecting "overelasticity" (a) as well as those due to "rate sensitivity" (b). An obvious and simple assumption would be to put

$$g = f_i \cdot f_i \quad (i = 1, 2, 3, 4), \quad (\text{VI.5})$$

where  $f$  is a scalar function of the stress tensor. This finally gives

A comparison with Eq. (V.1) shows that this expression formally takes the form of a yield criterion which explicitly depends on a certain parameter, like time or a time-dependent quantity, though the physical meaning and the structure of  $g$  are different now from that of  $\eta = \eta(t)$  (cf. also [2], [19b]).

In view of this analogy, it is easy to establish the criteria for the active (loading), the neutral, and the passive (unloading) processes. It is found that these criteria depend, besides on the velocities, also on the accelerations of the components of the stress and strain tensors.

This indicates that, when formulating the local conditions, which are related to the history of loading and which guarantee, e.g., the active character of the process, these involve not only the first but also the second time derivatives.

Therefore, also the investigations of uniqueness problems, which are related to the material classes considered in such studies, will essentially differ from the classical scheme.

Finally, assuming that the yield surface represents also the yield potential, the corresponding flow law has been established. So, e.g., the plastic strain rate can be expressed in the usual manner by

$$\dot{\varepsilon}_{ij}^p = \Lambda \frac{\partial f}{\partial \sigma_{ij}}, \quad \Lambda \geq 0, \quad (\text{VI.7})$$

where  $f(\sigma_{ij}, \dot{\varepsilon}_{ij}^p, t, \vartheta, \dots)$  represents the condition of the transition of the material into the plastic state (for unloading processes we have  $\Lambda = 0$ ).

In the case of ideally plastic materials, the factor  $\Lambda$  is undetermined, whereas for hardening processes it is obtained from the condition that, for an active process ( $\dot{\varepsilon}_{ij}^p \neq 0$ ), the point which characterizes the

state has to remain on the yield surface. Thus, Eq. (VI.7) leads to [13]

$$\begin{aligned}\dot{F} = 0 &= \frac{\partial F}{\partial \sigma_{ij}} \dot{\sigma}_{ij} + \frac{\partial F}{\partial \epsilon_{ij}} \dot{\epsilon}_{ij} + \frac{\partial F}{\partial \alpha_{ijk}} \dot{\alpha}_{ijk} + \frac{\partial F}{\partial \beta_{ijk}} \dot{\beta}_{ijk} = \\ &= \frac{\partial F}{\partial \sigma_{ij}} \left( \dot{\sigma}_{ij} + \Lambda \frac{\partial F}{\partial \epsilon_{ij}} + \Lambda, k \frac{\partial F}{\partial \beta_{ijk}} \right) + \frac{\partial F}{\partial \alpha_{ijk}} (\dot{\sigma}_{ij}), k + \Lambda \frac{\partial F}{\partial \beta_{ijk}} \left( \frac{\partial F}{\partial \sigma_{ij}} \right), k.\end{aligned}\quad (\text{VI.8})$$

If stresses  $\sigma_{ij}$ , plastic strains  $\epsilon_{ij}^P$  as well as their gradients  $\alpha_{ijk}$  and  $\beta_{ijk}$  are known, and if, furthermore, the rates of changes of stresses and their gradients  $\dot{\alpha}_{ijk}$  are given (because of  $\alpha_{ijk}$ , knowledge of the acceleration of the stress tensor is required), the factor can be found by solving the differential equation (VI.8) with respect to  $\Lambda$  (when taking  $F \equiv 0$  in account).

If, on the other hand, the yield condition is independent of the deformation gradient  $\beta_{ijk}$ , Eq. (VI.8) degenerates into an algebraic relation, from which the factor  $\Lambda$  can immediately be found in the form

$$\Lambda = - \left[ \frac{\partial F}{\partial \alpha_{ijk}} (\dot{\sigma}_{ij}), k + \frac{\partial F}{\partial \sigma_{ij}} \dot{\sigma}_{ij} \right] \cdot \left[ \frac{\partial F}{\partial \epsilon_{ij}^P} \cdot \frac{\partial F}{\partial \sigma_{ij}} \right]^{-1}. \quad (\text{VI.9})$$

For practical applications, the Belgian experimental programme has theoretically been analyzed. This mainly was focussed on elastic-plastic bending of steel elements. The increase of the plastic limit due to the stress gradient can be given a theoretical explanation. Nevertheless, further investigations are still necessary. Cf. Fig. 7, Fig. 8, Fig. 9.

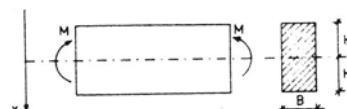


Fig. 7 : Belgian experiments [4]

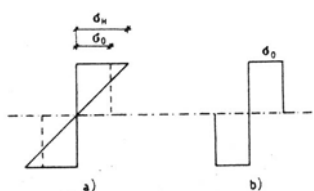


Fig. 8 : "Overelasticity" [4], [13]

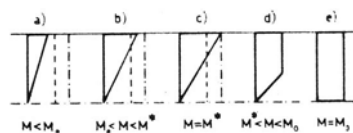


Fig. 9 : Evolution of stress field [13]

### VII. Final Methodical Remark

For our considerations, we might also have chosen the inverse way of presentation and start with the most general models (Sections VI and V). Only afterwards by introducing appropriate limitations in the generality of assumptions we might have, step by step, derived all the simpler situations and adequately represent them as particular cases, already contained in such a quite general final approach.

Thus, by eliminating the assumption of the space and time variability of stress and strain fields, further by successively dropping the notions of nonstationarity ( $\eta = 0$ ), of rheological response ( $\dot{\gamma} \rightarrow \infty$ ), of work-hardening ( $\alpha = 0$ ), of material anisotropy and nonhomogeneity, we would finally arrive at the known classical starting point: the transition to the simple Prandtl-Reuss material.

We prefer, however, the method adopted here which, moreover, corresponds to the historical evolution of actual research trends and progress.

References

- [1] E. Beltrami, Sulle condizioni di resistenza dei corpi elastici. Rend. Ist. Lomb., Ser. 2, vol. 18, 1885, p. 704.
- [2] B.A. Boley and J.E. Wiener, Theory of Thermal Stresses. Wiley & Sons Inc., New York-London, 1960.
- [3] W. Burzyński, (a) Studium nad hipotezami wytężenia (in Polish). Lwów 1928. (b) Über Anstrengungshypothesen. Schweizerische Bauzeitung, vol. 94, 1929, p. 259.
- [4] F. Campus, (a) Plastification de l'acier doux en flexion plane simple. Bull. de la Classe des Sciences, Série 5, vol. 49, 4, 1963. (b) Plastification de l'acier doux en flexion composée. Bull de la Classe des Sciences, Sér. 5, vol. 49, 4, 1963. (c) La plastification de l'acier doux en flexion simple et composée et ses effets sur le flambage par compression des pièces droites élastoplastiques. Bull. de la Classe des Sciences, Série 5, vol. 49, 5, 1963.
- [5] F. Campus et K. Gamski, Abaissement de la limite apparente d'élasticité des acier par fluage après une amorce d'écrissement à température ordinaire. C.R. Ac. Sci de Paris, 1955.
- [6] Ch. A. Coulomb, Essai sur une application de règle de Maximis et Minimis à quelques problèmes statiques relatifs à l'architecture. Mém. de math. et phys., vol. 7, 1773, p. 343.
- [7] N.M. Dehoussé, Note relative à un phénomène de surélasticité en flexion constatée lors d'un essais de barreau en acier doux. Bull. de la Classe des Sciences, Série 5, vol. 48, 1962.
- [8] Galileo Galilei, Discorsi e dimostrazioni matematiche. Leyde 1638.
- [9] H. Hencky, Zur Theorie plastischer Deformationen und der hierdurch im Material hervorgerufenen Nebenspannungen. Proc. 1st Internat. Congr. Appl. Mech., Delft, 1924, p. 312-317. Cf. also Zeitschr. für Angewandte Mathematik und Mechanik, vol. 4, 1924, p. 323-334.
- [10] R. Hill, (a) Mathematical Theory of Plasticity. Oxford University Press, 1950. (b) A note on estimating the yield point loads in a plastic-rigid body. Phil. Mag., vol. 43, 1952, p. 353-355.
- [11] K. Hohenemser and W. Prager, Über die Ansätze der Mechanik isotroper Kontinua. Zeitschr. für Angewandte Mathematik und Mechanik, vol. 12, 1932, p. 216.
- [12] M.T. Huber, Właściwa praca odkształcenia jako miara wytwżenia materiału (in Polish). Czasopismo Techniczne, Lwów, vol. 22, 1904, p. 81. Reprinted in Pisma, vol. 2, Państwowe Wydawnictwo Naukowe (PWN), Warsaw 1956.

- [13] J.A. König and W. Olszak, The yield criterion in the general case of nonhomogeneous (nonuniform) stress and deformation fields. Proc. Symp. "Topics in Applied Continuum Mechanics", (Ed. J.L. Zeman and F. Ziegler), Springer-Verlag, Wien-New York 1974.
- [14] C. Maiden and J.D. Campbell, The static and dynamic strength of a carbon steel at low temperatures. Phil. Mag., vol. 3, 1958, p. 872.
- [15] F. Mariotte, *Traité du mouvement des eaux et des autres fluides*. Paris 1686
- [16] R. von Mises, (a) Mechanik der festen Körper im plastisch deformablen Zustand. Göttinger Nachrichten, Math. phys. Klasse, 1913, p. 582-592. (b) Mechanik der plastischen Formänderung von Kristallen. Zeitschr. für Angewandte Mathematik und Mechanik, vol. 8, 1928, p. 161-185.
- [17] Z. Mróz, (a) On the description of anisotropic work-hardening, J. Mech. Phys. Solids, vol. 15, 1967, p. 163-175. (b) An attempt to describe the behaviour of metals under cyclic loads using a more general work-hardening model. Acta Mechanica, ovl. 7, 1969, p. 199-212. (c) A description of work-hardening of metals with application to variable loading. Proc. Intern. Symp. "Foundations of Plasticity", (Ed. A. Sawczuk), Noordhoff Intern. Publ., Groningen 1973.
- [18] W. Olszak, (a) O podstawach teorii ciuł elasto-plastycznych niejednorodnych (in Polish). Arch. Mech. Stos., 3, 4, 1955. (b) La nonhomogénéité plastique en tant que phénomène physique et problème scientifique. Prof. F. Campus Anniv. Volume, Brussels 1964. (c) Les critères de transition en elasto-visco-plasticité. Bull. Acad. Pol. Sci., Série Sci. Techn., 1, 1966. (d) Les critères de plasticité non-classiques. Considération de base. In "Topics of Contemporary Mechanics", CISM Courses and Lectures N° 210, Udine 1974, p. 185-189.
- [19] W. Olszak and P. Perzyna, (a) On elastic-viscoplastic soils. In "Rheology and Soil Mechanics", Proc. of the IUTAM Symp. Grenoble 1964, Springer 1966, p. 47-57. (b) The constitutive equations of the flow theory for a non-stationary yield condition. In "Applied Mechanics", Proc. of the Eleventh Congr. of Appl. Mech., Munich 1964, (Ed. H. Görtler), Springer 1966, p. 545-553. (c) Sur la théorie des phénomènes visco-plastiques. Rendic. Semin. Matem. e Fis., vol. 38, 2, 1968 (Milan). (d) Stationary and nonstationary viscoplasticity. Symp. on Inelastic Behaviour of Solids, Columbus, Ohio, 1970.
- [20] W. Olszak, J. Rychlewski and W. Urbanowski, Plasticity under nonhomogeneous conditions. Advances in Applied Mechanics, vol. 7, Acad. Press, New York-London 1962, p. 131-214.
- [21] W. Olszak and W. Urbanowski, (a) The generalized distortion energy in the theory of anisotropic bodies. Bull. Acad. Pol. Sci., Sér. Sci. Techn., 5, 1957, p. 29-37. (b) The tensor of moduli of plasticity. Bull. Acad. Pol. Sci., Sér. Sci. Techn., 5, 1957, p. 39-45. (c) The flow function and the yield condition for nonhomogeneous orthotropic bodies. Bull. Acad. Pol. Sci., Sér. Sci. Techn., 4, 1957.

- [22] P. Perzyna, (a) The constitutive equations for rate-sensitive plastic materials. *Quart. Appl. Math.*, 20, 1963, p. 321. (b) The constitutive equations for work-hardening and rate-sensitive plastic materials. *Proc. Vibr. Probl.*, 4, 1963, p. 281.
- [23] P. Perzyna and T. Wierzbicki, (a) Temperature dependent and strain rate-sensitive plastic materials. *Arch. Mech. Stos.*, 16, p. 135. (b) Fundamental problems in viscoplasticity. *Advances in Applied Mechanics*, vol. 9, Academic Press, New York-London 1966.
- [24] A. Phillips and H. Moon, An experimental investigation concerning yield surfaces and loading surfaces. *Rep. Yale University, Dept. of Engineering and Applied Science*, 1976. Cf. *Acta Mechanica*.
- [25] A. Phillips and M. Ricciutti, Fundamental experiments in plasticity and creep of aluminum. Extension of previous results. *Int. J. of Solids Structures*, vol. 12, 1976, p. 159-171.
- [26] W. Prager, (a) Mécanique des solides isotropes au delà du domaine élastique. *Mém. des Sci. Math.*, vol. 87, Gauthier-Villars, Paris 1937. (b) isothermal plastic deformation. *Proc. Koninkl. Akad. Wet. (B)* 61, 1958 p. 176-182 (Amsterdam).
- [27] W. Prager and P.G. Hodge, *Theory of Perfectly Plastic Solids*. John Wiley & Sons Inc., New York 1951.
- [28] L. Prandtl, (a) Über die Eindringungsfestigkeit (Härte) plastischer Baustoffe und die Festigkeit von Schneiden. *Zeitschr. für Angewandte Mathematik und Mechanik*, vol. 1, 1921, p. 15-21. (b) Spannungsverteilung in plastischen Körpern. *Proc. 1st Internat. Congr. Appl. Mech.*, Delft, 1924, p. 43-54 (c) Ein Gedankenmodell zur kinetischen Theorie fester Körper. *Zeitschrift für Angewandte Mathematik und Mechanik*, vol. 8, 1928, p. 85-106. (a), (b), (c) reprinted in "Gesammelte Abhandlungen zur angewandten Mechanik, Hydro- und Aerodynamik", 1. Teil (Ed. H. Görtler, H. Schlichting, W. Tollmien, F.W. Riegels), Springer-Verlag, Berlin-Göttingen-Heidelberg
- [29] M. Reiner and K. Weissenberg, Rheology Leaflet, N° 10, 1939, p. 12-20
- [30] E. Reuss, Berücksichtigung der elastischen Formänderungen in der Plastizitätstheorie. *Zeitschr. für Angewandte Mathematik und Mechanik*, vol. 1 1930, p. 266-274.
- [31] B. de Saint-Venant, Mémoire sur l'établissement des équations différentielles des mouvements intérieurs opérés dans les corps solides ductiles au-delà des limites où l'élasticité pourrait les ramener à leur premier état. *C. Acad. Sci.*, 70, 1870, p. 473-480 (Paris).
- [32] W. W. Sokolowskij, Rasprastranieme uprugo-viazko-plasticheskikh volnov v stierzhniakh (in Russian). *Dokl. AN SSSR*, 60, 5, 1948, p. 775-778.
- [33] H. Tresca, Mémoire sur l'écoulement des corps solides. *Mém. prés. p. div. sav.*, vol. 18, 1868, p. 733-799